ISSN (1230-0322)
2023, Vol. 73, No. 3

Food

Polish Journal of Food and Nutrition Sciences

formerly Acta Alimentaria Polonica

Published
by Institute of Animal Reproduction and Food Research of the Polish Academy of Sciences, Olsztyn

Published since 1957 as
Roczniki Chemii i Technologii Żywności and Acta Alimentaria Polonica (1975–1991)

SCOPE: The Journal covers fundamental and applied research in food area and nutrition sciences with a stress on interdisciplinary studies in the areas of food, nutrition and related subjects.

POLICY: Editors select submitted manuscripts in relation to their relevance to the scope. Reviewers are selected from the Advisory Board and from Polish and international scientific centres. Identity of reviewers is kept confidential.

AUTHORSHIP FORMS referring to Authorship Responsibility, Conflict of Interest and Financial Disclosure, Copyright Transfer and Acknowledgement, and Ethical Approval of Studies are required for all authors.

FREQUENCY: Quarterly – one volume in four issues (March, June, September, December).

COVERED by Web of Science, Current Contents/Agriculture, Biology & Environmental Sciences, Journal Citation Reports and Science Citation Index Expanded, BIOSIS (Biological Abstracts), SCOPUS, FSTA (formerly: Food Science and Technology Abstracts), CAS (Chemical Abstracts), AGRICOLA, AGRO-LIBREX data base, EBSCO, FOODLINE, Leatherhead FOOD RA data base FROSTI, AGRIS and Index Copernicus data bases, Biblioteka Nauki ICM, Biblioteka Narodowa – POLONA, and any www browser; ProQuest: The Summon, Bacteriology Abstracts, Immunology Abstracts.

EDITORIAL AND BUSINESS CORRESPONDENCE: Submit contributions (see Instructions to Authors) and address all communications regarding subscriptions, changes of address, etc. to:

CORRESPONDENCE TO: Ms. Joanna Molga
Polish Journal of Food and Nutrition Sciences
Institute of Animal Reproduction and Food Research
of Polish Academy of Sciences
ul. Tuwima 10, 10-747 Olsztyn, Poland
e-mail: pjfns@pan.olsztyn.pl; http://journal.pan.olsztyn.pl

Polish Journal of Food and Nutrition Sciences

ADVISORY BOARD OF PJFNS 2023–2026

Contents

ORIGINAL PAPERS

covered by CURRENT CONTENTS/AGRICULTURE, BIOLOGY & ENVIRONMENTAL SCIENCES, JOURNAL CITATION REPORTS AND SCIENCE CITATION INDEX EXPANDED, BIOSIS, SCOPUS, IFIS Publishing and CAS abstracts, and AGRO-Librex, FROSTI, PSJC, AGRIS and Index Copernicus data bases

Ministerstwo
Edukacji i Nauki

W latach 2022–2024 kwartalnik naukowy ***Polish Journal of Food and Nutrition Sciences*** realizuje projekt nr RCN/SP/0520/2021/1 finansowany ze środków budżetu państwa – Ministerstwo Edukacji i Nauki w ramach programu „Rozwój czasopism naukowych". Dofinansowanie wynosi 120 000 zł. W ramach projektu podejmowane są działania zmierzające do podniesienia poziomu praktyk wydawniczych i edytorskich, zwiększenia wpływu czasopism na rozwój nauki oraz utrzymania się czasopism w międzynarodowym obiegu naukowym.

Ministry of Education and Science
Republic of Poland

In the years 2022–2024, the scientific quarterly ***Polish Journal of Food and Nutrition Sciences*** accomplishes a project no. RCN/SP/0520/2021/1 financed from the state budged – Ministry of Education and Science Republic of Poland in the framework of a program "Development of scientific journals". The financing amounts to 120,000 PLN. The program aims at improving the level of publishing and editing practices, increasing the impact of scientific journals on science development, and extending the international range of scientific journals.

Subscription
2023 – One volume, four issues per volume. Annual subscription rates are: Poland 150 PLN, all other countries 80 EUR. Prices are subject to exchange rate fluctuation. Subscription payments should be made by direct bank transfer to Bank Gospodarki Żywnościowej, Olsztyn, Poland, account No 17203000451110000000452110 SWIFT code: GOPZPLWOLA with corresponding banks preferably. Subscription and advertising offices at the Institute of Animal Reproduction and Food Research of Polish Academy of Sciences, ul. J. Tuwima 10, 10-747 Olsztyn, Poland, tel./fax (48 89) 5234670, fax (48 89) 5240124, e-mail: pjfns@pan.olsztyn.pl; http://journal.pan.olsztyn.pl

Zamówienia prenumeraty: Joanna Molga (e-mail: pjfns@pan.olsztyn.pl)

Wersja pierwotna (referencyjna) kwartalnika PJFNS: wersja papierowa (ISSN 1230–0322)
Nakład: 70 egz.; Ark. wyd. 16; Ark. druk. 13
Skład i druk: ITEM

ORIGINAL ARTICLE
http://journal.pan.olsztyn.pl

Polish Journal of Food and Nutrition Sciences
2023, Vol. 73, No. 3, 205–213
DOI: 10.31883/pjfns/168233
ISSN 1230-0322, e-ISSN 2083-6007

Optimization of Lycopene Extraction from Tomato Pomace and Effect of Extract on Oxidative Stability of Peanut Oil

Dinh Thi Tran[1]*, Lan Thi Hoang Nguyen[1], Cuong Ngoc Nguyen[2], Maarten L.A.T.M. Hertog[3, 4], Bart Nicolaï[3, 4, 5], David Picha[6]

[1]Faculty of Food Science and Technology, Vietnam National University of Agriculture, Trauquy, Gialam, Hanoi, Vietnam
[2]Faculty of Engineering, Vietnam National University of Agriculture, Trauquy, Gialam, 100000 Hanoi, Vietnam
[3]BIOSYST-MeBioS, KU Leuven, Willem de Croylaan 42, 3001 Leuven, Belgium
[4]Plant Institute (LPI), KU Leuven, Kasteelpark Arenberg 31, 3001 Leuven, Belgium
[5]VCBT, Flanders Centre of Postharvest Technology, Willem de Croylaan 42, 3001 Leuven, Belgium
[6]School of Plant, Environmental and Soil Sciences, Louisiana State University, Baton Rouge, Louisiana, U.S.A.

Lycopene, the pigment principally responsible for the red colour of tomatoes, is well-known for its strong antioxidant property and substantial health benefits. In this study, the optimal combination of factors for lycopene extraction from tomato pomace was identified using response surface methodology. The best practically feasible results maximising both lycopene yield and antioxidant activity of the extract were obtained by applying a ratio of ethyl acetate to tomato waste of 35:1 (*v/w*), at a temperature of 55°C for 100 min of extraction. The extract was then added to the peanut oil to evaluate its oxidative stability during 60 days of storage at 40°C. It was shown that the addition of 2 g extract/kg oil offered the lowest level of peroxide value, *p*-anisidine value, and total oxidation value, followed by the oils with 50 mg butylated hydroxytoluene /kg oil and 1 g extract/kg oil, indicating the effect of lycopene-rich extract on enhancing the oxidative stability of peanut oil. The results in this study suggest that incorporation of extract rich in lycopene from tomato waste products may be an effective method to reduce oxidation and extend the shelf-life of peanut and other vegetable oils.

Key words: antioxidant, lycopene, extraction, optimization, response surface methodology, peanut oil stability

INTRODUCTION

Lycopene is the principal carotenoid present in high amount in tomatoes and tomato-derived products. It is an acyclic, open chain, unsaturated carotenoid with 13 double bonds, 11 of which are conjugated and organised linearly [Egydio *et al.*, 2010; Fernandez-Ruiz *et al.*, 2010]. In biological systems, lycopene is the most effective singlet oxygen quencher among carotenoids [Young & Lowe, 2001]. It can remove singlet oxygen atoms two and ten times more efficiently than β-carotene and α-tocopherol, respectively [Przybylska, 2020]. Due to its strong antioxidant potential, lycopene has been shown to provide protection against various types of cancer, including prostate, stomach, and lung [Cheng *et al.*, 2020; Stahl & Sies, 1996], and other forms of oxidative damage. It has also been shown to decrease the risk of chronic diseases including coronary heart disease as well as neurodegenerative diseases such as Alzheimer's and Parkinson's diseases [Przybylska, 2020; Willcox *et al.*, 2003]. In addition to its antioxidant capabilities, lycopene induces cell-to-cell contact and modulates the hormonal and immunological systems as well as other metabolic pathways [Cheng *et al.*, 2020; Fuhramn *et al.*, 1997]. Moreover, it is a natural red pigment utilised as a colouring ingredient in the dyeing of various foods [Castro *et al.*, 2021]. Its

***Corresponding Author:**
tel: +84 626 177 18; fax: +84 43 8276 554; e-mail: ttdinh@vnua.edu.vn (D.T. Tran)

Submitted: 28 April 2023
Accepted: 12 June 2023
Published on-line: 5 July 2023

significance is growing as the food industry uses more natural pigments than synthetic colourants and as law regarding the use of food additives becomes more stringent. Therefore, lycopene is in high demand by pharmaceutical companies and the food, feed, and cosmetic industries.

Tomatoes and tomato products are the primary sources of lycopene in the human diet [Dasgupta & Klein, 2014]. Typically, 80–90% of the total carotenoids in tomato fruit are lycopene [Shi & Maguer, 2000]. Lycopene and other carotenoids are mostly found in the water-insoluble fraction and have shown to be five times more concentrated in the peel and seeds, as compared to the tomato pulp [Toor & Savage, 2005]. Therefore, a large amount of lycopene is lost as waste during tomato processing [Baysal *et al.*, 2000].

The tomato processing industry generates substantial volumes of solid waste, and between 10–40% of the tomatoes processed in a facility are skins and seeds [Al-Wandawi *et al.*, 1985; Topal *et al.*, 2006]. In Vietnam, the production area of tomatoes has been progressively expanding in recent decades for both fresh consumption and processing. Thus, large amounts of low-grade fruit and processing waste are land filled or used as compost and animal feed without significant treatment. Therefore, valorisation of the tomato waste stream by extracting a highly added-value component, such as lycopene, from the waste will contribute to food sustainability and environmental protection. So far, the most common methods for lycopene extraction from plant tissues are based on extraction with organic solvents or supercritical fluid extraction [Deng *et al.*, 2021; Guerra *et al.*, 2021]. The latter requires high capital costs and limits its application to research and industrial scale [Montesano *et al.*, 2008]. The organic solvent extraction method has been more widely utilised due to the lower cost and better lycopene recovery [Pandya *et al.*, 2015].

Vegetable oils are rich in polyunsaturated fatty acids, yet they are extremely vulnerable to oxidation. This results in rancid odours, disagreeable flavours, and discolouration, causing negative alterations in sensory and nutritional qualities and a loss in shelf life [Machado *et al.*, 2022]. Commonly, synthetic antioxidants, such as butylated hydroxyanisole (BHA), butylated hydroxytoluene (BHT), and tert-butyl hydroquinone (TBHQ), are added to edible oils to increase their shelf life. Recent reports indicate these synthetic antioxidants may cause adverse side effects to human health [Mika *et al.*, 2023; Zhang *et al.*, 2023]. Consequently, there is significant interest in enriching oils with natural antioxidants, such as lycopene, tocopherols, polyphenols, to hinder lipid oxidation [Bodoira *et al.*, 2017; Omer *et al.*, 2014; Xie *et al.*, 2018; Zahran & Najafi, 2020].

The goal of this work was to obtain extract rich in lycopene from tomato pomace obtained after pressing the juice and using it to enhance the oxidative stability of peanut oil. Our objectives were to (1) optimise the lycopene extraction process from tomato processing waste using design of experiment (DOE) in combination with a multiple response criterion, and (2) utilise the extract rich in lycopene to enhance the oxidative stability of peanut oil. In this study, peanut oil was chosen to assess the extract's effect as it is prone to be oxidised due to a relatively high amount of polyunsaturated fatty acids and widely used in the food industry.

MATERIALS AND METHODS

Materials and reagents

The fruits of tomato cv. Savior were manually harvested at the red ripe stage from a commercial field in Nam Dinh province, Vietnam. After harvest, tomatoes were transported under ambient conditions to the food processing laboratory at the Vietnam National University of Agriculture in Hanoi. The fruits were washed, drained, and mechanically pressed to extract the juice. The tomato pomace was dried in a natural convection oven (UN55, Memmert, Schwabach, Germany) at 40°C until the moisture content reached 6.2 g/100 g. The dried pomace was ground using a grindomixer (GM200, Retsch, Haan, Germany). The powder was passed through a 0.15 mm sieve and used for lycopene extraction.

Peanuts were collected from a commercial plantation in Bac Ninh province, Vietnam. Peanut oil extraction was carried out in a single step with a pilot scale screw press. The moisture content of the peanuts averaged 12 g/100 g, the pressing temperature was 28°C, the screw speed was 20 rpm, and the restriction die was 6 mm [Martínez *et al.*, 2012]. The extracted oil was filtered through filter press and stored until use in amber glass bottles in a freezer at −20°C.

The analytical grade reagents included a lycopene standard, 6-hydroxy-2,5,7,8-tetramethylchroman-2-carboxylic acid (Trolox), 2,2-diphenyl-1-picrylhydrazyl (DPPH) radical, butylated hydroxytoluene (BHT), and *p*-anisidine, all purchased from Sigma-Aldrich (Saint Louis, MO, USA). All other reagents were also of analytical grade and obtained from Merck (Darmstadt, Germany) and Himedia (Mumbai, India). Distilled water of high-performance liquid chromatography (HPLC) grade was used throughout the experiments.

Response surface experimental design for optimisation of lycopene extraction from dried tomato pomace

To identify the potential factors and their working range for optimising lycopene extraction in the current study, the screening experiments were first conducted in which the dried tomato pomace was extracted using various organic solvents at different temperatures and solvent to dried tomato pomace ratios. As the extract will then be added to the edible oil for human consumption, only the solvents with food-grade were tested, *i.e.*, petroleum ether, ethyl ether, ethyl acetate, acetone, and ethanol. From the screening experimental results, ethyl acetate was determined as the most efficient solvent for the next experiments as it gave the highest lycopene extraction yield and economic efficiency and ensured food safety. Therefore, in this study, three independent variables having great influence on the lycopene content and antioxidant activity were retained for optimisation, namely: the ratio of ethyl acetate to material (X_1), extraction temperature (X_2), and extraction time (X_3) using the response surface methodology (RSM). For these three variables, a Box-Behnken design based on 15 trials involving three center points was constructed using the JMP software, version 10.0 (SAS Institute, Inc., Cary, NC, USA) (Table 1). The extraction experiments were carried

out randomly to minimise the effect of unexpected variability in the response variables. During extraction, the mixture was stirred using a magnetic stirrer under darkness. After extraction, the extract was analysed for its lycopene content and antioxidant activity. Next, the experimental results of the RSM were fitted with a second-order polynomial equation (Equation (1)) consisting of linear, quadratic and first-order interaction terms by multiple regression.

$$Y = \beta_0 + \sum_{i=1}^{k}\beta_i X_i + \sum_{i=1}^{k}\beta_{ii} X_i^2 + \sum_{1\le i\le j}^{k}\beta_{ij} X_i X_j + \varepsilon \quad (1)$$

where: Y is one of the output variables; β_i, β_{ii}, β_{ij} are regression coefficients for the major factors and interaction terms; X_i, X_j are the independent variables; k is the number of variables; and ε is the remaining unexplained error. The multiple-least square regression was used to estimate regression coefficients by minimising the sum of squares of the errors. Using analysis of variance (ANOVA), the significance of the overall model and each regression coefficient was determined. Lastly, response surface optimisation based on the Derringer's desirability function was used as previously described by Tran *et al.* [2016] to discover the ideal combination of parameters that maximise the lycopene content and antioxidant activity. The JMP software, version 10.0, was utilised for data analysis (SAS Institute).

Oxidative stability assessment of extract-enriched peanut oil

The oxidative stability assessment of the extract-enriched oil was performed as follows. Lycopene was extracted from dried tomato pomace under the optimised conditions. After removing the solvent using a vacuum evaporator (R-300, Buchi, Flawil, Switzerland) at 40°C and 240 mbar, the extract powder was added to the peanut oil in a range of 1–2 g/kg oil. BHT with concentration of 50 mg/kg oil was used to compare the effect of extract with a synthetic antioxidant. The antioxidants (extract or BHT) were uniformly dissolved in the peanut oil by using a shaker until a homogeneous oil was obtained. The peanut oil without any antioxidant was used as the control. The mixed oils were transferred separately to amber glass bottles containing 1 L of peanut oil and stored in a dark chamber at 40±1°C for up to 60 days. All the enriched and control oil samples were prepared in triplicate and the quality attributes were monitored every 14th day by analysing the peroxide value (PV), *p*-anisidine value (p-AV), and total oxidation (TOTOX).

Analytical methods

Determination of lycopene content

The lycopene content was quantified by using an LC-10AI HPLC system equipped with an SPD-M20A detector (Shimadzu, Kyoto, Japan). The chromatographic analysis was performed using the method developed by Kimura *et al.* [2007] with some modifications. Briefly, after tomato dried pomace extraction, a 20 µL aliquot of the extract was injected into an ODS C18 column (4.6×250 mm, 5 µm particle size; Agilent, Santa Clara, CA, USA). The mobile phase comprised distilled water (A), and acetone (B). The combined solvent flow rate was 1.2 mL/min; the column temperature was set at 30°C. The gradient program lasted for 26 min and was as follows: 80% B for 0–7 min; 95% B for 7–20 min;

Table 1. Box-Behnken design matrix of variables (X_1, X_2 and X_3), and measured responses (Y_1 and Y_2) for lycopene extraction from dried tomato pomace.

Run	Ratio of solvent: material (X_1)	Temperature (°C) (X_2)	Time (min) (X_3)	Lycopene content (mg/g DW) (Y_1)	Antioxidant activity (µmol TE/g DW) (Y_2)
1	10:1	30	90	4.24±0.07	4.54±0.05
2	50:1	30	90	5.49±0.05	6.32±0.02
3	10:1	70	90	6.75±0.04	7.52±0.03
4	50:1	70	90	8.23±0.08	10.01±0.05
5	10:1	50	30	6.58±0.03	7.43±0.07
6	50:1	50	30	7.61±0.05	10.22±0.02
7	10:1	50	150	6.82±0.09	8.20±0.03
8	50:1	50	150	8.69±0.12	12.43±0.06
9	30:1	30	30	4.53±0.05	4.92±0.05
10	30:1	70	30	7.67±0.12	9.21±0.04
11	30:1	30	150	4.85±0.18	5.12±0.02
12	30:1	70	150	8.37±0.23	12.05±0.14
13	30:1	50	90	8.76±0.22	12.32±0.03
14	30:1	50	90	8.63±0.11	12.18±0.07
15	30:1	50	90	8.51±0.14	12.26±0.04

Data values are accompanied by standard deviation of the mean with *n*=3. TE, Trolox equivalent; DW, dry weight.

100% B for 20-25 min; 80% B for 25–26 min. Absorbance was monitored at 470 nm. The lycopene standard was used to establish the calibration curve for quantifying lycopene in the sample. The lycopene content was expressed as mg per g of the pomace dry weight (DW) and per g of the dried extract.

Determination of antioxidant activity

Antioxidant activity of the extract was evaluated based on the scavenging activity of the DPPH radical. The sample preparation was performed according to Martinez & Maestri [2008]. Briefly, reaction mixtures containing 0.1 mL of the extract and 3.9 mL of a DPPH solution at a concentration of 0.1 mM in toluene were incubated for 30 min at room temperature. The absorbance at 515 nm was measured using a UV-VIS DR3900 spectrophotometer (Hach, Ames, IA, USA). The antioxidant activity was calculated using the Trolox calibration curve and expressed as µmol Trolox equivalent (TE) per g pomace DW and per g of the dried extract.

Oil quality analysis

Standard American Oil Chemists' Society (AOCS) methods were used to determine PV (method Cd 8b-90) [AOCS, 2009] and p-AV (method Cd 18-90) [AOCS, 2017]. TOTOX was derived using the formula (2) [Shahidi & Wanasundara, 2002].

$$TOTOX = 2PV + p\text{-}AV \quad (2)$$

Statistical analysis

Statistical differences among treatments were estimated from the ANOVA test at the 5% level of significance for all parameters evaluated. The differences between means were determined by Tukey's multiple comparison test using the JMP software version 10 (SAS Institute).

RESULTS AND DISCUSSION

Optimization of lycopene extraction by response surface methodology

The amounts of lycopene extracted from dried tomato pomace at the ratio of solvent to tomato pomace powder of 10:1, 30:1, and 50:1 (*v/w*) and temperatures of 30, 50, and 70°C for incubation periods up to 150 min are presented in Table 1. The lowest amount of lycopene (4.24 mg/g DW) was extracted at the ratio of 10:1 and a temperature of 30°C. Lycopene in the extract increased sharply from 4.24 to 8.76 mg/g DW when the ratio of solvent to material increased from 10:1 to 30:1 and extraction temperature ranged from 30 to 50°C. The positive effect of temperature on lycopene extraction found in this research is consistent with a previous study by Kumcuoglu *et al.* [2014] who found that increasing the temperature from 20 to 60°C during solvent extraction of lycopene from tomato processing waste resulted in a 20 mg/kg increase in lycopene content. In addition to temperature, the extraction time significantly contributed to the lycopene content for the duration from 30–90 min, after which no further improvements were detected (Table 1). When the ratio of solvent to solid is high, the solvent more easily diffuses through the tomato tissue and can extract lycopene. Moreover, it creates stronger diffusion dynamics to accelerate the mass transfer and extraction rate, facilitating the release of lycopene. However, further increasing the ratio of solvent to solid to 50:1 did not significantly change the lycopene content, likely because the mass transfer process between solvent solution and solid had reached its maximum. Although increasing temperature accelerates thermodynamic reactions, if the temperature is too high (>70°C) lycopene can lose stability and be degraded due to its long chain of conjugated carbon-carbon double bonds in the molecular structure [Calvo *et al.*, 2007; Ganje *et al.*, 2018].

The antioxidant activity of the extract was also influenced by the ratio of solvent to tomato pomace, temperature, and time in a similar manner as the lycopene content. The highest antioxidant activity of the extract (>12 µmol TE/g DW) was obtained from treatments 8, 13, 14, 15 when the ratio of solvent to waste material was 30:1–50:1, the temperature was 50°C, and the extraction time was 90–150 min (Table 1). The lowest antioxidant activity of 4.54 µmol TE/g DW was obtained when the ratio of solvent to tomato pomace was 10:1 and the temperature was 30°C. The high correlation of lycopene content and antioxidant activity was because lycopene has high antioxidant activity. Generally, a higher lycopene content will provide more antioxidant activity.

The lycopene content obtained in this study is in the same range as that published by Eh & Teoh [2012] in which the yield of all-*trans* lycopene was 5.11 mg/g DW extracted from tomato using ultrasonic-assisted extraction. Lavecchia & Zuorro [2008] obtained a lower lycopene content (450 mg/100 g DW) using cell wall degrading enzymes during the extraction process. Silva *et al.* [2019] extracted the lycopene from tomato processing by-product with innovative hydrophobic eutectic mixture (DL-menthol as a hydrogen-bond acceptor (HBA) and lactic acid as a hydrogen-bond donor (HBD)) using ultrasound-assisted extraction. Under

Table 2. Coefficients of the second-order models for lycopene content and antioxidant activity of the lycopene extraction from dried tomato pomace.

Components	Lycopene content (mg/g DW)	Antioxidant activity (µmol TE/g DW)
Intercept	3.482	3.416
Ratio of solvent:material (X_1)	0.035	0.071
Temperature (°C) (X_2)	0.074	0.112
Time (min) (X_3)	0.005	0.013
X_1^2	-0.002	-0.004
$X_1 \times X_2$	0.0001*	0.0004*
X_2^2	-0.004	-0.009
$X_1 \times X_3$	0.0002	0.0003
$X_2 \times X_3$	6.04×10^{-5}*	0.0006
X_3^2	-0.0015	-0.0003
Model (*p*-value)	<0.0001	<0.0001
R^2	0.9872	0.9703

*Data value was not significant ($p \geq 0.05$). TE, Trolox equivalent; DW, dry weight.

the optimal extraction condition of 8:1 mol HBA to mol HBD ratio, solvent to sample ratio of 120 mL/g, at 70°C for 10 min, the optimal yield of lycopene was 1446.6 µg/g DW. Kehili *et al.* [2019] showed the highest lycopene content of 1,223.72 mg/kg DW obtained when refined olive oil was used as the extractant, and a biomass to oil ratio was 2.5% (*w/v*), temperature was 80°C, and magnetic stirring was continued at 400 rpm for 45 min. The higher lycopene content obtained in the present study might be due to differences in tomato source, moisture content, and solvent extraction method. Tomato lycopene content varies depending on cultivar, maturity stage, and agronomic and environmental conditions during growth [Sumalan *et al.*, 2020; Taoukis & Assimakopoulos, 2010].

To evaluate the effect of three experimental factors on lycopene content (Y_1) and antioxidant activity (Y_2), the experimental results were fitted to the quadratic equation given in Equation (1).

Table 2 presents the fitting results for each response variable. The models were significant for both lycopene and antioxidant activity ($p<0.0001$). The coefficient of determination (R^2) was 0.9872 for lycopene content and 0.9703 for antioxidant activity, demonstrating that 98.72% and 97.03% of the variability in these response variables could be explained by the model. Interestingly, only the second-order interactions $X_1 \times X_3$ for lycopene content and $X_1 \times X_3$ and $X_2 \times X_3$ for antioxidant activity were statistically significant at the 5% level, all having a positive effect (Table 2). On the contrary, all the quadratic terms (X_1^2, X_2^2, X_3^2) were significant and negatively related to the response variables. In other words, excessive high temperature and longer extraction time may lead to lycopene degradation and isomerisation [Ganje *et al.*, 2018]. The results found in this study are consistent with those published by Dhakane-Lad & Kar [2021] who reported

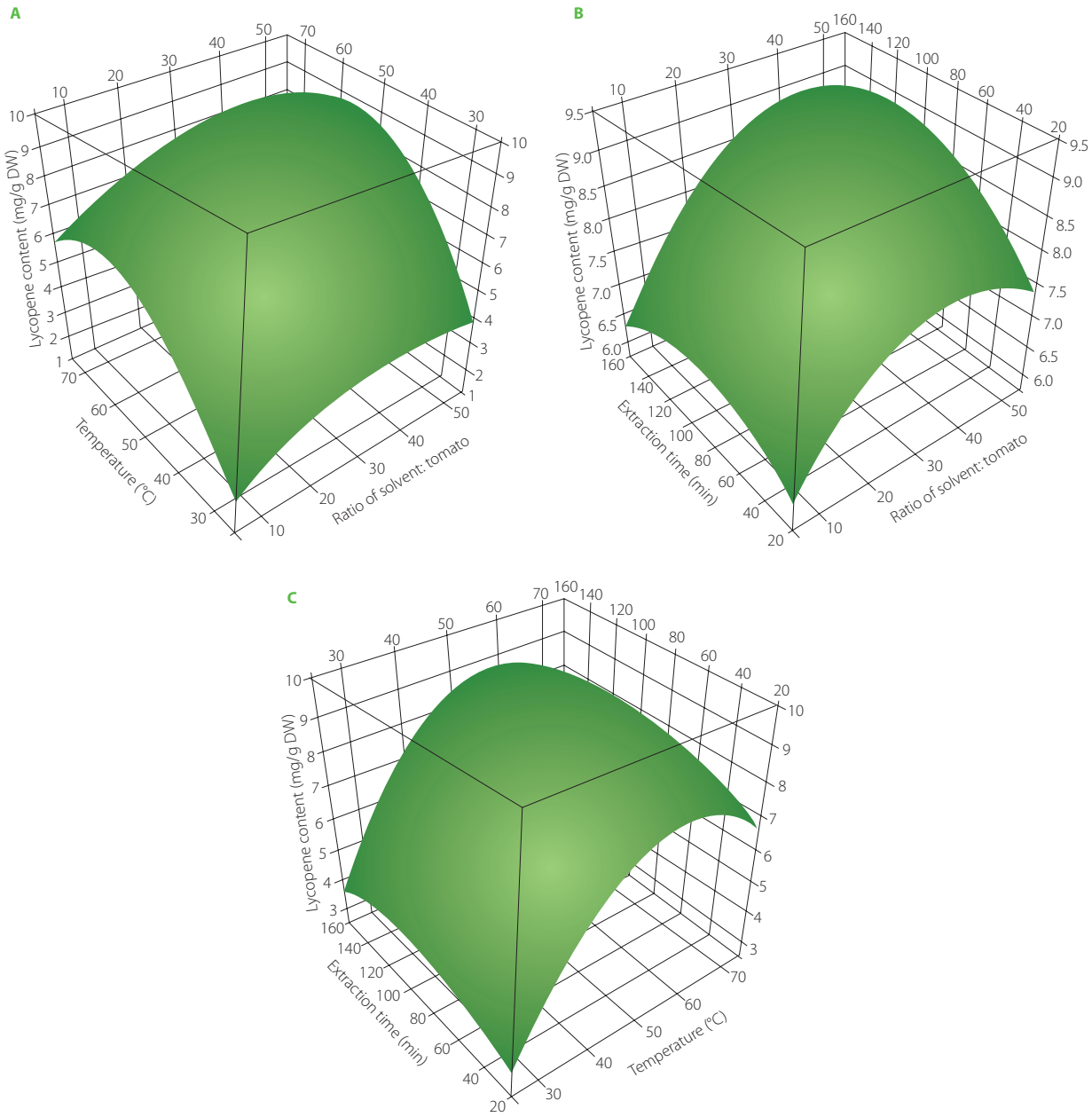

Figure 1. Three-dimensional response surface plots showing the effect of solvent to dried tomato pomace ratio *vs.* temperature (**A**), solvent to tomato dried pomace ratio *vs.* time (**B**), and temperature *vs.* time (**C**) on lycopene content.

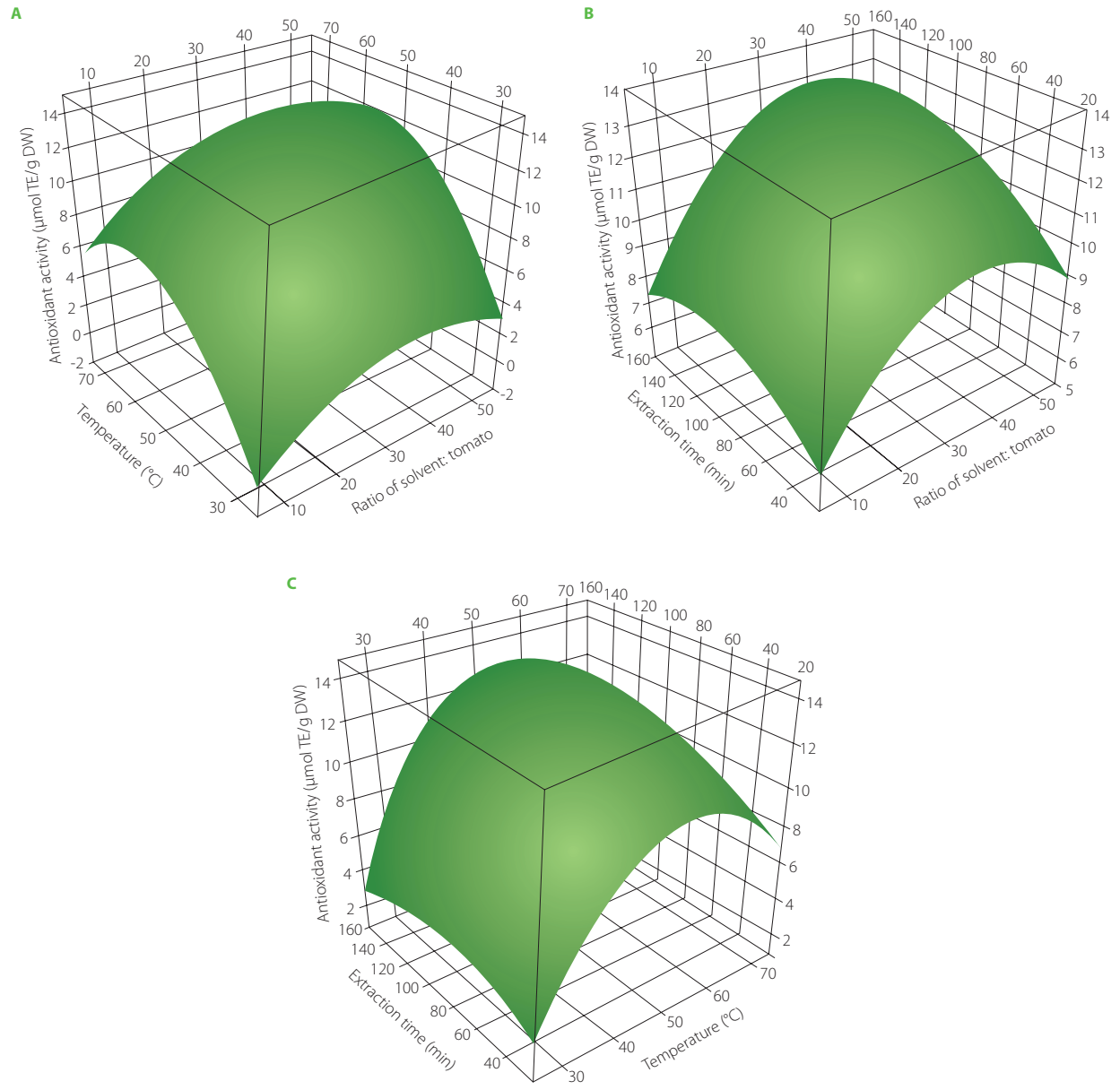

Figure 2. Three-dimensional response surface plots showing the effect of solvent to dried tomato pomace ratio *vs*. temperature (**A**), solvent to dried tomato pomace ratio *vs*. time (**B**), and temperature *vs*. time (**C**) on antioxidant activity.

a serious loss of lycopene from pink grapefruit when supercritical extraction was conducted at temperature above 74°C.

Figure 1 illustrates the graphical depiction of the global desirability function for optimising the lycopene content, while Figure 2 depicts the three-dimensional representations of the global function in the space of the distinct variables. However, these are only partial representations, as one of the three main factors was held constant at its optimal value. Their optimal areas were comparable for various extraction factor combinations, reaching 9.09 mg/g DW for lycopene content and 12.99 mol TE/g DW for antioxidant activity.

To determine the optimal values for the three main factors of the extraction process that maximise the lycopene yield and antioxidant activity, these output variables served as new variables for the desirability function to gain the global desirability score. The optimisation results indicated that the maximum lycopene content and antioxidant activity were achieved when lycopene extraction process was carried out at the ratio of ethyl acetate to tomato material of 35:1 (*v/w*), at 55°C for 100 min (Figure 3). After that, the effectiveness of the predicted regression was assessed by three replicate experiments conducted under the optimised conditions. The extraction efficiency of the samples was in line well (98.6%) with that predicted by the RSM experiments. The extract was then used to evaluate the oxidative stability of peanut oil.

Oxidative stability assessment of lycopene-enriched peanut oil during storage

Lycopene-rich powder was obtained by extraction under the optimal conditions, *i.e.*, ratio of ethyl acetate to tomato

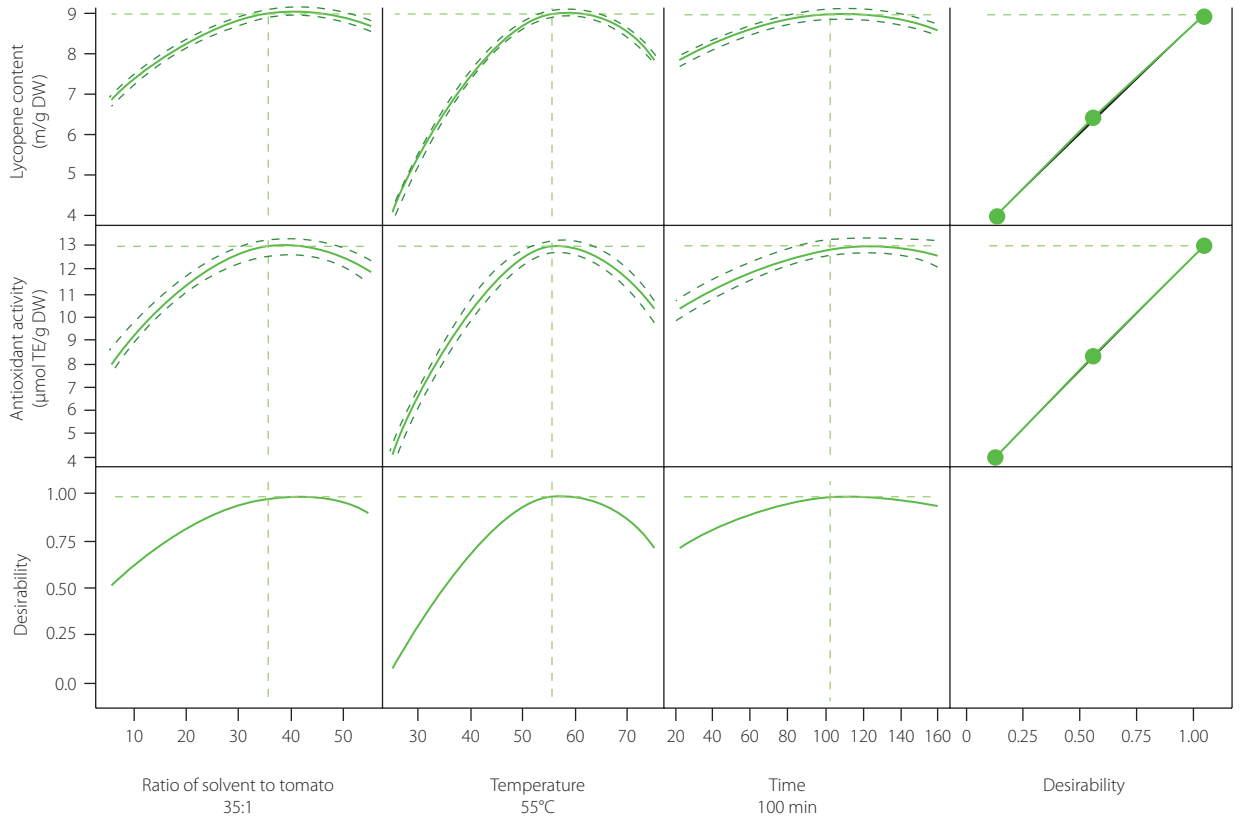

Figure 3. Profile showing the optimal extraction conditions of lycopene from dried tomato pomace. The optimal values for the extraction factors were determined by maximising the desirability function which was a combination of lycopene content and antioxidant activity.

pomace of 35:1 (*v/w*), at 55°C for 100 min, followed by solvent evaporation prior to its addition to the peanut oil. The dried extract had the lycopene content and antioxidant activity of 0.89 g/g, and 0.82 mmol TE/g respectively. The oxidative stability of the untreated and antioxidant-enriched oils is presented in Table 3. During storage, the oxidative indexes, including PV, p-AV, and TOTOX, increased in all treatments. The oil oxidation process is proportional to the storage time. However, within one storage time point, there were variations in oxidation for the different treatments. Specifically, the untreated oil (control

Table 3. Quality indexes of peanut oil without (control) and with the extract from dried tomato pomace during storage at 40°C.

Quality index	Oil sample	Storage time (day)					
		0	14	28	32	46	60
Peroxide value (meq O_2/kg)	Control	3.58±0.12	6.38±0.13^a	8.63±0.30^a	11.05±0.52^a	13.06±0.46^a	16.29±0.20^a
	BHT	3.58±0.12	5.01±0.19^b	7.32±0.21^b	8.50±0.30^b	9.23±0.45^b	9.76±0.12^b
	L_1	3.58±0.12	4.88±0.11^b	7.15±0.18^c	8.62±0.34^b	9.32±0.16^b	9.83±0.21^b
	L_2	3.58±0.12	3.74±0.18^c	4.52±0.49^d	5.02±0.26^c	6.96±0.20^c	8.55±0.23^c
p-Anisidine value	Control	1.52±0.05	1.81±0.03^a	2.52±0.03^a	2.77±0.05^a	3.08±0.04^a	3.67±0.04^a
	BHT	1.52±0.05	1.61±0.05^b	1.85±0.04^b	1.96±0.03^b	2.22±0.04^b	2.55±0.01^b
	L_1	1.52±0.05	1.59±0.05^b	1.89±0.06^b	1.93±0.03^b	2.25±0.04^b	2.39±0.04^c
	L_2	1.52±0.06	1.54±0.03^b	1.58±0.04^c	1.64±0.02^c	1.88±0.06^c	2.02±0.05^d
TOTOX	Control	8.68±0.26	14.57±0.04^a	19.78±0.03^a	24.87±0.06^a	29.19±0.06^a	36.24±0.06^a
	BHT	8.68±0.26	11.64±0.08^b	16.50±0.15^b	18.96±0.16^b	20.68±0.15^b	22.08±0.15^b
	L_1	8.68±0.26	11.35±0.07^b	16.19±0.01^b	19.18±0.10^b	20.89±0.14^b	22.14±0.14^b
	L_2	8.68±0.26	8.96±0.03^c	10.62±0.05^c	11.68±0.12^c	15.80±0.05^c	19.12±0.11^c

Data values are accompanied by standard deviation of the mean with n=3. Within a column, separately for each index, results with the same letter were not significantly different ($p \geq 0.05$). TOTOX, total oxidation; BHT, peanut oil with butylated hydroxytoluene addition of 50 mg/kg oil; L_1, peanut oil with extract addition of 1 g/kg oil; L_2, peanut oil with extract addition of 2 g/kg oil.

sample) always had the highest PVs while the peanut oil with 2 g extract/kg oil had the lowest levels during 60 days of storage. There were no significant differences ($p \geq 0.05$) in PVs between the oils with 50 mg BHT/kg oil and those with 1 g extract/kg oil on days 14, 32, 46, and 60, except for day 28 when the extract added peanut oil had a significantly lower PV than BHT added peanut oil. Low PVs in the extract-enriched oil indicate the effective antioxidant activity of lycopene in retarding primary oxidation to form peroxide compounds. According to the Codex Alimentarius standard 210-1999 [CODEX STAN, 2015], PV for cold-pressed and virgin oils is allowed up to 15 meq O_2/kg oil. Therefore, after 60 days of storage, peanut oils with BHT or lycopene-rich extract of 1 g/kg oil and 2 g/kg oil were still acceptable, as their PVs were 9.76, 9.83, and 8.55 meq O_2/kg respectively. The untreated oil with PV of 16.29 meq O_2/kg exceeded the threshold value. Data obtained in the current research are consistent with those published by Omer *et al.* [2014] in which lycopene-rich extract at the concentration of 1,000 ppm was proved to retard lipid oxidation in the refined sunflower oil. Li *et al.* [2011] also demonstrated the positive effect of lycopene at the concentration of 0.01% on oxidative stability of soybean oil as determined by measuring the peroxide value and acid value.

The p-AV generally shows the magnitude of aldehydic secondary oxidation products thus, it is an indicator of the freshness of vegetable oil. Results showed that at every storage time, the p-AVs of the control sample were significantly ($p<0.05$) higher compared to those of the oils with synthetic antioxidant (BHT) or extract addition (Table 3). The p-AVs of the BHT-added oil were statistically different ($p<0.05$) from those with 1 g extract/kg oil at the end of storage time. The oil with 2 g extract/kg oil had the lowest oxidation level and its p-AVs reached 2.02 after 60 days of storage. The p-AV of peanut oil with the addition of lycopene-rich extract analysed in the current study was higher than that of linseed oil with 80 mg lycopene extract/kg oil whose value only reached 0.23 [Condori *et al.*, 2020]. Zahran & Najafi [2020] reported the positive effect of olive leaves extract at concentrations of 1,000 and 1,500 ppm on reducing the p-AV in refined soybean oil; however, its value was much higher than that in our study, reaching 23.0 after 21 days of storage at 60°C. The variation in p-AVs could be due to differences in antioxidant activity of the extracts, oil properties, and storage conditions.

TOTOX, an indicator of the oxidative state of the oil, was calculated from the PV and p-AV, therefore its changes follow a similar trend to PV and p-AV. The untreated oil had the highest oxidation level with the TOTOX value increasing from 8.68 on day 0 to 36.24 on day 60. While the peanut oil stabilized with 2 g extract/kg oil had the smallest value of 19.12 on day 60. This was a similar level to the control sample on day 28, indicating it was the most stable, followed by the oils with 50 mg BHT/kg and with 1 g extract/kg oil. Our findings were consistent with the study by Chong *et al.* [2015], which indicated that 200 ppm mangosteen peel extracts exhibited superior reduction in the TOTOX value in sunflower oil compared to 200 ppm BHT after 24 d of storage at 65°C.

CONCLUSIONS

The results clearly demonstrated the effect of the ratio of ethyl acetate to tomato waste, extraction temperature, and time of extraction on the lycopene content and antioxidant activity of the extract. By using response surface methodology, it was possible to identify the optimal extraction condition for lycopene from tomato dried pomace. This was estimated to be the ratio of solvent to tomato waste material of 35:1 (*v/w*), at 55°C for 100 min. Addition of 2 g extract/kg oil to the peanut oil significantly enhanced its oxidative stability. Incorporation of lycopene from tomato by-products may extend the shelf-life and improve the acceptability and valorisation of edible oils.

ACKNOWLEDGEMENTS

The authors are grateful to the staff and students of the Faculty of Food Science and Technology, Vietnam National University of Agriculture for their kind assistance.

RESEARCH FUNDING

This research is funded by Vietnam National Foundation for Science and Technology Development (NAFOSTED) under Grant Number FWO.106-NN.2017.01.

CONFLICT OF INTERESTS

The authors declare that they have no conflict of interest or competing interests.

ORCID IDs

M.L.A.T.M. Hertog http://orcid.org/0000-0002-3840-5746
C.N. Nguyen https://orcid.org/0009-0003-7102-3410
L.T.H. Nguyen https://orcid.org/0000-0001-8126-7767
B. Nicolaï http://orcid.org/0000-0001-5267-1920
D.T. Tran https://orcid.org/0000-0002-3432-6557

REFERENCES

1. Al-Wandawi, H., Abdul-Rahman, M., Al-Shaikhly, K. (1985). Tomato processing wastes as essential raw materials source. *Journal of Agricultural and Food Chemistry*, *33*(5), 804-807. https://doi.org/10.1021/jf00065a009
2. AOCS. (2009). In Official Methods and Recommended Practices of the American Oil Chemists Society, 5th edition. Champaign, Il, USA: AOCS Press.
3. AOCS. (2017). In Official Methods and Recommended Practices of the American Oil Chemists Society, 5th edition. Champaign, Il, USA: AOCS Press.
4. Baysal, T.A.N.E.R., Ersus, S.E.D.A., Starmans, D.A.J. (2000). Supercritical CO2 extraction of β-carotene and lycopene from tomato paste waste. *Journal of Agricultural and Food Chemistry, 48*(11), 5507-5511. https://doi.org/10.1021/jf000311t
5. Bodoira, R.M., Penci, M.C., Ribotta, P.D., Martínez, M.L. (2017). Chia (*Salvia hispanica* L.) oil stability: Study of the effect of natural antioxidants. *LWT – Food Science and Technology*, *75*, 107-113. https://doi.org/10.1016/j.lwt.2016.08.031
6. Calvo, M.M., Dado, D., Santa-María, G. (2007). Influence of extraction with ethanol or ethyl acetate on the yield of lycopene, β-carotene, phytoene and phytofluene from tomato peel powder. *European Food Research and Technology*, *224*, 567-571. https://doi.org/10.1007/s00217-006-0335-8
7. Castro, T.A., Leite, B.S., Assunção, L.S., de Jesus Freitas, T., Colauto, N.B., Linde, G.A., Otero, D.M., Machado, B.A.S., Ribeiro, C.D.F. (2021). Red tomato products as an alternative to reduce synthetic dyes in the food industry: A review. *Molecules*, *26*(23), art. no. 7125. https://doi.org/10.3390/molecules26237125
8. Cheng, J., Miller, B., Balbuena, E., Eroglu, A. (2020). Lycopene protects against smoking-induced lung cancer by inducing base excision repair. *Antioxidants*, *9*(7), art. no. 643. https://doi.org/10.3390/antiox9070643

9. Chong, Y.M., Chang, S.K., Sia, W.C.M., Yim, H.S. (2015). Antioxidant efficacy of mangosteen (*Garcinia mangostana Linn.*) peel extracts in sunflower oil during accelerated storage. *Food Bioscience, 12*, 18-25. https://doi.org/10.1016/j.fbio.2015.07.002
10. CODEX STAN 210-1999 (amended 2015). Standard for named vegetable oil. Codex Alimentarius, Rome.
11. Condori, M.A.V., Chagman, G.J.P., Barriga-Sanchez, M., Vilchez, L.F.V., Ursetta, S., Pérez, A.G., Hidalgo, A. (2020). Effect of tomato (*Solanum lycopersicum* L.) lycopene-rich extract on the kinetics of rancidity and shelf-life of linseed (*Linum usitatissimum* L.) oil. *Food Chemistry*, *302*, art. no. 125327. https://doi.org/10.1016/j.foodchem.2019.125327
12. Dasgupta, A., Klein, K. (2014). *Antioxidants in Food, Vitamins, and Supplements: Prevention and Treatment of Disease*. 1st edition, Elsevier, Paperback ISBN: 9780128101049, eBook ISBN: 9780124059177.
13. Deng, Y., Zhao, S., Yang, X., Hou, F., Fan, L., Wang, W., Xu, E., Cheng, H., Guo, M., Liu, D. (2021). Evaluation of extraction technologies of lycopene: Hindrance of extraction, effects on isomerization and comparative analysis – A review. *Trends in Food Science & Technology*, *115*, 285-296. https://doi.org/10.1016/j.tifs.2021.06.051
14. Dhakane-Lad, J., Kar, A. (2021). Supercritical CO_2 extraction of lycopene from pink grapefruit (*Citrus paradise* Macfad) and its degradation studies during storage. *Food Chemistry, 361*, art. no. 130113. https://doi.org/10.1016/j.foodchem.2021.130113
15. Egydio, J.A., Moraes, Â.M., Rosa, P.T. (2010). Supercritical fluid extraction of lycopene from tomato juice and characterization of its antioxidation activity. *The Journal of Supercritical Fluids*, *54*(2), 159-164. https://doi.org/10.1016/j.supflu.2010.04.009
16. Eh, A.L.S., Teoh, S.G. (2012). Novel modified ultrasonication technique for the extraction of lycopene from tomatoes. *Ultrasonics Sonochemistry*, *19*(1), 151-159. https://doi.org/10.1016/j.ultsonch.2011.05.019
17. Fernández-Ruiz, V., Torrecilla, J.S., Cámara, M., Mata, M.C.S., Shoemaker, C. (2010). Radial basis network analysis of color parameters to estimate lycopene content on tomato fruits. *Talanta*, *83*(1), 9-13. https://doi.org/10.1016/j.talanta.2010.08.020
18. Fuhrman, B., Elis, A., Aviram, M. (1997). Hypocholesterolemic effect of lycopene and β-carotene is related to suppression of cholesterol synthesis and augmentation of LDL receptor activity in macrophages. *Biochemical and Biophysical Research Communications*, *233*(3), 658-662. https://doi.org/10.1006/bbrc.1997.6520
19. Ganje, M., Jafari, S.M., Farzaneh, V., Malekjani, N. (2018). Kinetics modelling of color deterioration during thermal processing of tomato paste with the use of response surface methodology. *Heat Mass Transfer*, *54*, 3663-3671. https://doi.org/10.1007/s00231-018-2394-3
20. Guerra, A.S., Hoyos, C.G., Molina-Ramírez, C., Velásquez-Cock, J., Vélez, L., Gañán, P., Eceiza, A., Goff, H.D., Zuluaga, R. (2021). Extraction and preservation of lycopene: A review of the advancements offered by the value chain of nanotechnology. *Trends in Food Science & Technology*, *116*, 1120-1140. https://doi.org/10.1016/j.tifs.2021.09.009
21. Kehili, M., Sayadi, S., Frikha, F., Zammel, A., Allouche, N. (2019). Optimization of lycopene extraction from tomato peels industrial by-product using maceration in refined olive oil. *Food and Bioproducts Processing*, *117*, 321-328. https://doi.org/10.1016/j.fbp.2019.08.004
22. Kimura, M., Kobori, C.N., Rodriguez-Amaya, D.B., Nestel, P. (2007). Screening and HPLC methods for carotenoids in sweet potato, cassava and maize for plant breeding trials. *Food Chemistry*, *100*(4), 1734-1746. https://doi.org/10.1016/j.foodchem.2005.10.020
23. Kumcuoglu, S., Yilmaz, T., Tavman, S. (2014). Ultrasound assisted extraction of lycopene from tomato processing wastes. *Journal of Food Science and Technology*, *51*, 4102-4107. https://doi.org/10.1007/s13197-013-0926-x
24. Lavecchia, R., Zuorro, A. (2008). Improved lycopene extraction from tomato peels using cell-wall degrading enzymes. *European Food Research and Technology*, *228*, 153-158. https://doi.org/10.1007/s00217-008-0897-8
25. Li, X.H., Liu, C., Sun, Y.J., Du, J., Xing, Y.G., Tang, Y. (2011). Effects of lycopene on oxidative stability of soybean oil. *Advanced Materials Research*, *236-238*, 2303-2306. https://doi.org/10.4028/www.scientific.net/AMR.236-238.2303
26. Machado, M., Rodriguez-Alcalá, L.M., Gomes, A.M., Pintado, M. (2022). Vegetable oils oxidation: mechanisms, consequences, and protective strategies. *Food Reviews International*. https://doi.org/10.1080/87559129.2022.2026378
27. Martínez, M.L., Maestri, D.M. (2008). Oil chemical variation in walnut (*Juglans regia* L.) genotypes grown in Argentina. *European Journal of Lipid Science and Technology*, *110*(12), 1183-1189. https://doi.org/10.1002/ejlt.200800121
28. Martínez, M.L., Marín, M.A., Faller, C.M.S., Revol, J., Penci, M.C., Ribotta, P.D. (2012). Chia (*Salvia hispanica* L.) oil extraction: Study of processing parameters. *LWT – Food Science and Technology*, *47*(1), 78-82. https://doi.org/10.1016/j.lwt.2011.12.032
29. Mika, M., Antończyk, A., Wikiera, A. (2023). Influence of synthetic antioxidants used in food technology on the bioavailability and metabolism of lipids - *in vitro* studies. *Polish Journal of Food and Nutrition Sciences*, *73*(1), 95-107. https://doi.org/10.31883/pjfns/161366
30. Mohammadi, M., Hajeb, P., Seyyedian, R., Hossein Mohebbi, G., Barmak, A. (2013). Evaluation of oxidative quality parameters in imported edible oils in Iran. *British Food Journal, 115*(6), 789-795. https://doi.org/10.1108/BFJ-Feb-2011-0035
31. Montesano, D., Fallarino, F., Cossignani, L., Bosi, A., Simonetti, M.S., Puccetti, P., Damiani, P. (2008). Innovative extraction procedure for obtaining high pure lycopene from tomato. *European Food Research and Technology*, *226*, 327-335. https://doi.org/10.1007/s00217-006-0541-4
32. Omer, E., Thapa, M., Hong, L., Lianfu, Z. (2014). The influence of lycopene and other natural antioxidants on refined sunflower oil stability. *International Journal of Engineering Research and Technology*, *3*(3), 86-91.
33. Pandya D.P, Akbari, S.H, Bhatt, H.G, Joshi, D.C., Darji, V.B. (2015). Identification of suitable solvent system for efficient extraction of lycopene from tomato pomace. *Journal of Food Research*, 3(2), 83-86.
34. Przybylska, S. (2020). Lycopene – a bioactive carotenoid offering multiple health benefits: a review. *International Journal of Food Science & Technology*, *55*(1), 11-32. https://doi.org/10.1111/ijfs.14260
35. Shahidi, F., Wanasundara, U.N. (2017). Chapter 19: Methods for measuring oxidative rancidity in fats and oils, In C. Akoh, D.B. Min (Eds.). *Food Lipids: Chemistry, Nutrition, and Biotechnology*, 4th edition, CRC Press, pp. 519-539.
36. Shi, J., Maguer, M.L. (2000). Lycopene in tomatoes: Chemical and physical properties affected by food processing. *Critical Reviews in Food Science and Nutrition*, *40*(1), 1-42. https://doi.org/10.1080/10408690091189275
37. Silva, Y.P.A., Ferreira, T.A.P.C., Jiao, G., Brooks, M.S. (2019). Sustainable approach for lycopene extraction from tomato processing by-product using hydrophobic eutectic solvents. *Journal of Food Science and Technology*, *56*, 1649-1654. https://doi.org/10.1007/s13197-019-03618-8
38. Stahl, W., Sies, H. (1996). Lycopene: a biologically important carotenoid for humans? *Archives of Biochemistry and Biophysics*, *336*(1), 1-9. https://doi.org/10.1006/abbi.1996.0525
39. Sumalan, R.M., Ciulca, S.I., Poiana, M.A., Moigradean, D., Radulov, I., Negrea, M., Crisan, M.E., Copolovici, L., Sumalan, R.L. (2020). The antioxidant profile evaluation of some tomato landraces with soil salinity tolerance correlated with high nutraceutical and functional value. *Agronomy*, *10*(4), art. no. 500. https://doi.org/10.3390/agronomy10040500
40. Taoukis, D., Assimakopoulos, J. (2010). Effect of growth season and slow--release fertilizers on quality characteristics of tomatoes. *Communications in Soil Science and Plant Analysis*, *41*(8), 945-955. https://doi.org/10.1080/00103621003646030
41. Toor, R.K., Savage, G.P. (2005). Antioxidant activity in different fractions of tomatoes. *Food Research International*, *38*(5), 487-494. https://doi.org/10.1016/j.foodres.2004.10.016
42. Topal, U., Sasaki, M., Goto, M., Hayakawa, K. (2006). Extraction of lycopene from tomato skin with supercritical carbon dioxide: effect of operating conditions and solubility analysis. *Journal of Agricultural and Food Chemistry*, *54*(15), 5604-5610. https://doi.org/10.1021/jf0606407
43. Tran, D.T., Hertog, M., Nicolaï, B.M. (2016). Hierarchical response surface methodology for optimization of postharvest treatments to maintain quality of litchi cv. 'Thieu'during cold storage. *Postharvest Biology and Technology*, *117*, 94-101. https://doi.org/10.1016/j.postharvbio.2016.01.006
44. Willcox, J.K., Catignani, G.L., Lazarus, S. (2003). Tomatoes and cardiovascular health. *Critical Reviews in Food Science and Nutrition*, *43*(1), 1-18. https://doi.org/10.1080/10408690390826437
45. Xie, C., Ma, Z.F., Li, F., Zhang, H., Kong, L., Yang, Z., Xie, W. (2018). Storage quality of walnut oil containing lycopene during accelerated oxidation. *Journal of Food Science and Technology*, *55*, 1387-1395. https://doi.org/10.1007/s13197-018-3053-x
46. Young, A.J., Lowe, G.M. (2001). Antioxidant and prooxidant properties of carotenoids. *Archives of Biochemistry and Biophysics*, *385*(1), 20-27. https://doi.org/10.1006/abbi.2000.2149
47. Zahran, H., Najafi, Z. (2020). Enhanced stability of refined soybean oil enriched with phenolic compounds of olive leaves. *Egyptian Journal of Chemistry*, *63*(1), 215-224. https://doi.org/10.21608/ejchem.2019.16592.2010
48. Zhang, X.J., Diao, M., Zhang, Y.F. (2023). A review of the occurrence, metabolites and health risks of butylated hydroxyanisole (BHA). *Journal of the Science of Food and Agriculture*, https://doi.org/10.1002/jsfa.12676

ORIGINAL ARTICLE
http://journal.pan.olsztyn.pl

Polish Journal of Food and Nutrition Sciences
2023, Vol. 73, No. 3, 214–223
DOI: 10.31883/pjfns/168709
ISSN 1230-0322, e-ISSN 2083-6007

Is it Possible to Produce Carrier-Free Fruit and Vegetable Powders by Spray Drying?

Alicja Barańska*, Aleksandra Jedlińska, Katarzyna Samborska

Department of Food Engineering and Process Management, Institute of Food Sciences, Warsaw University of Life Sciences (WULS-SGGW), Nowoursynowska 159C str., 00-776 Warsaw, Poland

The application of low-temperature, dehumidified air-assisted spray drying was evaluated as a method to produce carrier-free powders of selected sugar-rich and acid-rich food materials: blackcurrant juice concentrate, mango puree, purple carrot juice concentrate, sauerkraut juice, kiwiberry pulp, and tomato pulp. As a consequence of decreased drying air humidity, inlet/outlet air temperature was lowered to 80/55°C. In order to validate this new approach, the conventional spray drying was conducted as well at 180/80°C inlet/outlet air temperature. The powder recovery, physical properties and color parameters of powders were determined. For blackcurrant juice concentrate, mango puree, purple carrot juice concentrate and sauerkraut juice it was possible to obtain carrier-free powders only by low-temperature drying, while for kiwiberry pulp and tomato pulp both variants of spray drying were effective. Decreased drying temperature positively influenced some properties of powders; *i.e.*, median particle size diameter and hygroscopicity of the powders obtained by spray drying with dehumidified air were lower compared to those of the powders dried by conventional spray drying. Carrier-free powders of some raw materials (blackcurrant juice concentrate, mango puree, purple carrot juice concentrate, sauerkraut juice) were spray dried solely with dehumidified air, underlining its importance in the production of "clean label" products.

Key words: dehumidified air, powder recovery, clean label, glass transition, stickiness

INTRODUCTION

The most popular method to produce powder in single and quick operation is spray drying. It enables obtaining powders from aqueous solutions, suspensions or emulsions by spraying them and then evaporating the solvent from the droplets using hot air at a certain temperature and pressure. The inlet air temperature typically used in the conventional spray drying method is 160–220°C. Recently, it was presented in some published works, that the inlet air temperature can be lowered to even 75°C while reducing the humidity of the drying air [Samborska *et al.*, 2020, 2021]. The reduction of air humidity increases the driving force of water evaporation and makes it possible to remove water at lower temperature. Such modification increases the opportunities of spray drying application for some materials of special requirements, *i.e.*, sugar-rich and acid-rich materials, including fruit juices/concentrates/pulps or honey, characterized by low glass transition temperature (T_g) [Muzaffar *et al.*, 2015]. The problem of drying sugar-rich materials is explained by the concept of T_g. According to this theory: 1) the product shows the greatest stability at T_g and below it, 2) there is a reduction in the stability of the food above T_g; the stability decreases with the increasing temperature difference between the temperature reached by the material during drying and its T_g [Champion *et al.*, 2000]. At the same time, the material in the glass amorphous state can easily change into a rubbery amorphous state, when temperature

***Corresponding Author:**
e-mail: alicja_baranska@sggw.edu.pl (A. Barańska)

Submitted: 18 March 2023
Accepted: 20 June 2023
Published on-line: 11 July 2023

increases over the material's T_g. The rubbery amorphous state is unacceptable in spray drying – rubber sticks to the drying chamber, reduces the efficiency of the process, or even makes it impossible to obtain free-flowing powder [Barańska *et al*., 2021; Truong *et al*., 2005]. It is impossible to obtain the powder at the outlet temperature 20°C higher than T_g of the dried material [Shrestha *et al*., 2007], which is why it is crucial to apply dehumidified air to reduce drying temperature. Carriers' addition can be considered as a drawback of spray drying, the application of dehumidified air affords the possibility to reduce the carrier content, which is added to increase material T_g. Typically, the powder obtained by conventional spray drying contains about 50% of carriers in solids, while dehumidified air application and low-temperature spray drying enables decreasing the carrier content even down to 10–25% [Barańska *et al*., 2021; Samborska *et al*., 2020, 2022]. Thus, the powder obtained by low-temperature spray drying with dehumidified air can be classified as "more natural", similar in chemical composition to raw material. In our previous study, white mulberry molasses was spray dried using dehumidified air to lower drying temperature and successfully obtain a product with a carrier (nutriose) content reduced to 10% [Samborska *et al*., 2022]. In addition, buckwheat honey powder was produced using the same technique with a low content (25%) of the carrier (skim milk powder or maltodextrin) [Barańska *et al*., 2021]. So far, few studies have been published on spray drying of carrier-free powders including carrier-free powders from kiwiberry fruit pulp, durian pulp, tomato pulp, mango pulp and juçara pulp [Chin *et al*., 2008; Goula *et al*., 2004; Jedlińska *et al*., 2022; Pereira *et al*., 2020; Zotarelli *et al*., 2017]. Nowadays, consumers have greater nutritional knowledge and are looking for products with a short list of ingredients, without the additives [Asioli *et al*., 2017]. Despite the interest in producing "clean label" products, very few materials were taken into consideration while producing carrier-free powders. Thus, in this context, it seems crucial to take up the challenge of producing powders of different materials with no additional carriers, which would have satisfactory physiochemical properties.

The aim of the present study was to investigate the possibility of producing carrier-free powders of different fruit/vegetable juice/pulp/concentrate using dehumidified air-assisted spray drying and determine powder recovery and selected physical properties of the produced powders. In the case of materials for which conventional high-temperature spray-drying was possible, the physicochemical properties of the carrier-free powders obtained with both methods were compared.

MATERIALS AND METHODS

Materials

Juices and pulps were bought from the market: purple carrot juice concentrate (Maspex, Wadowice, Poland), mango puree (Purena, Złoty Potok, Poland), blackcurrant juice concentrate (Maspex, Wadowice, Poland), tomato pulp (EkoWital, Warszawa, Poland), and sauerkraut juice (Słoneczne Pole, Kalisz, Poland). Sauerkraut juice was concentrated to 27.2°Bx using a Rotavapor R-124 evaporator (BUCHI, Flawil, Switzerland). Kiwiberry (mini kiwi) pulp was prepared from the whole fruits of Weiki variety (Poland) using an NS-621CES squeezer (Kuvings, Buk-gu, Korea).

Spray drying of materials

A mobile minor laboratory spray dryer (GEA, Søborg, Denmark) was used to obtain powders of blackcurrant juice concentrate (BC), mango puree (M), purple carrot juice concentrate (PC), sauerkraut juice (S), kiwiberry pulp (KB), and tomato pulp (T). Conventional spray drying (SD) and dehumidified air-assisted spray drying (DASD) were carried out, and the variants of the produced powders are listed in Table 1. Every drying was performed in duplicate and liquid feed of 500 g was supplied each time. The parameters of the spray drying process were as follows: rotation speed 26,000 rpm; liquid feed speed 0.25 mL/s; inlet/outlet temperature 180/80°C for SD, 80/55°C for DASD; humidity of drying air during DASD <0.5 g/m^3. To conduct DASD, the spray dryer was equipped with an air dehumidification system including a TAEevo TECH020 cooling unit (MTA, Codogno, Italy) and an ML270 concentration-adsorption unit (MUNTERS, Kista, Sweden). Powder recovery (R_p) was calculated as the ratio of solids content in the obtained powder to the amount of solids in the liquid feed. Powders were put into PET/PE sealed bags and stored at a temperature of 4°C in the dark until analyzed. Analyses were done 24 h after each drying.

Table 1. Variants of powders produced using conventional spray drying (SD) and dehumidified air-assisted spray drying (DASD).

Raw material	Variant	Spray drying method	Drying air temperature (inlet/outlet)
Blackcurrant juice concentrate	BC/DASD	DASD	80/55°C
Mango puree	M/DASD	DASD	80/55°C
Purple carrot juice concentrate	PC/DASD	DASD	80/55°C
Sauerkraut juice	S/DASD	DASD	80/55°C
Kiwiberry pulp	KB/DASD	DASD	80/55°C
Kiwiberry pulp	KB/SD	SD	180/80°C
Tomato pulp	T/DASD	DASD	80/55°C
Tomato pulp	T/SD	SD	180/80°C

Particle morphology analysis

Particle morphology of the powders was analyzed using an XL Phenom World scanning electron microscope (SEM) (Thermo Fisher Scientific, Waltham, MA, USA) at 1,000× magnification (voltage 5 kV). Samples were prepared by placing a small amount of powder on the double sticky tape, removing the excess of the powder with compressed air, and sputtering the surface with a layer of gold by an Cressington 108auto automatic coater (EO Elektronen-Optik-Service GmbH, Dortmund, Germany).

Particle size determination

Powder particle size was determined with the laser light diffraction method conducted using a CILAS 1190 apparatus (Cilas, Orléans, France). The powder was suspended in ethanol at 10% obscuration. The results were presented as particle size distribution and cumulative particle size distribution curves, and as a median diameter (D_{50}) derived by Size Expert software (Cilas).

Moisture content and water activity measurement

Moisture content (MC) was determined using the oven method, where 1 g of powder was dried at 104°C for 4 h [Janiszewska, 2014]. Water activity (a_w) was analyzed by means of a Hygro Lab1 apparatus (Rotronic, Bassersdorf, Switzerland) at 25±1°C.

Hygroscopicity analysis

The aliquot of 1 g of each powder was incubated at 25°C and 75% relative humidity (over saturated NaCl solution) for 168 h. The hygroscopicity (H) was calculated as the amount of water absorbed per 100 g of powder solids and expressed in percentage [Samborska *et al*., 2020].

Bulk density and flowability analysis

A cylinder (25 mL) was filled with powder and weighed to determine loose bulk density (D_L). Tapped density (D_T) was determined after 100 taps by using a STAV 2003 automatic volumeter (Engelsmann AG, Ludwigshafen am Rhein, Germany). The Hausner ratio (HR) calculated according to Equation (1) was employed to express flowability [Barańska *et al*., 2021].

$$HR = D_L/D_T \quad (1)$$

Water solubility index determination

Water solubility index (WSI) was analyzed as described by Jafari *et al*. [2017] with some minor modifications. An aliquot of 2 g (m_0) of the sample (of known solids content, *DB*) was suspended in 30 mL of distilled water at ambient temperature in a centrifuge tube. The suspension was mixed for 1 min on a vortex mixer and then placed in a water bath at 37°C for 30 min. The suspension was centrifuged for 20 min at 2,054×*g* at ambient temperature. Supernatant (15 mL) was placed into a Petri dish of known weight and dried at 105°C for 24 h. The final mass of the residue (m_1) was recorded. WSI was calculated according to Equation (2):

$$WSI = \frac{m_1}{\frac{m_0}{2} \times DB} \times 100 \quad (2)$$

Color measurement

Color of the powders was measured using a CR-5 colorimeter (Konica-Minolta, Tokyo, Japan) in the CIELab color space. Lightness (L^*), the contribution of red and green color (a^*), and the contribution of yellow and blue color (b^*) were evaluated.

Statistical methods

The results were shown as mean values with standard deviation. The analysis of variance (ANOVA) and Tukey test were performed (α=0.05) to identify the significant differences between the mean values. The Pearson correlation coefficient was determined to examine the correlations between powder parameters. Hierarchical cluster analysis (HCA) was employed to plot a dendrogram graph showing the similarities between the variants of spray dried powders. The statistical analysis was conducted using STATISTICA 13.3 software (Statsoft, Tulsa, OK, USA). All analyses were done in triplicate.

RESULTS AND DISCUSSION

Powder recovery

All of the powders were successfully obtained using dehumidified air as a drying medium. Their appearance immediately after drying is presented in Figure 1. It should be underlined that only two powders from kiwiberry and tomato pulps could be produced at high drying temperature without any carrier (KB/SD, T/SD, respectively). This result corroborates the viability of dehumidified air as a drying medium in the production of "clean label" powders.

Powder recovery (R_p) determined for all drying variants is presented in Table 2. Laboratory and pilot scale spray drying is deemed successful when R_p exceeds 50%, while at the industrial scale its R_p should be higher than 60% to consider it as satisfactory [Bhandari *et al*., 1997; Wang *et al*., 2011]. Accordingly, the R_p of PC/DASD and BC/DASD can be classified as acceptable. However, the fact that other carrier-free powders could be produced even at low R_p, is an important progress in spray drying development of difficult sugar-rich materials. Only few studies have been published so far on spray drying of carrier-free powders. In our previous research, significantly higher R_p was determined for dried kiwiberry pulp, ranging from 75% to 93% [Jedlińska, *et al*., 2022]; however, it should be underlined that kiwiberry pulps were dried at different temperatures in both studies. Pereira *et al*. [2020] reported R_p of 66% of juçara pulp powder spray dried without a carrier. It should be emphasized that these authors determined the highest values for the powders produced with the highest carrier content (35%). In this research, a highly acceptable result (60.9%) was noted for purple carrot juice concentrate powder (PC/DASD) with no additional carrier, as a result of decreased drying temperature and stickiness, possibly due to the application of dehumidified air. Dehumidified air-assisted spray drying has also been recently applied for honey [Matwijczuk *et al*., 2022] and sour cherry juice concentrate [Barańska *et al*., 2023]. For this type of materials, it also showed significant improvement in carrier content reduction (from 50% to 30% solids) but not its complete elimination.

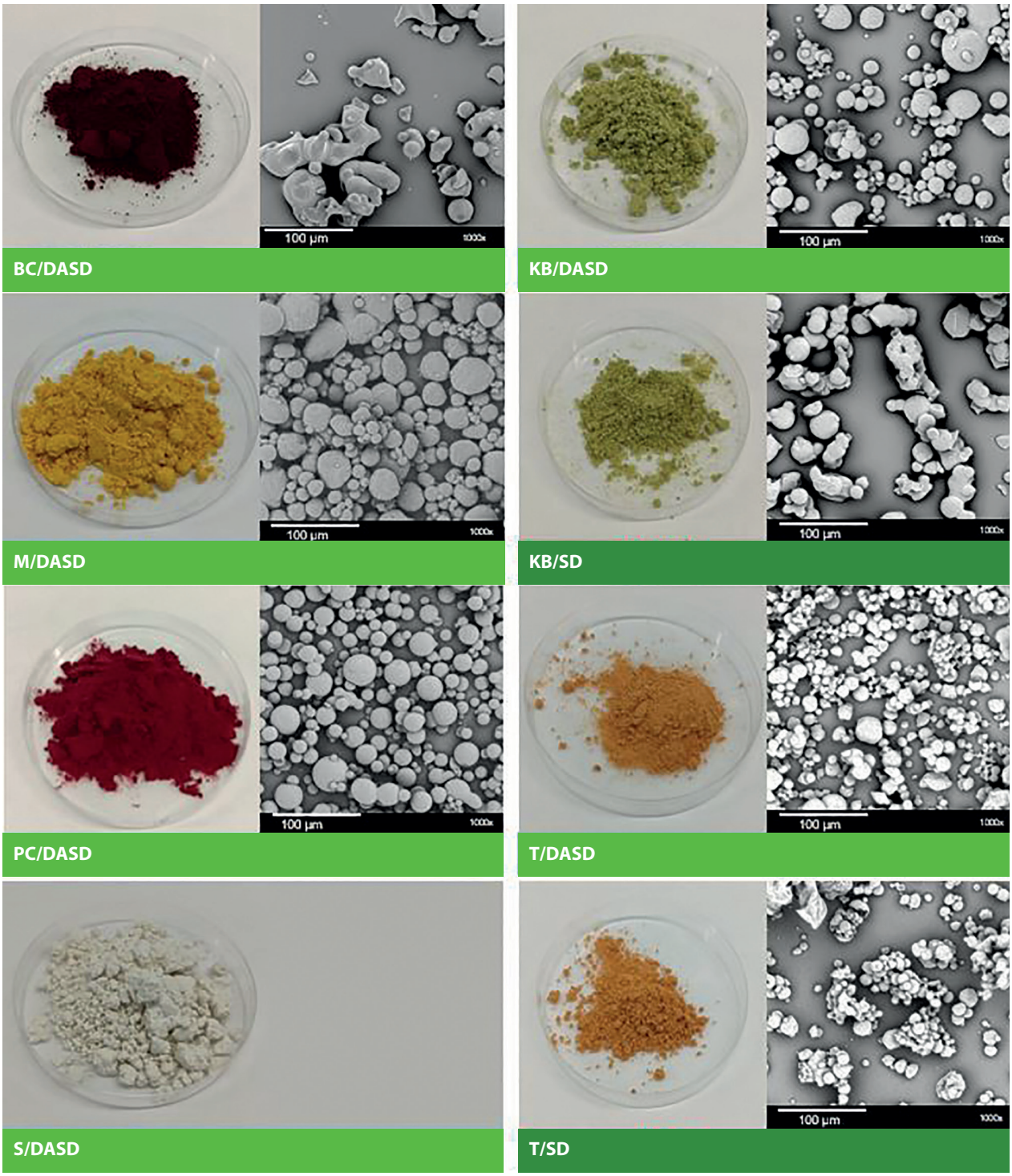

Figure 1. Carrier-free powders produced by conventional high-temperature spray drying (SD) and/or with the application of dehumidified air at low temperature (DASD) from blackcurrant juice concentrate (BC), mango puree (M), purple carrot juice concentrate (PC), sauerkraut juice (S), kiwiberry pulp (KB), and tomato pulp (T), as well as their scanning electron microscope (SEM) microphotographs (mag. 1,000×).

Kiwiberry and tomato pulps were the only materials that could be successfully dried also at higher temperature. It could result from their composition – high contents of pectin and dietary fiber that act as natural carriers [Baranowska-Wójcik & Szwajgier, 2019; Del Valle *et al*., 2006; Jedlińska *et al*., 2022]. Moreover, kiwiberry contains sucrose as a major sugar, which presents higher T_g (62°C than fructose (5°C) or glucose (31°C)) [Bhandari *et al*., 1997; Latocha, 2015]. These factors were probably responsible for obtaining carrier-free powders of only these two variants in the case of spray drying at high temperature. For kiwiberry pulp, the R_p of the variant spray dried with dehumidified air was significantly ($p<0.05$) higher than R_p obtained upon conventional drying (Table 2).

Sauerkraut juice powder (S/DASD) was the only sample that could not be further analyzed, as it turned into rubbery state after few minutes at ambient temperature without any

Table 2. Powder recovery (R_p), median diameter (D_{50}), moisture content (MC), water activity (a_w), hygroscopicity (H), loose bulk density (D_L), tapped bulk density (D_T), flowability (HR), and water solubility index (WSI) of carrier-free powders produced by conventional high temperature spray drying (SD) and/or with the application of dehumidified air at low temperature (DASD).

	BC/DASD	M/DASD	PC/DASD	S/DASD	KB/DASD	KB/SD	T/DASD	T/SD
R_p (%)	73.7±6.7^{a}	41.7±4.7^{bc}	60.9±1.7^{a}	31.7±0.5^{cde}	41.7±0.7^{b}	28.1±4.5^{de}	23.9±0.5^{e}	23.8±1.9^{e}
D_{50} (µm)	68.0±1.3^{a}	23.7±1.3^{d}	22.5±2.3^{d}	-	29.2±4.9^{c}	36.9±4.0^{b}	14.9±2.7^{e}	19.3±1.7^{de}
MC (g/100 g)	14.5±1.7^{b}	5.3±0.3^{c}	13.6±0.3^{b}	-	6.1±0.5^{c}	3.8±0.2^{d}	16.0±1.4^{a}	12.9±1.3^{b}
a_w	0.135±0.002^{c}	0.161±0.008^{b}	0.155±0.004^{b}	-	0.123±0.004^{d}	0.098±0.003^{e}	0.196±0.002^{a}	0.074±0.002^{f}
H (%)	35.9±0.4^{b}	27.3±0.4^{d}	33.7±0.3^{c}	-	25.1±0.6^{f}	26.1±0.9^{e}	36.3±0.5^{b}	37.9±0.2^{a}
D_L (g/mL)	0.62±0.01^{a}	0.61±0.03^{a}	0.52±0.01^{b}	-	0.42±0.01^{c}	0.54±0.02^{b}	0.42±0.01^{c}	0.43±0.02^{c}
D_T (g/mL)	0.78±0.03^{ab}	0.82±0.02^{a}	0.67±0.01^{c}	-	0.64±0.03^{c}	0.76±0.02^{b}	0.54±0.01^{d}	0.63±0.02^{c}
HR (-)	1.21±0.04^{d}	1.34±0.06^{bc}	1.32±0.04^{bc}	-	1.43±0.09^{ab}	1.41±0.04^{ab}	1.29±0.05^{cd}	1.47±0.06^{a}
WSI (%)	92.3±3.3^{a}	95.5±2.1^{a}	92.4±2.1^{a}	-	71.5±2.5^{c}	69.2±2.9^{c}	55.1±2.5^{d}	83.8±4.6^{b}

The differences between values with the same letter (a–f) in rows were statistically not significant ($p \geq 0.05$). BC/DASD, DASD dried blackcurrant juice concentrate; M/DASD, DASD dried mango puree; PC/DASD, DASD dried purple carrot juice concentrate; S/DASD, DASD dried sauerkraut juice; KB/DASD, DASD dried kiwiberry pulp; KB/SD, SD dried kiwiberry pulp; T/DASD, DASD dried tomato pulp; T/SD, SD dried tomato pulp. S/DASD powder analysis was not possible due to the caking of powder immediately after drying.

Table 3. Pearson correlation coefficients showing a strength of correlations between physiochemical parameters and color parameters of carrier-free powders produced by conventional high temperature spray drying (SD) and/or with the application of dehumidified air at low temperature (DASD).

	a_w	D_L	D_T	HR	D_{50}	WSI	L^*	a^*	b^*	H
MC	0.158	-0.266	-0.568	-0.344	-0.045	0.002	-0.647	0.858*	-0.536	0.975*
a_w		0.093	-0.193	-0.681	-0.184	-0.160	-0.110	0.293	0.042	0.083
D_L			0.909*	-0.581	0.699	0.671	-0.311	0.065	-0.057	-0.145
D_T				-0.200	0.578	0.654	-0.013	-0.250	0.164	-0.432
HR					-0.523	-0.201	0.642	-0.525	0.442	-0.347
D_{50}						0.334	-0.526	0.019	-0.520	0.005
WSI							-0.416	0.358	-0.107	0.071
L^*									0.900*	-0.629
a^*									-0.595	0.854*
b^*										-0.474

MC, moisture content; a_w, water activity; D_L, loose bulk density; D_T, tapped bulk density; HR, flowability; D_{50}, median diameter; WSI, water solubility index; L^*, a^*, b^*, color parameters. Significant correlations ($p<0.05$) are marked with asterisk.

packaging. Such behavior of this sample was not unexpected, as sauerkraut juice has a high content of organic acids of low T_g, which poses problems with stickiness and caking [Muzaffar *et al.*, 2015; Satora *et al.*, 2021].

Particle morphology and size

SEM microphotographs of powders showing their particle morphology are presented in Figure 1. Powders had spherical, scattered particles, which is typical for powders after spray drying with no stickiness observed, or powders of low stickiness. However, some differences were noted in the morphology of the obtained carrier-free powders depending on raw material and drying approach followed. BC/DASD particles differed from the other variants – they were less spherical and formed some conglomerates with liquid bridges. It may be assumed that blackcurrant juice concentrate was more difficult to spray dry due to its possible stickiness. However, it was not manifested in low R_p, as it was the highest among all powders examined (Table 2). A bigger particle size could as well be responsible for this result, which in consequence enhanced cyclone recovery. Kiwiberry pulp and tomato pulp powders obtained at lower drying temperature (KB/DASD and T/DASD) had less conglomerated particles than the variants produced by high-temperature spray drying (KB/SD and T/SD) (Figure 1). This again confirms the positive impact of air dehumidification and the lowering of drying temperature to 80/50°C (inlet/outlet) on the reduction of stickiness during spray drying.

Figure 2 presents particle size distribution and cumulative particle size distribution curves of powders, while the median diameters (D_{50}) are reported in Table 2. Most of the powders

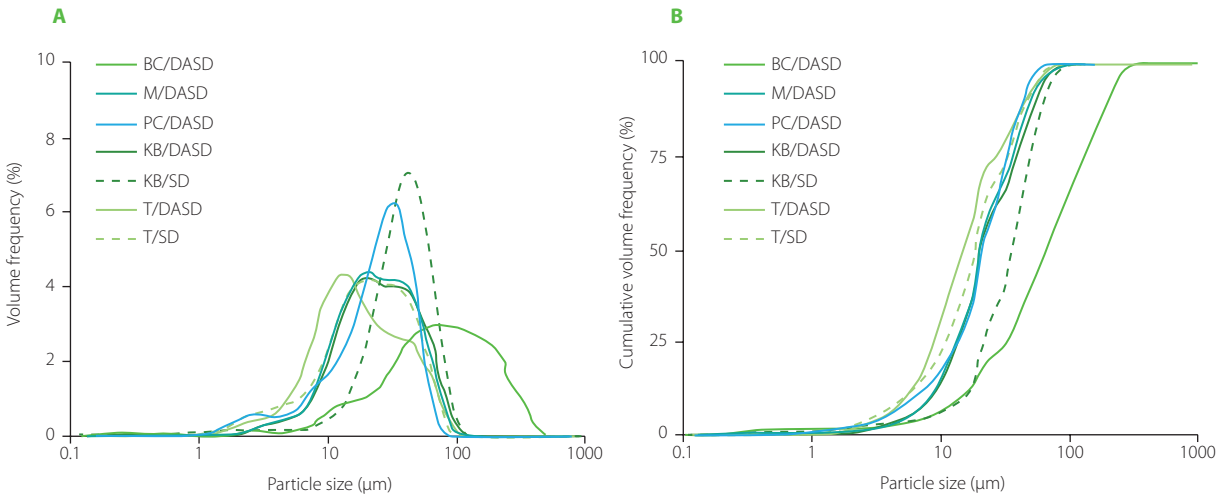

Figure 2. Particle size distribution (**A**) and cumulative particle size distribution (**B**) of carrier-free powders produced by conventional high temperature spray drying (SD) and/or with the application of dehumidified air at low temperature (DASD) fromblackcurrant juice concentrate (BC), mango puree (M), purple carrot juice concentrate (PC), sauerkraut juice (S), kiwiberry pulp (KB), and tomato pulp (T).

demonstrated bimodal and/or wide particle size distribution (Figure 2). This phenomenon indicates the presence of smaller, loose particles that can fill the spaces between bigger particles, which could be observed as well on SEM microphotographs (Figure 1). Blackcurrant juice concentrate powder (BC/DASD) had the widest particle size distribution and the highest D_{50} (Table 2). As mentioned earlier, this was the effect of stickiness during drying but was surprisingly helpful to increase R_p due to enhanced cyclone efficiency. On the contrary, KB/SD had the narrowest particle size distribution, almost no particles had diameters below 10 µm, which absence could also be observed in SEM microphotographs.

D_{50} of powder particles ranged from 14.9 to 68.0 µm (Table 2) and a significant (p<0.05) positive effect of dehumidified air application was noted for the kiwiberry pulp powders (BK/SD *vs*. BK/DASD). The effect of drying method of tomato pulp (T/SD *vs*. T/DASD) was not statistically significant (p<0.05). Zotarelli *et al*. [2017] spray dried conventionally mango puree without any carriers and noted D_{50} of 198 µm; thus, it can be concluded that dehumidified air application and decrease of drying temperature in this research affected positively the particle size of mango puree powder (M/DASD). Moreover, Jedlińska *et al*. [2022] described in their study properties of carrier-free powders produced from different varieties of kiwiberry and reported higher D_{50} values for Weiki variety powders than in the present research (111.2 and 166.8 µm, respectively). The authors produced powders at higher drying temperature (inlet 100 and 120°C); thus, the evidence from this study implies that lowering drying temperature is favorable in the case of kiwiberry pulp spray drying. Taken together, these findings confirm the role of dehumidified air in facilitating the course of drying.

Moisture content, water activity and hygroscopicity

There was a significant influence of dehumidified air application and type of material used on moisture content (MC) of the powders (Table 2). Although MC of some powders was relatively high (even above 15g /100 g), their a_w was lower than 0.2. This suggests that water was bounded structurally and hence was not available for microbial growth and biochemical reactions, which points to powder's storage stability [Shi *et al*., 2013]. Among T and KB powders, lower MC was noted for the variants spray dried conventionally (KB/SD and T/SD) – the rate of heat and mass transfer increased at higher temperature, and in consequence water evaporated more effectively. The lowest MC was reported for kiwiberry pulp spray dried at high temperature (KB/SD). These results are in contrast with earlier findings of Jedlińska *et al*. [2022], who spray dried carrier-free kiwiberry pulp, and reported much higher MC ranging from 10.3 g to 14.1 g/100 g. It may be assumed that the crust formed on the particles' surface as a result of drying at higher temperatures and made it more difficult for water to evaporate, thus the aforementioned authors obtained higher MC values. Zotarelli *et al*. [2017] spray dried mango pulp powders with no carrier and noted 1.5 g/100 g of MC, which was lower that the MC determined in our study for the carrier-free mango puree powder. However, as aforementioned, this powder variant was classified as safe and stable as its MC was below 6 g/100 g. It seems likely that differences compared to the mentioned literature data were due to different drying parameters, such as drying air temperature and humidity, and different origin of mango puree. Blackcurrant juice concentrate powder (BC/DASD) had one of the highest MC values (Table 2), probably due to a high content of glucose and fructose in this raw material [Stój & Targoński, 2005]. As raw material is stickier due to high content of low-molecular-weight sugars, the drying rate decreases and thus the water content of the final product is higher [Goula & Adamopoulos, 2008]. Bhandari & Hartel [2002] reported that a high content of low-molecular-weight sugars, such as glucose and fructose, corresponded with a higher water content of sucrose powder.

Hygroscopicity (H) of the produced powders was reported in Table 2. According to the classification proposed by Dolivet *et al*. [2012], the powders in our study were extremely hygroscopic. This could be an effect of eliminating carrier and high sugar content of raw materials. In general, glucose and fructose have high H; thus, powders that had majority of these sugars in their composition, presented higher H values [Bhandari *et al*., 1997]. Sucrose is a major sugar of kiwiberries [Latocha, 2017], which could be the main reason of the lowest H values determined for KB/SD and KB/DASD among all the carrier-free powders. In the case of the mango puree powder (M/DASD), H determined in our study (Table 2) confirmed findings reported by Zotarelli *et al*. [2017], who spray dried mango pulp without additional carrier and obtained H= 26.9%. Both tomato pulp powders had the highest H values (Table 2), which seemed to be an effect of small particle size, which enlarged specific total surface area for moisture sorption. Finally, it should be highlighted that dehumidified air application decreased H values of the powders obtained using both methods (KB and T), which is important for their storage stability.

Bulk density and flowability

Tontul *et al*. [2016] analyzed tomato powders with different vegetable proteins as carriers and observed increasing bulk density (D_L) with an increasing median particle size diameter. However, such a correlation was not observed in our work dealing with various powders of different origin, *i.e.*, no significant ($p \geq 0.05$) Pearson's correlation between D_{50} and D_L correlation was noted (Table 3). No effect of dehumidified air application on D_L was observed for tomato pulp powders (T/SD, T/DASD) (Table 2); however, the influence of drying temperature was noted in the case of kiwiberry pulp powders (KB/SD, KB/DASD). The unfavorable effect of dehumidified air application was reported, which was not expected. Higher D_L favors less free spaces between particles that are filled with air, decreasing the risk of bioactive compounds degradation [García-Segovia *et al*., 2021]. However, it is likely that this unfavorable phenomenon was due to MC, as D_L decreases with higher MC [Koç *et al*., 2021]. Zotarelli *et al*. [2017] analyzed carrier-free mango powders and determined D_L equal to 0.45 g/mL; however, dehumidified air was not applied as a drying medium to lower drying temperature. In this study, the produced mango puree powder was of higher bulk density as a consequence of dehumidified air application, which enhances the powder properties. Archaina *et al*. [2018] produced blackcurrant juice and extract powders from processing waste at 150°C and with 40% (*w/w*) addition of maltodextrin as a carrier, and reported D_L of 0.39 g/mL. As before, dehumidified air in this research enabled spray drying of blackcurrant juice concentrate with no additional carrier to powder with higher D_L. This is beneficial because the costs of transportation, packaging, handling and storage of the powders are reduced [Koç *et al*., 2021].

Geldart *et al*. [1984] classified powders based on the Hausner ratio (HR) as of good flowability (<1.25), average flowability (1.25–1.4) and cohesive (>1.4). The positive effect of decreased drying temperature as a consequence of dehumidified air application on HR was noted for tomato pulp powders (T/SD, T/DASD) – the variant spray dried using an innovative method had significantly ($p<0.05$) better flowability (Table 2). The best flowability among all tested powders was noted for the blackcurrant powder (BC/DASD), which, as described earlier, had the biggest particle size (Table 2). As was discussed, bigger particle size can imply the problematical course of drying due to stickiness, while bigger particles can at the same time promote powder recovery and flowability. This supports previous findings of Barańska *et al*. [2021, 2023] and Nishad *et al*. [2017], who observed that powders with smaller particles were more cohesive. However, the general correlation between D_{50} and HR determined for all powders was not significant ($p \geq 0.05$; Table 3), because other powders (M/DASD, PC/DASD, T/DASD) obtained by DASD, with significantly smaller particles, had medium flowability.

Water solubility index

Water solubility index (WSI) is an important parameter that describes powder's behavior in water and as a consequence, determines the reconstitution properties of a final product [Jafari *et al*., 2017]. As consumers' attention is focused on the dissolution of powders, it is crucial to characterize this parameter. Murali *et al*. [2015] spray dried purple carrot juice at 150–225°C with tapioca starch, gum Arabic and maltodextrin as carriers, and determined WSI values varying from 11.1 to 98.9%. Archaina *et al*. [2018] produced blackcurrant powder using spray drying at 150°C with 40% (*w/w*) content of maltodextrin as a carrier and reported its 94.2% solubility. Zotarelli *et al*. [2022] evaluated the solubility of mango pulp powders obtained at 150°C with and without maltodextrin as a carrier. They determined 77.2 and 78.6% solubility and no significant difference between the powders with and without a carrier. In the present research, similar or higher solubility was obtained for comparable raw materials at significantly lower drying temperature with no additional carrier (Table 2). This finding underlines the importance of dehumidified air application in designing "clean label" powders of high quality and satisfactory reconstitution properties. Moreover, the influence of the applied drying method was reported as well, but only for tomato powders. The variant produced at higher drying temperature had better solubility (T/SD), presumably due to MC of the analyzed samples. Lower MC of the variant spray dried at higher drying temperature (T/SD) facilitated the solubilization. A similar relationship was reported by Goula & Adamopoulos [2005], who produced tomato pulp powders as well.

The effect of the type of raw material used on WSI values was noted in the study (Table 2). According to Zotarelli *et al*. [2022], the presence of insoluble fiber plays an essential role in solubility of the final powder. It was confirmed by the present study results – materials that were initially in form of pulps (T and KB) had significantly ($p<0.05$) lower WSI values than juice concentrates (BC and PC) and clear mango puree (M).

Color parameters

The results of measurements of color parameters of the carrier-free powders produced are presented in Figure 3. In general,

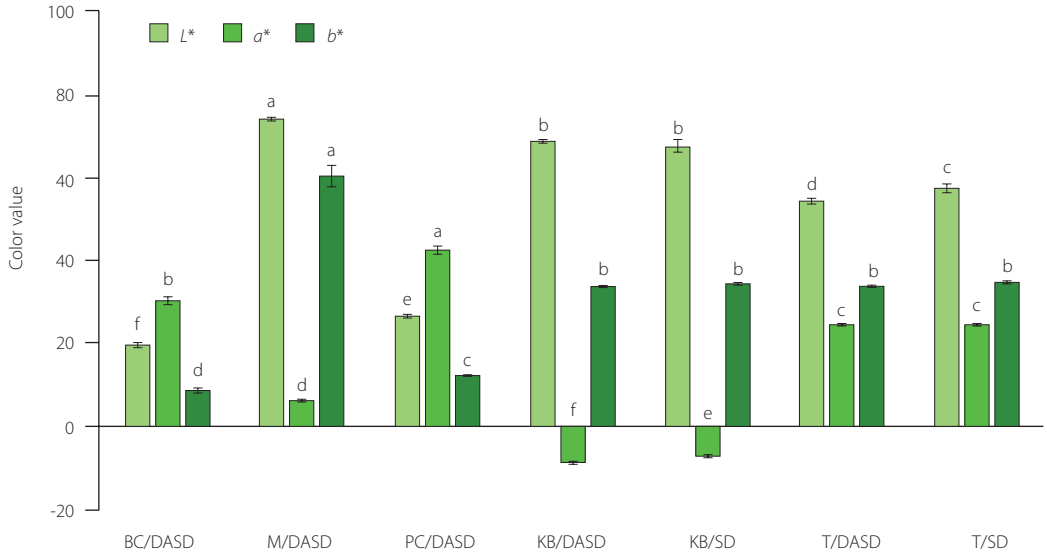

Figure 3. Color parameters (L^*, a^*, b^*) of carrier-free powders produced by conventional high temperature spray drying (SD) and/or with the application of dehumidified air at low temperature (DASD) from blackcurrant juice concentrate (BC), mango puree (M), purple carrot juice concentrate (PC), sauerkraut juice (S), kiwiberry pulp (KB), and tomato pulp (T). The differences between mean values marked with the same letter (a–f) for each parameter separately were statistically not significant ($p \geq 0.05$).

the values differed significantly between powders because of the differences in raw materials; however, attention should be focused more on the differences between the powders made of the same materials obtained using both spray drying methods. There was no statistically significant ($p \geq 0.05$) difference in L^* parameter values between KB/SD and KB/DASD. However, the difference ($p < 0.05$) was noted for tomato pulp powders (T/SD, T/DASD). In contrast to findings from our earlier study with sour cherry juice concentrate [Barańska *et al.*, 2023], tomato pulp powder obtained by DASD was darker than the powder produced at high drying temperature. The values of a^* parameter, which describes the contribution of red and green in the sample color, differed significantly ($p < 0.05$) between KB/SD and KB/DASD. The favorable effect of decreased drying temperature was noted, as the contribution of green color in the DASD sample was stronger. Thus, it can be concluded that chlorophylls, which are responsible for green color of kiwiberry berries [Lawes, 1989], were better preserved in the powder produced at low drying temperature, as they are susceptible to high temperature. The differences in the values of b^* parameter, that describes yellow hues in samples, were not significant ($p \geq 0.05$) for the variants spray dried using both methods; thus, the effect of lowering drying temperature on b^* parameter was not observed.

Hierarchical cluster analysis

HCA analysis enables presenting results in the form of a dendrogram that shows the hierarchy, organization and similarity of tested variants [Granato *et al.*, 2018; Senior *et al.*, 2012]. The dendrogram displays the horizontal axis representing the distance, thus the similarity between clusters. Four clusters were formed: first cluster of PC/DASD and BC/DASD, second cluster with single M/DASD, third with KB/DASD and KB/SD, and fourth cluster with T/DASD and T/SD (Figure 4). The strongest similarity was observed for the variants in cluster 3, as the distance was only 8. The effect of the type of raw material used was more evident than that of the drying method applied, as the distance between variants spray dried using both methods were small, indicating strong similarities.

CONCLUSIONS

Food products with a short list of ingredients have spurred a growing interest among consumers whose awareness on food formulation has substantially increased over the past decade. Dehumidified air application to produce powders by spray drying enables not only decreasing carrier content, but also eliminating it entirely in some types of raw materials. This study has investigated the possibility of producing carrier-free powders from sauerkraut juice, purple carrot juice concentrate, mango puree, blackcurrant juice concentrate, kiwiberry pulp, and tomato pulp using high temperature – conventional spray drying and low temperature – dehumidified air-assisted spray drying. Decreasing drying temperature as a consequence of low drying air humidity was the only possible solution to produce carrier-free powders of sauerkraut juice, purple carrot juice concentrate, mango puree, and blackcurrant juice concentrate. Moreover, considering process performance, the satisfactory powder recovery (over 60%) was noted in the case of two variants: purple carrot juice concentrate and blackcurrant juice concentrate. For kiwiberry and tomato pulps that were spray dried using both methods, some of the physiochemical properties were enhanced when the dehumidified air was applied. Median particle size diameter, that indicates the ease of the course of drying, was favorably smaller, hygroscopicity was reported to decrease and flowability

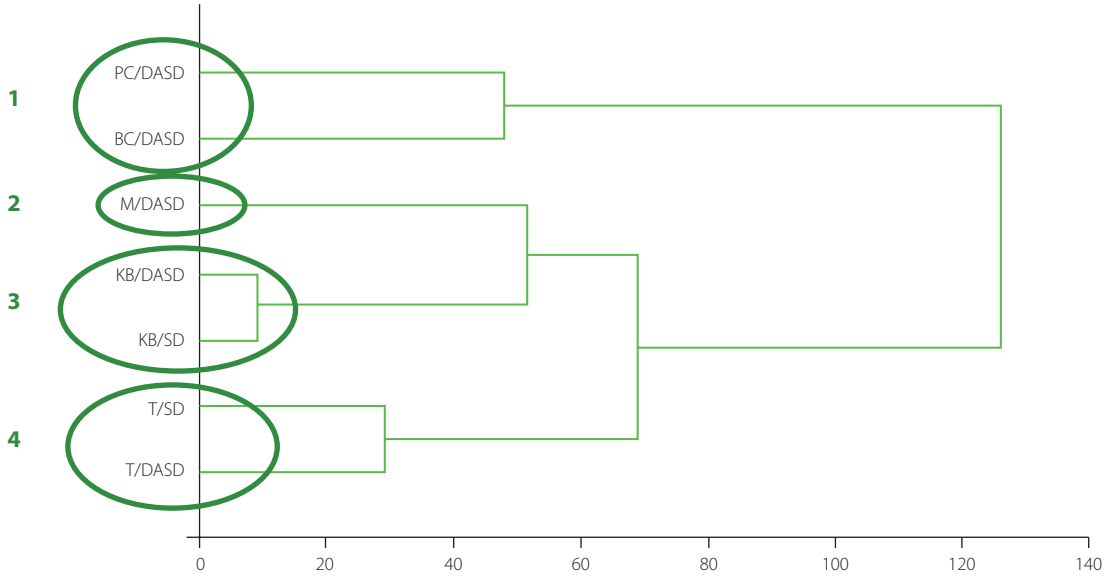

Figure. 4. Dendrogram plot derived from hierarchical cluster analysis (HCA) for physiochemical and color parameters of carrier-free powders produced by conventional high temperature spray drying (SD) and/or with the application of dehumidified air at low temperature (DASD) from blackcurrant juice concentrate (BC), mango puree (M), purple carrot juice concentrate (PC), sauerkraut juice (S), kiwiberry pulp (KB), and tomato pulp (T).

was improved when the inlet drying temperature was lower (flowability only for tomato pulp powders). Taken together, the differences between the variants spray dried with both methods were minor; however, selected properties of the powders produced using dehumidified air were more beneficial than these of the powders dried conventionally.

This research provided results demonstrating that lowering drying air humidity is a vital factor in designing powders of carrier-free juice/concentrate/pulp. Dehumidified air application enables lowering drying temperature, which consequently decreases the risk of stickiness and problems during drying, allowing the successful production of powders. The approach presented in this study has the potential to be applied in the formulation and production of clean label powders, meeting expectations of modern consumers.

ACKNOWLEDGEMENTS

The research for this publication was carried out with the use of equipment purchased as part of the "Food and Nutrition Centre – modernization of the WULS campus to create a Food and Nutrition Research and Development Centre (CŻiŻ)" co-financed by the European Union from the European Regional Development Fund under the Regional Operational Programme of the Mazowieckie Voivodeship for 2014–2020 (Project No. RPMA.01.01.00-14-8276/17).

CONFLICTS OF INTERESTS

The authors declare no conflicts of interests.

ORCID IDs

A. Barańska https://orcid.org/0000-0003-2711-6073
A. Jedlińska https://orcid.org/0000-0003-4387-8537
K. Samborska https://orcid.org/0000-0002-1221-7261

REFERENCES

1. Archaina, D., Leiva, G., Salvatori, D., Schebor, C. (2018). Physical and functional properties of spray-dried powders from blackcurrant juice and extracts obtained from the waste of juice processing. *Food Science and Technology International, 24*(1), 78-86. https://doi.org/10.1177/1082013217729601
2. Asioli, D., Aschemann-Witzel, J., Caputo, V., Vecchio, R., Annunziata, A., Næs, T., Varela, P. (2017). Making sense of the "clean label" trends: A review of consumer food choice behavior and discussion of industry implications. *Food Research International*, *99*, Part 1, 58-71. https://doi.org/10.1016/j.foodres.2017.07.022
3. Baranowska-Wójcik, E., Szwajgier, D. (2019). Characteristics and pro-health properties of mini kiwi (*Actinidia arguta*). *Horticulture, Environment, and Biotechnology*, *60*, 217-225. https://doi.org/10.1007/s13580-018-0107-y
4. Barańska, A., Jedlińska, A., Samborska, K. (2021). Dehumidified-air-assisted spray drying of buckwheat honey with maltodextrin and skim milk powder as carriers. *Applied Sciences, 11*(7), art. no. 3150. https://doi.org/10.3390/app11073150
5. Barańska, A., Świeca, M., Samborska, K. (2023). Sour cherry juice concentrate powdered by high and low temperature spray drying with pea protein as a carrier — Physical properties, antioxidant activity and *in vitro* bioaccessibility. *Drying Technology*, *41*(3), 444-459. https://doi.org/10.1080/07373937.2022.2096060
6. Bhandari, B., Datta, N., Howes, T. (1997). Problems associated with spray drying of sugar-rich foods. *Drying Technology, 15*(2), 671-684. https://doi.org/10.1080/07373939708917253
7. Bhandari, B., Hartel, R. (2002). Co-crystallization of sucrose at high concentration in the presence of glucose and fructose. *Journal of Food Science, 67*(5), 1797-1802. https://doi.org/10.1111/j.1365-2621.2002.tb08725.x
8. Champion, D., Le Meste, M., Simatos, D. (2000). Towards an improved understanding of glass transition and relaxations in foods: Molecular mobility in the glass transition range. *Trends in Food Science & Technology, 11*(2), 41-55. https://doi.org/10.1016/S0924-2244(00)00047-9
9. Chin, S.T., Nazimah, S.A.H., Quek, S.Y., Che Man, Y.B., Abdul Rahman, R., Mat Hashim, D. (2008). Changes of volatiles' attribute in durian pulp during freeze- and spray-drying process. *LWT – Food Science and Technology, 41*(10), 1899-1905. https://doi.org/10.1016/j.lwt.2008.01.014
10. Del Valle, M., Cámara, M., Torija, M.E. (2006). Chemical characterization of tomato pomace. *Journal of the Science of Food and Agriculture, 86*(8), 1232-1236. https://doi.org/10.1002/jsfa.2474
11. Dolivet, A., Schuck, P., Jeantet, R. (2012). Determination of the Sorption Isotherm, Water Activity and Hygroscopicity of Powders. In P. Schuck, A. Dolivet, A.R. Jeantet (Eds.), *Analytical Methods for Food and Dairy Powders*, John Wiley & Sons, Ames, Iowa, USA, pp. 167–190.

12. García-Segovia, P., Igual, M., Martínez-Monzó, J. (2021). Beetroot microencapsulation with pea protein using spray drying: Physicochemical, structural and functional properties. *Applied Sciences*, *11*(14), art. no. 6658. https://doi.org/10.3390/app11146658
13. Geldart, D., Harnby, N., Wong, A. (1984). Fluidization of cohesive powders. *Powder Technology, 37*(1), 25-37. https://doi.org/10.1016/0032-5910(84)80003-0
14. Goula, A.M., Adamopoulos, K.G. (2005). Spray drying of tomato pulp in dehumidified air: II. The effect on powder properties. *Journal of Food Engineering, 66*(1), 35-42. https://doi.org/10.1016/j.jfoodeng.2004.02.031
15. Goula, A.M., Adamopoulos, K.G. (2008). Effect of maltodextrin addition during spray drying of tomato pulp in dehumidified air: II. Powder properties. *Drying Technology, 26*(6), 726-737. https://doi.org/10.1080/07373930802046377
16. Goula, A.M., Adamopoulos, K.G., Kazakis, N.A. (2004). Influence of spray drying conditions on tomato powder properties. *Drying Technology, 22*(5), 1129-1151. https://doi.org/10.1081/DRT-120038584
17. Granato, D., Santos, J.S., Escher, G.B., Ferreira, B.L., Maggio, R.M. (2018). Use of principal component analysis (PCA) and hierarchical cluster analysis (HCA) for multivariate association between bioactive compounds and functional properties in foods: A critical perspective. *Trends in Food Science & Technology, 72*, 83-90. https://doi.org/10.1016/j.tifs.2017.12.006
18. Jafari, S.M., Ghalenoei, M.G., Dehnad, D. (2017). Influence of spray drying on water solubility index, apparent density, and anthocyanin content of pomegranate juice powder. *Powder Technology, 311*, 59-65. https://doi.org/10.1016/j.powtec.2017.01.070
19. Janiszewska, E. (2014). Microencapsulated beetroot juice as a potential source of betalain. *Powder Technology*, *264*, 190-196. https://doi.org/10.1016/j.powtec.2014.05.032
20. Jedlińska, A., Samborska, K., Wiktor, A., Balik, M., Derewiaka, D., Matwijczuk, A., Gondek, E. (2022). Spray drying of pure kiwiberry pulp in dehumidified air. *Drying Technology*, *40*(7), 1421-1435. https://doi.org/10.1080/07373937.2020.1871006
21. Koç, B., Koç, M., Baysan, U. (2021). Food Powders Bulk Properties. In E. Ermiş (Ed.). *Food Powders Properties and Characterization,* Springer, Cham, pp. 1-36. https://doi.org/10.1007/978-3-030-48908-3_1
22. Latocha, P. (2017). The nutritional and health benefits of kiwiberry (*Actinidia arguta*) – a review. *Plant Foods for Human Nutrition*, *72*, 325-334. https://doi.org/10.1007/s11130-017-0637-y
23. Lawes, G.S. (1989). The effect of shading on the chlorophyll content of 'Hayward' kiwifruit. *New Zealand Journal of Crop and Horticultural Science*, *17*(3), 245-249. https://doi.org/10.1080/01140671.1989.10428039
24. Matwijczuk, A., Budziak-Wieczorek, I., Czernel, G., Karcz, D., Barańska, A., Jedlińska, A., Samborska, K. (2022). Classification of honey powder composition by FTIR spectroscopy coupled with chemometric analysis. *Molecules*, *27(12)*, art. no. 3800. https://doi.org/10.3390/molecules27123800
25. Murali, S., Kar, A., Mohapatra, D., Kalia, P. (2015). Encapsulation of black carrot juice using spray and freeze drying. *Food Science and Technology International, 21*(8), 604-612. https://doi.org/10.1177/1082013214557843
26. Muzaffar, K., Nayik, G.A., Kumar, P. (2015). Stickiness problem associated with spray drying of sugar and acid rich foods: a mini review. *Journal of Nutrition & Food Sciences*, *S12*, art. no. S12003. https://doi.org/10.4172/2155-9600.S12-003
27. Nishad, J., Selvan, C.J., Mir, S.A., Bosco, S.J.D. (2017). Effect of spray drying on physical properties of sugarcane juice powder (*Saccharum officinarum* L.). *Journal of Food Science and Technology, 54*, 687-697. https://doi.org/10.1007/s13197-017-2507-x
28. Pereira, D.C.d.S., Beres, C., Gomes, F.d.S., Tonon, R.V., Cabral, L.M. (2020). Spray drying of juçara pulp aiming to obtain a "pure" powdered pulp without using carrier agents. *Drying Technology, 38*(9), 1175-1185. https://doi.org/10.1080/07373937.2019.1625363
29. Samborska, K., Barańska, A., Szulc, K., Jankowska, E., Truszkowska, M., Ostrowska-Ligęza, E., Wołosiak, R., Szymańska, E, Jedlińska, A. (2020). Reformulation of spray dried apple concentrate and honey for the enhancement of drying process performance and the physicochemical properties of powders. *Journal of the Science of Food and Agriculture, 100*(5), 2224-2235 https://doi.org/10.1002/jsfa.10247
30. Samborska, K., Bonikowski, R., Kalemba, D., Barańska, A., Jedlińska, A., Edris, A. (2021). Volatile aroma compounds of sugarcane molasses as affected by spray drying at low and high temperature. *LWT – Food Science and Technology, 145*, art. no. 111288. https://doi.org/10.1016/j.lwt.2021.111288
31. Samborska, K., Edris, A., Jedlińska, A., Barańska, A. (2022). The production of white mulberry molasses powders with prebiotic carrier by dehumidified air-assisted spray drying. *Journal of Food Process Engineering*, *45*(1), art. no. e13928. https://doi.org/10.1111/jfpe.13928
32. Satora, P., Skotniczny, M., Strnad, S., Piechowicz, W. (2021). Chemical composition and sensory quality of sauerkraut produced from different cabbage varieties. *LWT – Food Science and Technology*, *136*, Part 1, art. no. 110325. https://doi.org/10.1016/j.lwt.2020.110325
33. Senior, S., Hamed, E., Masoud, M., Shehata, E. (2012). Characterization and dating of blue ballpoint pen inks using principal component analysis of UV–Vis absorption spectra, IR spectroscopy, and HPTLC. *Journal of Forensic Sciences, 57*(4), 1087-1093. https://doi.org/10.1111/j.1556-4029.2012.02091.x
34. Shi, Q., Fang, Z., Bhandari, B. (2013). Effect of addition of whey protein isolate on spray-drying behavior of honey with maltodextrin as a carrier material. *Drying Technology*, *31*(13-14), 1681-1692. https://doi.org/10.1080/07373937.2013.783593
35. Shrestha, A.K., Ua-Arak, T., Adhikari, B.P., Howes, T., Bhandari, B.R. (2007). Glass transition behavior of spray dried orange juice powder measured by differential scanning calorimetry (DSC) and thermal mechanical compression test (TMCT). *International Journal of Food Properties, 10*(3), 661-673. https://doi.org/10.1080/10942910601109218
36. Stój, A., Targoński, Z. (2005). Use of sugar content analysis for the estimation of berry juice authenticity. *Polish Journal of Food and Nutrition Sciences*, *55*(4), 403-409.
37. Tontul, I., Topuz, A., Ozkan, C., Karacan, M. (2016). Effect of vegetable proteins on physical characteristics of spray-dried tomato powders. *Food Science and Technology International, 22*(6), 516-524. https://doi.org/10.1177/1082013216629528
38. Truong, V., Bhandari, B.R., Howes, T. (2005). Optimization of co-current spray drying process of sugar-rich foods. Part I — Moisture and glass transition temperature profile during drying. *Journal of Food Engineering, 71*(1), 55-65. https://doi.org/10.1016/j.jfoodeng.2004.10.017
39. Wang, S., Konkol, E., Langrish, T.A.G. (2011). Spray drying of fruit juice using proteins as additives. *Drying Technology, 29*(16), 1868-1875. https://doi.org/10.1080/07373937.2011.589552
40. Zotarelli, M.F., da Silva, V.M., Durigon, A., Hubinger, M.D., Laurindo, J.B. (2017). Production of mango powder by spray drying and cast-tape drying. *Powder Technology, 305*, 447-454. https://doi.org/10.1016/j.powtec.2016.10.027
41. Zotarelli, M.F., Durigon, A., da Silva, V.M., Hubinger, M.D., Laurindo, J.B. (2022). Rehydration of mango powders produced by cast-tape drying, freeze drying, and spray drying. *Drying Technology, 40*(1), 175-187. https://doi.org/10.1080/07373937.2020.1777562

ORIGINAL ARTICLE
http://journal.pan.olsztyn.pl

Polish Journal of Food and Nutrition Sciences
2023, Vol. 73, No. 3, 224–232
DOI: 10.31883/pjfns/169425
ISSN 1230-0322, e-ISSN 2083-6007

Discrimination of Selected Cold-Pressed and Refined Oils by Untargeted Profiling of Phase Transition Curves of Differential Scanning Calorimetry

Mahbuba Islam[1], Magdalena Montowska[2], Emilia Fornal[3], Jolanta Tomaszewska-Gras[1]*

[1]Department of Food Quality and Safety Management, Poznan University of Life Sciences, ul. Wojska Polskiego 31/33, 60-637 Poznan, Poland
[2]Department of Meat Technology, Poznan University of Life Sciences, ul. Wojska Polskiego 31, 60-624 Poznan, Poland
[3]Department of Bioanalytics, Faculty of Biomedicine, Medical University of Lublin, Jaczewskiego 8b, 20-090 Lublin, Poland

The authenticity assessment of edible oils is crucial to reassure consumers of product compliance. In this study, a new approach was taken to combining untargeted profiling by using differential scanning calorimetry (DSC) with chemometric methods in order to distinguish cold-pressed oils (flaxseed, camelina, hempseed) from refined oils (rapeseed, sunflower, soybean). The whole spectrum of DSC melting profiles was considered as a fingerprint of each oil. Flaxseed and hempseed oils exhibited four endothermic peaks, while three peaks with one exothermic event were detected for camelina seed oil. In the case of refined oils, two endothermic peaks were detected for rapeseed oil, three for sunflower oil and four for soybean oil. Thermodynamic parameters, such as peak temperature, peak heat flow and enthalpy, differed for each type of oil. Principal component analysis (PCA) and orthogonal partial least squares-discriminant analysis (OPLS-DA) were used for processing data consisting of the whole spectrum of heat flow variables of melting phase transition. PCA demonstrated a clear separation between refined and cold-pressed oils as well as six individual oils. The OPLS-DA showed a distinct classification in six classes according to the types of oils. High OPLS-DA coefficients including $R^2X(cum)=0.971$, $R^2(cum)=0.916$ and $Q^2X(cum)=0.887$ indicated good fitness of the model for oil discrimination. Variables influence on projection (VIP) plot indicated the most significant variables of the heat flow values detected at temperatures around −29°C, −32°C, −14°C, −10°C, −24°C and −41°C for the differentiation of oils. The study ultimately demonstrated great potential of the untargeted approach of using the whole melting DSC profile with chemometrics for the discrimination of cold-pressed and refined oils.

Key words: authentication, plant oils, chemometrics, multivariate data analysis, melting profiles, orthogonal partial least squares-discriminant analysis, differential scanning calorimetry

INTRODUCTION

Authentication of cold-pressed oils can be carried out by means of adulteration detection and quality assessment. Edible oils are susceptible to adulteration with lower-quality oils or substances, which can have a detrimental effect on their nutritional value, safety, and sensory properties [Islam *et al.*, 2022]. Authenticity analysis employs a combination of chemical and physical tests to determine the composition, purity, and quality of the oil. The authenticity analysis becomes increasingly important in the case of the high-value oils, like cold-pressed oils (*e.g.*, flaxseed oil, camelina seed oil, hemp seed oil, olive oil, and avocado oil), which are commonly targeted by fraudulent practices, including

***Corresponding Author:**
tel.: +48 618487512; e-mail: jolanta.tomaszewska-gras@up.poznan.pl (J. Tomaszewska-Gras)

Submitted: 3 June 2023
Accepted: 10 July 2023
Published on-line: 2 August 2023

adulteration with other substances or blending with cheaper oils [De Souza *et al.*, 2015; Jović & Jović, 2017; Nikolaichuk *et al.*, 2022; Van Wetten *et al.*, 2015; Yanty *et al.*, 2011]. Refined oils, characterized by a neutral flavor, high smoke point and longer shelf life, have been one of the most commonly used and cheapest oils. Therefore, it is also crucial to know the characteristics of widely consumed refined oils (*e.g.*, rapeseed, soybean, sunflower oils), since they can be used as adulterants.

Several factors should be considered when evaluating the authenticity of cold-pressed and refined oils, for instance, the oil's origin can provide insights into its authenticity [Karim *et al.*, 2015; Piravi-vanak *et al.*, 2022; Rajagukguk *et al.*, 2022; Zhang *et al.*, 2011]. Cold-pressed oils are usually extracted from high-quality seeds or nuts, while refined oils may be sourced from raw materials of average quality. Furthermore, the oil's color and clarity can be crucial in authenticity assessment. Cold-pressed oils tend to have a darker and cloudier appearance, whereas refined oils have a lighter color due to the elimination of impurities and color pigments during the refining process [Aydeniz Güneser *et al*., 2017; Gharby, 2022; Vaisali *et al*., 2015]. The authenticity of an oil can be inferred from its chemical composition. Cold-pressed oils, for instance, may contain more antioxidants and other beneficial compounds than refined oils [Gogolewski *et al*., 2000; Wroniak *et al.*, 2008].

The analysis of the authenticity of cold-pressed and refined oils usually entails a list of physical, chemical, and sensory tests. Several analytical techniques are employed for this purpose, *e.g.*, gas chromatography (GC) [Xu *et al.*, 2015], high-performance liquid chromatography (HPLC) [Ratusz *et al.*, 2018], and various spectroscopy methods such as UV-visible spectroscopy [Karbasian *et al.*, 2015], nuclear magnetic resonance (NMR) [Siudem *et al.*, 2019], and Fourier transform infrared spectroscopy (FTIR) [Moigradean *et al.*, 2015] being the most widely deployed. However, thermal analysis is an emerging technique that has proved useful in authenticating oil products. Differential scanning calorimetry (DSC) is a thermal analysis technique that measures the amount of heat absorbed or released by a sample as it is heated or cooled, which is often used to analyze oil melting behavior and thermal stability. This information can provide insight into the oil's purity and authenticity, as well as its thermal stability. Different exothermic or endothermic curves obtained by DSC technique can provide information about the energy changes that occur inside fats or oils during phase transitions, such as melting [Islam *et al.*, 2023] or crystallization [Brożek *et al.*, 2022]. These curves are determined by the structure and behavior of triacylglycerols (TAG), which are the major constituents of fats and oils. Assessment of TAG components showed their influence on polymorphic behavior during phase transition, which affects unique DSC curves [Rousseau *et al.*, 2005; Sato *et al.*, 2013]. Furthermore, degree of unsaturation, indicated by the number of double bonds in the fatty acid chains, influences the energy required for crystallization or melting phase transition [Zhang *et al.*, 2022]. Thus, any added adulterants, such as low-quality oils or other substances, can affect the oil's thermal properties and can be detected through thermal analysis. In brief, if an oil sample has been adulterated with a lower-grade oil or a non-food-grade substance, the melting and solidification points of the sample will be different from those of the pure oil, and this difference can be detected using DSC [Angiuli *et al.*, 2009; Marikkar, 2014; Dyszel & Baish, 1992; Rudakov *et al.*, 2021].

The aim of this study was to use the whole thermal profiles of melting phase transition of selected edible oils (both cold-pressed and refined oils) for discrimination purposes. A novel approach was taken to combining an untargeted method of DSC with chemometrics in order to distinguish three cold-pressed oils, *i.e.*, flaxseed, camelina, and hempseed oils from such refined oils as rapeseed, sunflower, and soybean oil. Multivariate data analysis tools, *i.e.*, principal component analysis (PCA) and orthogonal partial least squares-discriminant analysis (OPLS-DA), were used to investigate a dataset with a large number of variables. The originality of this study lies in the fact that chemometric methods (PCA, OPLS-DA) were employed for the first time to analyze the whole thermal spectrum of melting phase transition to authenticate cold-pressed oils. To the best of the authors' knowledge, the use of untargeted analysis of the whole DSC spectrum for the authentication of edible oils has never been reported and is yet to be fully explored.

MATERIALS AND METHODS

Materials

For the experiment, primarily 15 kg of seeds of each cultivar or batch of flax, camelina and hemp were obtained from different sources and then cold-pressed to obtain oils. In the case of flax (*Linum usitatissimum* L.), seeds of *Bukoz* cultivar from the Polish Institute of Natural Fibers and Medicinal Plants (Poznań, Poland), *Dolguniec* cultivar from SEMCO manufactory (Śmiłowo, Poland), *Szafir* cultivar from two different suppliers, *i.e.*, from SEMCO manufactory and Hodowla Roślin Strzelce Sp. z o.o. (Strzelce, Poland) and seeds of unknown variety from VitaCorn company (Poznań, Poland) were collected. All hemp (*Cannabis sativa* L.) seeds of the *Henola* cultivar originated from five different suppliers and were collected from the Polish Institute of Natural Fibers and Medicinal Plants. Three cultivars of camelina (*Camelina sativa*) seeds originated from five suppliers; seeds of a spring *Omega* cultivar were purchased from the Poznań University of Life Sciences (Agriculture Research Station Dłoń, Miejska Górka); two camelina seed cultivars (*Luna* and *Śmiłowska*) were collected from SEMCO manufactory, which purchased seeds from different suppliers: *Luna* – a winter variety from two different suppliers and *Śmiłowska* – a spring variety from two different suppliers. All seeds were pressed in the SEMCO manufactory to obtain the oils at the same conditions, *i.e.*, keeping the temperature below 50°C. The pressed oils were left for 24 h for decantation and stored in brown glass bottles. A total of nine refined oils (three for each type of oil: rapeseed, sunflower, and soybean) were purchased from local Polish markets.

Melting phase transition analysis by differential scanning calorimetry

Melting phase transition analysis of oils was carried out according to the method used for butterfat [Tomaszewska-Gras, 2016] with

some modifications, using a DSC 8500 Perkin Elmer differential scanning calorimeter (Waltham, MA, USA), equipped with an Intracooler II and running with Pyris software. Nitrogen (99.999% purity) was the purge gas. Oils (6–7 mg) were weighed into 20-µL aluminum pans (Perkin Elmer, No. 0219-0062) and hermetically sealed. The reference was an empty, hermetically sealed aluminum pan. Analysis started with the oil sample being cooled at a scanning rate of 2°C/min from a temperature of 30°C to –65°C, after which it was heated at a scanning rate of 5°C/min from –65°C to 30°C. For each measurement at a given scanning rate, the calibration procedure was completed with the correct scanning rate. After the analysis, the DSC files were converted to the ASCII format and then analyzed using Origin Pro software, version 2023 (OriginLab Corporation, Northampton, MA, USA). All curves were normalized and the baseline was subtracted to project the DSC curves of all investigated samples in the same scale. Peak temperature (T, °C), peak heat flow (h, W/g), and enthalpy (ΔH, J/g) were measured from the melting curves. Peak temperature was determined at the maximum heat flow on the curve for the selected peak. Peak heat flow was established as the maximum value of heat flow for the normalized peaks. Enthalpy was determined by integrating the area under the curve of the heat flow (J/s) *vs.* temperature (°C). The number of analytical repetitions was two for each oil sample. Therefore, for each cold-pressed oils, five samples were analyzed in duplicate, and for each refined oils, three samples were analyzed in duplicate.

Statistical analysis

Mean and standard deviation were calculated in order to present results that were obtained from ten measurements (n=10) for each cold-pressed oil and from six measurements (n=6) for each refined oil. The SIMCA software version 16.1 (Sartorius Stedim Data Analytics AB, Umea, Sweden) was used to conduct multivariate data analysis, *i.e.*, PCA and OPLS-DA. Both PCA and OPLS-DA models were cross-validated, and the OPLS-DA models were also validated using permutation testing. For these models, X represents the normalized heat flow data matrix obtained from 7471 variables, Y represents the types of oils, and the predictive variables in X were used to classify and predict the oil types. To assess the quality of the models, the model statistics parameters: R^2X(cum), R^2(cum), R^2Y(cum), Q^2(cum), were obtained through cross-validation. Model performance was evaluated by examining the explained variation R^2(cum), which represents the goodness of fit for X- and Y-variables, and the predictive variation Q^2(cum), which represents the goodness of prediction for the fit of predicted variables.

RESULTS AND DISCUSSION

DSC melting profiles of cold-pressed and refined oils

Cold-pressed (flaxseed, camelina seed and hempseed) and refined (rapeseed, soybean and sunflower seed) oils were analyzed for phase transition during heating to establish their melting profile by considering the full spectrum of the DSC curves as fingerprint of the oil. DSC is a highly regarded thermal analysis technique that can explain various properties of these oils,

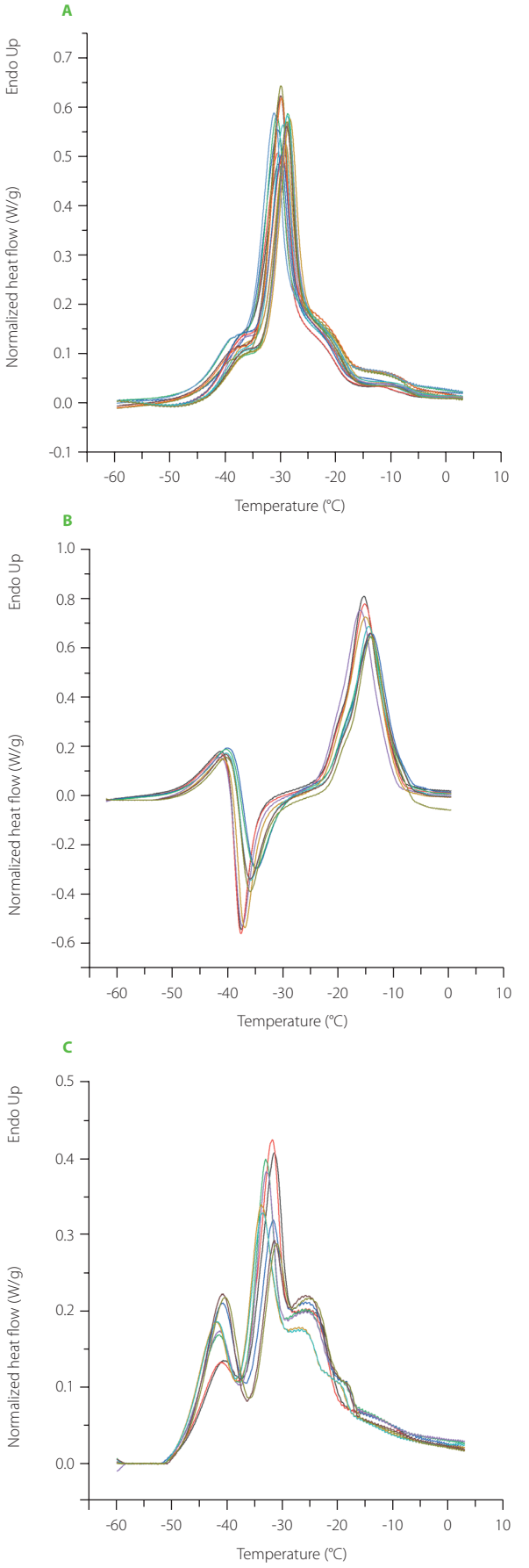

Figure 1. Differential scanning calorimetry (DSC) melting curves of cold-pressed oils at a scanning rate 5°C/min; (**A**) flaxseed oils; (**B**) camelina seed oils; (**C**) hempseed oils. Different color curves represent oil samples from different suppliers.

such as their phase transition temperature and magnitude of the thermal effect (heat flow) during individual processes of transition, and enthalpy as energy changes involved in the process. Figure 1 presents the melting curves of cold-pressed oils. To plot the melting curves, all those oils were subjected to crystallization before starting the heating program. The formation of peaks during the melting phase transition is a manifestation of the energy required to overcome the intermolecular forces holding the crystals together, which is absorbed by the sample during heating, resulting in endothermic peaks. As can be seen from Figures 1A and 1C, four peaks appeared on the melting curves, *i.e.*, at −36°C, −30°C, −25°C and −13°C for flaxseed oil; and at −41°C, −32°C, −24°C and −17°C for hempseed oil. In turn, the melting profiles of seed oils of all camelina cultivars were definitely different compared to the profiles of flaxseed and hempseed oils. The second peak was manifested as an exothermic thermal event at −34°C, whereas the other two peaks at −38°C and −12°C were clearly endothermic in nature (Figure 1B). The exothermic peak appeared as a downward deflection in the baseline of the DSC curve of camelina seed oil, which indicates that the sample is undergoing a polymorphic transition by recrystallization. The presence of an exothermic peak during the melting phase transition of camelina seed oil was also reported by other authors [Rudakov *et al.*, 2021]. Recrystallization of the polymorphic crystals of triacylglycerols into a more stable form was observed for flaxseed, hempseed and canola oil, especially at lower heating rates, *i.e.*, 1°C/min [Teh & Birch, 2013]. Although seeds of different plant cultivars were analyzed in the experiment, melting curves showed similarities between the samples of individual oil types, thus unique thermal profiles were obtained for each oil type. The melting process of flaxseed oils of all cultivars started at the temperature around −48°C, after which the initiation of the first peak occurred. The second peak appeared at around −30°C, which is the major peak of the transition, with two more shoulder peaks as the third and fourth peak at the end of transition (at temperatures of −25 and −13°C, respectively). For camelina and hempseed oils, the onset of the melting process was earlier than for flaxseed oils (for both at around −52°C). Although the curves for hempseed oils show the same number of endothermic peaks as for flaxseed oils (four peaks), their melting profile was noticeably different from that of flaxseed oils.

The behavior of oils during the phase transitions was quantified by the thermodynamic parameters, such as peak temperature, peak heat flow and enthalpy. Results are presented in Table 1. These parameters can be substantial for the authenticity assessment of oils. The peak temperatures are presented as T1, T2, T3 and T4 from the first to the fourth peak appearing while oil crystals were melted. The magnitude of transition measured as peak heat flow was also calculated for all peaks after the normalization of the melting curve. A normalized heat flow of the major peak (h2) for flaxseed oil was higher (0.49 W/g) than that of the major peak (h2) for hempseed oil (0.35 W/g). However, the greatest magnitude of transition was observed for the fourth peak (h4) of camelina oils (0.70 W/g). The first and third peak identified for hempseed oil had the higher heat flows (0.20 and 0.19 W/g, respectively) than those of flaxseed oils (0.13 and 0.14 W/g, respectively). For flaxseed and hempseed oil, the major peak (h2) appeared when the peak temperature reached approximately −30°C and −32°C, whereas for camelina oil the main peak was observed at the end of the melting transition when peak temperature reached approximately −12°C. In turn, the exothermic peak of camelina oil had peak heat flow minimum (h2) of −0.40 W/g. Enthalpy can provide insight into the degree of crystallinity or molecular weight, or amorphousness of the samples. Amongst the cold-pressed oils, flaxseed oils showed the lowest ΔH value (62.73 J/g), compared to camelina seed oil (65.09 J/g) and hempseed oil (69.53 J/g). Other authors determined the melting enthalpy for different transformants of camelina oil in the range from 42 to 57 J/g [Rodríguez-Rodríguez *et al.*, 2021] and for flaxseed oil from 54 to 62 J/g [Punia *et al.*, 2020; Zhang *et al.*, 2011].

The melting profiles of flaxseed and camelina seed oils in our study are consistent with the results obtained by Rudakov *et al.*

Table 1. Differential scanning calorimetry (DSC) parameters of the melting curves of cold-pressed oils.

Parameter		Flaxseed oil	Camelina seed oil	Hempseed oil
Peak temperature (°C)	T1	−36.37±0.72	−38.07±0.66	−40.96±0.56
	T2	−30.26±0.83	−33.61±1.08	−32.03±1.06
	T3	−24.66±0.50	-	−24.11±0.74
	T4	−12.79±0.91	−11.97±0.71	−17.11±2.88
Peak heat flow (W/g)	h1	0.13±0.02	0.20±0.01	0.20±0.03
	h2	0.49±0.06	−0.40±0.11	0.35±0.05
	h3	0.14±0.01	-	0.19±0.01
	h4	0.02±0.00	0.70±0.06	0.08±0.02
Enthalpy (J/g)	ΔH	62.73±2.05	65.09±2.69	69.53±1.52

All values are mean ± standard deviation (n=10); T1, T2, T3 and T4 represent the first, second, third and fourth peak temperatures, respectively; h1, h2, h3 and h4 mean heat flow for the first, second, third and fourth peak, respectively; ΔH represents enthalpy for the whole melting phase transition.

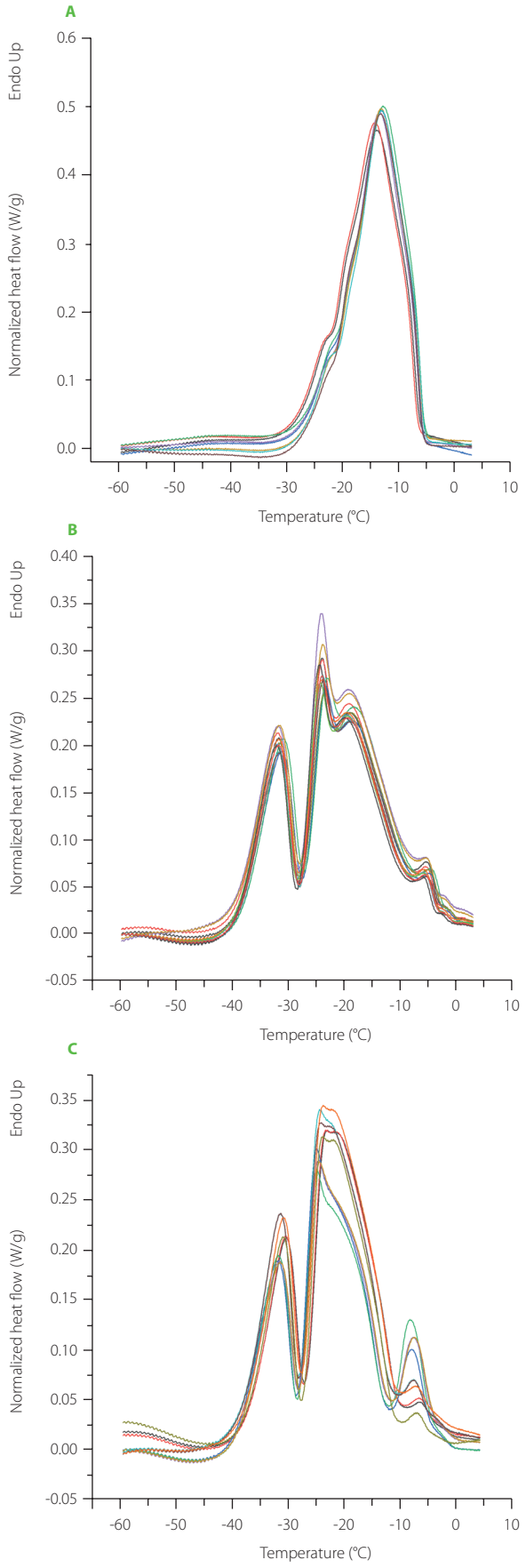

Figure 2. Differential scanning calorimetry (DSC) melting curves of refined oils at a scanning rate 5°C/min; (**A**) rapeseed oils; (**B**) soybean oils; (**C**) sunflower seed oils. Different color curves represent oil samples from different suppliers.

[2021] who used DSC at 5°C/min heating rate. These authors mentioned that the characteristics of the melting curves depended on the triacylglycerol (TAG) profile of the oil samples, which causes differences in the number of peaks, peak temperature values, and the magnitude and temperature ranges of melting transition, as well as enthalpy of transition. Similarly to this study, they also observed four endothermic peaks appearing for flaxseed oils, and three peaks for camelina seed oils (where the second peak was exothermic). Similar four peaks at −38, −31, −24, −13°C were identified by Zhang *et al.* [2014] for the melting profiles of flaxseed oil obtained with the same heating rate of 5°C/min. Our previous study showed that the melting profiles of oils were very strongly influenced by the scanning rate used for heating [Islam *et al.*, 2023; Tomaszewska-Gras *et al.*, 2021]. In turn, Teh & Birch [2013] compared the melting profiles of cold-pressed flaxseed and hempseed oils at a lower heating rate of 1°C/min, for which they determined two endothermic peaks at −40°C and −18°C for hempseed oil and at −36°C and −15°C for flaxseed oil, as well as one exothermic peak at −39°C for hempseed and at −30°C for flaxseed oils. They suggested that the polymorphic transitions indicating the recrystallization of unstable structures were due to the low heating rate. Another study, carried out with a higher scanning rate of 10°C/min, showed that flaxseed hull oils exhibited three peaks of the melting transitions at −33°C, −25°C and −14°C [Oomah & Sitter, 2009], which indicates that a higher heating rate may reduce peak resolution.

Authentication of cold-pressed oils requires knowledge and verification of the characteristics of oils which can be used as adulterants. These most often used ones include refined oils, because they are colorless and odorless, but also because they are cheap and widely available. The melting characteristics of refined rapeseed, soybean and sunflower oils are presented in Figure 2. The melting curves of rapeseed oils were characterized by two endothermic peaks, where the second peak was the major peak, appearing at −13°C, while the melting temperature range was from −30°C to −5°C. In the case of DSC profiles of soybean and sunflower oils, four and three endothermic peaks were identified, respectively, within the transition temperature range from −45°C to 0°C for both oils. For soybean and sunflower oils, the main peak was at a similar temperature, around −24°C. However, there were two peaks (at −18°C and −5°C) after the main peak for soybean oil and one peak at −9°C for sunflower oil. For soybean and sunflower oils, the curves showed differences in the number of peaks; however, corresponding peaks had similar magnitudes of transition and there was a similar temperature range of melting transition. These can be more explicitly described by analyzing the results shown in Table 2 collating DSC parameters, like peak temperature, peak heat flow and enthalpy of the refined oils. The highest transition magnitude was observed for the second peak (h2) of the rapeseed oil samples, *i.e.*, 0.48 W/g, whereas the main peak heat flows of the soybean oils and sunflower oils were 0.28 and 0.31 W/g, respectively. Additionally, during melting transition, two more shoulder peaks were detected for soybean oils, and one for sunflower oils. Comparing ΔH determined for the whole melting process, soybean oils show

Table 2. Differential scanning calorimetry (DSC) parameters of the melting curves of refined oils.

Parameter		Rapeseed oil	Soybean oil	Sunflower oil
Peak temperature (°C)	T1	−23.18±0.50	−32.23±0.68	−32.16±0.28
	T2	−13.49±0.65	−24.09±0.40	−24.83±0.87
	T3	-	−18.06±0.47	−8.57±0.33
	T4	-	−5.20±0.39	-
Peak heat flow (W/g)	h1	0.13±0.01	0.20±0.01	0.21±0.02
	h2	0.48±0.01	0.28±0.02	0.31±0.02
	h3	-	0.23±0.01	0.06±0.04
	h4	-	0.06±0.01	-
Enthalpy (J/g)	ΔH	63.91±0.94	58.42±2.78	61.14±3.18

All values are mean ± standard deviation (n=6); T1, T2, T3 and T4 represent the first, second, third and fourth peak temperatures, respectively; h1, h2, h3 and h4 mean heat flow for the first, second, third and fourth peak, respectively; ΔH represents enthalpy for the whole melting phase transition.

the lowest value (58.42 J/g), in contrast to rapeseed oils, for which the highest enthalpy was measured (63.91 J/g). A similar experimental approach was presented by other authors [Tan & Che Man, 2000], who characterized canola, soybean and sunflower oils after heating at a rate of 5°C/min and identified two peaks for canola and four peaks for the soybean and sunflower oils, where the position of peaks differed from that found in our study. Comparable results obtained for the melting profiles at a heating rate of 5°C/min for sunflower oils with three peaks (−36°C, −27°C, and −11°C) and rapeseed oil with two peaks (−23°C and −15°C) were reported by Rudakov *et al.* [2021]. Other authors [Teh & Birch, 2013] reported two major endothermic peaks at −23°C and −9°C for cold-pressed canola oils with a 1°C/min program, which is comparable to the results of our study.

Chemometric analysis of melting profiles of cold--pressed and refined oils

The main goal of this study was to use data obtained from the DSC technique to authenticate three cold-pressed oils and to differentiate them from the refined oils by analyzing the melting phase transitions. Since it could be seen (Figure 1 and 2) that the DSC profiles obtained for all oils (cold-pressed and refined) were visually different, it was necessary to decide at this stage which results and methods to choose for discrimination. To solve this problem, two potential approaches were considered in this study. The first was to compare the parameters determined from the curves, which are presented in Table 1 and Table 2. The second approach was based on comparing the entire phase transition spectrum using chemometric methods. The disadvantage of the first approach was the fact that melting profiles consist of a different number of peaks at different positions, which makes it difficult to compare them with each other. Thus, the authors decided to compare the whole melting profiles of oils expressed by normalized heat flow (W/g), which were tested as variables using SIMCA software. Multivariate data analyses, *i.e.*, PCA and OPLS-DA, were conducted to assess the usability of DSC melting profiles in classifying and distinguishing cold-pressed and refined oils. The first step was to compare two groups of oils, refined oils *vs.* cold-pressed oils. PCA – a widely used, unsupervised analysis – was employed to uncover and visualize the underlying patterns of variations within a dataset. Figure 3A shows a score plot with oils separated into two groups: refined and cold-pressed ones. Based on the DSC data matrix, the two principal components, t[1] and t[2] were established, which accounted for 80.8% of the variation in the values of normalized heat flow of the melting profiles. Next, an OPLS-DA model was built on the same data matrix, which focused on the separation of two oil classes: refined and cold-pressed ones (Figure 3B). The OPLS-DA is a multivariate statistical method that is commonly used for the classification and prediction of data with multiple variables. The OPLS-DA model separates the systematic variation in X (normalized heat flow) into two parts: one that is linearly related (and therefore predictive) to Y (representing classes), and one that is orthogonal to Y. The Y-predictive part represents the between-class variation and the Y-orthogonal part constitutes the within-class variation. A score plot of cold-pressed and refined oils classified into six classes in the space of two components: t[1] – predictive and t_o[1] – orthogonal, is shown in Figure 3B. The model fit was described by the coefficient R^2X(cum)=0.807, which is the cumulative R^2X of the fractions of the X variation modeled in the component, using the X model, the R^2(cum)=0.978, which is the cumulative R^2 of the fractions of Y variation modeled in the component, using the X model, and Q^2(cum)=0.977, which is cumulative Q^2 of fractions of Y variation predicted according to cross-validation in the component, using the X model. It can also be noticed that the separation in both classes, occurring relative to components t[1] and t[2], is additionally connected with the appearance of two subclasses for each class, which are located on opposite sides (Figure 3A). However, the difference between subclasses is smaller for refined oils compared to cold-press oils. This suggests some similarities inside both classes, leading to their differentiation. The existence of subclasses inside each class was confirmed

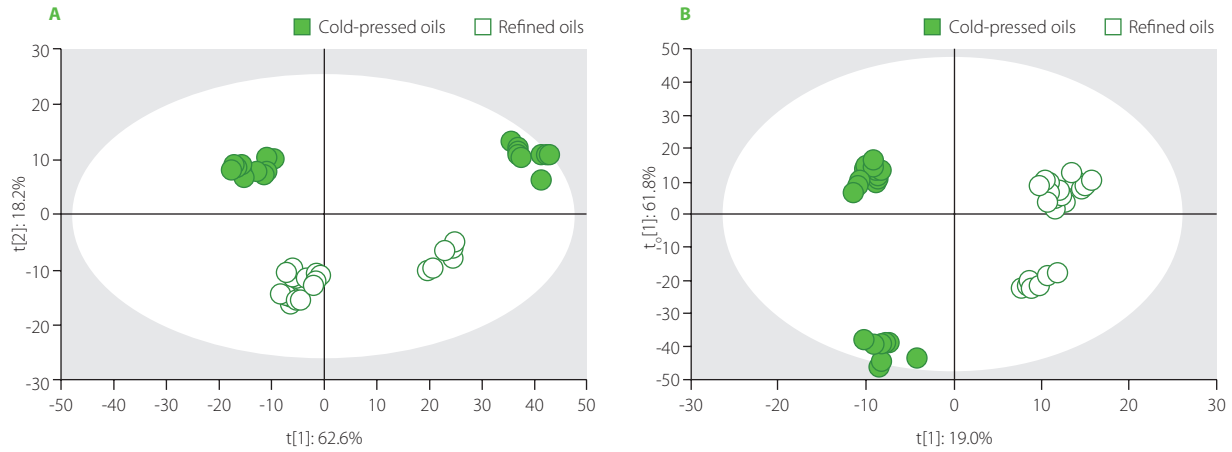

Figure 3. Differentiation between cold-pressed and refined oils based on their differential scanning calorimetry (DSC) melting profiles; (**A**) principal component analysis (PCA) score plot; where t[1] and t[2] are the first and second principal components, respectively; (**B**) orthogonal partial least square-discriminant analysis (OPLS-DA) score plot; where t[1] and t_o[1] are predictive and orthogonal components, respectively.

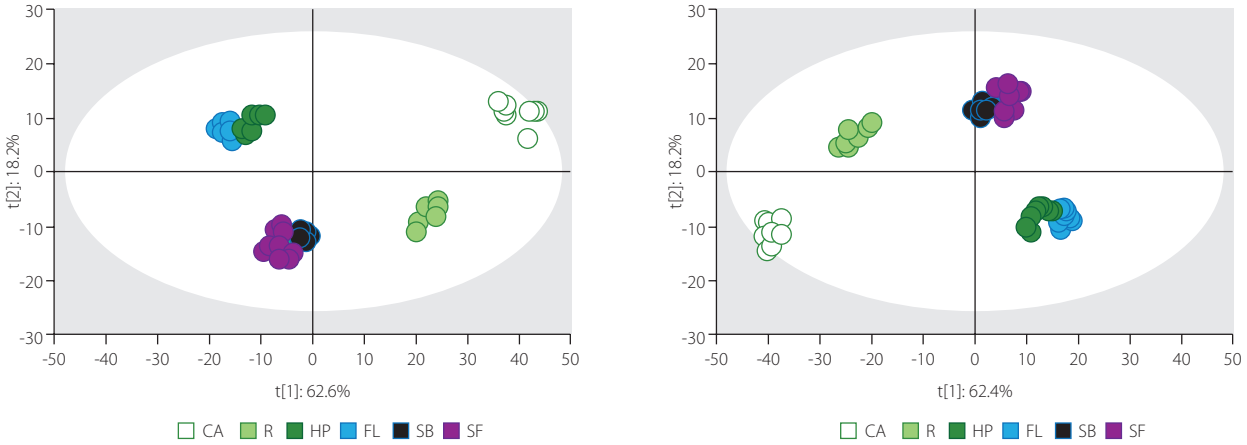

Figure 4. Distinguishing oils based on their differential scanning calorimetry (DSC) melting profiles; (**A**) principal component analysis (PCA) score plot; where t[1] and t[2] are the first and second principal components, respectively; (**B**) orthogonal partial least square-discriminant analysis (OPLS-DA) score plot; where t[1] and t[2] are predictive and orthogonal components, respectively. CA, camelina seed oil; FL, flaxseed oil; HP, hempseed oil; R, rapeseed oil; SB, soybean oil; SF, sunflower seed oil.

by the OPLS-DA method, where orthogonal component t_o[1] also shows differentiation inside the class of unrefined oils (Figure 3B).

Since the orthogonal component in X was significant ($R^2X = 0.618$), indicating that the variation within the class of cold-pressed oils and within the class of refined oils was high (Figure 3B), the next step was to analyze all six types of oils as six classes by using PCA (Figure 4A) and OPLS-DA (Figure 4B). Figure 4A shows a score plot of the PCA results with the oils separated into six groups: three refined oils (rapeseed, soybean and sunflower) and three cold-pressed oils (flaxseed, camelina, hempseed), in the space of the two first principal components t[1] and t[2], which accounted for 80.8% of the total variation. The score plot with the clear classification and discrimination of six types of oils conducted by means of the OPLS-DA is shown in Figure 4B. Five predictive components (P1-P5) and two orthogonal components in X (O1, O2) were calculated by the OPLS-DA. The variation modelled for X using all predictive components and orthogonal components in X gave the value of $R^2X(cum)=0.971$, which is a measure of model fit. The next parameters of OPLS-DA, $R^2(cum)$ and $Q^2X(cum)$, were equal to 0.916 and 0.887, respectively. Individual values of Q^2 calculated for five components are the fractions of the Y variation predicted according to cross-validation in the component using the X model. All Q^2 values were in the range from 0.143 to 0.198 and all were higher than the limit of 0.01, which is the critical value of Q^2 below which the component is insignificant.

Summing up, it can be stated that all parameters ($R^2X(cum)$, $R^2(cum)$ and $Q^2X(cum)$) indicated that the model established by the OPLS-DA fitted the data of DSC profiles and enabled reliable classification of oils into six classes. The variables influence on projection (VIP) plot shown in Figure 5 reflects selected variables, which are of the highest importance for oil differentiation. Normalized VIP values were in the range from 0.3 to 1.6, while the average squared VIP value was 1. Since only variables with VIP values above 1 are important, only such variables are shown in Figure 5. It can be seen that, in this model, the most important

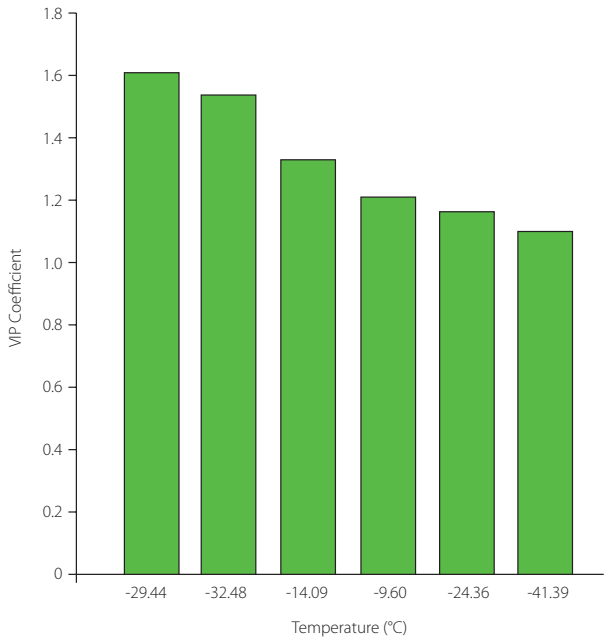

Figure 5. Variables influence on projection (VIP) plot showing the most important variables of heat flow values detected at different temperatures.

for oil discrimination were the heat flow values of the DSC profiles measured at temperatures of −29.44±0.32°C, −32.48±1.80°C, −14.09±1.61°C, −9.60±0.71°C, −24.36±0.94°C, and −41.39±0.77°C.

CONCLUSIONS

This study presents a novel approach for authenticating oils by using the whole spectrum of their DSC melting profiles. The DSC profiles combined with advanced chemometric methods of OPLS-DA were used to distinguish cold-pressed oils (flaxseed, camelina, hempseed) from refined oils (rapeseed, sunflower, soybean) in order to establish a model for their classification. The results showed that the DSC melting profiles can be considered as a fingerprint of each oil, since they differed in the number of peaks and their position. Flaxseed and hempseed oils exhibited four endothermic peaks, in contrast to camelina seed oil, for which three peaks with one exothermic event were detected. For the refined oils, two endothermic peaks were detected for rapeseed oil, three for sunflower oil and four for soybean oil. Additionally, it was stated that thermodynamic parameters, such as peak temperature, peak heat flow and enthalpy, differed for each type of oil. The results from the PCA and OPLS-DA showed successful classification of different edible oils into two classes (refined and cold-pressed), as well as into six classes according to the oil type. The model fitted the data well, as indicated by the R^2X(cum), R^2(cum), and Q^2X(cum) values, which assessed the variation in the X (normalized heat flow) and Y (classes) data. Furthermore, it was shown that certain heat flow values measured at specific temperatures were crucial for differentiating the oils. These variables played a significant role in the discrimination of oils based on their melting profiles.

The study provides practical information on the utility and the potential of the DSC profiles for the detection of frauds, as it was in the case of olive oil scandal in Western Europe in 2019, where refined sunflower oil was colored with chlorophylls and beta-carotene to mirror olive oil and sold as extra virgin olive oil. The approach presented in this study could lead to future research addressing more expensive and highly nutritious plant fats and oils available on the market, to build a database of their fingerprints to be analyzed by chemometric methods for authentication.

RESEARCH FUNDING

This research was funded by the National Science Centre, Poland, grant number: 2018/31/B/NZ9/02762.

CONFLICT OF INTERESTS

The authors declare that they have no competing interests.

ORCID IDs

E. Fornal https://orcid.org/0000-0002-0503-0706
M. Islam https://orcid.org/0000-0003-1860-3718
M. Montowska https://orcid.org/0000-0002-6331-5726
J. Tomaszewska-Gras https://orcid.org/0000-0003-3964-8093

REFERENCES

1. Angiuli, M., Bussolino, G.C., Ferrari, C., Matteoli, E., Righetti, M.C., Salvetti, G., Tombari, E. (2009). Calorimetry for fast authentication of edible oils. *International Journal of Thermophysics*, *30*(3), 1014–1024. https://doi.org/10.1007/s10765-009-0592-4
2. Aydeniz Güneser, B., Yilmaz, E., Ok, S. (2017). Cold pressed *versus* refined winterized corn oils: Quality, composition and aroma. *Grasas y Aceites*, *68*(2), art. no. e194. https://doi.org/10.3989/gya.1168162
3. Brożek, O., Kiełczewska, K., Bohdziewicz, K. (2022). Characterisation of selected emulsion phase parameters in milk, cream and buttermilk. *Polish Journal of Food and Nutrition Sciences*, *72*(1), 5–15. https://doi.org/10.31883/pjfns/144223
4. De Souza, L.M., De Santana, F.B., Gontijo, L.C., Mazivila, S.J., Borges Neto, W. (2015). Quantification of adulterations in extra virgin flaxseed oil using MIR and PLS. *Food Chemistry*, *182*, 35–40. https://doi.org/10.1016/j.foodchem.2015.02.081
5. Dyszel, S.M., Baish, S.K. (1992). Characterization of tropical oils by DSC. *Thermochimica Acta*, *212*(C), 39–49. https://doi.org/10.1016/0040-6031(92)80218-L
6. Gharby, S. (2022). Refining vegetable oils: Chemical and physical refining. *Scientific World Journal*, *2022*, art. no. 6627013. https://doi.org/10.1155/2022/6627013
7. Gogolewski, M., Nogala-Kalucka, M., Szeliga, M. (2000). Changes of the tocopherol and fatty acid contents in rapeseed oil during refining. *European Journal of Lipid Science and Technology*, *102*(10), 618–623. https://doi.org/10.1002/1438-9312(200010)102:10<618::aid-ejlt618>3.3.co;2-y
8. Islam, M., Bełkowska, L., Konieczny, P., Fornal, E., Tomaszewska-Gras, J. (2022). Differential scanning calorimetry for authentication of edible fats and oils - What can we learn from the past to face the current challenges? *Journal of Food and Drug Analysis*, *30*(2), art. no. 2. https://doi.org/10.38212/2224-6614.3402
9. Islam, M., Kaczmarek, A., Tomaszewska-Gras, J. (2023). DSC melting profile of cold-pressed hemp seed oil as an authenticity fingerprint influenced by scanning rate. *Applied Sciences, 13*(6), art. no. 3975. https://doi.org/10.3390/app13063975
10. Jović, O., Jović, A. (2017). FTIR-ATR adulteration study of hempseed oil of different geographic origins. *Journal of Chemometrics*, *31*(12), art. no. e2938. https://doi.org/10.1002/cem.2938
11. Karbasian, M., Givianrad, M.H., Ramezan, Y. (2015). A rapid method for detection of refined olive oil as adulterant in extra virgin olive oil by Differential Scanning Calorimetry. *Oriental Journal Of Chemistry*, *31*(3), 1735–1739. https://doi.org/10.13005/ojc/310354
12. Karim, M., Karim, S., Rana, A., Masum, S., Mondol, A., Israt, S. (2015). ATR-FTIR spectroscopy and chemometric techniques for the identification of edible vegetable oils. *Bangladesh Journal of Scientific and Industrial Research*, *50*(4), 233–240. https://doi.org/10.3329/bjsir.v50i4.25830

13. Marikkar, M.N., (2014). DSC as a valuable tool for the evaluation of adulteration of oils and fats. In E. Chiavaro (Ed.) *Differential Scanning Calorimetry: Applications in Fat and Oil Technology*, 1st ed., CRC Press, Boca Raton, USA. https://doi.org/10.1201/b17739
14. Moigradean, D., Poiana, M.A., Gogoasa, I. (2015). Use of ATR-FTIR spectroscopy to detect the changes in extra virgin olive oil by adulteration with soybean oil and high temperature heat treatment. *Open Chemistry*, *13*(1), 689–698. https://doi.org/10.1515/chem-2015-0110
15. Nikolaichuk, H., Przykaza, K., Kozub, A., Montowska, M., Wójcicka, G., Tomaszewska-Gras, J., Fornal, E. (2022). Shotgun lipidomic analysis for differentiation of niche cold pressed oils. *Molecules*, *27*(6), art. no. 1848. https://doi.org/10.3390/molecules27061848
16. Oomah, B.D., Sitter, L. (2009). Characteristics of flaxseed hull oil. *Food Chemistry*, *114*(2), 623–628. https://doi.org/10.1016/j.foodchem.2008.09.096
17. Piravi-vanak, Z., Azadmard-Damirchi, S., Kahrizi, D., Mooraki, N., Ercisli, S., Savage, G.P., Rostami Ahmadvandi, H., Martinez, F. (2021). Physicochemical properties of oil extracted from camelina (*Camelina sativa*) seeds as a new source of vegetable oil in different regions of Iran. *Journal of Molecular Liquids*, *345*, art. no. 117043. https://doi.org/10.1016/j.molliq.2021.117043
18. Punia, S., Sandhu, K.S., Dhull, S.B., Kaur, M., Siroha, A. K. (2020). Kinetic, rheological and thermal studies of flaxseed (*Linum usitatissiumum* L.) oil and its utilization. *Journal of Food Science and Technology*, *57*(11), 4014–4021. https://doi.org/10.1007/s13197-020-04434-1
19. Rajagukguk, Y.V., Utcu, M.A., Islam, M., Muzolf-Panek, M., Tomaszewska-Gras, J. (2022). Authenticity assessment from sesame seeds to oil and sesame products of various origin by Differential Scanning Calorimetry. *Molecules*, *27*(21), art. no. 7496. https://doi.org/10.3390/molecules27217496
20. Ratusz, K., Symoniuk, E., Wroniak, M., Rudzińska, M. (2018). Bioactive compounds, nutritional quality and oxidative stability of cold-pressed camelina (*Camelina sativa* L.) oils. *Applied Sciences (Switzerland)*, *8*(12), art. no. 2606. https://doi.org/10.3390/app8122606
21. Rodríguez-Rodríguez, M.F., Moreno-Pérez, A.J., Makni, S., Troncoso-Ponce, M.A., Acket, S., Thomasset, B., Sánchez, R., Venegas-Calerón, M., Garcés, R., Martínez-Force, E., Salas, J.J. (2021). Lipid profiling and oil properties of *Camelina sativa* seeds engineered to enhance the production of saturated and omega-7 fatty acids. *Industrial Crops and Products*, *170*, art. no. 113765. https://doi.org/10.1016/j.indcrop.2021.113765
22. Rousseau, D., Hodge, S.M., Nickerson, M.T., Paulson, A.T. (2005). Regulating the beta prime to beta polymorphic transition in food fats. *JAOCS – Journal of the American Oil Chemists' Society*, *82*(1), 7–12. https://doi.org/10.1007/s11746-005-1035-z
23. Rudakov, O.B., Saranov, I.A., Van, A.N., Rudakova, L.V., Polyanskiy, K.K. (2021). Differential Scanning Calorimetry as a method for the control of vegetable oils. *Journal of Analytical Chemistry*, *76*(2), 258–266. https://doi.org/10.1134/S1061934821020118
24. Sato, K., Bayés-García, L., Calvet, T., Cuevas-Diarte, M.À., Ueno, S. (2013). External factors affecting polymorphic crystallization of lipids. *European Journal of Lipid Science and Technology*, *115*(11), SI, 1224–1238. https://doi.org/10.1002/ejlt.201300049
25. Siudem, P., Wawer, I., Paradowska, K. (2019). Rapid evaluation of edible hemp oil quality using NMR and FT-IR spectroscopy. *Journal of Molecular Structure*, *1177*, 204–208. https://doi.org/10.1016/j.molstruc.2018.09.057
26. Tan, C.P., Che Man, Y.B. (2000). Differential scanning calorimetric analysis of edible oils: Comparison of thermal properties and chemical composition. *JAOCS – Journal of the American Oil Chemists' Society*, *77*(2), 143–155. https://doi.org/10.1007/s11746-000-0024-6
27. Teh, S.S., Birch, J. (2013). Physicochemical and quality characteristics of cold-pressed hemp, flax and canola seed oils. *Journal of Food Composition and Analysis*, *30*(1), 26–31. https://doi.org/10.1016/j.jfca.2013.01.004
28. Tomaszewska-Gras, J. (2016). Multivariate analysis of seasonal variation in the composition and thermal properties of butterfat with an emphasis on authenticity assessment. *Grasas y Aceites*, *67*(4), art. no. e167. https://doi.org/10.3989/gya.0453161
29. Tomaszewska-Gras, J., Islam, M., Grzeca, L., Kaczmarek, A., Fornal, E. (2021). Comprehensive thermal characteristics of different cultivars of flaxseed oil (*Linum usittatissimum* L.). *Molecules*, *26*(7), art. no. 1958. https://doi.org/10.3390/molecules26071958
30. Vaisali, C., Charanyaa, S., Belur, P.D., Regupathi, I. (2015). Refining of edible oils: A critical appraisal of current and potential technologies. *International Journal of Food Science and Technology*, *50*(1), 13–23. https://doi.org/10.1111/ijfs.12657
31. Van Wetten, I.A., Van Herwaarden, A.W., Splinter, R., Boerrigter-Eenling, R., Van Ruth, S.M. (2015). Detection of sunflower oil in extra virgin olive oil by fast differential scanning calorimetry. *Thermochimica Acta*, *603*, 237-243. https://doi.org/10.1016/j.tca.2014.11.030
32. Wroniak, M., Krygier, K., Kaczmarczyk, M. (2008). Comparison of the quality of cold pressed and virgin rapeseed oils with industrially obtained oils. *Polish Journal of Food and Nutrition Sciences*, *58*(1), 85–89.
33. Xu, B., Li, P., Ma, F., Wang, X., Matthäus, B., Chen, R., Yang, Q., Zhang, W., Zhang, Q. (2015). Detection of virgin coconut oil adulteration with animal fats using quantitative cholesterol by GC × GC-TOF/MS analysis. *Food Chemistry*, *178*, 128–135. https://doi.org/10.1016/j.foodchem.2015.01.035
34. Yanty, N.A.M., Marikkar, J.M.N., Long, K. (2011). Effect of varietal differences on composition and thermal characteristics of avocado oil. *JAOCS – Journal of the American Oil Chemists' Society*, *88*(12), 1997–2003. https://doi.org/10.1007/s11746-011-1877-x
35. Zhang, Z., Wei, Y., Guan, N., Li, B., Wang, Y. (2022). Changes in chemical composition of flaxseed oil during thermal-induced oxidation and resultant effect on DSC thermal properties. *Molecules*, *27*(20), art. no. 7135. https://doi.org/10.3390/molecules27207135
36. Zhang, Z.S., Li, D., Zhang, L.X., Liu, Y.L., Wang, X.D. (2014). Heating effect on the DSC melting curve of flaxseed oil. *Journal of Thermal Analysis and Calorimetry*, *115*(3), 2129–2135. https://doi.org/10.1007/s10973-013-3270-5
37. Zhang, Z.S., Wang, L.J., Li, D., Li, S.J., Ozkan, N. (2011). Characteristics of flaxseed oil from two different flax plants. *International Journal of Food Properties*, *14*(6), 1286–1296. https://doi.org/10.1080/10942911003650296

ORIGINAL ARTICLE
http://journal.pan.olsztyn.pl

Polish Journal of Food and Nutrition Sciences
2023, Vol. 73, No. 3, 233–241
DOI: 10.31883/pjfns/169483
ISSN 1230-0322, e-ISSN 2083-6007

Sensory Characteristics and Consumer Liking of Basil Syrups (*Ocimum basilicum L.*) in Different Sensory Settings

Ervina Ervina[1]*, Kyle Bryant[1], Dwi L. Nur Fibri[2], Wahyudi David[3]

[1]Food Technology Department, Faculty of Engineering, Bina Nusantara University, Jakarta 11480, Indonesia
[2]Department of Food and Agricultural Product Technology, Faculty of Agricultural Technology, Universitas Gadjah Mada, Yogyakarta, Central Java 55281, Indonesia
[3]Department of Food Science and Technology, Bakrie University, Jakarta 12920, Indonesia

The objective of this study was to investigate the sensory profiles of basil syrups formulated with different contents of basil leaf extract and sugar, and to determine the key attributes of consumer liking. Moreover, this study also measured consumers' perceptions in two sensory evaluation settings of blind and non-blind (informed) tests. Sixty adult consumers were involved in the evaluation. The basil leaf extract and sugar contents influenced the sensorial characteristic of basil syrups. Moreover, consumers had different perceptions and changed their preferences for this product in different sensory evaluation settings. Information related to ingredients and sugar contents was demonstrated to consumers to enable the shift in their preferences. Consumers perceived the basil syrups as significantly healthier in the non-blind setting (p<0.001) compared to the blind test (p=0.110). Moreover, the liking showed to be significantly higher in the non-blind setting compared to the blind test (p=0.050), especially for the sugar-free samples. This research could be used as a preliminary study to further develop functional drinks made from basil leaves and to consider the information regarding food ingredients provided to consumers.

Key words: blind test, check-all-that-apply, informed test, consumer perception, sugar

INTRODUCTION

The demand for functional food and nutraceuticals increased tremendously during the Covid-19 pandemic [Lestari, 2021], suggesting the shifting of food intake patterns from satisfying hunger to promoting health and wellness [Farzana *et al.*, 2022; Lestari, 2021]. Today, consumers want to take responsibility for their healthcare and well-being, and functional food is aimed to address these specific needs. The development of functional food should involve consumers because they have specific health and nutritional needs [Alongi & Anese, 2021]. Bioactive compounds from plants and traditional herbs frequently become a target for functional food development since these ingredients confer many potential health benefits [Chandrasekara & Shahidi, 2018; Serrano *et al.*, 2018].

Basil (*Ocimum basilicum* L.) is one of the traditional herbs that has the potential to be developed as a functional food product. The plant belongs to the mint family and is indigenous to tropical regions, including Indonesia. *O. basilicum* also well known as wild basil or *Kemangi* in Bahasa Indonesia [Shahrajabian *et al.*, 2020], is an aromatic herb that has been widely used in many cuisines. Basil confers many health benefits and traditionally has been used for the treatment of fever, cough, flu, asthma, and diarrhea [Shahrajabian *et al.*, 2020]. Moreover, the leaves also contain bioactive compounds responsible for their anticancer, radioprotective, antimicrobial, anti-inflammatory, anti-stress, antidiabetic,

***Corresponding Author:**
e-mail: ervina002@binus.ac.id (E. Ervina)

Submitted: 9 February 2023
Accepted: 11 July 2023
Published on-line: 2 August 2023

and hypolipidemic effects, and high antioxidant activity [Dhama *et al.*, 2023; Kozlowska *et al.*, 2021; Sestili *et al.*, 2018; Teofilović *et al.*, 2021; Zhan *et al.*, 2020]. The basil leaves have been used broadly in different foods and beverages [Mäkinen & Pääkkönen, 1999; Uzun & Oz, 2021]. Most of the plant's leaves have been used as herbs in meals [Baliga *et al.*, 2016] or consumed as fresh vegetables in mixed salads. The most well-known application of basil leaves is in Italian pesto [Snežana, 2017] while in another study, the leaves were added in cheese to improve taste and aroma [Ribas *et al.*, 2019]. A recent publication utilized basil leaves to increase the antioxidant and acceptance levels in roselle (hibiscus) drinks [Abidoye *et al.*, 2022].

Understanding the key characteristics of a food product is important in order to determine product's acceptability. Moreover, sensory profiles of the products were able to significantly affect consumer acceptability [Chambers, 2019; Topolska *et al.*, 2021]. The appearance, texture, flavor, taste, aroma and even sound of foods can impart a desire to eat and promote liking [Chambers, 2019]. In addition, there was a strong and positive correlation between sensory profiles and consumption of functional food products, suggesting that taste and aroma play a significant role in determining consumer acceptability of a new functional food [Urala & Lähteenmäki, 2004].

Sensory descriptive analysis can be used to distinguish sensory characteristics of specific food and highlight their differences [Marques *et al.*, 2022; Yang & Lee, 2019], whereas consumer research can be deployed to identify factors that affect food acceptability [Ruiz-Capillas & Herrero, 2021]. The main objective of this study was to identify the sensory characteristic of syrups made from *O. basilicum* leaves and the key consumer liking drivers using the check-all-that-apply (CATA) method. In addition, two methods of consumer testing, *i.e.*, comparing blind test (without any information provided, coded samples) and non-blind test (with information regarding the samples, non-coded samples) were applied in this study. This was aimed to evaluate consumer perceptions and preferences in an informed setting. Based on previous literature, consumers were shown to have different perceptions towards foods in blind and non-blind settings, demonstrating that information may be able to influence their preferences [Bemfeito *et al.*, 2021; Fibri & Frøst, 2020; Mazhangara *et al.*, 2022]. This is the first study to investigate the sensory characteristics and the key driver of consumer liking of basil syrups in different formulations and at the same time evaluate consumers' perceptions in the different sensory evaluation settings (blind *vs*. non-blind test).

MATERIALS AND METHODS

Preparation of the basil syrups

The syrups were made using fresh basil leaves (purchased in Sekolah Seniman Pangan, Javara Indonesia), sugar, and water as the main ingredients. The main formulation had followed the previous study with modification [Pratama *et al.*, 2013]. The first step was to make a sugar solution by adding caster sugar (100 g) and water in a 1:1 (*w/v*) ratio. The solution was then mixed and boiled until the sugar dissolved. The second step was to make the basil extract by blending the chopped basil leaves (100 g) using an HR2223 blender (Philips, Jakarta, Indonesia) with water in a 1:1 (*w/v*) ratio for 2 min and filtering the mixture using a stainless-steel filter mesh (20 mesh, BZ Wire Mesh Products Co., Anping, China) to separate the liquid (extract) and the sediment. The basil extract was then heated until it reached 100°C for around 2 min and blended with the syrup solution in various proportions. The basil syrups were then placed in sterilized glass jars for the cooling process. Afterwards, they were sealed and packaged in closed 10-mL disposable cups to be evaluated by consumers. Before evaluation, the samples were stored at ambient temperature.

This study evaluated the different addition levels of basil leaf extract to the syrup solution, *i.e.*, 5%, 10%, 15% and 20% (*v/v*) (samples F1, F2, F3 and F4, respectively). In addition, three alternative sugar versions were analyzed, including: 10% (*v/v*) of basil extract with 50% sugar reduction (the sugar portion (50 g) was replaced with 4 g of steviol glycosides (Stevia, Tropicana Sweetener, Nutrifood, Cikarang, Indonesia) (sample F5), 10% (*v/v*) of basil extract with no added sugar (100% sweeteners; the sugar portion (100 g) was replaced with 8 g of steviol glycosides) (sample F6), and 10% (*v/v*) of basil extract with the addition of 50 g of honey (Madurasa, Natural Honey, Banten, Indonesia) instead of sugar (sample F7). All formulations were presented in Table 1. Three batches were prepared for each of the formulations.

Table 1. Formulations of basil syrups.

Syrup code	Content of basil extract in syrup	Composition of sweetening ingredients of the syrup
F1:5%	5% (*v/v*)	100% sugar
F2:10%	10% (*v/v*)	100% sugar
F3:15%	15% (*v/v*)	100% sugar
F4:20%	20% (*v/v*)	100% sugar
F5:10%+SR	10% (*v/v*)	50% sugar reduction (SR) (replaced by sweetener (SWE) – steviol glycosides)
F6:10%+SWE	10% (*v/v*)	Sugar 100% replaced by SWE – steviol glycosides
F7:10%+HN	10% (*v/v*)	Sugar 100% replaced by honey (HN)

Determination of CATA method attributes

All the attributes were generated and discussed during the focus group discussion (FGD) session by eight trained panels (5 women and 3 men, mean age: 28.6 years) from the Food Technology Department, Bina Nusantara University, Jakarta, Indonesia. Each of the panelists was served all the samples and asked to write all the sensations that they perceived [Ervina *et al.*, 2020]. In addition, raw basil leaves, sugar, lemongrass, mint, honey, fresh cut lemon, fresh cut grass, and raw leafy vegetables were also presented as the references to confirm the perceived sensation from the samples. The similar attributes generated by panelists were then grouped together (*i.e.*, thin, watery, water-like and water merged as thin). The CATA questions for the non-sensory attributes were adapted from the previous study [Kim *et al.*, 2013].

Procedures in consumer tests

In total, 60 untrained panelists participated in this study (50% men and 50% women, mean age: 24.5 years). Prior to the tests, an introduction regarding the study was explained and the digital consent forms were collected by asking the respondents to thick the "agreed" box in the online questionnaire if they were willing to participate. In addition, a verbal consent was also asked at the beginning of the evaluation, all the participations was voluntary. The list of the ingredients used in the samples were provided to the consumers at the beginning of the test to avoid recruiting someone with food allergies or dietary restrictions with one of the ingredients. The participants were also informed that all the data and information collected will be processed and stored as anonymous. The study has been approved by the ethical committee of the Research and Technology Transfer Office (RTTO), Bina Nusantara University, Jakarta, Indonesia (referral code: 60/VR.RTT/IV/year 2022) and has followed the World Medical Association (WMA) declaration of Helsinki [WMA, 2013].

The tests were divided into two parts. The first part was the blind test, all the samples were coded in a three-digit--random number and served monadically to the participants in a random order. The second part was the non-blind test, the participants were provided with the information regarding the samples (*i.e.*, the ingredient list, sugar content such as 100% sugar, 50% reduced sugar, no sugar added or replaced with sweetener and honey). Noteworthy is that the consumers had no information that the first and second part was actually evaluating the same samples. The blind test evaluated all the samples presented in Table 1. This evaluation included the overall liking and all the CATA attributes, while the non-blind test evaluated only samples F2, F5, F6 and F7 and focused on evaluating the overall liking and the non-sensory attributes only. Consumer liking was measured using a 9-point hedonic scale and was always evaluated first followed by the CATA questions. The participants were asked to tick the attribute (check-all-that-apply) if it was perceived in the sample [Piochi *et al.*, 2021; Tarancón *et al.*, 2020]. They were also asked to rinse their mouth with water before tasting and in between sample tasting. A short break for around two minutes was provided to ensure all the sensation from the previous sample had vanished before the participants continued to the next sample. The results of CATA questions were expressed as percentage of frequency of perception of each attribute by consumers.

Statistical analysis

The CATA results were analyzed using Cochran's Q test [Galler *et al.*, 2020]. The attribute with a significant difference ($p \leq 0.05$) was then further analyzed using McNemar-Bonferroni test. The correspondence analysis was employed to map the associations between the attributes and the samples. In addition, the penalty analysis was conducted to evaluate which attributes significantly impacted liking. To evaluate the differences between the blind and the non-blind test setting on liking, a Student's *t*-test was conducted. All the data was analyzed using XLSTAT Sensory version (Addinsoft, Paris, France, Version 2019.2.2).

RESULTS AND DISCUSSION

Sensory characteristics of the basil syrups

Thirty-two attributes of basil syrups were determined and used in the CATA method. They consisted of 3 visual attributes, 9 aromas, 10 tastes, 2 textures and 8 non-sensory attributes. The complete attributes are listed in Table 2. CATA can incorporate both sensory and non-sensory properties such as emotion or feeling when consumers tasted the products or the perception related to price, usage occasions, and product positioning [Ruiz-Capillas *et al.*, 2021; Varela & Ares, 2012], which makes this method very consumer oriented. CATA method has been reported as a valid method to discriminate products' characteristics using untrained panel or consumers [Tarancón *et al.*, 2020].

The frequency of consumer-perceived CATA sensory attributes of each basil syrup recipe in a blind test is presented

Table 2. Check-all-that-apply (CATA) attributes.

Visual	Aroma	Taste	Texture	Non-sensory
Light green	Sweet	Sweet	Thick (viscous)	Fresh
Dark green	Bitter	Bitter	Thin (watery)	Innovative
Transparent	Basil	Umami (savory)		Herbal drink
	Lemongrass	Basil		Traditional drink
	Sour, citrus	Lemongrass		Calming
	Earthy	Sour, citrus		Healthy drink
	Grassy	Earthy		Vegetables
	Mint	Grassy		Sugary drink
	Honey	Mint		
		Honey		

in Table 3. For the texture attribute, most of the samples had thin and watery-like characteristic with F6 having the most watery texture (perceived by 100% of the participants) followed by F5 (90% of the participants). F6 is the formula of basil syrup without any sugar addition (replaced by sweetener), while F5 is the formula with 50% sugar reduction (substitute with sweetener). In beverages, sugar is not only used to sweeten taste but also to improve texture and mouthfeel [Wagoner *et al.*, 2018], therefore reducing or replacing sugar with sweetener will decrease the viscosity of the syrups.

For the color attributes, F7 (formulation with honey) appeared to be the most transparent and did not have dark green color (Table 3). The green color of basil may be covered with the yellow-to-dark amber color from honey [Aparna & Rajalakshmi, 1999]. The addition of basil extract at 10–20%, *v/v* (F2, F3, and F4) significantly increased the dark green color of the syrup, this may be due to the chlorophyl content of the basil leaves [Dadan *et al.*, 2021]. Interestingly, the dark green color was significantly less perceived when the sugar content was reduced or replaced by sweetener in F5 and F6, respectively. These phenomena can be explained due to the formation of sugar degradation product due to the heating process in the sample making [Hubbermann *et al.*, 2006]. The more sugar added in the formula enhanced the formation of the sugar-degradation product. This condition will contribute to the darker color of the final product [García *et al.*, 2017].

The basil aroma was perceived by more than 50% of the consumers in most of the formulations except for F7 (honey) and this trend was similar for the basil taste (Table 3). The taste and aroma of grassy were perceived high in the sample with 20% (*v/v*) addition of basil extract (F4). The *cis*-3-hexanal is abundant in green plants, including basil, and this aromatic compound contributes to the fresh-cut grass aroma or grassy odor [van Nieuwenburg *et al.*, 2019]. Interestingly, the taste and aroma of lemongrass

Table 3 The frequency of perception by consumers (%) of the sensory check-all-that-apply (CATA) attributes of the basil syrups with different contents of basil extract and sugar.

Attributes	F1:5%	F2:10%	F3:15%	F4:20%	F5:10%+RS	F6:10%+SWE	F7:10%+HN
Thin watery	61.7^{cd}	45.0^{d}	46.7^{d}	40.0^{d}	90.0^{ab}	100.0^{a}	80.0^{ab}
Thick viscous	38.3^{ab}	55.0^{a}	53.3^{a}	60.0^{a}	10.0^{cd}	0.0^{d}	20.0^{bc}
Light green	45.0^{b}	8.3^{cd}	1.7^{d}	5.0^{cd}	80.0^{a}	43.3^{b}	25.0^{bc}
Dark green	50.0^{b}	90.0^{a}	95.0^{a}	91.7^{a}	11.7^{c}	10.0^{c}	0.0^{c}
Transparent	5.0^{c}	1.7^{c}	3.3^{c}	3.3^{c}	8.3^{c}	46.7^{b}	75.0^{a}
Aroma sour/citrus	13.3^{b}	5.0^{b}	20.0^{ab}	8.3^{b}	26.7^{ab}	21.7^{ab}	51.7^{a}
Aroma honey	8.3^{b}	3.3^{b}	8.3^{b}	11.7^{b}	3.3^{b}	5.0^{b}	46.7^{a}
Aroma mint	6.7^{a}	8.3^{a}	3.3^{a}	10.0^{a}	5.0^{a}	5.0^{a}	16.7^{a}
Aroma basil	56.7^{b}	73.3^{ab}	80.0^{a}	76.7^{ab}	65.0^{ab}	56.7^{b}	28.3^{c}
Aroma sweet	46.7^{a}	31.7^{ab}	30.0^{ab}	25.0^{ab}	20.0^{b}	16.7^{b}	35.0^{ab}
Aroma grassy	25.0^{ab}	28.3^{ab}	21.7^{ab}	41.7^{a}	26.7^{ab}	31.7^{a}	6.7^{b}
Aroma bitter	0.0^{a}	6.7^{a}	1.7^{a}	3.3^{a}	8.3^{a}	15.0^{a}	1.7^{a}
Aroma lemongrass	30.0^{a}	40.0^{a}	30.0^{a}	36.7^{a}	21.7^{a}	21.7^{a}	21.7^{a}
Aroma earthy	1.7^{a}	6.7^{a}	8.3^{a}	11.7^{a}	6.7^{a}	15.0^{a}	8.3^{a}
Taste sour/citrus	13.3^{ab}	5.0^{b}	6.7^{b}	8.3^{ab}	6.7^{b}	11.7^{ab}	26.7^{a}
Taste honey	28.3^{bc}	35.0^{b}	35.0^{b}	21.7^{bc}	36.7^{b}	11.7^{c}	81.7^{a}
Taste mint	5.0^{a}	11.7^{a}	6.7^{a}	18.3^{a}	6.7^{a}	3.3^{a}	8.3^{a}
Taste basil	41.7^{ab}	56.7^{ab}	63.3^{a}	60.0^{a}	53.3^{ab}	26.7^{bc}	15.0^{c}
Taste sweet	91.7^{a}	88.3^{a}	85.0^{a}	80.0^{ab}	83.3^{ab}	56.7^{b}	71.7^{ab}
Taste grassy	6.7^{a}	11.7^{a}	20.0^{a}	23.3^{a}	13.3^{a}	26.7^{a}	8.3^{a}
Taste bitter	0.0^{b}	1.7^{b}	3.3^{b}	1.7^{b}	10.0^{b}	73.3^{a}	10.0^{b}
Taste lemongrass	23.3^{a}	20.0^{a}	18.3^{a}	16.7^{a}	16.7^{a}	15.0^{a}	8.3^{a}
Taste earthy	0.0^{a}	1.7^{a}	3.3^{a}	3.3^{a}	0.0^{a}	11.7^{a}	3.3^{a}
Taste umami/savory	1.7^{a}	3.3^{a}	5.0^{a}	3.3^{a}	3.3^{a}	5.0^{a}	3.3^{a}

Different letters in row showing significant differences based on McNemar-Bonferroni test ($p \leq 0.05$). SR, sugar reduction; SWE, sweetener; HN, honey. Syrup codes and their formulations are detailed in Table 1.

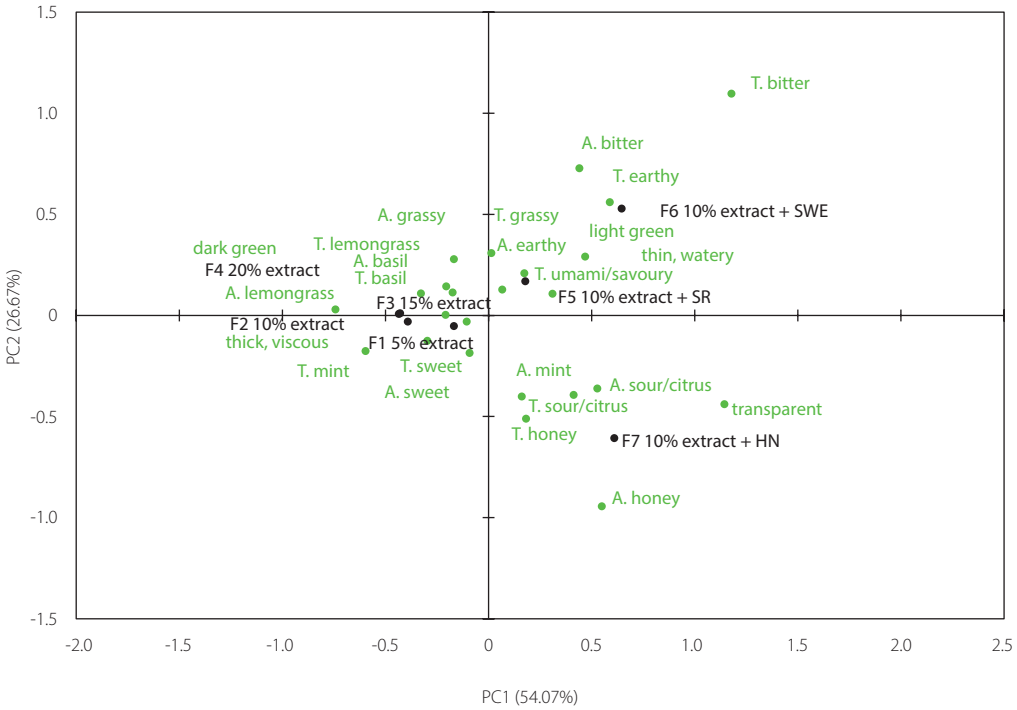

Figure 1. Plot of correspondence analysis of sensory attributes of basil syrups with different contents of basil extract and sugar. SWE, sweetener; SR, sugar reduction (50% sugar); HN, honey; A, aroma; T, taste. Syrup codes and their formulations are detailed in Table 1.

was also perceived in most of the samples, indicating that basil leaves contain similar odorants with lemongrass, such as linalool (contributes to floral and sweet notes), citral (lemon, citrus, sour), and myrcene (spices) [Patel *et al.*, 2021; Skaria *et al.*, 2006]. The bitter taste was perceived as extremely high in F6 (100% sweetener). The addition of sweetener to fully replace sugar in F6 may result in bitter note and bitter aftertaste of the basil syrups. Steviol glycosides were used as sweeteners in this study. This class of compounds has been reported to provide a strong bitterness intensity and bitter aftertaste [Hellfritsch *et al.*, 2012; Tao & Cho, 2020]. The stevia compounds were selected in this study because they are the natural-non-caloric sweetener and well-known by consumer [Tao & Cho, 2020]. The bitterness of steviol glycosides became the main challenge of food industries to use stevia as a non-nutritive sweetener [Hellfritsch *et al.*, 2012; Tian *et al.*, 2022]. Sweetness was perceived in most of the basil syrup samples except for F6. The sweetness intensity in F6 may be covered by the lingering bitter taste sensation from stevia and this may reduce the sweetness sensation [Tian *et al.*, 2022].

The sensory characteristics of each formulation were also mapped in a symmetric plot and presented in Figure 1. The two principal components of PC1 and PC2 contributed to 81% of variability. Based on the CATA mapping, the sensory profile between F1 (5% extract, *v/v*), F2 (10% extract, *v/v*), F3 (15% extract, *v/v*) and F4 (20% extract, *v/v*) lies on a similar group and in proximity. These samples were characterized with taste and aroma of sweet, lemongrass, basil, and dark green color. Moreover, samples made with 100% sugar (F1, F2, F3, and F4) lay on left quadrants and were separated with the samples made with sweetener or honey (F5, F6, and F7) which lay on right quadrant based on PC1. In addition, F5 and F6 were also separated with F7 based on PC2. Based on the mapping, F5 and F6 were associated with thin, watery, bitter aroma and bitter taste, while F7 was closely related to taste and aroma of citrus, honey, and was transparent in color. The sensory profiles of each formula presented in the mapping from Figure 1 were in line with what was described based on data in Table 3.

Blind test *vs.* non-blind test: Impact on consumers' perception and liking

This study also investigated the consumer perception for non-sensory attributes and their liking in different settings of blind test and non-blind test. Based on Cochran's Q test (Table 4), "healthy drink" was perceived as an important attribute in the non-blind test ($p<0.001$) but not in the blind test evaluation ($p=0.110$). Sugar content in the basil syrups may relate with health perceptions, because sugar is commonly associated with metabolic diseases such as diabetes, overweight and obesity [Reis *et al.*, 2017]. The consumers were informed regarding the sugar content of the samples (reduced sugar, replaced by sweetener, honey) in the non-blind test. The disclosure of health-related information of a product could significantly increase the willingness of consumers to try and to buy a product, and this information could positively modulate consumer perception [Grasso *et al.*, 2017]. In the case of sugar content, consumers may think that the sugar-reduced and the sugar-free version of the basil syrup is associated with healthiness, such as diabetes prevention, reduced calorie intake, and prevention of overweight and obesity, and thus able

Table 4. Cochran's Q test *p*-values for the non-sensory check-all-that-apply (CATA) attributes of the basil syrups in the blind test and non-blind test.

Attribute	Blind test	Non-blind test
Fresh	0.009	<0.001
Innovative	0.887	0.402
Herbal drink	<0.001	<0.001
Traditional drink	0.002	0.003
Calming	0.427	0.172
Healthy drink	0.110	<0.001
Vegetable	0.029	0.036
Sugary drink	<0.001	<0.001

to positively impact consumers perception and their acceptability [Reis *et al.*, 2017; Wardy *et al.*, 2018].

Table 5 presents the consumer perception for the non-sensory attributes in the blind and non-blind test of each basil syrup formula. The "healthy drink" attribute was perceived as significantly higher in the non-blind testing compared to the blind test, especially for the samples with sugar reduction (F5), no sugar (F6) and honey (F7). Sugar reduction has been closely correlated with health status as the WHO suggests to reduce sugar intake by less than 10% of the total dietary intake with a further reduction of 5% providing additional health benefits [Deliza *et al.*, 2021; WHO, 2015]. Moreover, previous studies have reported the association between sugar reduction and consumer perceptions [Deliza *et al.*, 2021; de Souza *et al.*, 2021; Wardy *et al.*, 2018] showing that consumers will provide positive attitude and prefer sugar-reduced or sugar-free version for health reasons. However, the perception of "sugary drink" was similar in both settings. We assume this could be influenced by the texture of the basil syrups. In the blind test, consumers already perceived the sugar-free samples as less sugary even though they had no information regarding the sugar content. The sugar-free version was characterized as thin, watery and having bitter taste, thus this might have influenced consumers perception regarding the sugar levels [Wagoner *et al.*, 2018].

The information provided to the consumers before the test could influence their perception to the product directly. For example, the information regarding coffee quality before tasting was reported to significantly increase consumers preferences [Bemfeito *et al.*, 2021]. Moreover, another study suggests that the nutritional information, such as sugar content, was able to influence consumer perception regarding physical health and emotional aspects of wellbeing [Reis *et al.*, 2017]. The same study also showed that consumer perception was significantly changed when they were provided information regarding the sugar content of the juice, in which consumers preferred juice without added sugar (sugar-free) [Reis *et al.*, 2017]. The use of sweetener is associated with less calorie foods, and consumers may have expectation that this product will provide health benefits [Deliza *et al.*, 2021; Wardy *et al.*, 2018].

The hedonic aspect was also evaluated to compare the liking score of the basil syrups in the blind and the non-blind setting. Based on the Student's *t*-test, the liking showed to be significantly higher (p=0.050) for the basil syrup with sweetener (no added sugar) in the non-blind test (mean liking score 4.72) compared to the blind test (4.03), while there were no significant differences for the other samples (Table 6). In addition, the results of the penalty analysis for the non-sensory attributes were different in the blind test and the non-blind test. The mean impact is presented in Table 7. The results show that "sugary drink" positively affected consumer liking in the blind test but not in the non-blind test setting. Moreover, "fresh", "innovative" and "healthy drinks" were able to significantly promote liking while "herbal drink" was found to decrease liking in the non-blind test. However, the results were different in the blind testing, as only the "sugary drink" positively impacted liking. The non-nutritive sweetener used in the syrup formulation may provide a "healthy" perception for consumers. Based on the penalty analysis, the "healthy drink"

Table 5. The frequency of perception by consumers (%) of non-sensory check-all-that-apply (CATA) attributes of basil syrups in the blind test and non-blind test.

Attribute	Blind test				Non-blind test			
	F2:10%	F5:10%+SR	F6:10%+SWE	F7:10%+HN	F2:10%	F5:10%+SR	F6:10%+SWE	F7:10%+HN
Fresh	16.7^{b}	10.0^{b}	6.7^{b}	25.0^{ab}	21.7^{ab}	11.7^{b}	8.3^{b}	38.3^{a}
Innovative	26.7^{a}	26.7^{a}	26.7^{a}	30.0^{a}	28.3^{a}	35.0^{a}	25.0^{a}	33.3^{a}
Herbal drink	25.0^{b}	18.3^{b}	58.3^{a}	33.3^{ab}	26.7^{ab}	15.0^{b}	51.7^{a}	35.0^{ab}
Traditional drink	3.3^{a}	5.0^{a}	21.7^{a}	8.3^{a}	6.7^{a}	6.7^{a}	26.7^{a}	18.3^{a}
Calming	11.7^{a}	6.7^{a}	6.7^{a}	13.3^{a}	15.0^{a}	10.0^{a}	5.0^{a}	16.7^{a}
Healthy drink	13.3^{b}	18.3^{b}	26.7^{b}	26.7^{b}	13.3^{b}	33.3^{a}	45.0^{a}	48.3^{a}
Vegetable	20.0^{a}	10.0^{a}	18.3^{a}	5.0^{a}	11.7^{a}	15.0^{a}	18.3^{a}	3.3^{a}
Sugary drink	75.0^{a}	76.7^{a}	30.0^{b}	41.7^{b}	85.0^{a}	66.7^{a}	28.3^{b}	31.7^{b}

Different letters in row show significant differences based on McNemar-Boferroni test ($p \leq 0.05$). SR, sugar reduction; SWE, sweetener; HN, honey. Syrup codes and their formulations are detailed in Table 1.

Table 6. Consumers' liking in the blind and non-blind test.

Samples	Blind test	Non-blind test	*p*-Value
F2:10%	6.38±1.49	6.12±1.35	0.308
F5:10%+SR	5.35±1.44	5.70±1.37	0.174
F6:10%+SWE	4.03±1.97	4.72±1.79	0.050
F7:10%+HN	5.93±1.72	6.17±1.64	0.448

p-Value was calculated based on Student's *t*-test. SR, sugar reduction; SWE, sweetener; HN, honey. Syrup codes and their formulations are detailed in Table 1.

Table 7. Results of penalty analysis in the blind test and non-blind test.

Attribute	Blind test		Non-blind test	
	Mean impact	*p*-Value	Mean impact	*p*-Value
Fresh	1.18	0.285	1.24	<0.001
Innovative	0.25	0.359	0.47	0.043
Herbal drink	−0.47	0.065	−0.48	0.036
Traditional drink	−0.85	0.170	0.05	0.224
Calming	1.12	0.121	1.26	0.554
Healthy drink	0.43	0.146	0.43	0.050
Vegetable	0.05	0.740	−0.57	0.441
Sugary drink	0.54	0.026	0.19	0.377

attribute significantly (p=0.050) influenced liking (mean impact of 0.43). This may promote consumer acceptability towards the samples since a non-nutritive sweetener is associated with non-caloric food and sugar intake reduction [Deliza *et al.*, 2021] as well as weight and diabetes management [Farhat *et al.*, 2021; Lohner *et al.*, 2017], which is closely related with healthiness aspect. The liking of basil syrups was influenced by the different attributes in the blind test and the non-blind test, suggesting that consumer perception can be modulated by the information provided prior to testing.

Our study found that the drivers of liking for non-sensory attributes were different when comparing the blind and the non-blind test evaluation. The information provided to consumers prior to tasting can influence their perception and liking. Our study corroborates previous studies [Bemfeito *et al.*, 2021; Fibri & Frøst, 2020; Henrique *et al.*, 2015; Mazhangara *et al.*, 2022] that also found similar results in comparing consumers perception in the blind and the non-blind setting. For example, information regarding the label of organic foods was able to influence consumers' perception of the products and increase their purchase interest [Asioli *et al.*, 2018]. Further, information regarding coffee quality was shown to change consumer preferences and increase their liking significantly compared to the blind testing [Bemfeito *et al.*, 2021]. A similar result was also reported for sausages [Mazhangara *et al.*, 2022] and cooked ham [Henrique *et al.*, 2015], suggesting that the information obtained regarding the samples (ingredients, processing, origin) in a non-blind setting can shift consumer perception and preferences. A previous study reported that when consumers were presented with information regarding salt-reduction in the biscuit samples their liking was higher compared to a normal-salt biscuit [Vazquez *et al.*, 2009]. However, when the same biscuits were tested in the blind test setting the liking was similar between normal-salt and reduced-salt biscuit. Sensory and non-sensory cues may interact to build consumer perception, and the interaction between these cues depends on such factors as the product characteristics, familiarity, brand, sensory profiles, prices or any additional claim related to health and wellness [Carrillo *et al.*, 2012], which can influence consumer preferences.

CONCLUSIONS

This study investigated the sensory profiling of basil syrups with different contents of basil extract and different sugar formulations using the CATA method. The different addition levels of basil extracts significantly impacted the sensory profiles of the basil syrups. Moreover, the sugar content was found to significantly modify sensory profiles of the samples. Interestingly, the consumer perception of the basil syrups showed to be different in the blind and the non-blind testing. The information provided in the non-blind sensory evaluation setting may be able to change consumer preferences of the basil syrup. There was a shift for the key liking attribute from "sugary drink" in the blind testing into "fresh", "innovative" and "healthy drink" in the non-blind testing. This concludes that information provided to consumers can modulate their perception and liking. Our study also suffers from some limitations.

We suggest involving more participants with a wider age group for next studies to confirm the finding. To date, this is the first study that investigates sensory profiles of basil syrups using CATA method and the results could be used as a preliminary study to develop healthy beverages made from basil with consideration of healthy information provided to consumers.

ACKNOWLEDGEMENTS

We would like to thank all the participants who have been involved in this research.

RESEARCH FUNDING

We would like to thank Bina Nusantara University for the research funding of PTB (research grant contract No: 060/VR.RTT/IV/2022).

CONFLICT OF INTERESTS

The authors declare that there is no conflict of interests.

ORCID IDs

K. Bryant https://orcid.org/0000-0003-4940-0219
W. David https://orcid.org/0000-0002-7611-0076
E. Ervina https://orcid.org/0000-0002-6503-6907
D.L. Nur Fibri https://orcid.org/0000-0001-9130-1957

REFERENCES

1. Abidoye, A.O., Ojedokun, F.O., Fasogbon, B.M., Bamidele, O.P. (2022). Effects of sweet basil leaves (*Ocimum basilicum* L.) addition on the chemical, antioxidant, and storage stability of roselle calyces (*Hibiscus sabdariffa*) drink. *Food Chemistry*, *371*, art. no. 131170. https://doi.org/10.1016/j.foodchem.2021.131170
2. Alongi, M., Anese, M. (2021). Re-thinking functional food development through a holistic approach. *Journal of Functional Foods*, *81*, art. no. 104466. https://doi.org/10.1016/j.jff.2021.104466
3. Aparna, A.R., Rajalakshmi, D. (1999). Honey — its characteristics, sensory aspects, and applications. *Food Reviews International*, *15*(4), 455-471. https://doi.org/10.1080/87559129909541199
4. Asioli, D., Wongprawmmas, R., Pignatti, E., Canavari, M. (2018). Can information affect sensory perceptions? Evidence from a survey on Italian organic food consumers. *AIMS Agriculture and Food*, *3*(3), 327-344. https://doi.org/10.3934/agrfood.2018.3.327
5. Baliga, M., Rao, S., Rai, M., Souza, P. (2016). Radio protective effects of the Ayurvedic medicinal plant *Ocimum sanctum* Linn. (Holy Basil): A memoir. *Journal of Cancer Research and Therapeutics*, *12*(1), 20-27. https://doi.org/10.4103/0973-1482.151422
6. Bemfeito, C.M., Guimarães, A.S., de Oliveira, A.L., Andrade, B.F., de Paula, L.M.A.F., Pimenta, C.J. (2021). Do consumers perceive sensory differences by knowing information about coffee quality? *LWT – Food Science and Quality, 138*, art. no. 110778. https://doi.org/10.1016/j.lwt.2020.110778
7. Carrillo, E., Varela, P., Fiszman, S. (2012). Effects of food package information and sensory characteristics on the perception of healthiness and the acceptability of enriched biscuits. *Food Research International*, *48*(1), 209-216. https://doi.org/10.1016/j.foodres.2012.03.016
8. Chambers, E. (2019). Analysis of sensory properties in foods: A Special Issue. *Foods (Basel, Switzerland)*, *8*(8), art. no. 291. https://doi.org/10.3390/foods8080291
9. Chandrasekara, A., Shahidi, F. (2018). Herbal beverages: Bioactive compounds and their role in disease risk reduction – A review. *Journal of Traditional and Complementary Medicine*, *8*(4), 451-458. https://doi.org/10.1016/j.jtcme.2017.08.006
10. Dadan, M., Tylewicz, U., Tappi, S., Rybak, K., Witrowa-Rajchert, D., Dalla Rosa, M. (2021). Effect of ultrasound, steaming, and dipping on bioactive compound contents and antioxidant capacity of basil and parsley. *Polish Journal of Food and Nutrition Sciences*, *71*(3), 311-321. https://doi.org/10.31883/pjfns/141430
11. de Souza, L.B.A., Pinto, V.R.A., Nascimento, L.G.L., Stephani, R., de Carvalho, A.F., Perrone, Í.T. (2021). Low-sugar strawberry yogurt: Hedonic thresholds and expectations. *Journal of Sensory Studies*, *36*(3), art. no. e12643. https://doi.org/10.1111/joss.12643
12. Deliza, R., Lima, M.F., Ares, G. (2021). Rethinking sugar reduction in processed foods. *Current Opinion in Food Science*, *40*, 58-66. https://doi.org/10.1016/j.cofs.2021.01.010
13. Dhama, K., Sharun, K., Gugjoo, M.B., Tiwari, R., Alagawany, M., Iqbal Yatoo, M., Thakur, P., Iqbal, H.M.N., Chaicumpa, W., Michalak, I., Elnesr, S.S., Farag, M.R. (2023). A comprehensive review on chemical profile and pharmacological activities of *Ocimum basilicum*. *Food Reviews International*, *39*(1), 119-117. https://doi.org/10.1080/87559129.2021.1900230
14. Ervina, E., Berget, I., Nilsen, A., Almli, V.L. (2020). The ability of 10-11-year-old children to identify basic tastes and their liking towards unfamiliar foods. *Food Quality and Preference, 83*, art. no. 103929. https://doi.org/10.1016/j.foodqual.2020.103929
15. Farhat, G., Dewison, F., Stevenson, L. (2021). Knowledge and perceptions of non-nutritive sweeteners within the UK adult population. *Nutrients*, *13*(2), art. no. 444. https://doi.org/10.3390/nu13020444
16. Farzana, M., Shahriar, S., Jeba, F.R., Tabassum, T., Araf, Y., Ullah, A., Tasnim, J., Chakraborty, A., Naima, T.A., Shain Marma, K.K., Rahaman, T.I., Hosen, M.J. (2022). Functional food: complementary to fight against COVID-19. *Beni-Suef University Journal of Basic and Applied Sciences, 11*, art. no. 33. https://doi.org/10.1186/s43088-022-00217-z
17. Fibri, D.L.N., Frøst, M.B. (2020). Indonesian millennial consumers' perception of tempe – And how it is affected by product information and consumer psychographic traits. *Food Quality and Preference*, *80*, art. no. 103798. https://doi.org/10.1016/j.foodqual.2019.103798
18. Galler, M., Næs, T., Almli, V.L., Varela, P. (2020). How children approach a CATA test influences the outcome. Insights on ticking styles from two case studies with 6–9-year old children. *Food Quality and Preference*, *86*, art. no. 104009. https://doi.org/10.1016/j.foodqual.2020.104009
19. García, J.M., Narváez, P.C., Heredia, F.J., Orjuela, Á., Osorio, C. (2017). Physicochemical and sensory (aroma and colour) characterisation of a non-centrifugal cane sugar ("panela") beverage. *Food Chemistry*, *228*, 7-13. https://doi.org/10.1016/j.foodchem.2017.01.134
20. Grasso, S., Monahan, F.J., Hutchings, S.C., Brunton, N.P. (2017). The effect of health claim information disclosure on the sensory characteristics of plant sterol-enriched turkey as assessed using the Check-All-That-Apply (CATA) methodology. *Food Quality and Preference*, *57*, 69-78. https://doi.org/10.1016/j.foodqual.2016.11.013
21. Hellfritsch, C., Brockhoff, A., Stähler, F., Meyerhof, W., Hofmann, T. (2012). Human psychometric and taste receptor responses to steviol glycosides. *Journal of Agricultural and Food Chemistry*, *60*(27), 6782-6793. https://doi.org/10.1021/jf301297n
22. Henrique, N.A., Deliza, R., Rosenthal, A. (2015). Consumer sensory characterization of cooked ham using the Check-All-That-Apply (CATA) methodology. *Food Engineering Reviews*, *7*(2), 265-273. https://doi.org/10.1007/s12393-014-9094-7
23. Hubbermann, E.M., Heins, A., Stöckmann, H., Schwarz, K. (2006). Influence of acids, salt, sugars and hydrocolloids on the colour stability of anthocyanin rich black currant and elderberry concentrates. *European Food Research and Technology*, *223*(1), 83-90. https://doi.org/10.1007/s00217-005-0139-2
24. Kim, I.-A., Kim, M.-A., van de Velden, M., Lee, H.-S. (2013). Psychological positioning of bottled tea products: A comparison between two Kansei profiling techniques. *Food Science and Biotechnology*, *22*(1), 257-268. https://doi.org/10.1007/s10068-013-0035-7
25. Kozlowska, M., Scibisz, I., Przybyl, J., Ziarno, M., Zbikowska, A., Majewska, E. (2021). Phenolic contents and antioxidant activity of extracts of selected fresh and dried herbal materials. *Polish Journal of Food and Nutrition Sciences*, *71*(3), 269-278. https://doi.org/10.31883/pjfns/139035
26. Lestari, L.A. (2021). Opportunities and challenges of functional foods and nutraceuticals development during Covid-19 pandemic. *BIO Web of Conferences, 41*, art. no. 02009. https://doi.org/10.1051/bioconf/20214102009
27. Lohner, S., Toews, I., Meerpohl, J.J. (2017). Health outcomes of non-nutritive sweeteners: analysis of the research landscape. *Nutrition Journal*, *16*(1), art. no. 55. https://doi.org/10.1186/s12937-017-0278-x
28. Mäkinen, S.M., Pääkkönen, K.K. (1999). Processing and use of basil in foodstuffs, beverages and in food preparation. In R. Hiltunen, Y. Holm (Eds.). *Basil: The Genus Ocimum*. Harwood Academic Publishing, UK, pp. 142-257.
29. Marques, C., Correia, E., Dinis, L.-T., Vilela, A. (2022). An overview of sensory characterization techniques: from classical descriptive analysis to the emergence of novel profiling methods. *Foods (Basel, Switzerland)*, *11*(3), art. no. 255. https://doi.org/10.3390/foods11030255
30. Mazhangara, I.R., Chivandi, E., Jaja, I.F. (2022). Consumer preference for the chevon sausage in blind and nonblind sensory evaluations: A comparative study. *International Journal of Food Science, 2022*, art. no. 8736932. https://doi.org/10.1155/2022/8736932

31. Patel, M., Lee, R., Merchant, E.V., Juliani, H.R., Simon, J.E., Tepper, B.J. (2021). Descriptive aroma profiles of fresh sweet basil cultivars (*Ocimum* spp.): Relationship to volatile chemical composition. *Journal of Food Science*, *86*(7), 3228-3239. https://doi.org/10.1111/1750-3841.15797
32. Piochi, M., Cabrino, G., Torri, L. (2021). Check-All-That-Apply (CATA) test to investigate the consumers' perception of olive oil sensory properties: effect of storage time and packaging material. *Foods (Basel, Switzerland)*, *10*(7), art. no. 1551. https://doi.org/10.3390/foods10071551
33. Pratama, S.B., Wijana, S., Mulyadi, A.F. (2013). Studi Pembuatan Sirup Tamarillo (Kajian Perbandingan Buah Dan Konsentrasi Gula) (Bahasa Indonesia). *Industria: Jurnal Teknologi dan Manajemen Agroindustri*, *1*(3), art. no. 14 (in Indonesian).
34. Reis, F., Alcaire, F., Deliza, R., Ares, G. (2017). The role of information on consumer sensory, hedonic and wellbeing perception of sugar-reduced products: Case study with orange/pomegranate juice. *Food Quality and Preference*, *62*, 227-236. https://doi.org/10.1016/j.foodqual.2017.06.005
35. Ribas, J.C.R., Matumoto-Pintro, P.T., Vital, A.C.P., Saraiva, B.R., Anjo, F.A., Alves, R.L.B., Santos, N.W., Machado, E., Agustinho, B.C., Zeoula, L.M. (2019). Influence of basil (*Ocimum basilicum Lamiaceae*) addition on functional, technological and sensorial characteristics of fresh cheeses made with organic buffalo milk. *Journal of Food Science and Technology*, *56*(12), 5214-5224. https://doi.org/10.1007/s13197-019-03990-5
36. Ruiz-Capillas, C., Herrero, A.M. (2021). Sensory analysis and consumer research in new product development. *Foods (Basel, Switzerland), 10*(3), art. no. 582. https://doi.org/10.3390/foods10030582
37. Ruiz-Capillas, C., Herrero, A.M., Pintado, T., Delgado-Pando, G. (2021). Sensory analysis and consumer research in new meat products development. *Foods (Basel, Switzerland)*, *10*(2), art. no. 429. https://doi.org/10.3390/foods10020429
38. Serrano, A., Ros, G., Nieto, G. (2018). Bioactive compounds and extracts from traditional herbs and their potential anti-inflammatory health effects. *Medicines*, *5*(3), art. no. 76. https://doi.org/10.3390/medicines5030076
39. Sestili, P., Ismail, T., Calcabrini, C., Guescini, M., Catanzaro, E., Turrini, E., Layla, A., Akhtar, S., Fimognari, C. (2018). The potential effects of *Ocimum basilicum* on health: a review of pharmacological and toxicological studies. *Expert Opinion on Drug Metabolism & Toxicology*, *14*(7), 679-692. https://doi.org/10.1080/17425255.2018.1484450
40. Shahrajabian, M.H., Sun, W., Cheng, Q. (2020). Chemical components and pharmacological benefits of basil (*Ocimum basilicum*): a review. *International Journal of Food Properties*, *23*(1), 1961-1970. https://doi.org/10.1080/10942912.2020.1828456
41. Skaria, B.P., Joy, P.P., Mathew, S., Mathew, G. (2006). Chapter 24 - Lemongrass. In K.V. Peter (Ed.) *Handbook of Herbs and Spices*, Woodhead Publishing, pp. 400-419. https://doi.org/10.1533/9781845691717.3.400
42. Snežana, F. (2017). Basil (*Ocimum basilicum* L.) a source of valuable phytonutrients. *International Journal of Clinical Nutrition & Dietetics 3*, art. no. 118. https://doi.org/10.15344/2456-8171/2017/118
43. Tao, R., Cho, S. (2020). Consumer-based sensory characterization of steviol glycosides (rebaudioside A, D, and M). *Foods (Basel, Switzerland)*, *9*(8), art. no. 1026. https://doi.org/10.3390/foods9081026
44. Tarancón, P., Tárrega, A., Aleza, P., Besada, C. (2020). Consumer description by Check-All-That-Apply Questions (CATA) of the sensory profiles of commercial and new mandarins. Identification of preference patterns and drivers of liking. *Foods (Basel, Switzerland)*, *9*(4), art. no. 468. https://doi.org/10.3390/foods9040468
45. Teofilović, B., Tomas, A., Martić, N., Stilinović, N., Popović, M., Čapo, I., Grujić, N., Ilinčić, B., Rašković, A. (2021). Antioxidant and hepatoprotective potential of sweet basil (*Ocimum basilicum* L.) extract in acetaminophen-induced hepatotoxicity in rats. *Journal of Functional Foods*, *87*, art. no. 104783. https://doi.org/10.1016/j.jff.2021.104783
46. Tian, X., Zhong, F., Xia, Y. (2022). Dynamic characteristics of sweetness and bitterness and their correlation with chemical structures for six steviol glycosides. *Food Research International*, *151*, art. no. 110848. https://doi.org/10.1016/j.foodres.2021.110848
47. Topolska, K., Florkiewicz, A., Filipiak-Florkiewicz, A. (2021). Functional food-consumer motivations and expectations. *International Journal of Environmental Research and Public Health*, *18*(10), art. no. 5327. https://doi.org/10.3390/ijerph18105327
48. Urala, N., Lähteenmäki, L. (2004). Attitudes behind consumers' willingness to use functional foods. *Food Quality and Preference*, *15*(7-8), 793-803. https://doi.org/10.1016/j.foodqual.2004.02.008
49. Uzun, I., Oz, F. (2021). Effect of basil use in meatball production on heterocyclic aromatic amine formation. *Journal of Food Science and Technology*, *58*(8), 3001-3009. https://doi.org/10.1007/s13197-020-04803-w
50. van Nieuwenburg, D., de Groot, J.H.B., Smeets, M.A.M. (2019). The subtle signaling strength of smells: A masked odor enhances interpersonal trust. *Frontiers in Psychology*, *10,* art. no. 1890. https://doi.org/10.3389/fpsyg.2019.01890
51. Varela, P., Ares, G. (2012). Sensory profiling, the blurred line between sensory and consumer science. A review of novel methods for product characterization. *Food Research International*, *48*(2), 893-908. https://doi.org/10.1016/j.foodres.2012.06.037
52. Vazquez, M.B., Curia, A., Hough, G. (2009). Sensory descriptive analysis, sensory acceptability and expectation studies on biscuit with reduced salt and increased fiber. *Journal of Sensory Studies*, *24*(4), 498-511. https://doi.org/10.1111/j.1745-459X.2009.00223.x
53. Wagoner, T.B., McCain, H.R., Foegeding, E.A., Drake, M.A. (2018). Food texture and sweetener type modify sweetness perception in whey protein-based model foods. *Journal of Sensory Studies*, *33*(4), art. no. e12333. https://doi.org/10.1111/joss.12333
54. Wardy, W., Jack, A.R., Chonpracha, P., Alonso, J.R., King, J.M., Prinyawiwatkul, W. (2018). Gluten-free muffins: effects of sugar reduction and health benefit information on consumer liking, emotion, and purchase intent. *International Journal of Food Science & Technology*, *53*(1), 262-269. https://doi.org/10.1111/ijfs.13582
55. WHO. (2015). Guideline: sugars intake for adults and children. In World Health Organization, Geneva, Switzerland.
56. W.M.A. (2013). World Medical Association Declaration of Helsinki: Ethical Principles for Medical Research Involving Human Subjects. *JAMA*, *310*(20), 2191-2194. https://doi.org/10.1001/jama.2013.281053
57. Yang, J., Lee, J. (2019). Application of sensory descriptive analysis and consumer studies to investigate traditional and authentic foods: A review. *Foods (Basel, Switzerland)*, *8*(2), art. no. 54. https://doi.org/10.3390/foods8020054
58. Zhan, Y., An, X., Wang, S., Sun, M., Zhou, H. (2020). Basil polysaccharides: A review on extraction, bioactivities and pharmacological applications. *Bioorganic & Medicinal Chemistry*, *28*(1), art. no. 115179. https://doi.org/10.1016/j.bmc.2019.115179

ORIGINAL ARTICLE
http://journal.pan.olsztyn.pl

Polish Journal of Food and Nutrition Sciences
2023, Vol. 73, No. 3, 242–252
DOI: 10.31883/pjfns/169729
ISSN 1230-0322, e-ISSN 2083-6007

Encapsulation of *Lactiplantibacillus plantarum* and Beetroot Extract with Alginate and Effect of Capsules on Rheological Properties and Stability of an Oil-in-Water Emulsion Model Food

Minerva Bautista-Villarreal, Sandra L. Castillo Hernández*, Salvador López Uriarte, María Porfiria Barrón González

Universidad Autónoma de Nuevo León, Facultad de Ciencias Biológicas. Departamento de Alimentos, Av. Universidad s/n Cd. Universitaria, San Nicolás de Los Garza Nuevo León, CP. 66455, Mexico

Alginate encapsulation is a viable alternative for the preservation of probiotics along the gastric route or within a food product during its shelf life. Furthermore, co-encapsulation with a vegetal material could act as a prebiotic and enhance the viability of the encapsulated probiotic. The rheological properties of dressing-type foods could be altered by adding an ingredient that would affect the quality of the final product. In this investigation, alginate beads loaded with *Lactiplantibacillus plantarum* and beetroot extract were obtained by two methods (emulsification and extrusion). They were characterized by size and morphology, encapsulation efficiency, and bacteria viability under simulated gastrointestinal conditions. Finally, they were added in an oil-in-water emulsion model food for which rheological properties and probiotic survival were monitored. The encapsulation efficiency ranged from 86.4 to 88%. Morphology and size of capsules varied depending on the method of encapsulation applied. No significant changes were evidenced in the rheological properties of the model food; the viscosity, the particle size ($d_{3,2}$), and the coalescence rate remained stable after the addition of the capsules. Survival of *L. plantarum* was significantly higher in the capsules with beetroot extract. These results suggest a prebiotic effect conferred by the beetroot extract when co-encapsulated. It is worth mentioning that the incorporation of capsules with beetroot extract does not cause any destabilization of the model food.

Key words: alginate bead, probiotic, co-encapsulation, dressing, storage, bacteria viability

ABBREVIATIONS

O/W, oil-in-water; %EE, encapsulation efficiency; NB, natural beads; BB, beetroot beads; DWB, dressing without beads; DNB, dressing with natural beads; DBB, dressing with beetroot beads; COD, commercial dressing; V_{24h}, viability after 24 h; LAB, lactic acid bacteria; cfu, colony forming unit.

INTRODUCTION

Probiotics such as *Lactiplantibacillus plantarum* are part of human intestinal microbes. They play a very important role in food fermentation processes [Nordström *et al.*, 2021]. In addition, they are live microorganisms which can confer health benefits by improving the host's intestinal microbial balance when administered in adequate amounts [Baek & Lee, 2009]. Likewise,

***Corresponding Author:**
tel.: + 52 8183 294 110 ext. 3670; e-mail: sandra.castilloh@uanl.mx (S. Castillo-Hernandez)

Submitted: 2 May 2023
Accepted: 18 July 2023
Published on-line: 28 August 2023

probiotics are being commercialized in many different forms, including supplements or fermented foods from animal or vegetal origin (dairy and non-dairy products, respectively). *L. plantarum* 299v is the most documented and popular *L. plantarum* strain in the world [Nordström *et al.*, 2021]. The consumption of probiotic foods is an actual demand and these products account for up to 70% of the total functional food market [Rajam & Subramanian, 2022]. On the other hand, prebiotics are defined as ingredients that promote the growth or metabolic activity of the beneficial bacteria; when probiotics and prebiotics are in combination, they are known as "synbiotics" and are designed to improve the survival of the microorganisms and their colonization [Vijaya Kumar *et al.*, 2015]. The trend of incorporating natural sources of bioactive compounds to obtain healthier food products has led researchers to investigate their prebiotic potential [Lazar *et al.*, 2022].

The beetroot (*Beta vulgaris* L.) is rich in bioactive compounds and confers health benefits due to its antioxidant and anti-inflammatory effects, among other features [Chhikara *et al.,* 2019; Mirmiran *et al.*, 2020]. It is applied as a functional ingredient due to its content of betalains, flavonoids, phenolic acids, and saponins [Otalora *et al.*, 2020; Płatosz *et al.*, 2020; Spórna-Kucab *et al.*, 2022]. Moreover, its benefits on the gut microbiota, due to the content of oligo- and polysaccharides, have also been demonstrated and therefore it has received special attention as a potential prebiotic [Alexandrino de Oliveira *et al.*, 2021].

The encapsulation of probiotic cells serves to protect them from hostile environments; this is how they can reach the intestine without being damaged. On the other hand, the probiotic cell is immobilized and could be added to a product in order to extend the cell viability, along with its shelf life [Vijaya *et al.*, 2015]. Dressings are oil-in-water (O/W) emulsions which are widely consumed by the population; for instance, a variety of products such as mayonnaise or dressings are available in the market. The tendency to consume foods based on natural ingredients compels producers to incorporate ingredients from vegetal origin into dressings that could improve their functional properties [Castillo *et al.*, 2021]. The quality of the final product based on O/W emulsions is governed by diverse rheological characteristics that can be affected during the incorporation of new ingredients [Ma & Boye, 2013]. Due to the reasons stated above, the aim of the present research was to study the viability of *L. plantarum* co-encapsulated with beetroot extract loaded into alginate beads, and the effect of capsules on rheological properties when incorporated as an ingredient in a model food (O/W emulsion). This information may provide valuable data for the development of new, healthier products.

MATERIALS AND METHODS

Microbial strain and culture conditions

A bacterial strain of *Lactiplantibacillus plantarum* 299v (*L. plantarum* Orla-Jensen 1919 Bergey *et al.* 1923 strain 17–5) was acquired from the American type culture collection (ATCC; Manassas, VA, USA) and donated by the Laboratory of Cell Biology of the Autonomous University of Nuevo León (San Nicolás de los Garza, Mexico). It was kept on De Man Rogosa Sharpe (MRS) broth (Difco, Becton & Dickinson, Sparks, MD, USA) in refrigeration until use. In order to obtain fresh cultures, an aliquot of 100 µL was taken from the refrigerated culture and placed in tubes containing 10 mL of MRS medium; they were incubated at 37°C for 24 h for further analyses. For the encapsulation, the cells were recovered by centrifugation (Hermle Labnet Z326, Labnet International, Inc., Wehingen, Germany) at 590×*g* for 20 min at 25°C and washed twice with 10 mL of 8.5 g/L of a saline solution. The cells were then suspended in 1 mL of the saline solution and used for the respective encapsulation method. A plate count method in MRS was used to determine the final count of cells in the suspension [Mahmoud *et al.,* 2020].

Preparation of beetroot material

The beetroots (*Beta vulgaris* L.) were purchased from retail markets in the metropolitan area of Monterrey, NL, Mexico. They were washed and disinfected with mycrodin® (Tavistock Group, Mexico City, Mexico) for 15 min. After that, the peel was separated and discarded. Then, the beetroots were chopped into small pieces using a knife (squares of 0.5 cm) and placed in a tunnel drier (model LO2001, Procomm, Mexico City, Mexico) at 45°C for 24 h. The dried material was ground in a mill (model 4 Wiley mill, Thomas Scientific, Swedesboro, NJ, USA) with a mesh of 1 mm and stored in a dry, sterile container protected from light [Castillo *et al.*, 2021]. This material was used later for the beetroot extract preparation.

Preparation of the beetroot extract

An aqueous extract of dried beetroot powder was prepared according to the procedure described by Sánchez *et al.* [2016], with minor modifications. Briefly, the dried material was soaked in sterile distilled water (20 g/L) and left at room temperature (25°C) for 48 h in a sterile screw-capped glass flask. After that, the aqueous material was recovered by filtration (Whatman No.1) and placed in a sterile glass container at 4°C until use. Finally, the extract was incorporated into the capsules according to the method mentioned below.

Preparation of capsules and their characterization

Two methods, including emulsification and extrusion, were used for the encapsulation of *L. plantarum* with alginate (natural beads, NB) and co-encapsulation of *L. plantarum* and beetroot extract with alginate (beetroot beads, BB). The particle size and morphology of the capsules obtained by both methods were determined. The encapsulation efficiency (%EE) was determined only for the method that gave the best results in terms of particle size and morphology of capsules.

Encapsulation by emulsification

The emulsification method was carried out according to the procedure described by Motalebi Moghanjougi *et al.* [2021], with minor modifications. First, a sodium alginate solution (10 g/L) was prepared and autoclaved (121°C/15 min). After that, 1 mL of the harvested cells of *L. plantarum* in saline solution was mixed

with 99 mL of the alginate solution. The mixture (20 mL) was then added dropwise with a sterile syringe with needles of different calibers (G22×32 mm, G27×13 mm, G31×6 mm), to a previously sterilized solution containing 100 mL of vegetable oil (canola) with 0.1% (*w/v*) Tween 80 (Sigma-Aldrich, Saint Louis, MO, USA); then, it was magnetically stirred for 5 min. Subsequently, 100 mL of cooled 0.15 M $CaCl_2$ were added slowly to the mixture to break the emulsion. The mixture was left at room temperature for 30 min and the capsules were formed. The oil layer was removed, and the probiotic beads were recovered by filtration (Whatman No.1). The beads were washed twice with 0.15 M $CaCl_2$ and stored at 4°C for the analyses. For the incorporation of the beetroot extract to the bead, the same procedure mentioned above was used, but part of the sterile alginate solution (10 mL) was replaced by the same volume of the plant extract.

Encapsulation by extrusion

The encapsulation of *L. plantarum* through the extrusion technique was performed according to the method reported by Mahmoud *et al.* [2020] and Krasaekoopt & Watcharapoka [2014], with some modifications. Briefly, 1 mL of the harvested probiotic culture of *L. plantarum* was added to 99 mL of alginate solution (10 g/L) previously prepared and autoclaved. The suspension was extruded dropwise with a syringe through needles of different calibers (G22×32mm, G27×13mm, G31×6mm) in a sterile 0.15 M $CaCl_2$ with gentle magnetic stirring. The encapsulated cells were then washed with 0.15 M $CaCl_2$ and stored in a sealed bag at 4°C in sterile peptone water. For the incorporation of the beetroot extract to the beads, the plant extract (10 mL) was added to the alginate solution (89 mL). After adding 1 mL of the *L. plantarum* suspension, the same procedures of extrusion and capsule washing were used as described above.

Analysis of particle size and morphology of capsules

The average diameter of particles and the morphology of the capsules were evaluated by optical microscopy using a Leica EZ4HD digital stereo microscope with a high-definition CMOS camera (Leica, Wetzlar, Germany) according to the method reported by Krasaekoopt & Watcharapoka [2014] and Holkem *et al.* [2016]. Magnification of 10× was used. The diameters of 100 randomly selected capsules were measured using the Image-Pro Plus 2D analysis software (Media Cybernetics, Rockville, MD, USA) with the caliper tool.

Encapsulation efficiency determination

Once the capsules were obtained using the protocol that produced the best results in particle size and morphology, the encapsulation efficiency as a function of percentage of entrapped cells was determined according to Krasaekoopt & Watcharapoka [2014]. Briefly, 1 g of fresh beads was blended in a stomacher for 1 min with 99 mL of sterile peptone solution (1 g/L) and then allowed to stand for 10 min to dissolve. Appropriate serial dilutions were made and then a plate count method was deployed onto MRS broth (Difco, Becton & Dickinson). The same procedure was carried out after 24 h of the encapsulation for monitoring the viability of *L. plantarum* in order to discard any antimicrobial activity.

The encapsulation efficiency (%EE) was calculated according to Equation (1), as suggested by Pupa *et al.* [2021].

$$\%EE = (\log N / \log N_0) \times 100 \quad (1)$$

where: N_0 is the initial population of *L. plantarum* before encapsulation, and N is the population of encapsulated *L. plantarum*.

The viability of bacteria after 24 h ($\%V_{24}$) was calculated from Equation (2):

$$\%V_{24} = (\log N_{24} / \log N) \times 100 \quad (2)$$

where: N is the initial population of encapsulated *L. plantarum,* and N_{24} is the remaining encapsulated population after 24 h.

Determination of *L. plantarum* viability under simulated gastrointestinal conditions

In order to determine the viability of *L. plantarum* under the gastrointestinal conditions, the method mentioned by Krasaekoopt & Watcharapoka [2014] and Chávarri *et al.* [2010] was used with minor modifications. One gram of freshly prepared beads was incubated in a tube containing 10 mL of simulated gastric juice (0.2% NaCl, 0.08 M of HCl, without pepsin and adjusted to pH 1.5 with HCl). This mixture was incubated at 37°C for 90 min; afterwards, the beads were recovered by filtration and resuspended in 9 mL of sterile simulated intestinal juice containing saline (0.5%) with pancreatin (0.1%) and bile salts (0.5%) at pH 8. This mixture was incubated at 37°C for 120 min. At the end of the process, the capsules with probiotics were recovered to determine their viability by means of a plate count (log cfu/g) as described above.

Determination of rheological properties and physical stability of model food with the capsules

A dressing (O/W emulsion) was used as model food. After addition of the capsules, the rheological properties, physical stability of model food, and the viability of encapsulated probiotics were determined throughout 28 days.

Preparation of the O/W emulsion food model

The ingredients used to formulate the O/W emulsion are presented in Table 1. The procedure performed according to Castillo *et al.* [2021] is described as follows: first, the water and egg yolk were placed in a bowl and mixed at 500 rpm for 5 min (T50 Digital Ultra Turrax, IKA, Wilmington, NC, USA). After that, vinegar, salt, sugar, and xanthan gum were added and mixed for 15 more min. Finally, the oil was added manually in a continuous manner until it was fully incorporated into the mix at 3,000 rpm for 2 min, and at 5,000 rpm for 3 more min. Once the emulsion was finished, the beads were added according to the formulations reported in Table 1. The first formulation was the dressing without the addition of beads (DWB), the second one was the dressing with the addition

Table 1. Composition (g/100 g) of oil-in-water emulsion dressings without beads (DWB), and with natural beads (DNB) obtained by encapsulation of *Lactiplantibacillus plantarum* with alginate and with beetroot beads (DBB) obtained by co-encapsulation of *L. plantarum* and beetroot extract with alginate.

Ingredient	DWB	DNB	DBB
Water	28.31	25.48	25.48
Egg yolk	3.0	2.7	2.7
Oil	50.0	45.0	45.0
Xanthan gum	0.29	0.26	0.26
White vinegar	11.50	10.35	10.35
Salt	1.15	1.04	1.04
Sugar	5.75	5.18	5.18
Natural beads	-----	10.0	----
Beetroot beads	-----	-----	10.0

of natural beads (DNB), and the third one was the dressing with the addition of beetroot beads (DBB). The formulated dressings were packed in a sealed bag and stored at 4°C.

Analysis of flow properties of the O/W emulsion food model

The flow curves of the O/W emulsions (DWB, DNB and DBB) were obtained for the shear rate in range from 1 to 100 1/s using a rotational test with a RheolabQC rheometer (Anton Paar, Mexico City, Mexico) and a CC27 geometry at a temperature of 25°C [Castillo *et al*., 2021]. Consistency indexes (*k*, Pa×s^n) and flow behavior indexes (*n*) were obtained according to the power law model described in Equation (3) [Sakin-Yilmazer *et al.,* 2014].

$$\text{Shear stress (Pa)} = k \times \text{shear rate}^n \quad (3)$$

The commercial dressing was used as a point of comparison. Analyses were carried out for fresh dressings and dressings stored for 28 days.

Droplet size and coalescence rate determination

The particle size of fresh emulsions and those stored for 14 and 28 days were monitored with the Malvern Mastersizer 3000 equipment (Malvern Instruments, Ltd, Worcestershire, UK) using the Hydro LV unit with water as a dispersant. Angular scattering intensity data from the analyzer were used to calculate the size of the particles that create the scattering pattern using Mie's theory of light scattering [Bautista Villarreal *et al.*, 2018]. The software Malvern Mastersizer v3.63 (Worcestershire, UK) was used to calculate the Sauter mean diameter ($d_{3,2}$). The optical properties of the emulsions were defined as follows: the refractive index was 1.460, while the absorption index was 0.100. The coalescence rate (K_c, 1/s) was obtained based on the first order kinetics and the Equation (4).

$$N_t/N_0 = e^{-K_c t} \quad (4)$$

where: N_t is the concentration in the number of drops at a time = (t), N_0 is the concentration in the number of the newly formed drops (time = 0), and K_c is the rate constant, which is related to the probability that the interfacial film will break at a certain time (t). The volume of the emulsion droplets remains constant when there is no oil release in the emulsion [Castillo *et al*., 2021].

Determination of *L. plantarum* viability in the food model under storage conditions

In order to monitor the viability of encapsulated *L. plantarum* over time in the food model, a plate count technique was used. Briefly, after preparation of the dressing, a portion of 10 g containing 1 g of respective beads was packed in a sealed bag and stored at 4°C. Each sample was processed in time intervals (on day 0, 2, 4, 8, 12, 18, 22 and 28), by serial dilutions and plating. Results were expressed as log cfu/g.

Statistical analysis

All measurements were performed three times in triplicate. To determine statistically significant differences between the values, a one-way analysis of variance (ANOVA) and a Tukey's test were used ($p<0.05$).

RESULTS AND DISCUSSION

Beetroot was selected as vegetal material to be included in the encapsulation of *L. plantarum* since it has been implicated in different health benefits and recognized as an important source of antioxidants [Chhikara *et al*., 2019]. It has also been reported as functional food [Chhikara *et al*., 2019; Płatosz *et al*., 2020]. Beetroot has become a very popular food and actually is one of the top ten planted vegetables associated with superior health benefits [Borjan *et al*., 2022]. On the other hand, some investigations have suggested the possibility of beetroot juice encapsulation to preserve its functional characteristics [Tumbas Šaponjac *et al*., 2020]. For this reason, in this research, beetroot aqueous extract was obtained and co-encapsulated with *L. plantarum*.

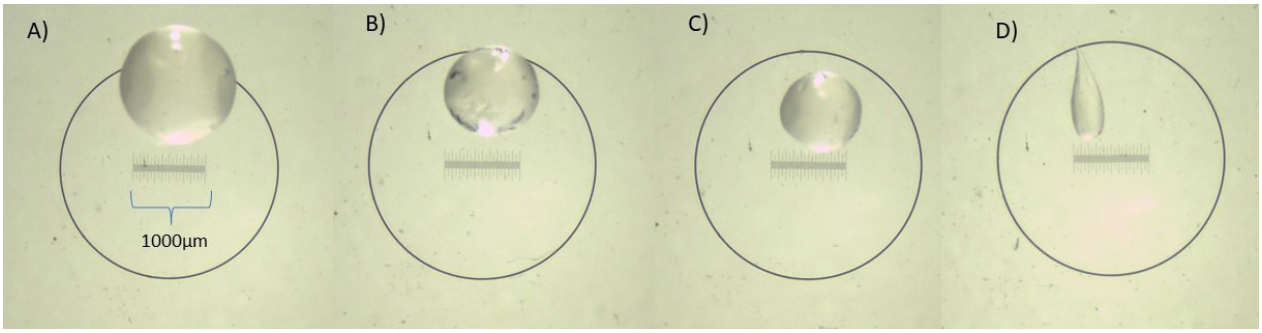

Figure 1. Morphology of the alginate beads loaded with *Lactiplantibacillus plantarum* co-encapsulated with beetroot extract obtained by extrusion (A–C) and emulsion (D) techniques using different needle calibers: G22×32 mm (A), G27×13 mm (B), G31×6 mm (C), G31×6 mm (D). Magnification was 10×. The measurements of the capsules were obtained with the Image-Pro Plus 2D analysis software with the caliper tool.

Characterization of capsules

Size and morphology

Considering that particle size can influence the aroma, texture, and appearance of the food, it may be deemed a very important physical parameter [Holkem *et al.*, 2016]. In our study, the alginate beads loaded with *L. plantarum* and with *L. plantarum* and beetroot aqueous extract varied in size and morphology depending on the protocol of capsule preparation used. However, the particle size was independent of the addition of beetroot extract (data not shown). The extrusion technique derived in spherical alginate beads (Figure 1) with an average particle diameter between 2,260 to 978 µm (for capsules with *L. plantarum* and beetroot extract), depending on the needle caliber used (Table 2). In general, the beads obtained by this protocol presented a homogeneous size for each needle caliber. On the other hand, beads obtained by the emulsion technique had an irregular morphology (Figure 1) and differed greatly in diameters. The average particle diameter of these beads ranged from 600 to 2,850 µm (Table 2). The smaller beads in size were obtained by the emulsification and needle calibers of G31×6 mm, G27×13 mm compared to analogous beads obtained using the extrusion technique. These results are in agreement with Capela *et al.* [2007], who reported a wide size distribution of alginate capsules loaded with *Lactobacillus acidophilus*, *L. casei* and *L. rhamnosus* when using the emulsion technique with bead sizes ranging from 200 to 1,000 µm. Also, Li *et al.* [2009] and Lopes *et al.* [2017], reported more uniform alginate beads loaded with probiotics obtained by the extrusion technique with diameters ranging from ~900 to 1,400 µm, which is consistent with our study results. Pupa *et al.* [2021] reported varied alginate-chitosan bead shapes and sizes depending on the preparation technique used, with mean diameters of ~1,500 µm for those obtained by extrusion, and ~500 µm for those obtained by emulsion technique, while Mahmoud *et al.* [2020] obtained alginate microcapsules loaded with *L. plantarum* and biopolymers by the extrusion technique with sizes ranging from ~501 to 1,200 µm. According to Holkem *et al.* [2016], particle sizes below 100 µm are desirable to avoid the negative impact on the sensory characteristics; however, some marketing strategies regarding flavor may help in the acceptance of the product. Nevertheless, the optimum size of the microcapsules could be debatable as it varies according to their applications. Actually, encapsulating lactic acid bacteria (LAB) and applying them in a food product is a challenge due to the large sizes of bacterial cells that lead to the production of large beads [Mahmoud *et al.*, 2020].

The variability in the beads' morphology could affect the encapsulation efficiency and the results could hardly be replicated. Due to the variability in size and morphology of the beads obtained by the emulsification, we selected the extrusion technique for further analyses. The smallest bead sizes produced by this last method were for the needle with the caliber of G31×6mm, thus it was chosen for bead production.

Encapsulation efficiency and viability of *L. plantarum* after 24 h

The counts of encapsulated *L. plantarum* (natural beads, NB) and *L. plantarum* co-encapsulated with beetroot extract (beetroot beads, BB), the count of bacteria in both types of beads after 24 h, as well as encapsulation efficiency (%EE) and percentage of bacteria viability after 24 h ($\%V_{24h}$) are presented in Table 3. The counts of encapsulated cells were 7.59 and 7.82 log cfu/g for NB and BB, respectively, with an encapsulation efficiency

Table 2. Average particle diameter ($d_{3,2}$, µm) of capsules of *Lactiplantibacillus plantarum* and beetroot extract with alginate obtained by different encapsulation techniques.

Needle caliber	Extrusion	Emulsion
G31×6mm	978±42^{e}	600±150^{f}
G27×13mm	1,250±37^{c}	1,050±120^{d}
G22×32mm	2,260±120^{b}	2,850±260^{a}

Results are expressed as mean of three repetitions in triplicate ± standard deviation. Different letters (a–f) represent significant differences of values (p<0.05).

Table 3. Encapsulation efficiency (%EE) of *Lactiplantibacillus plantarum* with alginate (natural beads, NB) and *L. plantarum* and beetroot extract with alginate (beetroot beads, BB), percentage of bacteria viability after 24 h ($\%V_{24h}$) and percentage of bacteria survival after incubation under simulated gastrointestinal conditions.

	NB	BB
Count of *L. plantarum* (log cfu/g)	7.59±0.21[a]	7.82±0.10[a]
%EE	86.4±2.1[a]	88.0±2.8[a]
Count of *L. plantarum* after 24 h (log cfu/g)	6.07±0.11[b]	7.28±0.41[a]
$\%V_{24h}$	80.2±2.2[b]	92.4±2.1[a]
Survival (%) under gastrointestinal conditions	57.4±3.1[b]	73.3±1.0[a]

Results are expressed as mean of three repetitions ± standard deviation. Initial count of *L. plantarum* before encapsulation was ≈8.89 log cfu/mL. Values with different letters (a,b) in the same row are significantly different ($p<0.05$).

of 86.4–88.0%. No significant differences ($p\geq0.05$) in %EE were evidenced between the different formulations when cells were incorporated. These results are in agreement with the study by Pupa *et al*. [2021], who reported an efficacy of alginate – *L. plantarum* encapsulation in the range from 73.64 to 94.10%. They found a higher efficiency in the extrusion method compared to the spray drying method. Mahmoud *et al.* [2020] reported an efficiency of up to 94% with no significant differences between different encapsulating agents (skim milk, dextrin and chitosan) in combination with the alginate loaded with *L. plantarum*. In addition, our results showing that the content of beetroot extract did not affect the %EE are in line with the literature data; according to Krasaekoopt & Watcharapoka [2014], the effectiveness of encapsulation is independent of the concentration of prebiotics incorporated. Otherwise, the encapsulated bacteria viability after 24 h ($\%V_{24h}$) varied among formulations with better survival noted in beetroot beads (Table 3). A significantly ($p<0.05$) lower bacterial count by 1.52 log cfu/g was evidenced after 24 h in NB. The much smaller loss of 0.54 log cfu/g was noted for BB. This last assay is important to determine any negative effect of the beetroot extract on *L. plantarum* cells. A significant decrease within 24 h in the number of bacteria co-encapsulated with beetroot extract could indicate the occurrence of antimicrobial activity; if that is the case, co-encapsulation would not be feasible. On the contrary, if the population is maintained or increased, we can infer that the presence of the beetroot extract does not exert a negative effect or that it may actually be beneficial for the bacteria. Our results indicate that the incorporation of the beetroot extract in the alginate beads does not exert negative effects on *L. plantarum*. Since *L. plantarum* showed higher viability after 24 h in BB than in NB (Table 3), the effect of beetroot extract incorporation was found positive. According to Shafizadeh *et al*. [2020], some compounds co-encapsulated with bacteria could confer certain protective effect. Other investigations reported that the viability of encapsulated probiotics was improved when adding prebiotics, *i.e.*, raftilose [Capela *et al*., 2006], inulin [Akhiar, 2010], galacto-oligosaccharides and fructo-oligosaccharides [Amine *et al*., 2014], as well as dextrin and whey [Mahmoud *et al*., 2020] among others. These previous reports are consistent with our results, in which the V_{24h} was higher in BB than NB. Based on this literature data and our results, it can be concluded that the beetroot extract acted as a prebiotic.

The results presented in Table 3, show that the encapsulation efficiency was less than 95% for the beads produced. Even though other investigations have reported %EE above 95%, this could be improved by increasing the number of initial cell counts [Pupa *et al.,* 2021].

Viability of *L. plantarum* under simulated gastrointestinal conditions

The survival percentages of *L. plantarum* encapsulated in NB and BB after the incubation under simulated gastrointestinal conditions are shown in Table 3. For this assay, the free *L. plantarum* was used as a respective control. Encapsulated *L. plantarum* had better viability compared with the free cells, which were not detectable at the end of the process. These results are in agreement with those reported by Khosravi *et al.* [2014], who found no survival of free *Bifidobacterium bifidum* after exposure to simulated gastrointestinal conditions. Several other studies have reported better survival of bacteria in the capsules than in the non-encapsulated form, during exposure to unfavorable conditions [Chávarri *et al*., 2010; Khosravi *et al*., 2014; Krasaekoopt & Watcharapoka, 2014; Mahmoud *et al*., 2020; Pupa *et al*., 2021]. Besides this, significant difference ($p<0.05$) in the survival percentage was evidenced between the NB and BB, proving that BB ensured a better cell survival rate (73.3%) when compared with NB (57.4%) (Table 3). The losses of bacteria were 3.1 and 2.0 log cfu/g for NB and BB, respectively. This could suggest that beetroot had a protective effect on *L. plantarum*, which allows major survival of the bacteria in the gastric environment, compared with the bead that does not contain beetroot. Other studies reported a protective effect generated by the incorporation of skim milk [Mahmoud *et al*. 2020] or amylomaize [Khosravi *et al*., 2014], with losses ranging from 2.5 to 4.6 log cfu/g after exposure to gastrointestinal conditions, depending on the bacteria and the co-encapsulated material. It has been reported that beetroot represents a rich source of bioactive compounds and contains certain amounts of nutrients (*i.e.*, carbohydrates and proteins) that could protect the bacterial cells and thus maintain their viability [Barbu *et al*., 2020]. Although it has been

reported that buffering capacity of some ingredients can protect probiotic bacteria in the product or during intestinal transit [Shori, 2017; Tripathy & Giri, 2014], with the data presented here we cannot ensure which compound of beetroot was specifically responsible for this protection. According to Mahmoud *et al.* [2020], this protection may be influenced by the strong structure of the bead, or the nutritional factor conferred by the incorporation of beetroot extract.

Effect of the addition of capsules on the rheological properties of model food

To obtain functional food with capsules, different formulations of dressings based on O/W emulsion were prepared (Table 1). For monitoring the stability of the products, flow properties, the droplet size and coalescence rate were monitored during storage. The dressing without the addition of beads (DWB) was used as the control.

Flow properties of dressings

The flow behavior of O/W emulsions is important because the behavior of different formulations can be compared and appropriate process conditions, as well as optimal quality control strategies may be chosen accordingly [Mun *et al.,* 2009]. In our study, to evaluate changes in viscosity of dressings over time, emulsion flow curves (the changes in apparent viscosity as a function of shear rate) were obtained at the initial time of storage (zero time) and at the end of storage (28 days). Flow curves are presented in Figure 2. The behavior of the different dressings was consistent with the power law. Overall, dressings with NB and BB added exhibited non-Newtonian stress thinning behavior and a creep point related to the systems' initial resistance to flow. The control sample and formulated dressings showed a similar trend. To identify the flow characteristics of the dressings, the values of consistency coefficient (*k*) and flow behavior index (*n*) were obtained as a function of the shear rate. The *k* is often used as an indicator of fluid viscosity, which is a measure of the fluid's ability to resist deformation; high values indicate high viscosity and a stronger and more stable network structure [Castillo *et al.*, 2021]. When evaluating the flow behavior index, a value less than 1 represents pseudoplasticity; this characteristic is desirable for obtaining a dressing with a good mouth feel [Ma & Boye, 2013; Primacella *et al.*, 2019]. On the other hand, a high *k* value is desirable for the stability of the system. The *k* and *n* values for the formulated dressings (DWB, DNB, and DBB) at zero time and after 28 days of storage are shown in Table 4. Additionally, a commercial dressing (COD) was analyzed as a point of comparison. The initial *k* values varied from 12.52 to 14.52 Pa×s^n, with no significant differences ($p \geq 0.05$) among the formulations prepared, including the COD, indicating a similar viscosity of all the formulations tested. When the initial flow behavior index was considered, low values (<1) were evidenced for all the formulations. The initial *n* values varied from 0.239 to 0.299. Significant difference ($p<0.05$) was noted only between the DWB and COD formulations. Anyway, there was $n<1$ for all the formulations, so we could expect a good texture of the product. After 28 days of storage, the *k* values ranged from 13.93 to 17.23 Pa×s^n. On the other hand, the *n* values ranged from 0.249 to 0.300. The results showed no significant changes ($p \geq 0.05$) in *k* and *n* values over the storage period (after 28 days) regardless of the formulation, which indicates that the addition of the capsules did not affect the rheological properties of the system.

Droplet size and coalescence rate of dressings

An incorporation of a new ingredient can destabilize the system and may affect shelf life. Stability of the system can be monitored through changes in the average particle diameter over time and also implies prevention of coalescence [Castillo *et al.*, 2021]. Averages of droplet size ($d_{3,2}$) of the formulations were measured at zero time and after 14 and 28 days of storage. Changes in droplet size varied along time in the three formulations (Table 5). A significant difference ($p<0.05$) was found on day fourteen of storage only for DNB ($d_{3,2}$=4.380) compared with DWB ($d_{3,2}$=3.942) and DBB ($d_{3,2}$=3.836). On the other hand, on day 28 of storage, significant differences ($p<0.05$) were found for DNB ($d_{3,2}$=4.326) and DBB ($d_{3,2}$=3.925) compared with DWB ($d_{3,2}$=3.488). Despite the differences in those points, no significant

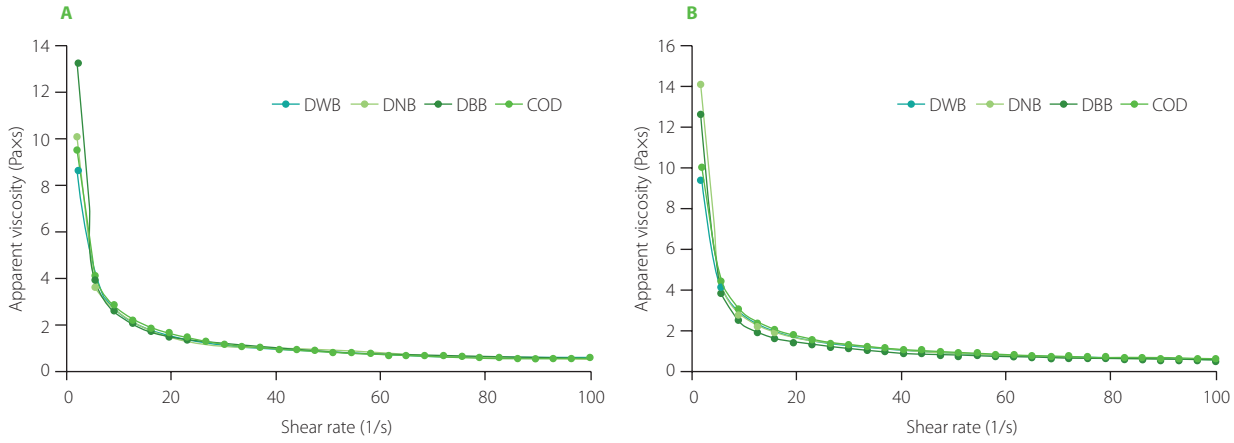

Figure 2. Apparent viscosity as a function of shear rate of the dressings at the initial (**A**) and final time of storage (28 days) (**B**). DWB, dressing without beads; DNB, dressing with encapsulated *Lactiplantibacillus plantarum* with alginate (natural beads); DBB, dressing with co-encapsulated *L. plantarum* and beetroot extract with alginate (beetroot beads); COD, commercial dressing.

Table 4. Consistency coefficient (*k*) and flow behavior index (*n*) of dressings at the initial (day 0) and final time (28 days) of storage, and coalescence rate (K_c) of model food.

Dressing	*k* (Pa×s^n)		*n*		K_c (1/s)
	0 day	28 days	0 day	28 days	
COD	14.29±0.89^{aA}	15.47±1.04^{aA}	0.239±0.020^{bA}	0.279±0.028^{aA}	−2×10^{-7a}
DWB	12.52±1.23^{aA}	13.93±1.11^{aA}	0.299±0.018^{aA}	0.300±0.015^{aA}	−4×10^{-8b}
DNB	13.20±3.61^{aA}	17.23±2.66^{aA}	0.279±0.044^{abA}	0.249±0.044^{aA}	−3×10^{-7a}
DBB	14.52±3.26^{aA}	15.85±2.77^{aA}	0.251±0.050^{abA}	0.251±0.039^{aA}	−1×10^{-7a}

Results are expressed as mean of three repetitions ± standard deviation. Values with different minor letters (a–c) in the same column are significantly different (p<0.05). Values with different capital letters (A, B) in the same row for each parameter separately (*k* or *n*) are significantly different (p<0.05). COD, commercial dressing; DWB, dressings without beads; DNB, dressing with encapsulated *Lactiplantibacillus plantarum* with alginate (natural beads); DBB, dressing with co-encapsulated *L. plantarum* and beetroot extract with alginate (beetroot beads).

Table 5. Average particle diameter ($d_{3,2}$, µm) of the dressings at 0, 14 and 28 days of storage.

Dressing	0 day	14 days	28 days	Mean
DWB	3.514±0.011^{a}	3.942±0.115^{b}	3.488±0.015^{b}	3.624±0.215^{a}
DNB	3.518±0.013^{a}	4.380±0.027^{a}	4.326±0.053^{a}	4.070±0.408^{a}
DBB	3.512±0.007^{a}	3.836±0.025^{b}	3.925±0.041^{a}	3.786±0.217^{a}

Results are expressed as mean of three repetitions in triplicate ± standard deviation. Different letters (a,b) in the same column represent significant differences (p<0.05). DWB, dressings without beads; DNB, dressing with encapsulated *Lactiplantibacillus plantarum* with alginate (natural beads); DBB, dressing with co-encapsulated *L. plantarum* and beetroot extract with alginate (beetroot beads).

differences (p≥0.05) were found in the global behavior throughout the 28 days.

Another parameter that provides important information about stability of the emulsion is the coalescence rate (K_c), which can be measured through changes in the average diameter of the drops over time. This parameter allows the collection of quantitative data on system stability. The coalescence rate of the different formulations is reported in Table 4. Despite a significant difference (p<0.05) was noted for DWB (−4×10^{-8}) compared with the other formulations, the coalescence rate for all the dressings tested had very low values with exponents −7 and −8. The formulations with encapsulated probiotic showed similar behavior compared with the COD with values ranging from −1×10^{-7} to −3×10^{-7}. According to Bautista *et al.* [2018], values at this level indicate a stable system. When the droplet coalescence rate is high, a decrease in the emulsion's viscosity may occur because the coalescence of emulsions is inversely related to the viscosity of the aqueous phase [Krstonošić *et al*., 2009]. We can observe in our results that *k* of the formulations did not decrease during storage (Table 4).

The coalescence of emulsions in storage conditions are influenced by different factors, as collision frequency and drainage time [Ye *et al.*, 2004]. This phenomenon could take place in different stages of emulsion formulation, *i.e.*, whipping process or storage [Petrut *et al.,* 2016]. The addition of certain ingredients including those with different functional characteristics could cause changes in stability. Preserving the original viscoelastic properties is very important to the quality of the product that is strongly influenced by its rheological properties and appearance attributes [Ma & Boye, 2013]. Losses in stability provoked by the increase in droplet mean diameter of the emulsion shorten the shelf life. Therefore, obtaining a product with an extended shelf life is a challenge during food product formulation [Traynor *et al.*, 2013].

Viability of encapsulated *L. plantarum* in a model food in storage conditions

The NB and BB loaded with *L. plantarum* were added to a dressing (DNB and DBB, respectively) and the viability of the probiotic was determined over time. Viable counts of *L. plantarum* during 28 days of storage at 4°C are presented in Figure 3A. Also, the percentage of viability was calculated and results are shown in Figure 3B. Even though the number of viable cells of *L. plantarum* decreased as time progresses in both models, the DBB maintained a greater viability of the probiotic over time, ranging from 7.09 to 4.3log cfu/g, and a percentage of viability ranging from 94.4% to 60.6% along the storage time, respectively. On the other hand, the levels of cells recovered for the DNB were significantly lower (p< 0.05) from the 8th day on. The bacterial population decreased from 6.90 to 2.1 log cfu/g at the end of storage for this last model, while the percentage of viability ranged from 79.2% to 30.6%, respectively. At the end of storage, a total diminution of 2.8 log cfu/g was detected for DBB and 4.8 log cfu/g for DNB, suggesting that encapsulated beetroot could act as a prebiotic ingredient. Our results are in agreement with Chavarri *et al.* [2010], who reported losses of encapsulated probiotic bacteria ranging from 2.1 to 3.4 log cfu/g along the time of storage (28 days), depending on the bead matrix. Additionally, Rodríguez Huezo *et al.* [2011] reported losses of 4.0 log cfu/g for encapsulated probiotics without prebiotic ingredient in a period of 25 days.

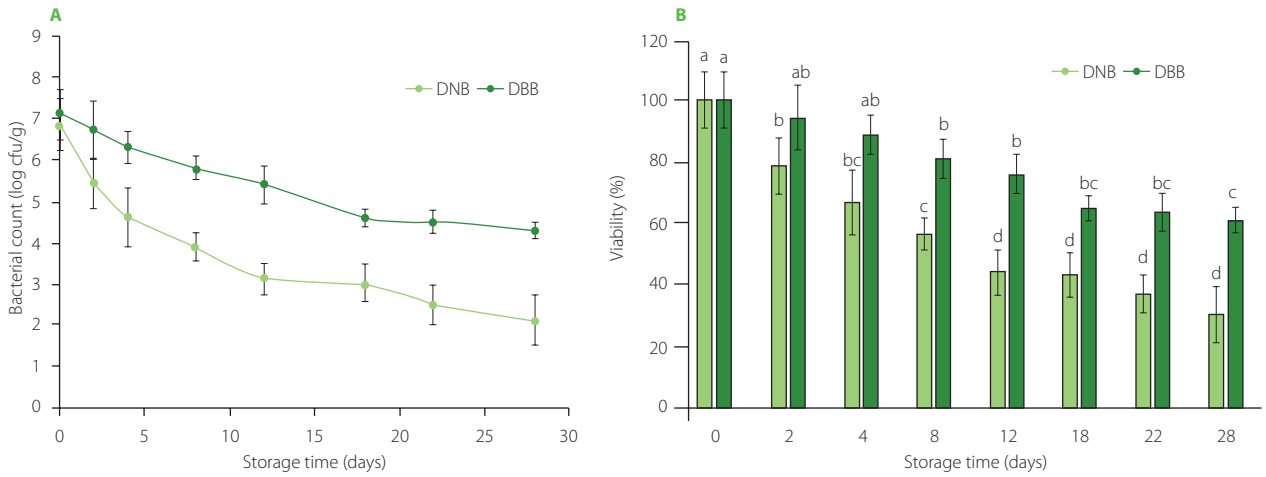

Figure 3. Viable counts of encapsulated *Lactiplantibacillus plantarum* along time of storage at 4°C in the model food (**A**). Percentage of viability of *L. plantarum* along storage time in the model food (**B**). Error bars represent standard deviation. Different letters in the top of the bars (a–d) represent significant differences ($p<0.05$). DNB, dressing with encapsulated *L. plantarum* with alginate (natural beads); DBB, dressing with co-encapsulated *L. plantarum* and beetroot extract with alginate (beetroot beads).

Although the population of *L. plantarum* continued to decline by the 28th day, the population remained over 60% in DBB, while the DNB model had less than 35% of viability at the end of storage. These results are consistent with other reports, in which greater viability of probiotics was observed when encapsulated with prebiotics rather than with natural beads [Capela *et al.,* 2006; Krasaekoopt & Watcharapoka, 2014; Mahomud *et al.,* 2020]. Krasaekoopt & Watcharapoka, [2014] reported greater viability of *L. casei* and *L. acidophilus* encapsulated with galacto-oligosaccharides compared with those without this prebiotic. The authors also reported minimal losses of population (0.5 to 2.5 log cfu/g) along four weeks of storage. Additionally, Mahomud *et al.* [2020] reported better survival in storage conditions for *L. plantarum* when co-encapsulated with skim milk, and in some cases, an increase in population was evidenced. According to Barbu *et al.* [2020], diverse factors may influence the growth of the probiotics; in these cases, it could be attributed to biocomposites and nutrients from the bead matrix that somehow protect the bacterial cells, and thus maintain their viability. In a dressing, a probiotic bacterium must be kept immobilized to prevent proliferation, and in this way prevent food decomposition; when encapsulating the bacteria, it remains immobilized, protecting the integrity of the food while maintaining its attributes, such as pH and texture. Likewise, it has been demonstrated that beetroot consumption has a beneficial effect on the gut microbiota in humans, induced by a prebiotic effect [Alexandrino de Oliveira *et al.,* 2021]. Our results have shown a higher microbial recovery during storage time in the DBB model, so this model could have been influenced by the presence of the beetroot extracts inside the capsules.

Industrially, encapsulated probiotic bacteria can be used in many products (*i.e.*, yogurt, cheese or frozen dairy desserts). This strategy provides higher stability of bacteria also protecting the components incorporated against nutritional loss [Anal & Singh, 2007; Khosravi *et al*., 2014].

CONCLUSIONS

The extrusion technique demonstrated greater feasibility compared to emulsification for obtaining capsules of *L. plantarum* with alginate and *L. plantarum* and beetroot extract with alginate with homogeneous morphology and size. The co-encapsulation of *L. plantarum* and beetroot extract with alginate conferred better protection for bacteria under gastrointestinal conditions than the encapsulation of *L. plantarum* along with alginate Although the protection exerted by beetroot on the bacteria was evidenced, due to the number of components that beetroot contains, it is difficult to determine the driving mechanisms of this protection. Further studies are ongoing on this aspect. When beads were incorporated to the O/W emulsion model food, they did not cause changes in the flow properties or droplet coalescence, indicating that the addition of the capsules does not cause system destabilization. Additionally, beetroot beads preserved the viability of *L. plantarum* during 28 days of storage in the product, indicating that the incorporation of beetroot in the capsule could have a prebiotic effect on *L. plantarum*. Future studies should be carried out to evaluate the acceptability of the developed product.

ACKNOWLEDGEMENTS

The authors acknowledge the Universidad Autónoma de Nuevo León for supporting this investigation by "Programa de apoyo a la investigación científica y tecnológica (Paicyt)-UANL". This manuscript is part of the PhD thesis of Salvador López Uriarte, who was supported by a PhD scholarship from the National Council of Science and Technology of México (CONACYT).

RESEARCH FUNDING

This research received no external funding.

CONFLICTS OF INTEREST

The authors declare no conflict of interests.

ORCID IDs

M.P. Barrón González https://orcid.org/0000-0002-8386-444X
M. Bautista-Villarreal https://orcid.org/0000-0001-7975-1488
S.L. Castillo Hernández https://orcid.org/0000-0001-8354-3200

REFERENCES

1. Akhiar, N.S.M. (2010). Enhancement of probiotics survival by microencapsulation with alginate and prebiotics. *MMG 445 Basic Biotechnology*, *6*, 13-18.
2. Alexandrino de Oliveira, S.P., do Nascimento, H.M.A., Sampaio, K.B., de Souza, E.L. (2021). A review on bioactive compounds of beet (*Beta vulgaris L. subsp. vulgaris*) with special emphasis on their beneficial effects on gut microbiota and gastrointestinal health. *Critical Reviews in Food Science and Nutrition*, *61*(12), 2022–2033. https://doi.org/10.1080/10408398.2020.1768510
3. Amine, K.M., Champagne, C.P., Salmieri, S., Britten, M., St-Gelais, D., Fustier, P., Lacroix, M. (2014). Effect of palmitoylated alginate microencapsulation on viability of *Bifidobacterium longum* during freeze-drying. *LWT – Food Science and Technology*, *56*(1), 111–117. https://doi.org/10.1016/j.lwt.2013.11.003
4. Anal, A.K., Singh, H. (2007). Recent advances in microencapsulation of probiotics for industrial applications and targeted delivery. *Trends in Food Science & Technology*, *18*(5), 240–251. https://doi.org/10.1016/j.tifs.2007.01.004
5. Baek, Y.J., Lee, B.H., (2009). Chapter 12 – Probiotics and prebiotics as bioactive components in dairy products. In Park, Y.W. (Ed.). *Bioactive Components of Milk and Dairy Products*., Willey- Blackwell, pp. 287–310. https://doi.org/10.1002/9780813821504.ch12
6. Barbu, V., Cotarlet, M., Bolea, C.A., Cantaragiu, A., Andronoiu, D.G., Bahrim, G.E., Enachi, E. (2020). Three types of beetroot products enriched with lactic acid bacteria. *Foods*, *9*(6), art. no. 786. https://doi.org/10.3390/foods9060786
7. Bautista Villarreal, M., Gallardo Rivera, C.T., García Márquez, E., Rodríguez Rodríguez, J., Núñez González, M.A., Chávez Montes, A., Báez González, J.G. (2018). Comparative reduction of egg yolk cholesterol using anionic chelating agents. *Molecules*, *23*(12), art. no. 3204. https://doi.org/10.3390/molecules23123204
8. Borjan, D., Šeregelj, V., Andrejč, D.C., Pezo, L., Tumbas Šaponjac, V., Knez, Ž., Vulić, J., Marevci, M.K. (2022). Green techniques for preparation of red beetroot extracts with enhanced biological potential. *Antioxidants*, *11*(5), art. no. 805. https://doi.org/10.3390/antiox11050805
9. Capela, P., Hay, T.K.C., Shah, N.P. (2006). Effect of cryoprotectants, prebiotics and microencapsulation on survival of probiotic organisms in yoghurt and freeze-dried yoghurt. *Food Research International*, *39*(2), 203–211. https://doi.org/10.1016/j.foodres.2005.07.007
10. Capela, P., Hay, T.K.C., Shah, N.P. (2007). Effect of homogenisation on bead size and survival of encapsulated probiotic bacteria. *Food Research International*, *40*(10), 1261–1269. https://doi.org/10.1016/j.foodres.2007.08.006
11. Castillo, S., Rodríguez, A., Bautista-Villarreal, M., García-Solano, N., Gallardo-Rivera, C., Báez-González, J.G., Sánchez-García, E., García-Alanis, K.G. (2021). Rheological and nutritional characterization of sweet corn by-product (cob) to develop a functional ingredient applied in dressings. *Frontiers in Nutrition*, *8*, art. No. 666654. https://doi.org/10.3389/fnut.2021.666654
12. Chávarri, M., Marañón, I., Ares, R., Ibáñez, F.C., Marzo, F., del Carmen Villarán, M. (2010). Microencapsulation of a probiotic and prebiotic in alginate-chitosan capsules improves survival in simulated gastro-intestinal conditions. *International Journal of Food Microbiology*, *142*(1–2), 185–189. https://doi.org/10.1016/j.ijfoodmicro.2010.06.022
13. Chhikara, N., Kushwaha, K., Jaglan, S., Sharma, P., Panghal, A. (2019). Nutritional, physicochemical, and functional quality of beetroot (*Beta vulgaris* L.) incorporated Asian noodles. *Cereal Chemistry*, *96*(1), 154–161. https://doi.org/10.1002/cche.10126
14. Holkem, A.T., Raddatz, G.C., Nunes, G.L., Cichoski, A.J., Jacob-Lopes, E., Grosso, C.R.F., de Menezes, C.R. (2016). Development and characterization of alginate microcapsules containing Bifidobacterium BB-12 produced by emulsification/internal gelation followed by freeze drying. *LWT – Food Science and Technology*, *71*, 302–308. https://doi.org/10.1016/j.lwt.2016.04.012
15. Khosravi Zanjani, M.A., Tarzi, B.G., Sharifan, A., Mohammadi, N. (2014). Microencapsulation of probiotics by calcium alginate-gelatinized starch with chitosan coating and evaluation of survival in simulated human gastro-intestinal condition. *Iranian Journal of Pharmaceutical Research: IJPR*, *13*(3), art. no. 843.
16. Krasaekoopt, W., Watcharapoka, S. (2014). Effect of addition of inulin and galactooligosaccharide on the survival of microencapsulated probiotics in alginate beads coated with chitosan in simulated digestive system, yogurt and fruit juice. *LWT – Food Science and Technology*, *57*(2), 761–766. https://doi.org/10.1016/j.lwt.2014.01.037
17. Krstonošić, V., Dokić, L., Dokić, P., Dapčević, T. (2009). Effects of xanthan gum on physicochemical properties and stability of corn oil-in-water emulsions stabilized by polyoxyethylene (20) sorbitan monooleate. *Food Hydrocolloids*, *23*(8), 2212–2218. https://doi.org/10.1016/j.foodhyd.2009.05.003
18. Lazar, S., Constantin, O., Horincar, G., Georgeta, D., Stanciuc, N., Muresan, C., Rapeanu, G. (2022). Beetroot by-product as a functional ingredient for obtaining value added mayonnaise. *Processes*, *10*(2), art. no. 227. https://doi.org/10.3390/pr10020227
19. Li, X.Y., Chen, X.G., Cha, D.S., Park, H.J., Liu, C.S. (2009). Microencapsulation of a probiotic bacteria with alginate gelatin and its properties. *Journal of Microencapsulation*, *26*(4), 315–324. https://doi.org/10.1080/02652040802328685
20. Lopes, S., Bueno, L., De Aguiar Júnior, F., Finkler, C.L.L. (2017). Preparation and characterization of alginate and gelatin micro-capsules containing *Lactobacillus rhamnosus*. *Anais Da Academia Brasileira de Ciencias*, *89*(3), 1601–1613. https://doi.org/10.1590/0001-3765201720170071
21. Ma, Z., Boye, J.I. (2013). Advances in the design and production of reduced--fat and reduced-cholesterol salad dressing and mayonnaise: A review. *Food and Bioprocess Technology*, *6*(3), 648–670. https://doi.org/10.1007/s11947-012-1000-9
22. Mahmoud, M., Abdallah, N.A., El-Shafei, K., Tawfik, N.F., El-Sayed, H.S. (2020). Survivability of alginate-microencapsulated *Lactobacillus plantarum* during storage, simulated food processing and gastrointestinal conditions. *Heliyon*, *6*(3), art. no. e03541. https://doi.org/10.1016/j.heliyon.2020.e03541
23. Mirmiran, P., Houshialsadat, Z., Gaeini, Z., Bahadoran, Z., Azizi, F. (2020). Functional properties of beetroot (*Beta vulgaris*) in management of cardio--metabolic diseases. *Nutrition & Metabolism*, *17*, art. no. 3. https://doi.org/10.1186/s12986-019-0421-0
24. Motalebi Moghanjougi, Z., Rezazadeh Bari, M., Alizadeh Khaledabad, M., Amiri, S., Almasi, H. (2021). Microencapsulation of *Lactobacillus acidophilus* LA-5 and *Bifidobacterium animalis* BB-12 in pectin and sodium alginate: A comparative study on viability, stability, and structure. *Food Science & Nutrition*, *9*(9), 5103-5111. https://doi.org/10.1002/fsn3.2470
25. Mun, S., Kim, Y.L., Kang, C.G., Park, K.H., Shim, J.Y., Kim, Y.R. (2009). Development of reduced-fat mayonnaise using 4αGTase-modified rice starch and xanthan gum. *International Journal of Biological Macromolecules*, *44*(5), 400-407. https://doi.org/10.1016/j.ijbiomac.2009.02.008
26. Nordström, E.A., Teixeira, C., Montelius, C., Jeppsson, B., Larsson, N. (2021). *Lactiplantibacillus plantarum* 299v (LP299V®): Three decades of research. *Beneficial Microbes*, *12*(5), 441-465. https://doi.org/10.3920/BM2020.0191
27. Otalora, C.M., Bonifazi, E., Fissore, E.N., Basanta, F., Gerschenson, L.N. (2020). Thermal stability of betalains in by-products of the blanching and cutting of *Beta vulgaris* L. var conditiva. *Polish Journal of Food and Nutrition Sciences*, *70*(1), 15-24. https://doi.org/10.31883/pjfns/116415
28. Petrut, R.F., Danthine, S., Blecker, C. (2016). Assessment of partial coalescence in whippable oil-in-water food emulsions. *Advances in Colloid and Interface Science*, 229, 25-33. https://doi.org/10.1016/j.cis.2015.12.004
29. Płatosz, N., Sawicki, T., Wiczkowski, W. (2020). Profile of phenolic acids and flavonoids of red beet and its fermentation products. does long-term consumption of fermented beetroot juice affect phenolics profile in human blood plasma and urine? *Polish Journal of Food and Nutrition Sciences*, *70*(1), 55–65. https://doi.org/10.31883/pjfns/116613
30. Primacella, M., Wang, T., Acevedo, N.C. (2019). Characterization of mayonnaise properties prepared using frozen-thawed egg yolk treated with hydrolyzed egg yolk proteins as anti-gelator. *Food Hydrocolloids*, *96*(06), 529–536. https://doi.org/10.1016/j.foodhyd.2019.06.008
31. Pupa, P., Apiwatsiri, P., Sirichokchatchawan, W., Pirarat, N., Muangsin, N., Shah, A.A., Prapasarakul, N. (2021). The efficacy of three double-microencapsulation methods for preservation of probiotic bacteria. *Scientific Reports*, *11*(1), art. no. 13753. https://doi.org/10.1038/s41598-021-93263-z
32. Rajam, R., Subramanian, P. (2022). Encapsulation of probiotics: Past, present and future. *Beni-Suef University Journal of Basic and Applied Sciences*, *11*(1), art. no. 26. https://doi.org/10.1186/s43088-022-00228-w
33. Rodríguez-Huezo, M.E., Lobato-Calleros, C., Reyes-Ocampo, J.G., Sandoval-Castilla, O., Perez-Alonso, C., Pimentel-Gonzalez, D.J. (2011). Survivability of entrapped *Lactobacillus rhamnosus* in liquid-and gel-core alginate beads during storage and simulated gastrointestinal conditions. *Revista Mexicana de Ingeniería Química*, *10*(3), 353–361.
34. Sakin-Yilmazer, M., Dirim, S.N., Di Pinto, D., Kaymak-Ertekin, F. (2014). Yoghurt with candied chestnut: freeze drying, physical, and rheological behaviour. *Journal of Food Science and Technology, 51*, 3949–3955. https://doi.org/10.1007/s13197-012-0890-x

35. Shori, A.B. (2017). Microencapsulation improved probiotics survival during gastric transit. *HAYATI Journal of Biosciences*, *24*(1), 1–5. https://doi.org/10.1016/j.hjb.2016.12.008
36. Sánchez, E., Morales, C.R., Castillo, S., Leos-Rivas, C., Misael, D., Martínez, O. (2016). Antibacterial and antibiofilm activity of methanolic plant extracts against nosocomial microorganisms. *Evidence Based Complementary and Alternative Medicine*, *2016,* art. no. 1572697. https://doi.org/10.1155/2016/1572697
37. Shafizadeh, A., Golestan, L., Ahmadi, M., Darjani, P., Ghorbani-HasanSaraei, A. (2020). Encapsulation of *Lactobacillus casei* in alginate microcapsules: improvement of the bacterial viability under simulated gastrointestinal conditions using flaxseed mucilage. *Journal of Food Measurement and Characterization*, *14*, 1901–1908. https://doi.org/10.1007/s11694-020-00437-w
38. Spórna-Kucab, A., Tekieli, A., Skalicka-Woźniak, K., Grzegorczyk, A., Świergosz, T., Wybraniec, S. (2022). Characterization of triterpene saponin composition of white, yellow and red beetroot (*Beta vulgaris* L.). *Polish Journal of Food and Nutrition Sciences, 72*(2), 159-170. https://doi.org/10.31883/pjfns/149515
39. Traynor, M., Burke, R., Frias, J.M., Gaston, E., Barry-Ryan, C. (2013). Formation and stability of an oil in water emulsion containing lecithin, xanthan gum and sunflower oil. *International Food Research Journal*, *20*(5), 2173–2181. https://doi.org/10.21427/d7d189
40. Tripathi, M.K., Giri, S.K. (2014). Probiotic functional foods: Survival of probiotics during processing and storage. *Journal of Functional Foods*, *9*, 225-241. https://doi.org/10.1016/j.jff.2014.04.030
41. Tumbas Šaponjac, V., Čanadanović-Brunet, J., Ćetković, G., Jakišić, M., Vulić, J.J., Stajčić, S., Šeregelj, V. (2020). Optimisation of beetroot juice encapsulation by freeze-drying. *Polish Journal of Food and Nutrition Sciences*, *70*(1), 25–34. https://doi.org/10.31883/pjfns/115153
42. Vijaya Kumar, B., Vijayendra, S.V., Reddy, O.V.S. (2015). Trends in dairy and non-dairy probiotic products-a review. *Journal of Food Science and Technology*, *52*, 6112-6124. https://doi.org/10.1007/s13197-015-1795-2
43. Ye, A., Hemar, Y., Singh, H. (2004). Enhancement of coalescence by xanthan addition to oil-in-water emulsions formed with extensively hydrolysed whey proteins. *Food Hydrocolloids*, *18*(5), 737–746. https://doi.org/10.1016/j.foodhyd.2003.11.010

ORIGINAL ARTICLE
http://journal.pan.olsztyn.pl

Polish Journal of Food and Nutrition Sciences
2023, Vol. 73, No. 3, 253–264
DOI: 10.31883/pjfns/170219
ISSN 1230-0322, e-ISSN 2083-6007

Formulation of a Ready-to-Cook Soup Mix Using Microencapsulated Protein Hydrolysate Obtained from Pink Perch By-Product

Asha Kumari[1,2], Nutan Kaushik[1]*, Rasa Slizyte[3], Khushboo[1]

[1]Amity Food and Agriculture Foundation, Amity University Uttar Pradesh, Noida, Uttar Pradesh, India
[2]Amity Institute of Food Technology, Amity University Uttar Pradesh, Noida, Uttar Pradesh, India
[3]Department of Fisheries and New Biomarine Industry, SINTEF Ocean, Trondheim, Norway

In fast-growing world, people have not enough time for the preparation of food and they have started depending on fast foods. However, consumption of fast foods causes malnutrition and nutrition-related diseases. Thus, there is a need to formulate nutrient-rich products that are easy to cook. In this study, lyophilized protein hydrolysate from pink perch by-product, microencapsulated protein hydrolysate and sun-dried whole fish powder were incorporated in the formulation of ready-to-cook (RTC) soup mixes. The chemical and physical properties, and consumer acceptability of RTC soup mixes were evaluated. The RTC soup mixes exhibited high solubility (41.0 to 43.0%) and non-Newtonian pseudoplastic behavior. RTC soup mix with microencapsulated protein hydrolysate (MPHS) had high overall acceptability among all RTC soup mixes. The accelerated shelf-life testing (40°C, 75% RH) revealed that RTC MPHS mix was stable for 6 days (equivalent to 24 days of storage at room temperature) without any preservatives and sterilization treatment. Therefore, RTC MPHS mix can be used as a nutrient-rich product in protein-deficient populations.

Key words: nutrient-rich soup, fish protein hydrolysate, viscosity, pasting properties, consumer assessment, storage stability

INTRODUCTION

Fish and seafoods are abundant sources of good protein, oil, and minerals for maintaining healthy body worldwide [Ravichandran *et al*., 2012]. While fish is being considered for various preparations, large amounts of fish by-products (head, viscera, skin, and bones) are generated (approximately 50–60% of total fish capture) during processing. In many countries, these fish by-products have not been utilized efficiently and their disposal as such can have large adverse impacts on the natural environment [Jafarpour *et al*., 2020]. Therefore, there is an urgent requirement to find ecologically-sustainable way for efficient utilization of fish by-products. The fish by-products are potential sources to obtain high-quality protein hydrolysates by using enzymatic hydrolysis [Opheim *et al*., 2015; Slizyte *et al*., 2018]. In our previous study we utilized fish head and viscera to produce protein hydrolysate using Alcalase which was then microencapsulated [Kumari *et al*., 2023].

In urban areas, people do not have enough time to cook foods due to their busy schedule, which results in the consumption of fast food having high sugar, fat, and salt contents, and being deficient in protein, fiber, vitamins, and minerals. Consumption of such types of foods causes malnourishment and nutrition-related diseases [Farzana *et al*., 2017]. The problem of malnutrition related to protein deficiency is a matter of great concern in both developing and developed countries. The daily allowance of protein recommended by National Institute

***Corresponding Author:**
e-mail: kaushikn2008@gmail.com, nkaushik5@amity.edu (N. Kaushik)

Submitted: 23 March 2023
Accepted: 1 August 2023
Published on-line: 28 August 2023

of Nutrition (ICMR NIN) in India is 54 g/day for men, 46 g/day for women and 23 g/day for children [ICMR NIN, 2020]. Nutrient-enriched foods, such as protein-enriched ready-to-cook soup, are one of the potential ways to fight against malnutrition as they are easy to cook and eat [Mohamed *et al*., 2020]. The underutilized fish or fish by-products are potential sources for the development of protein-rich products which can help both high- and low-income populations to fight against malnutrition and, on the other hand, the fish industry can also earn extra profit by producing value-added products and aid in eliminating harmful effects on the natural environment.

Fish have been utilized to produce protein-rich products, such as fish soup powder, fish protein concentrate, *etc*. [Shashidhar *et al*., 2014]. However, the products developed from fish-derived ingredients may have a low market acceptability due to sensory problems (flavor and fishy odor) despite their improved nutritional quality. Therefore, in this study, microencapsulated protein hydrolysate obtained from pink perch head and viscera was used to formulate a ready-to-cook soup mix. The developed ready-to-cook soup mix may have improved sensory and nutritional properties, which increases the market acceptability of fish products. The optimization of pink perch head and viscera protein hydrolysis, characterization of hydrolysate, and its controlled release from microencapsulate were studied in our previous study [Kumari *et al*., 2023]. Therefore, the aim of this study was to formulate a ready-to-cook (RTC) soup mix containing the microencapsulated protein hydrolysate of pink perch head and viscera and evaluate its physical and chemical characteristics as well as its consumer acceptability.

MATERIAL AND METHODS

Raw material

The pink perch (*Nemipterus japonicus*) head and viscera were procured from Ulka Seafood Pvt. Ltd. (Mumbai, India) and minced into Hobart mincer (model AE 200, Hobart, Offenburg, Germany) with 10 mm holes. Vegetables (bean, carrot, and pea) used in soup formulation were procured from the local market (Noida, Uttar Pradesh, India). The vegetables were cleaned and cut into pieces. The chopped vegetables were blanched and freeze-dried in a lyophilizer (SNS FD-50, SN Solutions, Noida, Uttar Pradesh, India) and stored at −20°C till further used. The other ingredients, such as: salt, sugar, potato starch, milk solid, wheat refined flour, sunflower oil and spice mix (turmeric, black pepper, and roasted cumin), were purchased from the local supermarket. The sun-dried whole fish powder was procured from Coastal Export Corporation (Mangalore, Karnataka, India). All the chemicals and reagents used were of analytical grade. Nutrient agar, Czapek dox agar, XLD agar and EMB agar media were procured from Himedia (Thane, Maharashtra, India).

Preparation of microencapsulated protein hydrolysate

The protein hydrolysate was prepared as *per* method of Kumari *et al*. [2023]. Pink perch head and viscera minced sample (100 g) was mixed with hot distilled water (100 mL). Alcalase® (Novozymes A/S, Bagsværd, Denmark) (0.15 mL) was added into the sample. The content was incubated at 58°C for 85 min on a rotating test tube mixer (Stuart SB3, Vernon Hills, IL, USA) to ensure homogenous mixing. After completion of hydrolysis, the enzyme was deactivated by heating the mixture at 90°C for 10 min. The mixture was centrifuged at 5,000×*g* for 15 min. After the centrifugation, the tubes containing three layers were frozen at −20°C. The middle layer containing the protein hydrolysate was separated by cutting the layer with a knife. The protein hydrolysate layer thus obtained was freeze-dried in a lyophilizer (SNS FD-50, SN Solutions). The freeze-dried protein hydrolysate was stored at −20°C.

The freeze-dried protein hydrolysate was microencapsulated as *per* method of Kumari *et al*. [2023]. Maltodextrin (dextrin maize starch), gum Arabic and sodium alginate (1:1:1 ratio, *w/w/w*) were used as wall material. The protein hydrolysate and wall material were used in 4:6 ratio (*w/w*). First, the protein hydrolysate was dissolved in distilled water (1:25 ratio, *w/v*) with continuous stirring on a magnetic stirrer. Then, the wall material was added gradually in the following order: first maltodextrin then gum Arabic followed by sodium alginate with continuous stirring on a magnetic stirrer for 4 h. The microencapsulated protein hydrolysate was freeze-dried in a lyophilizer. The freeze-dried microencapsulated protein hydrolysate was stored at −20°C until further used.

Formulation of ready-to-cook soup mixes

The freeze-dried microencapsulated protein hydrolysate was used for RTC soup (microencapsulated protein hydrolysates soup, MPHS) mix formulation (Figure S1). Freeze-dried protein hydrolysate alone and sun-dried whole fish powder-based RTC soup (protein hydrolysate soup, PHS, and fish power soup, FPS, respectively) mixes were also prepared and used as controls. The composition of three RTC soup mixes and blank sample are provided in Table 1. The RTC blank soup (BS) mix was prepared by traditional standard recipes. The RTC soup mixes were prepared by mixing all the ingredients, *i.e*., vegetables, potato starch, wheat refined flour, sunflower oil, salt, sugar, and spices mix, and were packed in metallic polyethylene zip lock bags (32-micron thickness) with proper hygiene in a laminar flow. The packages were stored at −20°C. The RTC soup mix (each type) was prepared in triplicate. The main idea of formulation was to use different sources of proteins/peptides/amino acids and achieve 15% protein equivalent content in all RTC soup mixes. Therefore, the amount of other ingredients varied or was adjusted to make the overall weight to 100 g. The formulated RTC soup mixes were also compared with commercially available chicken soup (CCS) and vegetables soup (CVS). The ingredient used in CCS were refined wheat flour (maida), sugar, milk solids, hydrolyzed vegetable protein, iodized salt, flavors (nature identical flavoring substances and garlic), dehydrated vegetables (onion, leeks), dehydrated chicken, stabilizers (E461 and E407), antioxidant (E300), palm oil, thickener (E415), flavor enhancers (E627 and E631), spices and condiments (black pepper) and food color (caramel IV). The ingredients used in CVS were maize starch, dehydrated vegetables (carrot flakes, cabbage flakes, green peas,

Table 1. Formulation of ready-to-cook soup mixes (g/100 g).

Ingredient	BS	MPHS	PHS	FPS
Microencapsulated protein hydrolysate	0.0	27.0	0.0	0.0
Protein hydrolysate	0.0	0.0	11.0	0.0
Sun dried whole fish powder	0.0	0.0	0.0	16.0
Potato starch	28.0	15.0	25.0	20.0
Dried beans	15.5	15.5	15.5	15.5
Dried carrot	15.5	15.5	15.5	15.5
Milk solid	10.0	10.0	10.0	10.0
Refined flour	15.0	5.0	10.0	10.0
Salt	7.0	5.0	6.0	6.0
Sugar	3.0	2.0	2.0	2.0
Sunflower oil	4.5	4.0	4.0	4.0
Spice mix	1.5	1.0	1.0	1.0

BS, blank soup; MPHS, microencapsulated protein hydrolysate soup; PHS, protein hydrolysate soup; FPS, sun dried whole fish powder soup.

corn, onion powder, leeks), refined wheat flour (maida), milk solids, iodized salt, sugar, hydrolyzed vegetables protein, palm oil, thickener (E415), spices and condiments, anticaking agent (E551) and flavor enhancers (E627 and E631).

Characterization of ready-to-cook soup mix

Proximate analysis

The moisture, lipid and ash contents of ready-to-cook soup mixes were determined as *per* the standard methods of AOAC International [AOAC, 2005]. The moisture content of RTC soup mixes was determined by hot air oven method (Method no: 935.29). The RTC soup mix (1 g) was kept at 105°C for 24 h in a hot air oven. The sample was cooled in a desiccator and then weighed. Lipid content of the ready-to-cook soup mixes was determined using a Soxhlet apparatus (Method no: 2003.05). Ash content of the ready-to-cook soup mix was determined with the gravimetric method using a muffle furnace. RTC soup mixes (1 g) were kept at 500°C for 24 h in a muffle furnace. After complete ashing, weight of the ash was measured after sample cooling in a desiccator (Method No: 942.05).

The total nitrogen content of the ready-to-cook soup mix was estimated by Dumas method [Feng *et al*., 2022] in an automated micro-analyzer (Elementar® Max N Exceed, Elementar Analysensysteme GmbH, Langenselbold, Germany). The sample (50 mg) was weighed in a tin crucible and kept in the combustion chamber. The standard (aspartic acid) of known nitrogen content was used to calculate the amount of nitrogen present in the sample. The total protein content was calculated by multiplying the total nitrogen content by a factor of 6.25 [Steinsholm *et al*., 2021].

The carbohydrate content of the soup mix (g/100 g) was calculated using formula (1) [Merrill & Watt, 1973].

$$\text{Carbohydrate content} = 100 - (\text{Moisture content} + \text{Protein content} + \text{Ash content} + \text{Lipid content}) \quad (1)$$

All the analyses were performed in duplicate.

Total soluble solid determination

Total soluble solid (TSS) content of the ready-to-cook soup mixes was measured using refractometer (CTL-REFM-BR32, LW Scientific, Lawrenceville, GA, USA) at room temperature. An aliquot of 3 g of the soup mix was dissolved into 40 mL of hot water and cooked for 5 min. A drop of sample was taken on a refractometer prism and observed through an eyepiece. The TSS of the sample was expressed in °Brix. The analysis was conducted in duplicate.

Bulk and tapped density determination

Bulk density (BD) and tapped density (TD) were determined following the method described by Fasogbon & Taiwo [2019]. The RTC soup mixes (5 g) were taken into a 10 mL empty graduated cylinder. The tapped density was determined after continuous tapping of the graduated cylinder (an average of 300 beats), as long as the volume of the dispersions of RTC soup mixes changed. The BD and TD were expressed as weight of sample *per* unit the volume occupied in the cylinder (g/mL). The flowability of RTC soup mixes was also determined by Hausner ratio (HR) and compressibility index (CI). The formulas (2) and (3) were used to calculate the HR and CI, respectively.

$$\text{Hausner ratio} = \frac{TD}{BD} \quad (2)$$

$$\text{Compressibility index} = \frac{TD - BD}{TD} \quad (3)$$

Solubility determination

The solubility of the RTC soup mixes was determined as *per* the method described in the paper of Cano-Chauca *et al.* [2005] with some modifications. The sample (1 g) was dissolved

in 100 mL of distilled water with a continuous stirring on a magnetic stirrer for 4 min. The solution was centrifuged at 5,000×*g* for 4 min. The supernatant (25 mL) was dried in an oven at 105°C for 3–5 h. Weight of the dried solid matter as a percentage of the initial powder was used to determine sample solubility in water.

Viscosity determination

The viscosity of the RTC soup mixes was determined as *per* the method of Noordraven *et al*. [2021] using an MCR 52 rheometer (Anton Paar, Graz, Austria). The RTC soup mixes were prepared by dissolving 10 g of RTC soup mix into 120 mL of hot water and boiling for 5 min. The prepared soup was taken into a concentric cylinder cup and placed in a rheometer. The measurement was done using an SC4 21 spindle and at constant temperature (60°C). The measurement of viscosity (Pa×s) was performed by increasing the shear rate from 1 to 100 1/s. Results were expressed as the curves of viscosity *vs*. shear rate and shear stress (Pa) *vs*. shear rate. All the measurements were done in duplicate.

Pasting properties determination

Pasting properties, *i.e.*, pasting temperature, peak time, peak viscosity, trough viscosity, final viscosity, breakdown (peak viscosity minus trough viscosity), and setback (final viscosity minus trough viscosity) were determined as *per* the method of Hanan *et al*. [2020] using a rheometer (MCR 52, Anton Paar). The 1 g sample was weighed in a starch pasting cell (ST 24-2D) and dissolved in 40 mL of distilled water. The soup dispersion was equilibrated at 50°C for 1 min and heated up to 95°C at the rate of 0.2°C/s rate. The soup dispersion was kept at 95°C for 2.5 min and then cooled to 50°C at the rate of 12°C/min rate. The dispersion was again held for 2 min at 50°C. The paddle rotated at 960 rpm speed for the first 10 s to mix the sample and then at a constant speed of 160 rpm. All the parameters were expressed in mPa×s except pasting temperature which was in °C and peak time which was in min.

Consumer assessment of the ready-to-cook soup mixes

The consumer test of the ready-to-cook soup mixes was performed using a 9-point hedonic scale [Watts *et al*., 1989]. The assessment was conducted in the semi-scale with 30 semi-trained assessors (15 men, 15 women, age range 24–45) recruited from students and employees of the Amity University Uttar Pradesh, Noida, India. The consumer assessment of RTC soup mixes was done after dissolving 10 g of RTC soup mix into 120 mL of hot water and boiling for 5 min in an open vessel. Unlabeled warm soup was served to each assessor in a paper cup. The assessors were asked to clean their palates with water before tasting the second sample. The 9-point hedonic scale was provided to rate the sample with 9 as liked extremely, 8 as like very much, 7 as like moderately, 6 as like slightly, 5 as neither like nor dislike, 4 as dislike slightly, 3 as dislike moderately, 2 as dislike very much, and 1 as dislike extremely. The assessors were asked to give their remarks about appearance, taste, odor, flavor and overall acceptability of each of the sample [Wang *et al*., 2010]. The overall acceptability means acceptability of the products by assessors in total as a combination of all sensory characteristics.

Determination of storage stability of the ready-to-cook soup mixes

The accelerated shelf-life testing (ASLT) was used to accelerate the rate of product deterioration without altering the mechanisms of change when stored at room temperature. ASLT was used to predict the shelf-life of products in short time. The storage study of the RTC soup mixes packed in metallized polyester zip lock bag (32 micron) was done at 40°C and 75% relative humidity (RH) for 15 days. The experiment was set-up in laminar air flow. The samples were drawn at regular intervals of 3 days [Bhatt *et al*., 2020] and subjected to analysis of lipid quality, pH, color parameters, and microbial count.

2-Thiobarbituric acid reactive substance estimation

2-Thiobarbituric acid reactive substance (TBARS) contents of the ready-to-cook soup mixes were determined as *per* the method of Schmedes & Holmer [1989]. The 5 g sample was dissolved in 25 mL of 20% (*w/v*) trichloroacetic acid solution. The contents were mixed thoroughly. The suspension was filtered to remove solid particles. An aliquot of 2 mL of the aqueous 2-thiobarbituric acid solution (0.02 M) was added to 2 mL of the filtrate in a test tube. The tube was incubated at 100°C for 30 min and then cooled under running tap water. Absorbance was measured at 532 nm using a UV-Vis spectrophotometer (LMSPUV1900S, Labman, Chennai, India). TBARS value was calculated from a malondialdehyde standard curve and expressed as mg malondialdehyde *per* kg of the ready-to-cook soup mix.

Peroxide value determination

The peroxide value (PV) of ready-to-cook soup mix was determined as *per* the AOAC method no: 965.33 [AOAC, 1999]. The portion of 3 g of ready-to-cook soup mix was weighed in a conical flask, and 30 mL of acetic acid-chloroform solution (3:2, *v/v*) was added to dissolve the lipids. The suspension was filtered through Whatman no. 1 filter paper to remove the solid particles. A saturated potassium iodide solution (0.5 mL) was added to the filtrate. A few drops of a starch solution were added to the filtrate and titrated with sodium thiosulfate (0.01 N). The PV was calculated using the formula (4) and expressed as milli equivalent peroxide *per* kg of ready-to-cook soup mix.

$$PV = \frac{S \times N}{W} \times 100 \quad (4)$$

where: S, volume of sodium thiosulphate used (mL); N, normality of sodium thiosulfate solution (0.01 N); W, weight of sample (g).

Free fatty acid value determination

The free fatty acid (FFA) value of the ready-to-cook soup mix was determined as *per* the method of Rukunudin *et al*. [1998] with

slight modification. To the ready-to-cook soup mix (5 g), 30 mL of chloroform was added. The suspension was homogenized for 1 min and filtered to remove solid particles. A few drops of the ethanolic phenolphthalein (1%) indicator were added to the filtrate which was then titrated with 0.01 N ethanolic potassium hydroxide (KOH) solution. The free fatty acid percentage was calculated according to formula (5).

$$\text{FFA} = \frac{\text{Titration volume} \times \text{Normality of KOH} \times 28.2}{\text{Weight of sample}} \quad (5)$$

Color analysis

The color of the soup was assessed using an NS810 colorimeter (Shenzhen Threenh Technology Co (3nh), Zengcheng, Guangzhou, China) based on the CIELab system (illuminant D65, observer 10°, illumination mode d/8 and caliber 8 mm). The colorimeter was calibrated against black (L^*=0, a^*=0, b^*=0) and white (L^*=100, a^*=0, b^*=0) standard provided with the instrument. The colorimeter was equipped with a light source (combined light-emitting diode sources) and a sensor (silicon photodiode array). The homogeneous RTC soup mix was taken into Petri dish and the parameters of color (L^*, a^*, b^*) were measured on the surface of the soup at three different locations. L^* denoted lightness, a^* – redness (positive values) or greenness (negative value), and b^* – yellowness (positive values) or blueness (negative value).

Microbiological analysis

The microbiological analysis of the ready-to-cook soup mix was performed using a spread plate technique as *per* the method of Tolasa *et al*. [2012]. The ready-to-cook soup mix (1 g) was suspended in 10 mL of peptone water (0.1%, *w/v*) and serially diluted from 10^{-1} to 10^{-4} dilution. An aliquot of 100 µL of the sample from different dilutions was plated on different agar plates by the spread plate technique. Nutrient agar, Czapek dox agar, XLD agar and EMB agar media were used for total plate count, yeast and mold count, *Salmonella* count and *Escherichia coli* count, respectively. The plates were incubated for 24 h at 37°C for total plate count, *Salmonella* and *E. coli* counts and at 28°C for 3 days for yeast and mold counts. Total plate count was calculated using the formula (6).

$$\text{Total plate count} = \log\left(\frac{\text{No. of colonies} \times \text{Dilution factor}}{\text{Weight of sample}}\right) \quad (6)$$

Results were expressed as log of colony-forming unit (cfu) count *per* g.

Statistical analysis

Microsoft Office Excel 2016 (Microsoft, Redmond, WA, USA) was used to analyze data for mean and standard deviation. IBM SPSS (version 26.0) software (IBM, Armonk, NY, USA) was used to compare data for the analysis of variance (ANOVA), and Duncan multiple range test.

RESULTS AND DISCUSSION

In our previous study, we optimized the microencapsulation of pink perch head and viscera protein hydrolysate using maltodextrin, sodium alginates, gum Arabic and carboxyl methyl cellulose as wall materials [Kumari *et al*., 2023]. The best microencapsulates (maltodextrin, sodium alginate and gum Arabic in a 1:1:1 ratio, *w/w/w*) had 76% encapsulation efficiency with improved physiochemical properties compared to the pink perch head and viscera protein hydrolysate. The obtained microencapsulated protein hydrolysate had smooth surface and amorphous structure with no fissures, crack and disruption which retained the antioxidant activity of protein hydrolysate [Kumari *et al.,* 2023]. The microencapsulation of protein hydrolysate reduces its bitter taste, hygroscopicity, and fishy odor, and aids in the controlled release of hydrolysates with time under gastrointestinal conditions. In the present study, we utilized microencapsulated protein hydrolysate for the preparation of ready-to-cook protein-enriched soup mix.

Chemical composition

The nutritional composition of RTC soup mixes depends on the type of ingredients used. The proximate analysis of the soup mix powder gives an idea about nutritional composition and nature of the products. In this study, the proximate composition of RTC soup mixes was given in Table 2. The moisture content of RTC soup mixes was in the range of 4.2 g/100 g to 4.6 g/100 g. However, there was no significant difference ($p \geq 0.05$) between the moisture content of different RTC soup mixes. Statistically,

Table 2. Chemical composition of ready-to-cook (RTC) soup mixes (g/100 g).

Mix	Moisture content	Lipid content	Protein content	Ash content	Carbohydrate content
BS	4.2±0.1^{a}	7.1±1.6^{b}	9.8±0.5^{e}	3.9±0.8^{ab}	75.4±0.2^{ab}
MPHS	4.3±0.3^{a}	7.5±1.0^{ab}	15.4±0.4^{c}	3.6±0.3^{b}	69.4±1.2^{cd}
PHS	4.5±0.1^{a}	8.0±2.0^{ab}	16.4±0.1^{b}	4.3±0.1^{ab}	66.7±1.0^{e}
FPS	4.6±0.5^{a}	11.5±0.9^{a}	18.7±0.2^{a}	5.1±0.4^{a}	60.2±0.5^{f}
CCS	4.4±0.4^{a}	5.5±1.7^{b}	14.2±0.1^{d}	4.4±0.5^{ab}	71.4±0.3^{bc}
CVS	4.5±0.4^{a}	6.5±2.1^{b}	8.2±0.3^{f}	4.6±0.2^{ab}	76.4±0.2^{a}

Results are shown as mean ± standard deviation (n=2). Different lowercase letters in column indicate significant differences between RTC soup mixes (p<0.05). BS, blank soup; MPHS, microencapsulated protein hydrolysate soup; PHS, protein hydrolysate soup; FPS, sun dried whole fish powder soup; CCS, commercial chicken soup; CVS, commercial vegetable soup.

the RTC MPHS, PHS, and FPS mixes contained more proteins ($p<0.05$) than commercial chicken and vegetable soups, *i.e.*, approximately ≥15%. The ash content of RTC MPHS mix was the lowest among all soup mixes, which indicated the presence of low amounts of minerals. Öztürk *et al*. [2019] reported comparable proximate composition of powdered soups prepared from different species of fish, which contained 28–30% protein, 5–7% fat, 8–10% moisture, 6–7% ash, and 40–50% carbohydrate. Moisture plays an important role in food quality because moist foods deteriorate due to growth of mold and clustering. The chemical composition of all the soups showed that their moisture content was under the limits of Food Safety and Standard Authority of India (FSSAI) standard for soup powder, which is set to be 5.0% [FSSAI, 2022].

Physical properties of RTC soup mixes

Solubility

Solubility affects sensory attributes, such as the taste, in the final products and consumption characteristics of powder products [Azizpour *et al*., 2016]. The solubility of the RTC soup mixes was between 41.0 to 43.0% (Table 3) and there were no statistically significant differences ($p\geq0.05$) between the RTC soup mixes. In the RTC soup mixes, soluble ingredients were: microencapsulated protein hydrolysate, protein hydrolysate, milk solid, salt and sugar; whereas insoluble ingredients were: vegetables and oil; and partially soluble ingredients were: sun-dried whole fish powder, potato starch, refined flour and spice mix, which affected the solubility of products. Taşkin & Savlak [2022] reported significantly lower solubility of instant soup powders reaching 18–23%. Ready-to-cook soup mixes are supposed to have high water solubility as they must dissolve quickly and be ready to drink in a short time.

pH and total soluble solid content

The pH values of the RTC soup mixes varied between 6.0 and 6.8 (Table 3). Statistically, there was no significant difference ($p\geq0.05$) between pH values of different RTC soup mixes. In the RTC soup mixes, sunflower oil and protein hydrolysates might have got hydrolyzed into free fatty acids and free amino acids, respectively, which may affect the pH of soups. The total soluble solid is defined as the amount of sugar and soluble minerals in the sample [Beckles, 2012]. The TSS of the RTC soup mixes was in the range of 5.5 to 6.8°Brix (Table 3), which was in line with the FSSAI limit for soup powder (more than 5°Brix) [FSSAI, 2022]. The total soluble solid is one of the parameters which affect the sensory properties (taste) of the food. TSS also has a significant effect on the storage stability of products because it depends on the sugar content.

Bulk and tapped density

The flow characteristics of the soup are important to determine the transportation condition, processing condition, quality, and structural behavior of the products [Kumari *et al*., 2023]. The flowability of powder was determined as the Hausner ratio (HR) and the compressibility index (CI). Flowability of RTC MPHS mix and RTC PHS mix was poor with HR of 1.44 and 1.43, respectively, which was similar to that of the CVS mix (1.35) (Table 3). The poor flowability was observed in all tested soup mixes, which indicated high difference between bulk density and tapped density values. The bulk density of CCS mix was the highest ($p<0.05$) among all the soup mixes, probably due to the presence of meat shreds in the soup mix. Fasogbon & Taiwo [2019] reported that dika kernel powder soups had poor flowability with HR and CI values in ranges of 1.1 to 1.4 and 10.6 to 30.0, respectively. The HR and CI depend on moisture content of products.

Viscosity

Viscosity of the RTC soup mixes decreased with increase in shear rates (Figure 1). The curves of shear stress *vs*. shear rate were also prepared (Figure 1B). Results shown that all the RTC soup mixes exhibited non-Newtonian pseudoplastic behavior. Previous studies also reported that different soups (such as tomato, vegetable, gbegiri, ewedu, karkashi and ogbano) showed non-Newtonian pseudoplastic behaviors [Fasogbon & Taiwo, 2019]. The mouthfeel (thickness) is mostly linked to the viscosity of the food products [De Wijk *et al*., 2003]. The thickness of food products is directly proportional to the shear stress at the surface of the tongue [Thomazo *et al*., 2019]. At a given stress, deformation rate is higher in low viscous products as

Table 3. Physical parameters of ready-to-cook (RTC) soup mixes.

Mix	Bulk density (g/mL)	Tapped density (g/mL)	Compressibility index (%)	Hausner ratio	Solubility (%)	pH	Total soluble solid (°Brix)
BS	0.45±0.06^{b}	0.69±0.08^{b}	34.0±1.41^{a}	1.52±0.03^{a}	41.0±2.8^{a}	6.7±0.1^{a}	5.50±0.71^{b}
MPHS	0.49±0.19^{b}	0.71±0.11^{b}	30.0±2.83^{ab}	1.44±0.05^{ab}	42.5±2.1^{a}	6.8±0.0^{a}	6.75±0.35^{a}
PHS	0.46±0.31^{b}	0.65±0.03^{b}	30.5±2.12^{ab}	1.43±0.06^{ab}	42.0±1.4^{a}	6.4±0.1^{a}	6.25±0.35^{ab}
FPS	0.48±0.38^{b}	0.73±0.04^{b}	33.5±2.12^{a}	1.50±0.04^{a}	41.0±1.4^{a}	6.0±0.2^{a}	5.60±0.28^{b}
CCS	0.69±0.01^{a}	1.02±0.02^{a}	32.5±0.71^{a}	1.48±0.02^{a}	42.0±2.8^{a}	6.1±0.8^{a}	6.25±0.35^{ab}
CVS	0.50±0.57^{b}	0.68±0.02^{b}	26.0±1.41^{b}	1.35±0.03^{b}	43.0±2.8^{a}	6.2±0.4^{a}	6.75±0.35^{a}

Results are shown as mean ± standard deviation ($n=2$). Different lowercase letters in column indicate significant differences between RTC soup mixes ($p<0.05$). BS, blank soup; MPHS, microencapsulated protein hydrolysate soup; PHS, protein hydrolysate soup; FPS, sun dried whole fish powder soup; CCS, commercial chicken soup; CVS, commercial vegetable soup.

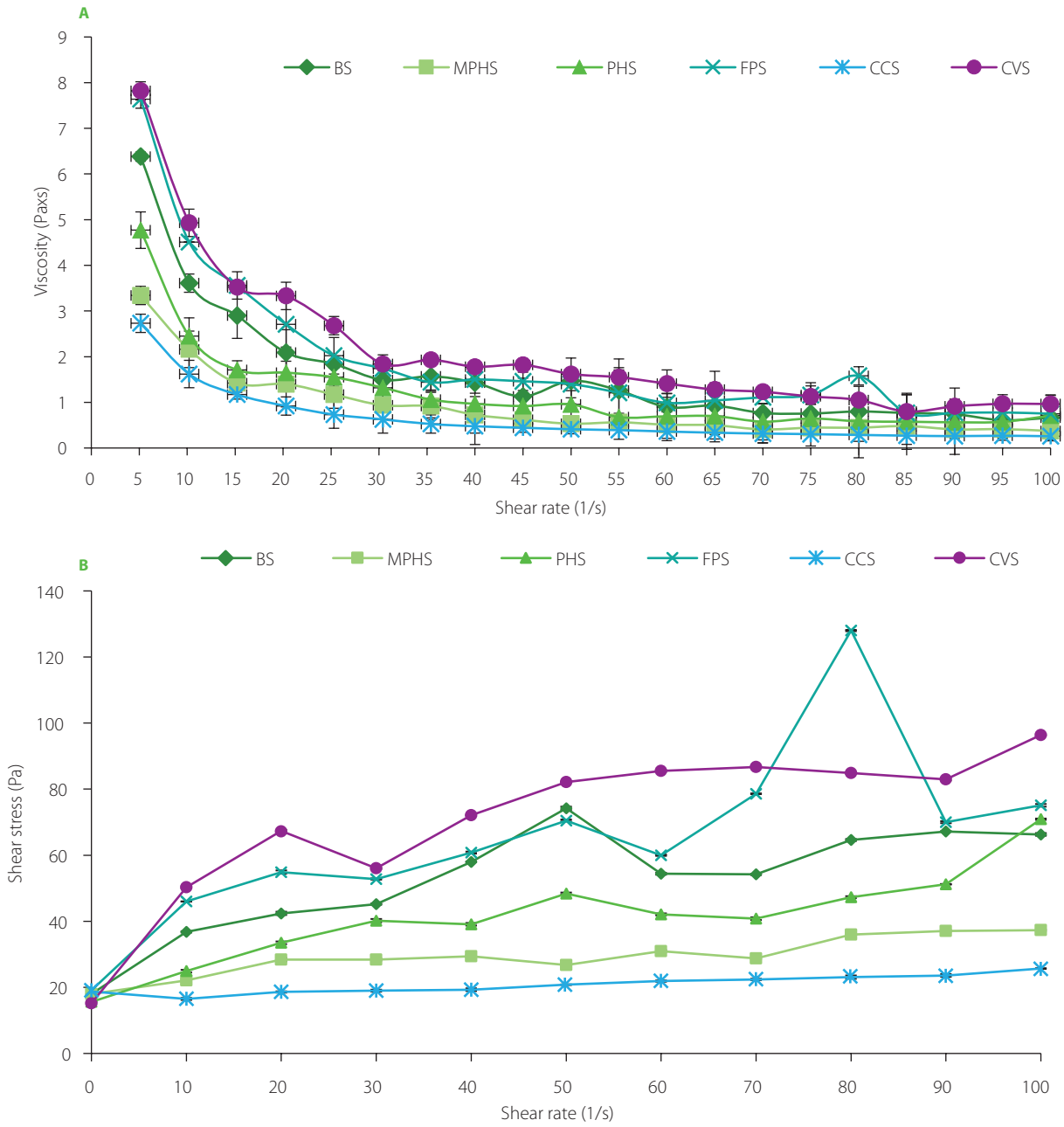

Figure 1. Viscosity at different shear rates (**A**) and shear stress at different shear rates (**B**) of ready-to-cook soup mixes. BS, blank soup; MPHS, microencapsulated protein hydrolysate soup; PHS, protein hydrolysate soup; FPS, sun dried whole fish powder soup; CCS, commercial chicken soup; CVS, commercial vegetable soup.

compared to the high viscous ones. Therefore, shear stress was used to predict the thickness of products [Abson *et al*., 2014]. In this study, the RTC MPHS mix was a low viscous product, which can be easily detectible with better mouth feel among other RTC soup mixes with the fish-derived additive.

Pasting properties

The pasting characteristics of different RTC soup mixes were presented in Table 4 and Figure S2. The RTC soup mixes attained their peak viscosity within 8.0–8.5 min. There was a significant ($p<0.05$) difference between peak viscosity of different RTC soup mixes. The peak viscosity of CVS (1,928.0 mPa×s) and CCS (1,577.0 mPa×s) was higher compared to RTC MPHS mix (293.8 mPa×s) and RTC FPS mix (291.3 mPa×s). This is due to the presence of a thickening agent in CVS and CCS mixes. The pasting temperature of the RTC MPHS mix was the lowest (64.7°C) among all the RTC soup mixes, although the value for FPS was not significantly ($p\geq0.05$) different. A lower peak viscosity as well as final viscosity of the RTC MPHS mix compared to other soup mixes could be due to the presence of maltodextrin, gum Arabic and sodium alginates which enable the powder to rehydrate and form crosslinks. The RTC MPHS mix showed low breaking down viscosity (24.9 mPa×s) followed by RTC PHS mix (131.3 mPa×s), RTC FPS mix (137.2 mPa×s), RTC BS mix (284.9 mPa×s), CVS (767.3 mPa×s), and CCS (914.5 mPa×s). Generally, the presence of protein and starch increases the viscosity [Wang *et al*., 2020]. However, in this case, the RTC soup mix contains microencapsulated protein hydrolysates which do not release peptides even after heating after 100°C. The protein hydrolysates are released from microcapsules under gastric conditions as *per* our previous study

Table 4. Pasting characteristics of ready-to-cook (RTC) soup mixes.

Mix	Peak time (min)	Peak viscosity (mPa×s)	Pasting temperature (°C)	Holding strength (mPa×s)	Breakdown viscosity (mPa×s)	Final viscosity (mPa×s)	Set back from peak (mPa×s)	Setback from trough (mPa×s)
BS	8.45±0.07^{ab}	929.1±1.3^{c}	69.85±0.49^{b}	644.0±1.4^{c}	284.9±0.5^{c}	1449.5±0.7^{c}	−521.6±0.6^{e}	806.4±0.1^{b}
MPHS	8.30±0.01^{bc}	293.8±0.3^{e}	64.72±0.03^{d}	269.5±0.8^{e}	24.9±0.2^{f}	468.9±0.4^{f}	−174.3±1.8^{b}	199.4±1.2^{f}
PHS	8.02±0.17^{d}	771.2±0.9^{d}	68.67±0.61^{bc}	639.4±0.8^{d}	131.3±0.6^{e}	1089.5±0.7^{d}	−318.4±0.6^{d}	406.5±1.4^{d}
FPS	8.54±0.08^{a}	291.3±0.9^{e}	66.25±0.73^{d}	153.7±0.8^{f}	137.2±0.4^{d}	556.0±0.1^{e}	−266.8±1.8^{c}	402.0±1.4^{e}
CCS	8.50±0.00^{ab}	1577.0±1.4^{b}	68.01±0.67^{c}	660.4±2.1^{b}	914.5±1.0^{a}	1614.0±2.8^{b}	−41.6±1.6^{a}	955.6±1.9^{a}
CVS	8.11±0.16^{cd}	1928.0±2.8^{a}	76.55±0.92^{a}	1158.5±2.1^{a}	767.3±1.9^{b}	1889.0±1.4^{a}	−38.31±1.9^{a}	730.3±2.3^{c}

Results are shown as mean ± standard deviation (n=2). Different lowercase letters in column indicate significant differences between RTC soup mixes (p<0.05). BS, blank soup; MPHS, microencapsulated protein hydrolysate soup; PHS, protein hydrolysate soup; FPS, sun dried whole fish powder soup; CCS, commercial chicken soup; CVS, commercial vegetable soup.

[Kumari *et al*., 2023]. Therefore, the RTC MPHS mix showed lower peak viscosity. Hanan *et al*. [2020] also reported the low pasting properties, including peak viscosity, final viscosity and break down viscosity, of a soup upon the incorporation of pea pod powder, gaur gum and locust bean gum.

Consumer assessment

The results of consumer assessment of appearance, taste, odor, flavor and overall acceptability of the RTC soup mixes are shown in Table 5. The RTC soup mixes exhibited overall acceptability scores ranging between 4.5 to 7.6 over the 9-point hedonic scale. The RTC soup mix formulated with microencapsulated protein hydrolysate was more preferred by the assessors among all soup mixes with overall acceptability of 7.6 and with more acceptable appearance, odor, taste and flavour among other soup mixes with the fish-derived additive. There was no significant (p≥0.05) difference between the overall acceptability of the RTC MPHS mix and instant commercial chicken soup. Among all RTC soup mixes, PHS and FPS mixes had significantly (p<0.05) lower overall acceptability scores due to fishy odors and bitter tastes. These results prove the theory that negative attributes like fishy odor and bitterness originated from fish ingredients can be masked by the technology of microencapsulation.

Storage stability of ready-to-cook soup mixes at accelerated shelf-life testing

The chemical composition, microbial contamination, storage conditions and type of packaging play an important role in the shelf-life of food products [Zarehgashti *et al*., 2019]. In our study, based on consumer assessment results, it was decided to evaluate the shelf-life of only RTC MPHS mix as the most promising formulation with the fish-derive additive. In addition, the shelf-life of RTC BS and CCS mixes (as controls) was estimated in ASLT (40°C, 75% RH). One day of ASLT condition is equivalent to 4 days of storage at room temperature [Subramaniam, 2009]. The aim of ASLT is to increase the rate of deterioration of the products without altering the mechanism of changes seen in the products under normal storage conditions (25–30°C). Estimation of shelf-life was an important part of the study for any food product formulation to keep the product safe for long period of time and to its further commercialization [Hemanth *et al*., 2020]. The spoilage factors chosen for the study were oxidation of lipids (evaluated by TBARS level, and peroxide value, and free fatty acid content), changes in pH and color, and microbiological quality.

pH

The pH values of soup mixes are shown in Table 6. There was statistically significant (p<0.05) relationship between the storage

Table 5. Consumer assessment of ready-to-cook (RTC) soup mixes.

Mix	Appearance	Taste	Odor	Flavor	Overall acceptability
BS	7.1±0.6^{b}	6.7±1.3^{b}	6.4±1.5^{a}	6.0±1.9^{b}	6.6±1.2^{b}
MPHS	7.7±0.9^{a}	7.5±1.4^{a}	7.0±0.9^{a}	7.2±1.2^{a}	7.6±0.9^{a}
PHS	6.7±1.3^{b}	5.5±1.5^{c}	4.4±1.5^{b}	5.3±1.3^{c}	5.6±1.0^{c}
FPS	5.8±1.1^{c}	4.2±1.3^{d}	3.2±1.5^{c}	4.4±1.3^{d}	4.5±0.9^{d}
CCS	7.3±1.3^{ab}	7.9±0.9^{a}	6.8±1.1^{a}	7.3±1.1^{a}	7.5±0.7^{a}
CVS	6.9±1.4^{b}	7.3±1.2^{ab}	6.4±1.3^{a}	6.5±1.8^{ab}	6.9±1.2^{ab}

Results are shown as mean ± standard deviation (n=30). Different lowercase letters in column indicate significant differences between RTC soup mixes (p<0.05). BS, blank soup; MPHS, microencapsulated protein hydrolysate soup; PHS, protein hydrolysate soup; FPS, sun dried whole fish powder soup; CCS, commercial chicken soup; CVS, commercial vegetable soup.

Table 6. Lipid quality parameters of ready-to-cook soup in accelerated shelf-life testing.

Storage time (day)	pH			Peroxide value (meq/kg)			TBARS content (mg malondialdehyde/kg)			Free fatty acid content (%)		
	BS	MPHS	CCS	BS	MPHS	CCS	BS	MPHS	CCS	BS	MPHS	CCS
0	6.5±0.0^{a}	6.7±0.1^{a}	6.7±0.1^{a}	2.07±0.09^{f}	1.57±0.14^{d}	1.37±0.05^{e}	1.89±0.06^{d}	1.27±0.06^{e}	1.05±0.01^{f}	1.54±0.06^{e}	1.34±0.06^{d}	1.10±0.08^{e}
3	6.4±0.0^{ab}	6.6±0.0^{b}	6.5±0.1^{b}	2.73±0.09^{e}	1.97±0.14^{cd}	1.97±0.05^{d}	2.07±0.15^{d}	2.10±0.01^{d}	1.68±0.03^{e}	1.80±0.16^{e}	1.85±0.34^{d}	1.41±0.08^{e}
6	6.2±0.1^{b}	6.3±0.0^{c}	6.2±0.2^{c}	3.27±0.09^{d}	2.27±0.09^{c}	2.23±0.05^{cd}	2.70±0.04^{c}	2.83±0.03^{c}	2.04±0.03^{d}	3.38±0.08^{d}	2.98±0.18^{c}	3.30±0.08^{d}
9	5.9±0.0^{c}	6.1±0.1^{d}	5.8±0.0^{d}	4.63±0.14^{c}	3.10±0.14^{b}	2.67±0.28^{c}	3.20±0.05^{b}	3.08±0.06^{c}	2.43±0.05^{c}	4.26±0.04^{c}	3.93±0.22^{b}	4.48±0.16^{c}
12	5.6±0.2^{d}	5.9±0.1^{e}	5.2±0.1^{e}	5.90±0.05^{b}	3.57±0.24^{b}	3.73±0.28^{b}	3.40±0.04^{b}	3.57±0.05^{b}	3.51±0.02^{b}	5.37±0.06^{b}	4.84±0.18^{a}	11.71±0.32^{b}
15	5.3±0.0^{e}	5.6±0.1^{f}	4.8±0.1^{f}	6.67±0.09^{a}	5.27±0.38^{a}	8.63±0.42^{a}	4.38±0.04^{a}	3.93±0.02^{a}	4.31±0.06^{a}	6.33±0.30^{a}	5.20±0.14^{a}	14.28±0.12^{a}

Results are shown as mean ± standard deviation (n=2). Different lowercase letters in column indicate significant differences between storage days (p<0.05). BS, blank soup; MPHS, microencapsulated protein hydrolysate soup; CCS, commercial chicken soup; TBARS, 2-thiobarbituric acid reactive substances.

Table 7. Color parameters of ready-to-cook soup mixes in accelerated shelf-life testing.

Storage time (day)	*L**			*a**			*b**		
	BS	MPHS	CCS	BS	MPHS	CCS	BS	MPHS	CCS
0	83.5±0.4^{a}	74.2±0.2^{a}	77.7±0.4^{a}	−0.04±0.2^{bc}	0.9±0.2^{c}	4.0±0.1^{d}	12.5±0.1^{d}	15.3±0.6^{e}	17.0±0.1^{b}
3	81.7±1.9^{bc}	69.5±1.8^{b}	76.1±0.8^{b}	−0.6±0.2^{c}	0.2±0.4^{d}	3.8±0.1^{d}	15.1±0.1^{c}	17.4±0.5^{c}	16.5±0.2^{c}
6	76.7±1.4^{d}	64.3±0.3^{c}	68.5±0.5^{e}	−0.7±0.6^{c}	2.2±0.2^{b}	4.0±0.3^{d}	11.8±0.7^{d}	15.5±0.2^{e}	15.1±0.6^{d}
9	79.4±3.0^{cd}	68.6±0.4^{b}	73.3±0.1^{c}	0.4±0.7^{ab}	2.1±0.1^{b}	5.1±0.0^{c}	13.1±1.8^{d}	18.7±0.5^{b}	18.0±0.0^{a}
12	76.8±1.7^{d}	68.5±0.2^{b}	68.2±0.0^{e}	−0.4±0.3^{c}	2.4±0.0^{b}	5.8±0.0^{b}	18.3±1.4^{b}	19.4±0.1^{a}	17.1±0.0^{b}
15	76.4±0.0^{d}	66.7±0.1^{c}	70.7±0.2^{d}	1.0±0.1^{a}	4.9±0.0^{a}	6.3±0.1^{a}	21.0±0.1^{a}	16.4±0.1^{d}	15.0±0.1^{d}

Results are shown as mean ± standard deviation (n=3). Different lowercase letters in column indicate significant differences between storage days (p<0.05). BS, blank soup; MPHS, microencapsulated protein hydrolysate soup; CCS, commercial chicken soup; L^*, lightness; a^*, redness (positive values) or greenness (negative value); b^*, yellowness.

time and the pH value. The pH value of the RTC BS mix decreases from 6.5 to 5.3. Whereas there was a slow decrease in pH in the case of RTC MPHS and CCS mixes during storage. The pH value of RTC soup mixes decreases due to chemical and microbial degradation. The pH of soup alone cannot be used as an indicator of soup quality. Therefore, other parameters should be determined along with the pH during storage. Mol [2005] also reported that the pH value of fish soup decreased during storage.

Free fatty acid content

Amount of free fatty acids is a quality indicator in the foods. In this study, day 6 of ASLT (equivalent to 24 days of storage at room temperature) was the beginning of most changes in the FFA content of the RTC soup mixes (Table 6). The FFA of RTC soup mixes significantly increased ($p<0.05$) during storage. Zarehgashti *et al*. [2019] studied the shelf-life of ready-to-eat shrimp soup powder and showed that its FFA content increased slowly during 6-month storage at room temperature).

Peroxide value

The peroxide value is used to determine the primary products (hydroperoxides) of lipid oxidation and mostly to detect oxidative rancidity in the products. In this study, the PV of all RTC soup mixes significantly ($p<0.05$) increased with days of ASLT, as shown in Table 6. The PV of the RTC BS mix increased from 2.07 to 6.67 meq/kg, that of RTC MPHS mix increased from 1.57 to 5.27 meq/kg, and that of CCS changed from 1.37 to 8.63 meq/kg. Zarehgashti *et al*. [2019] reported that the peroxide value of ready-to-eat shrimp soup powder increased from 0.09 meq/kg to 3.14 meq/kg after storage at room temperature within 6 months.

2-Thiobarbituric acid reactive substance content

During storage, meat-related products are prone to oxidative change. The TBARS estimation is the most widely used method for determination of lipid oxidation. The TBARS value of the RTC soup mixes significantly ($p<0.05$) increased during storage period, as given Table 6. The highest TBARS level after 15 days of ASLT has been found in RTC BS mix (4.4 mg malondialdehyde/kg) followed by commercial soup mix (4.3 mg malondialdehyde/kg) and RTC MPHS mix (3.9 mg malondialdehyde/kg). The lipid oxidation in RTC MPHS mix was low among all RTC soup mixes probably due to antioxidant activity of protein hydrolysates, which commercial chicken soup mix and RTC BS mix did not contain. The antioxidant properties of fish protein hydrolysates are documented in literature [Noman *et al*., 2022]. Sarkar *et al*. [2019] reported that the TBARS value of an instant soup mix blended with spent hen meat shred increased during storage from 0.37 to 0.42 mg malondialdehyde/kg. Öztürk *et al*. [2019] determined TBARS levels of fish powdered soups during storage at 65°C and 75% RH and found that they increased on average from 2.4 to 7.2 mg malondialdehyde/kg after 6-month storage.

Color

Color is a very important quality parameter because market acceptability, desirability and final price of food products mainly depend on their appearance and color [Azizpour *et al*., 2016]. The color parameters of stored RTC soup mixes are presented in Table 7. The color of RTC BS mix and RTC MPHS mix at initial day of storage was greenish yellow with L^* of 83.5 and 74.2, respectively, a^* of 0.04 and 0.9, respectively, and b^* of 12.5 and 15.3, respectively. The negative value of a^* indicates that the soup was more green in color. Statistically, there were significant ($p<0.05$) changes in color parameters of RTC soup mixes during storage (Figure S3). With increase in the number of days of ASLT, the color of RTC soups mixes became darker (moves towards reddish zone). It could be caused by chemical changes during ASLT storage. The results of this study indicated that the RTC MPHS mix was assumed to be more attractive to consumers as compared to CCS.

Microbiological quality

Microbiological quality of RTC soup mixes was studied in respect to total plate count, yeast and mold count, *E. coli* count, and *Salmonella* count during storage at accelerated conditions. The results are given in Table 8. There was significant ($p<0.05$) increase in microbial growth during storage for all types of mixes. This could be due to the gradual increase in the moisture content of samples. Total plate count and yeast and mold count were under the consumption limit of FSSAI standard for fish products (which is 1.0×10^6 cfu/g and 1.0×10^4 cfu/g, respectively [FSSAI, 2022]) till 6 days of storage under accelerated conditions which was equivalent to 24 days of storage at room temperature. Total plate count and yeast and mold count become uncountable at 9 days of ASLT, which indicated that the quality of RTC soup mixes started decreasing due to microbial spoilage. *E. coli* and *Salmonella* were not detected in all RTC soup mixes, which indicated that pathogenic bacteria were absent in all RTC soup mixes. The results of this study showed a positive correlation between changes in chemical parameters and microbial spoilage. This finding suggests that the RTC MPHS soup mix was stable and safe for consumption till 24 days at room temperature. The shelf-life of the product could be enhanced with proper sterilization techniques and packaging. Jayasinghe *et al*. [2016] reported that seaweed-based soup mix powder had shelf-life up to 3 months at ambient temperature when packed in airtight polystyrene packets.

CONCLUSIONS

The study proves that microencapsulated protein hydrolysate, originated from fish processing by-products, can be used as a value-added ingredient for the formulation of RTC soup mixes that have partial replacement potential for products commonly used by the food industry. Soup fortification with peptides and amino acids (15% protein equivalent) by incorporating microencapsulated protein hydrolysate obtained from pink perch by-products, represents a promising strategy to increase the nutritional value of ready-to-cook soup mixes. The developed RTC soup mixes will be an option especially for individuals suffering from protein deficiency. It can be concluded that microencapsulated protein hydrolysate can be effectively used to produce ready-to-cook

Table 8. Microbiological quality of ready-to-cook soup mixes in accelerated shelf-life testing.

Storage time (days)	BS				MPHS				CCD			
	Total plate count log(cfu/g)	Yeast & mold count log(cfu/g)	*Escherichia coli* count log(cfu/g)	*Salmonella* count log(cfu/g)	Total plate count log(cfu/g)	Yeast & mold count log(cfu/g)	*Escherichia coli* count log(cfu/g)	*Salmonella* count log(cfu/g)	Total plate count log(cfu/g)	Yeast & mold count log(cfu/g)	*Escherichia coli* count log(cfu/g)	*Salmonella* count log(cfu/g)
0	4.22±0.06^{c}	4.76 ±0.01^{c}	NIL	NIL	4.28±0.03^{c}	4.24±0.05^{c}	NIL	NIL	3.39 ±0.12^{c}	3.39 ±0.12^{c}	NIL	NIL
3	4.90 ±0.01^{b}	5.78±0.00^{a}	NIL	NIL	4.56±0.02^{b}	4.46±0.02^{b}	NIL	NIL	4.00 ±0.06^{b}	4.77 ±0.01^{b}	NIL	NIL
6	6.20 ±0.00^{a}	5.17±0.00^{b}	NIL	NIL	5.50±0.00^{a}	6.08±0.00^{a}	NIL	NIL	4.42±0.03^{a}	5.75±0.00^{a}	NIL	NIL
9	Uncountable	Uncountable	NIL	NIL	Uncountable	Uncountable	NIL	NIL	Uncountable	Uncountable	NIL	NIL
12	Uncountable	Uncountable	NIL	NIL	Uncountable	Uncountable	NIL	NIL	Uncountable	Uncountable	NIL	NIL
15	Uncountable	Uncountable	NIL	NIL	Uncountable	Uncountable	NIL	NIL	Uncountable	Uncountable	NIL	NIL

Results are shown as mean ± standard deviation (n=2). Different lowercase letters in column indicate significant differences between storage days (p<0.05). BS, blank soup; MPHS, microencapsulated protein hydrolysate soup; CCS, commercial chicken soup; NIL, no microbial growth.

soup mixes with improved nutritional and overall acceptability scores. The microencapsulated protein hydrolysate increased the overall acceptability of RTC soup mixes by masking bitter taste and fishy odor of protein hydrolysate. The ready-to-cook soup was suitable to be aerobically stored in metallized polyethylene zip lock bag (32-micron thickness) at 60°C and 75% RH for the period of 6 days in ASLT which is equivalent to 24 days of storage at room temperature without any deterioration in its quality and acceptability. The chemical analysis of RTC soup mixes showed that the RTC MPHS mix was at the same level or even better than commercial soups.

ACKNOWLEDGEMENTS

Dr. Nutan Kaushik and Asha Kumari would like to acknowledge the help extended by Dr. Shalini Gaur Rudra, Principal scientist, Indian Agricultural Research Institute (IARI), for the analysis (viscosity and pasting properties) of ready-to-cook soup mixes.

RESEARCH FUNDING

This work was supported by the Department of Biotechnology, Government of India (grant numbers BT/IN/INNO-INDIGO/12/NK/2017-18]) and The Research Council of Norway (grant numbers 281262).

CONFLICT OF INTERESTS

The authors declare no conflicts of interests.

ORCID IDs

Khushboo https://orcid.org/0000-0001-5768-7366
A. Kumari https://orcid.org/0000-0002-2554-5627
N. Kaushik https://orcid.org/0000-0002-3870-8093
R. Slizyte https://orcid.org/0000-0001-7589-2419

SUPPLEMENTARY MATERIALS

The following are available online at http://journal.pan.olsztyn.pl/Formulation-of-a-Ready-to-Cook-Soup-Mix-Using-Microencapsulated-Protein-Hydrolysate,170219,0,2.html; Figure S1. Flow diagram for formulation of ready-to-cook soup mixes. Figure S2. Pasting properties of ready-to-cook soup mixes. Figure S3. Appearance of blank soup mix, microencapsulated protein hydrolysate soup mix and commercial chicken soup mix during storage under accelerated conditions.

REFERENCES

1. Abson, R., Gaddipati, S.R., Hort, J., Mitchell, J.R., Wolf, B., Hill, S.E. (2014). A comparison of the sensory and rheological properties of molecular and particulate forms of xanthan gum. *Food Hydrocolloids*, *35*, 85-90. https://doi.org/10.1016/j.foodhyd.2013.04.018
2. AOAC International. (1999). Official Methods of Analysis of AOAC. 16th Edition, 5th Revision, Agricultural chemicals, contaminants, drugs. v. 1: Food composition, additives, natural contaminants. Gaithersburg, MD, USA.
3. AOAC International. (2005). Official Methods of Analysis. 18th Edition, Association of Official Analytical Chemists, Washington, DC, USA.
4. Azizpour, M., Mohebbi, M., Khodaparast, M.H.H. (2016). Effects of foam-mat drying temperature on physico-chemical and microstructural properties of shrimp powder. *Innovative Food Science and Emerging Technologies, 34*, 122-126. https://doi.org/10.1016/j.ifset.2016.01.002
5. Beckles, D.M. (2012). Factors affecting the postharvest soluble solids and sugar content of tomato (*Solanum lycopersicum L.*) fruit. *Postharvest Biology and Technology*, *63*(1), 129-140. https://doi.org/10.1016/j.postharvbio.2011.05.016

6. Bhatt, Z.K., Patel, N.V., Mayani, J.M., Raj, D. (2020). Development of technology for preparation of instant tomato (*Solanum lycopersicum* L.) soup mix powder. *International Journal of Chemical Studies*, *8*(2), 2034-2039. https://doi.org/10.22271/chemi.2020.v8.i2ae.9054
7. Cano-Chauca, M., Stringheta, P.C., Ramos, A.M., Cal-Vidal, J. (2005). Effect of the carriers on the microstructure of mango powder obtained by spray drying and its functional characterization. *Innovative Food Science and Emerging Technologies*, *6*(4), 420-428. https://doi.org/10.1016/j.ifset.2005.05.003
8. De Wijk, R.A., van Gemert, L.J., Terpstra, M.E., Wilkinson, C.L. (2003). Texture of semi-solids; sensory and instrumental measurements on vanilla custard desserts. *Food Quality and Preference*, *14*(4), 305-317. https://doi.org/10.1016/S0950-3293(02)00107-6
9. Farzana, T., Mohajan, S., Saha, T., Hossain, M.N., Haque, M.Z. (2017). Formulation and nutritional evaluation of a healthy vegetable soup powder supplemented with soy flour, mushroom, and moringa leaf. *Food Science and Nutrition*, *5*(4), 911-920. https://doi.org/10.1002/fsn3.476
10. Fasogbon, B.M., Taiwo, K.A. (2019). Modelling the flowing behaviour of dika kernel powder and soup as affected by moisture content, physical and rheological properties. *Journal of Food Science and Technology*, *56*(10), 4688-4695. https://doi.org/10.1007/s13197-019-03921-4
11. Feng, S., Whitfield, S., Ward, T. (2022). Analysis of a mass produced dried ready-to-use therapeutic food ingredient. *Journal of Nutritional Health & Food Engineering, 12*(2), 44-53. https://doi.org/10.15406/jnhfe.2022.12.00355
12. FSSAI (2022). https://www.fssai.gov.in/upload/uploadfiles/files/Compendium_Food_Additives_Regulations_03_03_2022.pdf
13. Hanan, E., Rudra, S.G., Sagar, V.R., Sharma, V. (2020). Utilization of pea pod powder for formulation of instant pea soup powder. *Journal* of *Food Processing* and *Preservation, 44*(11), art. no. e14888. https://doi.org/10.1111/jfpp.14888
14. Hemanth, K.J., Hema, M.S., Sinija, V.R., Hema, V. (2020). Accelerated shelf-life study on protein-enriched carbonated fruit drink. *Journal of Food Process Engineering*, *43*(3), art. no. e13311. https://doi.org/10.1111/jfpe.13311
15. ICMR-NIN (2020). https://www.im4change.org/upload/files/RDA_short_report%281%29.pdf
16. Jafarpour, A., Gomes, R.M., Gregersen, S., Sloth, J.J., Jacobsen, C., Sørensen, A.D.M. (2020). Characterization of cod (*Gadus morhua*) frame composition and its valorization by enzymatic hydrolysis. *Journal of Food Composition and Analysis*, *89*, art. no. 103469. https://doi.org/10.1016/j.jfca.2020.103469
17. Jayasinghe, P.S., Pahalawattaarachchi, V., Ranaweera, K.K.D.S. (2016). Formulation of nutritionally superior and low cost seaweed based soup mix powder. *Journal Food Processing Technology*, *7*(4), art. no. 571. https://doi.org/10.4172/2157-7110.1000571
18. Kumari, A., Kaushik, N., Slizyte, R., Khushboo (2023). Production and microencapsulation of protein hydrolysate of pink perch (*Nemipterus japonicus*) by-products obtained from surimi industry for its sustainable utilization. *Waste and Biomass Valorization*, *14*(1), 209-226. https://doi.org/10.1007/s12649-022-01853-3
19. Merrill, A.L., Watt, B.K. (1973). Energy value of foods: basis and derivation, revised. US Department of Agriculture, *Agriculture Handbook no. 74*. Washington, DC: US Government Printing Office.
20. Mohamed, R.S., Abozed, S.S., El-Damhougy, S., Salama, M.F., Hussein, M.M. (2020). Efficiency of newly formulated functional instant soup mixtures as dietary supplements for elderly. *Heliyon*, *6*(1), art. no. e03197. https://doi.org/10.1016/j.heliyon.2020.e03197
21. Mol, S. (2005). Preparation and the shelf-life assessment of ready-to-eat fish soup. *European Food Research and Technology*, *220*, 305-308. https://doi.org/10.1007/s00217-004-1030-2
22. Noordraven, L.E., Kim, H.J., Hoogland, H., Grauwet, T., Van Loey, A.M. (2021). Potential of chickpea flours with different microstructures as multifunctional ingredient in an instant soup application. *Foods*, *10*(11), art. no. 2622. https://doi.org/10.3390/foods10112622
23. Noman, A., Wang, Y., Zhang, C., Abed, S. (2022). Antioxidant activity of hybrid sturgeon (*Huso dauricus* × *Acipenser schrenckii*) protein hydrolysate prepared using bromelain, its fractions and purified peptides. *Polish Journal of Food and Nutrition Sciences*, *72*(1), 79-89. https://doi.org/10.31883/pjfns/146317
24. Opheim, M., Šližytė, R., Sterten, H., Provan, F., Larssen, E., Kjos, N.P. (2015). Hydrolysis of Atlantic salmon (*Salmo salar*) rest raw materials – Effect of raw material and processing on composition, nutritional value, and potential bioactive peptides in the hydrolysates. *Process Biochemistry*, *50*(8), 1247-1257. https://doi.org/10.1016/j.procbio.2015.04.017
25. Öztürk, F., Kalkan, S., Elmas, E., Elmas, S., Bariş, P., Demir, Ö. (2019). Some quality parameters of powdered soups prepared from different fish species. *Brazilian Archives of Biology and Technology*, *62*, art. no. e19180365. https://doi.org/10.1590/1678-4324-2019180365
26. Ravichandran, S., Sharmila Joseph, F.R., Kanagalakshmi, R., Ramya, M.S. (2012). Variation in nutritive composition of two commercially important marine fin fishes. *British Journal of Biomedical Science*, *8*(1), 43-51. https://doi.org/10.3923/ijzr.2012.43.51
27. Rukunudin, I.H., White, P.J., Bern, C.J., Bailey, T.B. (1998). A modified method for determining free fatty acids from small soybean oil sample sizes. *Journal of the American Oil Chemists' Society*, *75*(5), 563-568. https://doi.org/10.1007/s11746-998-0066-z
28. Sarkar, B., Upadhyay, S., Gogoi, P., Das, A., Hazarika, M., Rahman, Z., Datta, A. (2019). Development and quality evaluation of instant soup mix incorporated with spent hen meat shred. *Journal of Entomology and Zoology Studies*, *7*(2), 24-30.
29. Schmedes, A., Hølmer, G. (1989). A new thiobarbituric acid (TBA) method for determining free malondialdehyde (MDA) and hydroperoxides selectively as a measure of lipid peroxidation. *Journal of the American Oil Chemists' Society*, *66*(6), 813-817. https://doi.org/10.1007/BF02653674
30. Shashidhar, K., Ravishankar, C.N., Gopal, T.S., Joseph, J. (2014). Standardization of process parameters for ready-to-drink shrimp soup in reportable pouches. *Fishery Technology*, *51*, 43-46.
31. Slizyte, R., Mozuraityte, R., Remman, T., Rustad, T. (2018). Two-stage processing of salmon backbones to obtain high-quality oil and proteins. *Journal of Food Science and Technology, 53*(10), 2378-2385. https://doi.org/10.1111/ijfs.13830
32. Steinsholm, S., Oterhals, Å., Underhaug, J., Aspevik, T. (2021). Emulsion and surface-active properties of fish soluble based on direct extraction and after hydrolysis of Atlantic cod and Atlantic salmon backbones. *Foods, 10*(1), art. no. 38. https://doi.org/10.3390/foods10010038
33. Subramaniam, P.J. (2009). Chapter 12 – Shelf-life prediction and testing. In G. Talbot (Ed.). *Science and Technology of Enrobed and Filled Chocolate, Confectionery, and Bakery Products*. Woodhead Publishing Limited, pp. 233-254. https://doi.org/10.1533/9781845696436.2.233
34. Taşkın, B., Savlak, N. (2022). Functional, chemical, and sensorial properties of gluten-free fermented instant soup powders developed by use of mung bean and drum drying process. *Food Bioscience*, *47*, art. no. 101677. https://doi.org/10.1016/j.fbio.2022.101677
35. Thomazo, J.B., Contreras Pastenes, J., Pipe, C.J., Le Révérend, B., Wandersman, E., Prevost, A.M. (2019). Probing in-mouth texture perception with a biomimetic tongue. *Journal of the Royal Society Interface, 16*(159), art. no. 0362. https://doi.org/10.1098/rsif.2019.0362
36. Tolasa, S., Cakli, S., Kisla, D., Dincer, T. (2012). Quality and shelf-life assessment of pasteurized trout soup during refrigerated storage. *Journal of Aquatic Food Product Technology*, *21*(4), 321-329. https://doi.org/10.1080/10498850.2011.595054
37. Wang, L., Zhang, L., Wang, H., Ai, L., Xiong, W. (2020). Insight into protein-starch ratio on the gelatinization and retrogradation characteristics of reconstituted rice flour. *International Journal of Biological Macromolecules*, *146*, 524-529. https://doi.org/10.1016/j.ijbiomac.2020.01.048
38. Wang, R., Zhang, M., Mujumdar, A.S. (2010). Effect of food ingredient on microwave freeze drying of instant vegetable soup. *LWT – Food Science and Technology*, *43*(7), 1144-1150. https://doi.org/10.1016/j.lwt.2010.03.007
39. Watts, B.M., Ylimaki, G.L., Jeffery, L.E., Elias, L.G. (1989). Chapter 7 – Sensory Tests: Descriptions and Applications. In *Basic Sensory Methods for Food Evaluation*. International Development Research Centre, Ottawa, Ont., Canada, pp. 59-104.
40. Zarehgashti, G., Etemadian, Y., Valipour, A.R., Rahnama, M., Khodabandeh, F., Fahim, A. (2019). Production of a semi ready-to-eat shrimp soup powder and assessment of its shelf life. *Nutrition and Food Sciences Research, 6*(1), 41-50. https://doi.org/10.29252/nfsr.6.1.41

ORIGINAL ARTICLE
http://journal.pan.olsztyn.pl

Polish Journal of Food and Nutrition Sciences
2023, Vol. 73, No. 3, 265–277
DOI: 10.31883/pjfns/170870
ISSN 1230-0322, e-ISSN 2083-6007

Grain of Hybrids Between Spelt (*Triticum spelta* L.) and Bread Wheat (*Triticum aestivum* L.) as a New Raw Material for Breadmaking

Marian Wiwart[1*], Anna Szafrańska[2], Elżbieta Suchowilska[1]

[1]Department of Genetics, Plant Breeding and Bioresource Engineering, Faculty of Agriculture and Forestry, University of Warmia and Mazury in Olsztyn, pl. Łódzki 3, 10-724 Olsztyn, Poland
[2]Professor Wacław Dąbrowski Institute of Agricultural and Food Biotechnology – State Research Institute, Department of Grain Processing and Bakery, Rakowiecka 36, 02-532 Warsaw, Poland

The aim of this study was to determine differences in the technological quality of grain of hybrids between spelt (*Triticum spelta* L.) and bread wheat (*T. aestivum* L.) as compared with the grain of their parental forms, *i.e.*, modern bread wheat cultivars and spelt breeding lines. The content of basic nutrients in grain, milling quality of grain, rheological properties of dough, and bread quality were evaluated. Grain yields were around 18% lower in hybrid lines than in bread wheat. Gluten content was significantly higher in the grain of hybrid lines (34.0 *vs*. 27.5 g/100 g), and it did not differ significantly from that noted in spelt grain (36.1 g/100 g). The gluten index did not differ significantly between hybrid lines and bread wheat cultivars (77 *vs*. 85), and it was significantly higher than in spelt (43). Protein content was significantly higher in the flour obtained from hybrid lines than from bread wheat. Analyzed dough parameters in hybrid lines assumed intermediate values relative to parental forms, and protein parameters had a stronger discriminatory power than starch parameters. Bread made from the grain of single-cross hybrids between spelt and bread wheat was characterized by high quality and in many cases superior attributes relative to bread made from spelt flour. The study demonstrated that hybrids between *T. spelta* and *T. aestivum* can become a new, valuable source of grain for bread production.

Key words: bread wheat, spelt, hybrids, technological quality, rheological properties

INTRODUCTION

Modern consumers are increasingly aware of the nutritional value and health benefits of food products. New consumer behavior trends have decreased the interest in intensive farming crops and increased the demand for alternative crop species, including minor cereals such as hulled wheats [Boukid *et al.,* 2018]. Spelt (*Triticum spelta* L.) is the most popular species in this group of cereals. Spelt grain has a high nutritional value, and it is a rich source of bioactive compounds and essential micronutrients [Arzani & Ashraf, 2017; Shewry & Hey, 2015; Suchowilska *et al.,* 2012]. Although there are known studies suggesting that spelt delivers exceptional health benefits [Valli *et al.,* 2018; Wang *et al.,* 2020], according to some authors there is insufficient evidence to confirm this claim [Dinu *et al.,* 2018; Shewry, 2018]. The nutritional value of high-yielding bread wheat (*Triticum aestivum* L.) varieties was not affected by intensive farming practices [Shewry *et al.,* 2020], but the content of essential nutrients, in particular Fe, Zn, and Mg, continues to decrease in wheat grain [Fan *et al.,* 2008]. In general, spelt is not well suited for intensive agriculture, and high rates of nitrogen fertilization compromise the quality of spelt grain

***Corresponding Author:**
e-mail: marian.wiwart@uwm.edu.pl (M. Wiwart)

Submitted: 29 March 2023
Accepted: 3 August 2023
Published on-line: 28 August 2023

[Sugár *et al.,* 2019]. Spelt does not require intensive chemical protection, which decreases the cost of agricultural treatments and increases spelt's suitability for organic farming. The main challenges in the production and processing of spelt are low genetic yield potential, considerable susceptibility to lodging, and non-threshability [Packa *et al.,* 2015; Rapp *et al.,* 2017].

The technological suitability of wheat grain is determined mainly by its milling quality and the baking quality of flour. Flour yield is influenced by kernel size and the proportion of the seed coat in kernel mass, whereas the baking quality of flour is a complex trait that is determined by the quantity and quality of protein, including gluten, dough strength, α-amylase activity, and the degree of starch damage [Carson & Edwards, 2009]. Spelt grain is generally more abundant in protein than bread wheat grain, but the values of grain quality parameters, including gluten weakening, dough strength and stability, are usually lower in spelt [Rodríguez-Quijano *et al.,* 2019; Tóth *et al.,* 2022].

Bread wheat and spelt are allohexaploid species possessing the same AABBDD genomes [Dvorak *et al.,* 2012]. Considerable genetic similarities of both cereals promote introgression and the production of breeding lines that could combine the desirable traits of bread wheat with the high nutritional value of spelt [Gulyás *et al.,* 2012]. Therefore, the genetic potential of *T. aestivum* could be harnessed to develop new spelt varieties with high yield potential and resistance to lodging. Modern spelt cultivars are characterized by very high yield potential, satisfactory resistance to lodging, and less compact glumes than "true spelt", which facilitates dehulling [Dinkel, 2023; Winterspelz, Winterdinkel: Sorte Divimar, 2023]. However, information about the genetic origin of new spelt cultivars and the proportion of *T. aestivum* genes is rarely available. The phenotype of such spelt is similar to that of bread wheat, in particular as regards spike traits, plant height, and stalk rigidity. Despite the fact that modern spelt cultivars are not recognized as "true spelt" by some consumers and agricultural producers, especially organic farmers, the technological quality of grain and flour does not differ from that of traditional varieties, and the obtained bread receives high or very high scores in sensory analyses [Wiwart *et al.,* 2017].

Due to the high nutritional value of grain, relatively low soil requirements, and considerable resistance to fungal pathogens, *T. spelta* is highly suited for genetic recombination with bread wheat cultivars grown in intensive farming systems [Chrpová *et al.,* 2021; Rachoń *et al.,* 2020; Sugár *et al.,* 2019]. Breeding efforts aiming to produce hybrids between bread wheat and spelt are justified by the following observations: (1) sustainable farming practices should be incorporated in modern agricultural systems; (2) wheat is the most important small-grain cereal for human consumption; (3) agricultural production should be profitable and socially acceptable. The grain of the developed hybrids should be characterized by high technological quality and should be suitable for bread making. However, these parameters have not yet been more extensively studied in hybrids between bread wheat and spelt and literature data are only fragmentary and scarce [Ceglińska, 2003].

Therefore, the aim of this study was to determine differences in the processing suitability of grain in breeding lines derived from single-cross hybrids between *T. spelta* and *T. aestivum*. The content of basic nutrients in grain, milling quality of grain, rheological properties of dough, and bread quality were evaluated.

MATERIALS AND METHODS

Material

The experimental material comprised the grain of 36 spring breeding lines derived from single-cross hybrids between three bread wheat (*T. aestivum* L.) cultivars grown in an intensive farming system and five spelt (*T. spelta* L.) breeding lines, as well as the grain of the parental lines (Table 1).

Field experiment

The breeding lines of spring spelt (S10, S11, S12, S13 and S14) were selected at the Department of Genetics, Plant Breeding and Bioresource Engineering of the University of Warmia and Mazury in Olsztyn (Poland) from the accessions derived from the Polish Genebank (NCPGR) of the National Center for Plant Genetic Resources (Radzików, Poland). The analyzed parental lines fully meet "true spelt" criteria in terms of phenotypic and agronomic traits. Torka and Zebra are elite bread wheat cultivars (E) with the highest flour strength and high protein content, whereas Kontesa is a high-yielding variety of quality class A [Gacek, 2013]. The field experiment was performed at the Agricultural Experiment Station in Bałcyny in Poland (53°36' N latitude; 19°5' E longitude). Spikelets (spelt and breeding lines) or seeds (bread wheat) were sown in duplicate at a density of 200 spikelets/m^2 (spelt and breeding lines) and 400 seeds/m^2 in plots with an area of 9 m^2 each. The plots were fertilized with N/P/K at 80/25/80 kg/ha. Chemical plant protection was not applied. Grain (bread wheat) and spikelets (spelt and hybrids) were harvested in the over-ripe stage (BBCH 92) [Witzenberger *et al.,* 1989] with a Wintersteiger Classic (Ried im Innkreis, Austria) plot harvester. After harvesting, the yield and grain quality parameters listed in the next subsection were determined.

Grain milling

At least 2 kg of grain was harvested from the three wheat cultivars, five spelt breeding lines and most productive 17 hybrid lines for the assessment of grain baking properties. The milling quality of grain samples was evaluated before milling by determining grain weight [ISO 7971-3:2019], vitreousness using Pohl farinator for cutting grains (Bipea method Ref. 204-1104), and thousand kernel weight [ISO 520:2010]. Grain samples were cleaned and tempered to a moisture content of 16 g/100 g by adding water. Grain was conditioned for at least 24±1 h to promote rapid and complete separation of the endosperm. The samples were milled in a Bühler MLU-202 pneumatic laboratory mill (Bühler, Uzwil, Switzerland). Six flour streams were combined to obtain straight-grade white flour for quality analysis and baking trials. The flour yield (66.4% to 75.8%) and ash content [ISO 2171:2007] of each grain sample were determined. The flour

Table 1. Breeding lines and their parental components examined in the study. The origin of the lines is given in brackets.

Parental spelt line/ bread wheat cultivar		Breeding line (♀×♂)		Breeding line (♀×♂)		Breeding line (♀×♂)	
No		No	Origin	No	Origin	No	Origin
1	S10	9	(T×S10)	21	(Z×S13)^{I}	33	(S13×T)^{II}
2	S11	10	(K×S10)	22	(Z×S13)^{II}	34	(S13×T)^{III}
3	S12	11	(K×S11)	23	(Z×S13)^{III}	35	(S14×T)
4	S13	12	(K×S11)^{I}	24	(Z×S13)^{IV}	36	(S10×K)
5	S14	13	(K×S12)	25	(Z×S13)^{V}	37	(S10×K)^{I}
6	cv. Torka (T)	14	(K×S12)^{I}	26	(Z×S13)^{VI}	38	(S11×K)
7	cv. Zebra (Z)	15	(K×S12)^{II}	27	(Z×S13)^{VII}	39	(S12×K)
8	cv. Kontesa (K)	16	(K×S14)	28	(S10×T)	40	(S12×K)^{I}
		17	(Z×S10)	29	(S11×T)	41	(S13×K)
		18	(Z×S11)	30	(S11×T)^{I}	42	(S14×K)
		19	(Z×S11)^{I}	31	(S13×T)	43	(S14×K)^{I}
		20	(Z×S13)	32	(S13×T)^{I}	44	(S14×K)^{II}

S10…S14, parental spelt lines; K, T, Z, bread wheat cultivar Kontesa, Torka and Zebra, respectively; $^{I, II, III, IV, V, VI, VII}$, sister lines derived from the same combination of parents.

yield was calculated as the total flour obtained in the laboratory milling to all milling products including bran.

Analysis of the baking quality of flour

The bread-making potential of the flour samples was evaluated by examining the protein and starch complex. The protein complex was analyzed by determining protein content [ISO 20483:2013] using Kjeltec 2200 (Foss, Hilleroed, Denmark), gluten content, gluten index (GI) [ISO 21415-2:2015] using Glutomatic 2200 (PerkinElmer, Inc., Waltham, Ma, USA), and the Zeleny sedimentation index [ISO 5529:2007]. The starch complex was evaluated by determining the falling number [ISO 3093:2010] using Perten Falling Number® system (FN 1500 model, PerkinElmer) and starch damage [ISO 17715:2013] using SDmatic (KPM Analytics, Villeneuve-la-Garenne, France). The moisture content of flour was measured according to ISO standard [ISO 712:2009].

Analysis of the rheological properties of dough

The rheological properties of wholemeal flour and refined flour dough were analyzed in the Chopin Mixolab system (KPM Analytics) according to the procedure described by Suchowilska *et al.* [2019]. The Mixolab test was performed with the application of a standard Chopin+ protocol: dough weight – 75 g, kneading speed – 80 rpm, water temperature – 30°C and the following settings of the time and temperature in the phases of analyses: 8 min at 30°C, heating at 4°C/min for 15 min, holding at 90°C for 7 min, cooling to 50°C at 4°C/min for 10 min, and holding at 50°C for 5 min. Water absorption was expressed as the volume of water required to obtain dough with a consistency of 1.10 N×m (±0.05) at point C1 in the first test phase. The following protein characteristics of the tested flours were read from the Mixolab curve: dough development time (T1, min), stability time (min); C2, C10, C12, C14, C16, C18, C1-2, Cs (protein weakening, decrease in consistency due to mechanical shear stress in dough, followed by temperature increase; measured 10, 12, 14, 16 and 18 min after the beginning of the test, the calculated difference between points C1 and C2, N×m, and the stability measured 8 min after the test started), and slope α (indicator of protein weakening, N×m/min). The starch complex was analyzed based on the following Mixolab parameters: C3, C3--C2 (starch gelatinization, N×m); C4, C3-C4 (amylolytic activity, N×m), C5, C5-C4 (starch retrogradation, N×m), D2 and D3 (initial and final temperature of starch gelatinization, respectively, °C), time T2, T3, T4, T5 (respectively: initial and final time of starch gelatinization, time of dropping the consistency in point C4 during cooling process of a dough, final time of analysis, min), and slopes β and γ (starching speed and enzymatic degradation, respectively, N×m/min). D1, D4 and D5 (°C, correspond to an estimation of dough temperatures at test point characteristics: C1, C4 and C5, respectively). Six qualitative indices, including water absorption (WA), mixing (MIX), gluten+ (GLU+), viscosity (VIS), amylase activity (AMY) and starch retrogradation (RET), were converted from standard curve parameters and analyzed using the Chopin Profiler protocol. The results were expressed as the ratio of the values for the sample and the standard. All parameters were analyzed in duplicate.

Baking trials

Dough was prepared in a standard baking test with the use of the one-step method [Suchowilska *et al.,* 2019; Wiwart *et al.,* 2017]. Flour (600 g) was combined with water, compressed yeast (18 g), and salt (9 g) at 28–30°C in a laboratory mixer (KitchenAid, Benton Harbor, MI, USA). The moisture content [ISO 712:2009] of flour was determined to adjust flour weight to a moisture

content of 14 g/100 g. Water was added in an amount required to achieve the water absorption capacity indicated in the Mixolab system (KPM Analytics), and it was increased by 3 g/100 g until dough consistency reached 350 Brabender units (BU). Dough was fermented for 60 min in a laboratory proving cabinet at 30°C and 75% relative humidity (RH). After 30 min, dough was kneaded by hand for 60 s and divided into three portions of 250 g each. Each portion was rounded, placed in a baking tin, and kept in a laboratory proving cabinet at 30°C and 75% RH for the time required for optimal dough development (34–44 min). Loaves were baked at 230°C for 30 min in an oven (Piccolo Wachtel Winkler, Pulsnitz, Germany) (live steam was injected immediately after the loaves were placed in the oven). Baked loaves were brushed with water and stored in sealed plastic containers to prevent desiccation. After 24 h of cooling, each sample was weighed and analyzed for porosity, crumb elasticity, and specific volume with the rapeseed displacement method [Różyło *et al.,* 2015] (expressed in mL per 100 g of bread). Crumb hardness (expressed in newtons, N), namely the maximum force needed to achieve 50% deformation of a 3-cm-thick slice, was determined in five replicates with the Instron 1140 universal testing machine (Norwood, MA, USA). A probe with a diameter of 35 mm was used in the test, and crosshead speed was 50 mm/min. Crumb and crust color was determined in five replicates with a Minolta CR-310 colorimeter (Konica Minolta Sensing Americas, Inc, Ramsey, NJ, USA). The measurements were performed in the CIELab system (L^* – lightness, a^* –green-red coordinate, b^* –blue-yellow coordinate).

Statistical analysis

Statistical analyses were performed using the Statistica 13 program [TIBCO Software Inc., 2017]. After testing the condition of normality of distribution, the results were processed by analysis of variance (ANOVA), and the significance of differences between mean values was determined by the multiple Student-Newman-Keuls (SNK) test. Furthermore, the results were subjected to multivariate analyses (principal component analysis – PCA and hierarchical analysis). The non-parametric Kruskal-Wallis test was used to compare mean values of Mixolab indices.

RESULTS AND DISCUSSION

Grain yield and grain quality parameters

The grain yield and grain quality parameters of the analyzed hybrid lines and parental lines are presented in Table 2. As expected, grain yield was significantly highest in bread wheat (6.64 t/ha), and the grain yield of hybrid lines was higher in comparison with spelt (5.43 *vs*. 4.97 t/ha) but the difference was not statistically significant. No significant differences in grain yield were observed between hybrid lines. The content of protein and gluten in the grain of hybrid lines (15.2 g/100 g dry matter, d.m. and 34.0 g/100 g, respectively) assumed intermediate values between bread wheat (13.1 g/100 g d.m. and 27.5 g/100 g, respectively) and spelt (17.1 g/100 g d.m. and 36.1 g/100 g, respectively). The grain of hybrid lines where spelt was the maternal component was characterized by significantly higher protein and gluten content than the grain of hybrid lines where spelt was the paternal component. The starch content of hybrid grain (64.8 g/100 g d.m.) did not differ significantly from that noted in bread wheat (67.8 g/100 g d.m.) and spelt (62.1 g/100 g d.m.) grain, but the analyzed hybrids were characterized by significantly higher grain filling (average test weight of 79.5 kg/hL *vs*. 75.0 kg/hL in spelt) and relatively high thousand kernel weight. It should also be noted that the Zeleny index was significantly higher in hybrid lines than in bread wheat (62 mL *vs*. 45 mL), and the average values of this parameter were higher in hybrid lines where spelt was the maternal component than in hybrid lines where bread wheat was the maternal component (65 mL *vs*. 54 mL).

Dietary recommendations, current food trends, and the growing interest in new crops among farmers contribute to increasing the area under cereals characterized by high yields, satisfactory technological quality, and high nutritional value. These traits have been relatively well researched in spelt [Biel *et al.,* 2021; Bonafaccia *et al.,* 2000]. The present study was undertaken to examine unique hybrid lines between bread wheat and spelt which combine the attributes of their parental forms: high yield and resistance to lodging (bread wheat) and high processing suitability and resistance to fungal pathogens (spelt).

Technological quality of flour and rheological properties of dough

The mean values of the main parameters describing the technological quality of the tested flours of spelt, wheat and hybrids are presented in Table 3 and the values for flours of individual lines are shown in Table S1. Spelt flours were characterized by significantly highest protein (15.9 g/100 g d.m.) and gluten (45.4 g/100 g) content, but also the lowest quality (gluten index – 43). Bread wheat flours were characterized by the lowest protein (12.1 g/100 g d.m.) and lowest gluten content (28.6 g/100 g), as well as the highest gluten quality (gluten index – 85). Hybrid lines were characterized by a relatively high content of protein (13.2 g/100 g d.m.) of high quality (gluten index – 77). However, no significant differences were noted between the tested hybrids (W×S and S×W). The ash content of the examined flours ranged from 0.51 (S12×Kontesa) to 0.74 g/100 g d.m. (S11). Spelt flours had significantly higher ash content than bread wheat and hybrid flours. Significant differences were also observed between hybrid lines of different origin: ash content was significantly lower (more desirable) in S×W than W×S hybrids. Starch damage values ranged from 14.4 (S10×Torka) to 24.8 UCD (Zebra×S13) and were influenced by the origin of grain. On average, starch damage values were significantly lowest (17.5 UCD) in spelt flours and highest in bread wheat flours (23.0 UCD). Wheat flours were characterized by low α-amylase activity, as evidenced by falling number values above 250 s (338.5 to 365.5 s). Moderate α-amylase activity was noted in only one flour sample derived from Zebra as the maternal line (falling number – 162.5 s).

Dough torque at point C3 on the Mixolab curve (2.17 N×m on average) was highest in hybrid lines derived from spelt maternal lines and bread wheat cv. Torka as the paternal

Table 2. Grain yield and basic parameters describing the technological quality of the grain of hybrid lines and their parental lines.

	Yield (t/ha)	Test weight (kg/hL)	Vitreousness (%)	TKW (g)	Content			Zeleny index (mL)
					Protein (g/100 g d.m.)	Gluten (g/100 g)	Starch (g/100 g d.m)	
Spelt (S) (*n*=5)								
Mean	4.97^{b}	75.0^{b}	95	46.6	17.1^{a}	36.1^{a}	62.1^{b}	71^{a}
RSD (%)	12.7	3.9	0.9	8.9	10.4	11.1	4.1	10.3
Min÷max	3.93÷5.41	72.1÷79.2	94÷96	41.6÷52.4	15.1÷18.7	32.2÷40.9	59.4÷65.3	62÷75
Wheat (W) (*n*=3)								
Mean	6.64^{a}	78.3^{ab}	76.3	41.4	13.1^{b}	27.5^{b}	67.8^{a}	45^{c}
RSD (%)	7.3	8.7	19.7	6.8	4.5	7.6	1.1	12.7
Min÷max	6.20÷7.16	71.0÷84.4	62÷92	38.9÷45.5	12.7÷13.8	25.9÷29.9	66.9÷68.3	41÷52
Hybrids (*n*=36)								
Mean	5.43^{b}	79.5^{a}	85.9	48.4	15.2^{ab}	34.0^{a}	64.8^{ab}	62^{b}
RSD (%)	17.1	3.3	17.9	10.7	7.3	6.2	2.9	10.3
Min÷max	3.18÷6.84	72.2÷82.9	30÷95	39.8÷63.2	13.4÷19.1	28.2÷46.7	59.4÷68.0	49÷75
W×S hybrids (*n*=19)								
Mean	5.66	79.8	85.6	48.1	14.8^{y}	32.0^{y}	65.5^{x}	54^{y}
RSD (%)	10.9	3.5	23.1	11.4	6.0	8.2	1.9	10.4
Min÷max	4.44÷6 64	72.2÷82.9	30÷95	39.8÷63.2	13.4÷16.8	28.2÷38.5	63.4÷68.0	49÷72
S×W hybrids (*n*=17)								
Mean	5.17	79.1	86.3	48.8	15.8^{x}	35.3^{x}	64.1^{y}	65^{x}
RSD (%)	22.3	2.8	7.5	10.2	7.1	11.9	2.6	8.2
Min÷max	3.18÷6.84	72.2÷81.7	76÷94	41.0÷55.6	14.0÷19.1	29.7÷46.7	59.4÷67.0	55÷75

TKW, one thousand kernel weight; d.m., dry matter; RDS, relative standard deviation. Values followed by the different letters (a–c) within the column differ significantly at $p<0.05$ (for spelt, bread wheat and hybrids). Values with different letters x and y for S×W and W×S hybrids differ significantly at $p<0.05$.

component (Table S1). The lowest torque at point C3 (1.86 N×m on average) was noted in hybrids derived from cv. Kontesa as the maternal component. In turn, parameters C4 and C5 were lowest in hybrids derived from cv. Zebra as the maternal component (1.53 and 2.54 N×m on average, respectively) and highest in hybrids derived from cv. Torka as the paternal line (1.83 and 3.14 N×m on average, respectively). The initial (D2) and final (D3) temperatures of starch gelatinization were determined at 48.2–52.8°C and 70.0–84.2°C, respectively. The value of slope β, describing the starch pasting rate, ranged from 0.083 to 1.002 N×m/min, and no significant differences in this parameter were found between grain types. Starch damage had no significant effect on slope β, or on initial (D2) and final (D3) temperature of gelatinization. However, greater differences between points C1 and C2, and between points C3 and C2 were observed with an increase in starch damage.

The PCA results for 12 protein parameters and 12 starch parameters are presented in Figure 1. Protein parameters had greater discriminatory power because PC1 and PC2 explained 76.6% of total variance, whereas starch parameters explained only 52.2% of total variance. Eight protein parameters (C1, C2, C10, C12, C14, C16 C18, and C1-C2) were highly correlated with both PCs, as demonstrated by the location of the corresponding points in the vicinity of the circle with a radius of 1, which corresponded to the absolute value of the correlation coefficient *r*. Point C4 was positioned near the beginning of the coordinate system, which indicates that this parameter had the smallest discriminatory power. The areas corresponding to three bread wheat cultivars and five spelt lines are completely separate, and the distribution of parental components in hybrid lines (W×S and S×W) had no significant effect on their similarity to spelt or bread wheat.

The Mixolab profiler indices for the grain and flour of hybrid lines and their parental forms are presented in Table 4. In the grain analysis, water absorption capacity was characterized by the smallest variation and the highest similarity to the reference wheat cultivars and spelt lines. In the flour analysis, the same observations were made for viscosity. Grain milling significantly affected flour quality due to differences in starch damage values. The Mixolab profiles for wheat cultivars and spelt lines did not differ significantly, but retrogradation values were higher and gluten+ values were lower in spelt.

Table 3. Mean values, relative standard deviation (RSD), and range (min÷max) of basic parameters describing the technological quality of flour from the grain of single-cross hybrids between bread wheat and spelt, and their parental lines.

	Flour yield (%)	Water absorption (g/100 g)	Protein content (g/100 g d.m.)	Ash content (g/100 g d.m.)	Gluten content (g/100 g)	Gluten index	Falling number (s)	Starch damage (UCD)
Spelt (S) (*n*=5)								
Mean	72.0^{ab}	60.3	15.9^{a}	0.68^{a}	45.4^{a}	43^{b}	338.8	17.5^{b}
RSD (%)	3	4	10	7	15	51	2	9
Min÷max	70.0÷74.5	57.5÷62.7	13.7÷17.3	0.63÷0.74	37.3÷57.9	9÷65	326÷347	15.5÷19.8
Wheat (W) (*n*=3)								
Mean	74.5^{a}	58.3	12.1^{b}	0.62^{b}	28.6^{c}	85^{a}	354.3	23.0^{a}
RSD (%)	3	2	4	2	3	23	4	4
Min÷max	72.2÷75.8	56.7÷59.2	11.6÷12.6	0.61÷0.63	27.5÷29.3	60÷99	339÷366	22.0÷23.7
Hybrids (*n*=17)								
Mean	70.9^{b}	59.2	13.2^{b}	0.61^{b}	34.1^{b}	77^{a}	322.9	20.7^{ab}
RSD (%)	3	5	5	8	6	20	15	16
Min÷max	66.3÷74.2	55.8÷64.2	11.9÷14.6	0.51÷0.71	28.9÷38.1	45÷99	163÷379	14.4÷24.8
W×S hybrids (*n*=10)								
Mean	71.4	60.0	13.1	0.63^{x}	33.8	76	317.7	21.5
RSD (%)	2	5	5	7	7	22	18	15
Min÷max	68.0÷74.2	55.8÷64.2	11.9÷14.3	0.59÷0.71	28.9÷38.1	45÷99	163÷379	16.9÷24.8
S×W hybrids (*n*=7)								
Mean	70.2	57.9	13.4	0.59^{y}	34.5	78	330.6	19.4
RSD (%)	4	5	6	8	4	18	9	17
Min÷max	66.4÷73.4	52.9÷62.9	12.4÷14.6	0.51÷0.65	31.8÷36.2	58÷99	280÷372	14.4÷23.6

d.m., dry matter; RDS, relative standard deviation. Values followed by the different letters (a–c) within the column differ significantly at $p<0.05$ (for spelt, bread wheat and hybrids). Values with different letters x and y for S×W and W×S hybrids differ significantly at $p<0.05$.

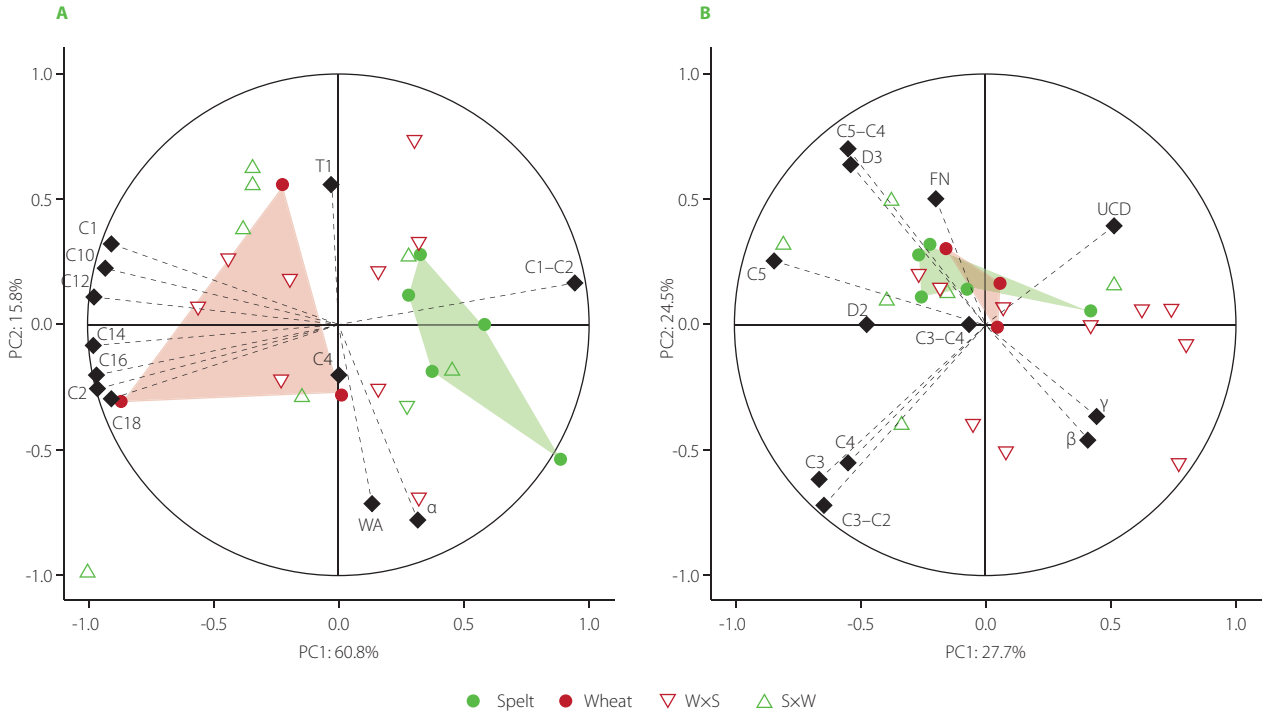

Figure 1. PCA biplot of the parameters associated with protein (**A**) and starch (**B**) quality in the grain of five spelt breeding lines, three bread wheat cultivars, and 17 single-cross hybrids between bread wheat × spelt (W×S) and spelt x bread wheat (S×W). C1, C2, C3, C4, C4, C5, C10, C12, C14, C16, C18, dough resistance (N×m) measured at point C1, C2, C3, C4 and C5, and after 10, 12 … 18 min of the analysis; T1, dough development time (min); D2 and D3, initial and final temperature of starch gelatinization (°C); WA, water absorption; FN, falling number (s); UCD, starch damage in UCD units; α, protein weakening (N×m/min); β and γ, starching speed and enzymatic degradation, respectively (N×m/min). The results were obtained in the Mixolab system (Chopin Technologies, France).

Table 4. Mean values of Mixolab Profiler indices, relative standard deviation (RSD,%), range (min÷max), the values of test function *H* for Kruskall-Wallis test and probabilities associated with *H* for grain and flour of studied cereals.

	Grain						Flour					
	WA	MIX	GLU+	VIS	AMY	RET	WA	MIX	GLU+	VIS	AMY	RET
	Mean						Mean					
Spelt	8.2	2.6	2.2	4.8	4.6	7.2	6.3	3.0	2.7	6.5	6.2	7.7
Bread wheat	8.0	3.7	3.0	5.7	5.0	5.0	5.0	4.7	5.7	7.2	4.8	7.8
Hybrids	8.1	3.9	3.7	4.6	4.8	6.9	5.1	3.8	4.9	7.0	5.1	6.9
	RSD (%)						RSD (%)					
Spelt	5	44	99	9	45	6	37	31	65	13	9	6
Bread wheat	0	42	67	10	35	35	35	22	20	4	49	4
Hybrids	7	42	43	33	54	25	48	25	44	18	41	19
	Min÷max						Min÷max					
Spelt	8÷9	1÷4	1÷6	4÷5	3÷8	7÷8	3.5÷8	2÷4	1÷5.5	5÷7	5.5÷7	7÷8
Bread wheat	8÷8	2÷5	1÷5	5÷6	4÷7	3÷6	3÷6	3.5÷5.5	5÷7	7÷7.5	3÷7.5	7.5÷8
Hybrids	6÷9	2÷7	1÷7	1÷7	1÷8	3÷9	2÷8	2÷5	1.5÷8	4÷8.5	1÷8	3÷8
	H value (2; *N*=44)						*H* value (2; *N*=25)					
	0.334	2.667	3.709	1.982	0.034	3.576	1.947	4.412	4.491	1.671	0.826	4.211
p-Value	0.846	0.264	0.157	0.371	0.983	0.167	0.378	0.110	0.106	0.434	0.662	0.122

WA, water absorption; MIX, mixing; GLU+,- gluten+; VIS, viscosity; AMY, amylase activity; RET, starch retrogradation.

The study demonstrated that bread wheat flours are characterized by the lowest protein and gluten content and the highest gluten quality, and it confirms previous observations made by Ceglińska [2003], Geisslitz *et al.* [2019], and Takač *et al.* [2021]. However, in the works of Ceglińska [2003] and Packa *et al.* [2019], flours obtained from hybrid lines inherited desirable traits from parental lines, including high protein content (spelt) and high gluten quality (bread wheat). Considerable variations in the protein and gluten content of hybrid lines were also reported by Diordiieva *et al.* [2018], and they suggest that effective selection for high content of both protein and gluten is possible. Average gluten content was nearly 25% lower in hybrids than in spelt, but the grain of hybrid lines was characterized by much higher gluten quality, as evidenced by the fact that gluten index values were 33 units higher on average in hybrids. Hybrid lines were highly similar to the studied bread wheat cultivars in terms of gluten content and quality, and their baking quality was higher in comparison with spelt. In the works of Tran *et al.* [2020] and Tóth *et al.* [2022], the gluten index was significantly lower in spelt than in bread wheat. Geisslitz *et al.* [2019] examined 75 genotypes of four *Triticum* species (*T. aestivum*, *T. spelta, T. dicoccon,* and *T. monococcum*) and found that the gliadin/glutenin ratio was more than 30% higher (3.3 *vs*. 2.5) in spelt gluten than in bread wheat gluten. Glutenins are good predictors of bread volume. In the current study, the total protein content of hybrid lines was significantly lower than in spelt (by approx. 20%), but it was around 9% higher than in bread wheat.

Starch damage is considered to be one of the most important criteria for assessing the baking quality of flour. This parameter affects the water absorption capacity of flour, the rheological properties of dough, dough fermentation, and crumb structure [León *et al.,* 2006; Litvyak, 2018]. In the present study, starch damage ranged from 14.4 (10×Torka) to 24.8 UCD (Zebra×13), and it was influenced by the origin of milled grain. Considerable variations in the starch damage values of the examined hybrids (14.4–24.8 UCD) indicate that these lines can be used in the production of a wide assortment of baked goods. Wheat flours intended for the production of bread and confectionery goods are generally characterized by a wide range of starch damage values, from 14 to 24 UCD [Liu *et al.,* 2018]. In a study by Dąbkowska [2009], starch damage values ranged from 13.9 to 17.7 UCD in spelt flour, and were determined at 19.3 UCD on average in bread wheat flour. According to Krawczyk *et al.* [2008], starch damage values are generally low in spelt flour (17.5 UCD). Wilson *et al.* [2008] reported lower starch damage values in spelt flour than in control wheat flour, and attributed these differences to the soft endosperm of spelt grain. Tóth *et al.* [2022] observed that variations in starch damage values were determined in 40.5% by genotype, and were significantly influenced by the interaction effects of genotype×environment (51.9%).

Flour ash content is a crucial parameter in the evaluation of grain milling characteristics. The milling efficiency index (MEI), which is defined as the ratio of total flour yield to flour ash content, is one of the most reliable indicators of milling

quality. The higher the value of MEI, the higher the milling quality of wheat grain [Dziki *et al.,* 2017]. High ash content of grain is not a desirable parameter because it decreases flour yield and reduces milling profits. However, ash content is a desirable trait from the nutritional point of view because it denotes high mineral content. In the present study, spelt flours were characterized by significantly highest ash content. In this respect, the examined hybrids were more similar to bread wheat than spelt, which implies that they have superior milling characteristics in comparison with *T. spelta*.

The water absorption capacity of wheat flour is influenced by several factors, mostly kernel size, grain hardness, starch damage, protein content, as well as the content and proportions of pentosans and arabinoxylans (AX) [Sapirstein *et al.,* 2018]. The water absorption capacity of gluten proteins is determined by their quality, and it generally ranges from 250 to 354% [Kaushik *et al.,* 2015]. In turn, the water absorption capacity of starch is affected by the degree of starch damage: whole grains retain around 40% of water on the surface (relative to their own weight), whereas damaged starch absorbs up to 300% of water [Jukić *et al.,* 2019; Sen *et al.,* 2016]. In the present study, higher starch damage values were significantly correlated (r=0.497, p<0.05) with increased water absorption capacity in all flours, and the strongest correlations were observed in the flours obtained from the grain of the examined hybrid lines (r=0.823, p<0.01).

The rheological properties of dough measured in the Mixolab system provide information about starch pasting properties, stability of the starch gel when heated, and starch retrogradation (torque at points C3, C4 and C5, respectively) [Banu *et al.*, 2011; Haros *et al.,* 2006; Kahraman *et al.,* 2008]. Dough torque at point C3 depends on slope β, *i.e.*, the rate of changes in starch pasting properties. High torque value at point C3 points to high dough flexibility and is characteristic of the flour fraction originating from the central part of the endosperm [Banu *et al.,* 2011; Mixolab Application Handbook 2012]. The discussed parameters were influenced by grain type, but no significant differences were found. Dough torque ranged from 1.61 to 2.68 N×m at point C3, from 1.07 to 2.52 N×m at point C4, and from 1.66 to 3.34 N×m at point C5. The mean values for bread wheat and spelt samples were higher than those noted in our previous study [Szafrańska *et al.,* 2015], which could be attributed to low α-amylase activity of the examined grain samples. Similarly to our study, no significant differences were found between bread wheat and spelt [Szafrańska *et al.*, 2015]. However, in the work of Zhygunov *et al.* [2020], spelt flours differed significantly in amylolytic activity and hot gel stability. Spelt flours had higher C4 values, and the difference between C3 and C4 was very small, which points to high thermal stability of starch gel. Wheat flours with lower amylolytic activity were characterized by higher starch damage values because hot dough continues to liquefy, which explains the high difference between C4 and C3. In a study by Dąbkowska [2009], flours obtained from different types of grain differed in initial starch gelatinization temperature determined with an amylograph. Initial starch gelatinization temperature was determined at 50.1–60.6°C in refined spelt flours and at 56.9–64°C in bread wheat flour, whereas the final temperature of gelatinization was determined at 65.9–90.8°C and 68.9–82.8°C, respectively. In the current study, the initial and final temperature of gelatinization was determined in the range of 48.2–52.8°C and 70.0–84.2°C, respectively.

The Profiler has been developed specifically to control quality and simplify the reading of data from Mixolab tests. This solution is not strictly a research tool, nor a tool for correcting potential flour defects, but it is a unique "translator" that converts complex technological data into six simple quality indicators [Dubat & Bock, 2018]. The Profiler is a highly convenient solution that facilitates the selection of the most desirable traits in quality breeding [Suchowilska *et al.,* 2019]. The hybrid lines evaluated in this study were characterized by considerable variations in all six quality indicators, which indicates that lines characterized by high technological quality can be selected and that bread wheat and spelt hybrids can be crossed to obtain varieties with high baking quality of flour.

Laboratory baking test

Cross-sectional images of bread made from the grain of bread wheat cultivars, spelt lines, and 15 single-cross hybrids between bread wheat and spelt are presented in Figure 2. The breads baked in laboratory trials were well risen, and they were characterized by desirable crust color and relatively even crumb porosity. Despite some variability between all tested materials in terms of color of crust, the differences proved to be statistically insignificant. The flours obtained from hybrid lines where elite bread wheat cv. Zebra was the maternal component were characterized by the highest baking quality (Table S1). Bread loaves baked from these flours had the largest average volume and lowest crumb hardness (Figure 3). Despite their low average gluten content, these flours were characterized by high values of the gluten index, water absorption, and dough stability time. High starch damage values and the highest proportion of particles smaller than 95 µm directly contributed to the high water absorption capacity of these flours. The resulting dough also had superior mechanical properties during processing in the dough rounder.

Four bread parameters for the 15 analyzed hybrids and their parental lines are presented in Figure 3. Significant differences were observed in bread yield and 100 g bread volume, whereas dough yield and bread crumb hardness did not differ significantly between the analyzed hybrids and their parental lines. Bread volume was lower for hybrid lines (318.3 mL on average) than for spelt (346.5 mL on average) and bread wheat (377.8 mL on average), but the obtained loaves were consistent with Polish quality standards regarding the minimum volume of bread loaves (200 mL) baked from type 750 wheat flour [PN-A-74105:1992]. Hybrid lines differed significantly from bread wheat in terms of bread yield (140.6 and 141.6 *vs*. 136.4%), but no significant differences in bread yield were found between hybrid lines and spelt (139.0%). Despite the absence of significant differences in crumb hardness, the average values of this parameter were

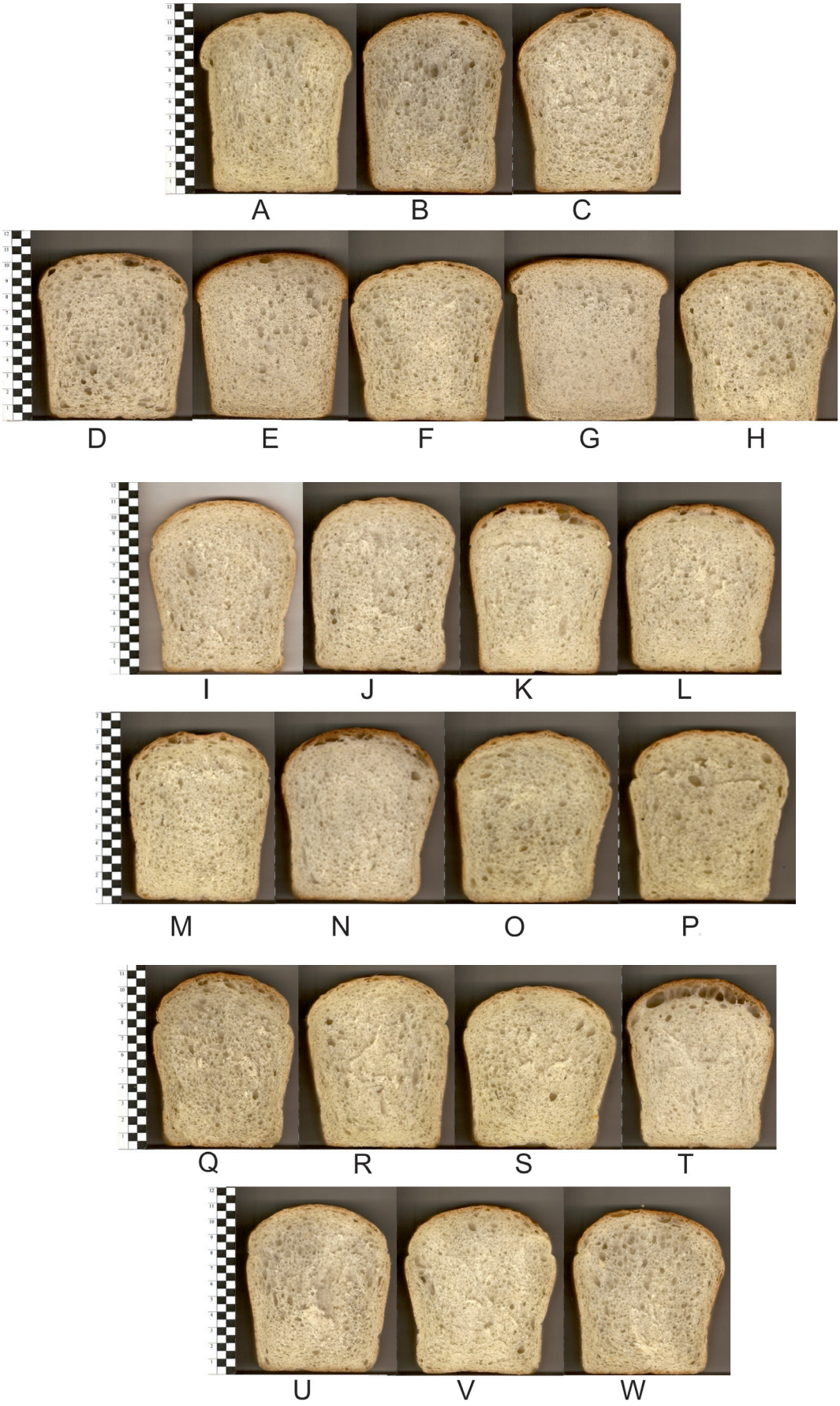

Figure 2. Cross-sectional images of bread loaves baked in laboratory trials from the flour of bread wheat cultivars (A–C) and spelt lines (D–H) as the parental components of single-cross hybrids (I–W). A, B, C, bread wheat cvs. Torka, Zebra, and Kontesa, respectively; D…H, spelt lines S10, S11, S12, S13, and S14; I, Kontesa ×10; J, 10×Kontesa; K, Kontesa×11; L, Kontesa ×11; M, (Kontesa ×14)'; N, Zebra×11; O, Zebra×13; P, (Zebra×13)'; Q, (Zebra×13)"; R, (Zebra×13)"'; S, 10×Torka; T, 11×Torka; U, 13×Torka; V, 12×Kontesa; W, 13×Kontesa.

higher in hybrid lines, in particular when spelt was the maternal component, than their parental lines (Figure 3).

The hierarchical cluster analysis of 10 bread parameters in 15 hybrid lines and their parental lines supported the discrimination of the examined cereals (Figure 4). The studied lines and cultivars were grouped in three clusters. The first cluster (I) comprised all spelt parental lines, bread wheat cvs. Kontesa and Zebra, and one hybrid line where bread wheat cv. Zebra was the maternal component. The second (II) and largest cluster consisted of 10 hybrid lines and bread wheat cv. Torka. The third cluster (III) contained six hybrid lines. Cluster I was characterized by high values of *a** for bread crumb and low values of bread yield and *L* for bread crumb; cluster II was characterized by high values of dough yield and bread yield, and low values of *L** for bread crust and *b** for bread crust; and cluster III was characterized by high values of bread crumb hardness, *L** for bread crust, and *b** for bread crust, and low values of dough yield, bread volume, and *a** for bread crumb. The above values had a high discriminatory power. It should also be noted that spelt was the maternal component in only three of the 10 hybrid lines in cluster II (33.3%).

The baking quality of flour can be directly and reliably evaluated in baking trials. Baking trials were conducted for 17 hybrid lines and eight parental lines. The lines were selected for the test based on the results of previous rheological analyses. Bread

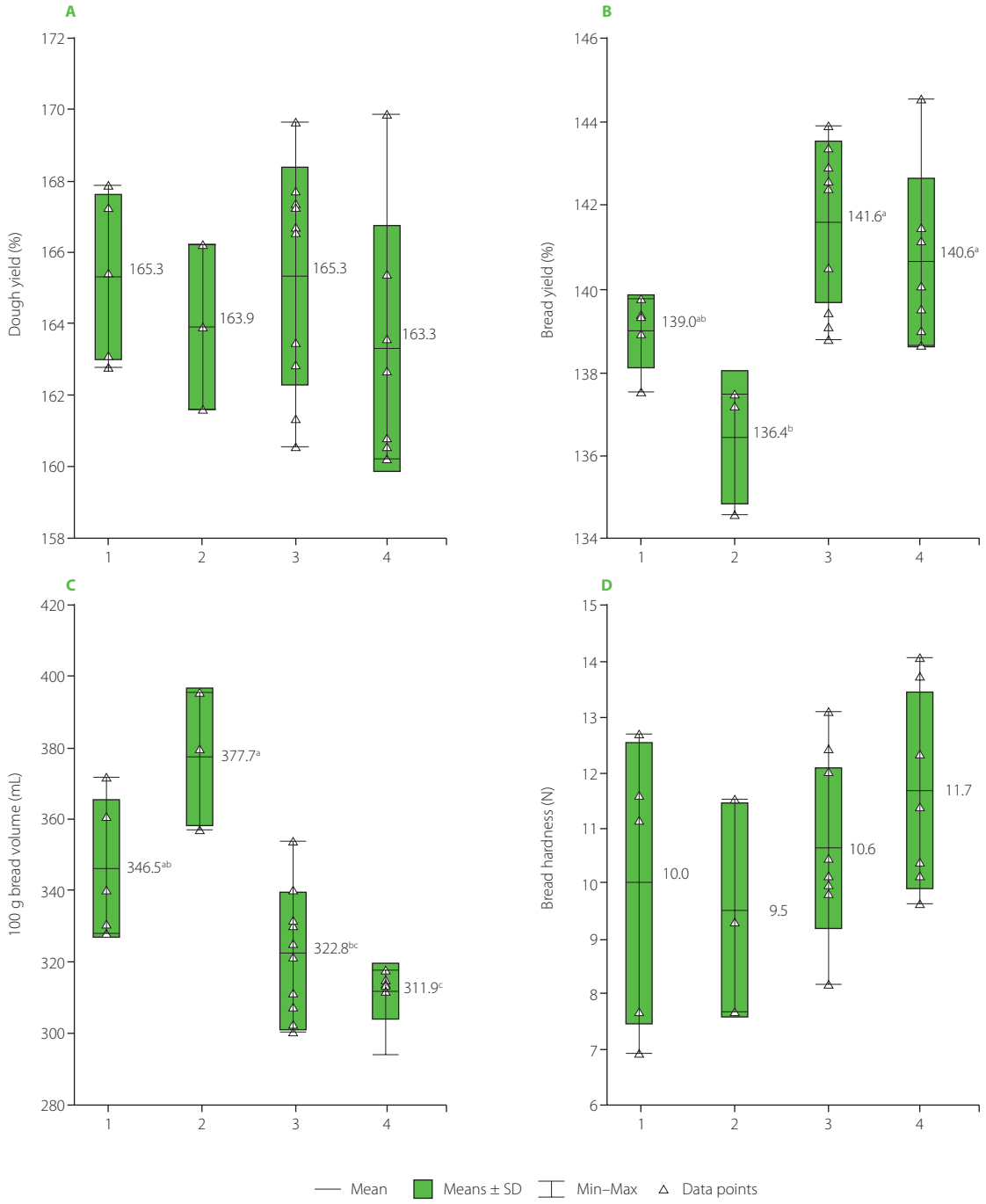

Figure 3. Dough yield (**A**), bread yield (**B**), 100 g bread volume (**C**), and bread crumb hardness (**D**) for for the hybrids and their parental lines: bread wheat, W (1), spelt, S (2), W×S hybrid lines (3), S×W hybrid lines (4).

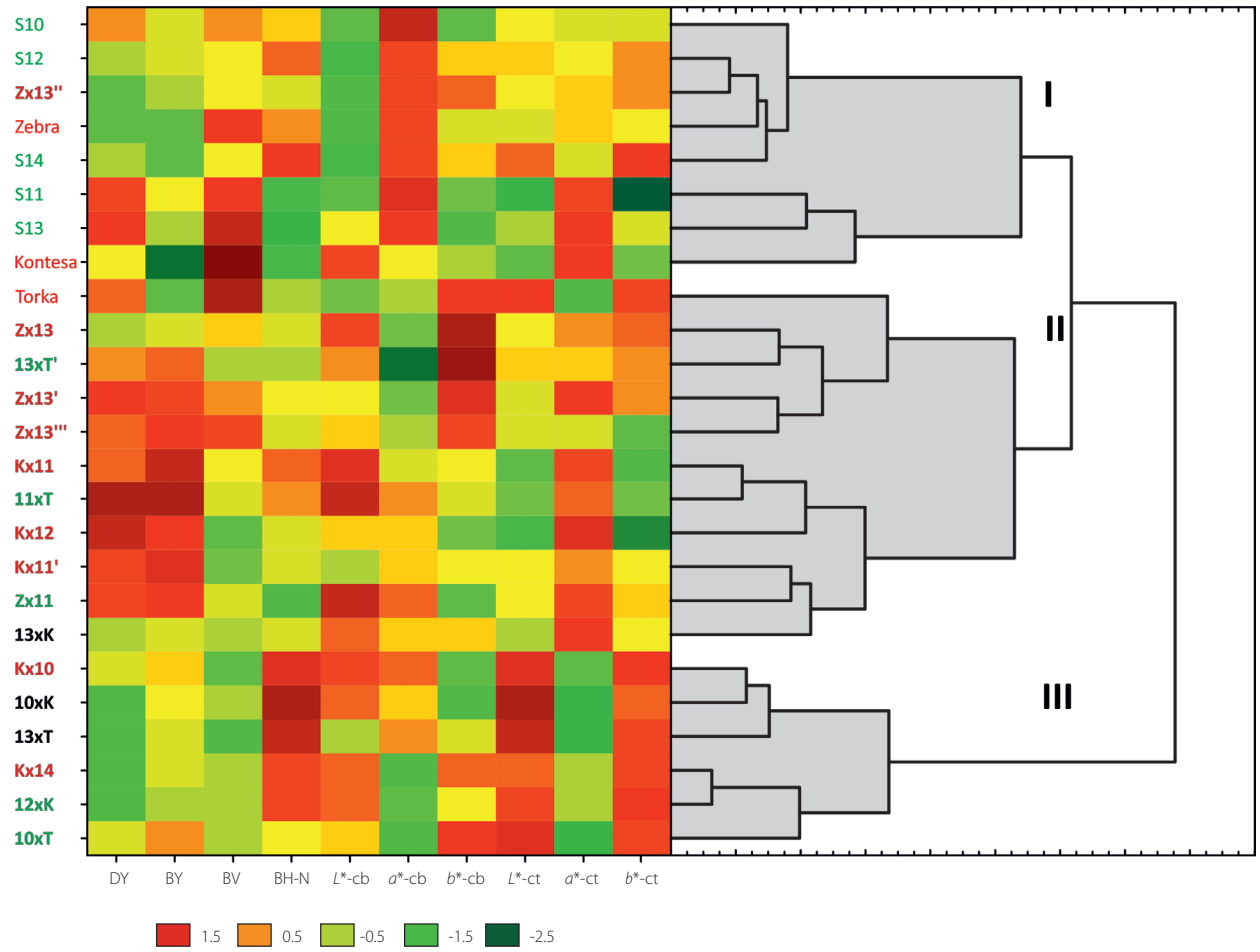

Figure 4. The results of the hierarchical cluster analysis of 10 bread parameters in 15 hybrid lines and their parental lines. DY, dough yield; BY, bread yield; BV, bread volume; BH-N, bread crumb hardness; *L**, *a**, *b**, color parameters of bread crumb (cb) and crust (ct): lightness (*L**), green-red coordinate (*a**), blue-yellow coordinate (*b**); I, II, III, cluster numbers.

loaves baked from spelt flour were characterized by the least desirable cross-sections. In contrast, loaves made from bread wheat flour were well-risen, had a visibly rounded top and desirable crumb structure. Bread loaves made from the flour of hybrid grain were more similar to the loaves baked from bread wheat flour than spelt flour, which suggests that bread wheat genes significantly improve the baking quality of spelt flour. However, there is no conclusive evidence to support the above claim. Some authors found that the rheological properties and baking quality of spelt flour were similar or higher in comparison with bread wheat flour [Rodríguez-Quijano, 2019; Sobczyk *et al.,* 2017], whereas other researchers reported contrary results [Frakolaki *et al.,* 2018]. These discrepancies could be attributed to differences in the experimental materials, environmental conditions, and farming systems. Similarly to bread wheat, spelt is a self-pollinating species that responds strongly to environmental variation. The flour of modern spelt cultivars harboring *T. aestivum* genes and designed for intensive cultivation is characterized by high baking quality [Wiwart *et al.,* 2017], and introgressive hybridization cannot be avoided in modern agriculture. Therefore, the proportion of *T. aestivum* genes can be expected to increase in newly bred *T. spelta* varieties. They are unlikely to attract the interest of organic farmers who have a preference for "true spelt", but the nutritional value of grain of modern spelt cultivars will surpass that of bread wheat grain.

The present study was undertaken to expand the existing knowledge about hybrids between bread wheat and spelt and to generate useful information for breeding purposes. In the studied hybrids, 50% of the genes were derived from each parent (*T. spelta* and *T. aestivum*), unlike in modern spelt cultivars intended for intensive farming, which harbor only a small proportion of bread wheat genes. The results clearly indicate that bread made from the flour of *T. spelta* × *T. aestivum* hybrids is characterized by superior attributes, compared with bread made from spelt flour. These hybrids represent a new category of crops with novel characteristics, in particular traits that are desirable from the agricultural point of view. The results of this study provide valuable inputs for expanding the biodiversity of agricultural phytocenoses, reducing pressure from pests and pathogens, and promoting sustainable cereal production.

CONCLUSIONS

The examination of 36 lines derived from single crosses between bread wheat and spelt indicates that gluten content was

significantly higher in the grain of hybrid lines than in bread wheat, and it did not differ significantly from that noted in spelt grain. The gluten index did not differ significantly between hybrid lines and bread wheat. Protein content was significantly higher in the flour obtained from hybrid lines than from bread wheat. Breads made from the grain of hybrids were characterized by high quality and superior attributes relative to breads made from spelt flour. The study demonstrated that hybrids between *T. spelta* and *T. aestivum* can become a new, valuable source of grain for bread production.

ACKNOWLEDGEMENTS

This research is the result of a long-term study carried out at the University of Warmia and Mazury in Olsztyn, Poland, Faculty of Agriculture and Forestry, Department of Genetics, Plant Breeding and Bioresource Engineering, topic number 30.610.007–110. The authors express their gratitude to A. Poprawska for language editing.

RESEARCH FUNDING

The study received no external funding.

CONFLICT OF INTERESTS

Authors declare no conflict of interest.

ORCID IDs

E. Suchowilska https://orcid.org/0000-0002-8999-6742
A. Szafrańska https://orcid.org/0000-0003-1038-7811
M. Wiwart https://orcid.org/0000-0003-2693-7021

SUPPLEMENTARY MATERIALS

The following are available online at http://journal.pan.olsztyn.pl/Grain-of-Hybrids-Between-Spelt-Triticum-spelta-L-and-Bread-Wheat-Triticum-aestivum,170870,0,2.html; Table S1. The values of flour parameters tested in the experiment. S10... S14, parental spelt lines; ^{I}, ^{II}, ^{III}, ^{IV},sister lines.

REFERENCES

1. Arzani, A., Ashraf, M. (2017). Cultivated ancient wheats (*Triticum* spp.): A potential source of health-beneficial food products. *Comprehensive Reviews in Food Science and Food Safety, 16*(3), 477-488. https://doi.org/10.1111/1541-4337.12262
2. Banu, I., Stoenescu, G., Ionescu, V., Aprodu, I. (2011). Estimation of the baking quality of wheat flours based on rheological parameters of the Mixolab curve. *Czech Journal of Food Sciences, 29*(1), 35-44. https://doi.org/10.17221/40/2009-CJFS
3. Biel, W., Jaroszewska, A., Stankowski, S., Sobolewska, M., Kępińska-Pacelik, J. (2021). Comparison of yield, chemical composition and farinograph properties of common and ancient wheat grains. *European Food Research and Technology, 247*, 1525-1538. https://doi.org/10.1007/s00217-021-03729-7
4. Bonafaccia, G., Galli, V., Francisci, R., Mair, V., Skrabanja, V., Kreft, I. (2000). Characteristics of spelt wheat products and nutritional value of spelt wheat-based bread. *Food Chemistry, 68*(4), 437-441. https://doi.org/10.1016/S0308-8146(99)00215-0
5. Boukid, F., Folloni, S., Sforza, S., Vittadini, E., Prandi, B. (2018). Current trends in ancient grains-based foodstuffs: insights into nutritional aspects and technological applications. *Comprehensive Reviews in Food Science and Food Safety, 17*(1), 123–136. https://doi.org/10.1111/1541-4337.12315
6. Carson, G.R., Edwards, N.M. (2009). Chapter 4 – Criteria of wheat and flour quality. In: K. Khan, P.R. Shewry (Eds.). *Wheat Chemistry and Technology, 4th edition*, AACC International Inc., pp. 97-118. https://doi.org/10.1094/9781891127557.004
7. Ceglińska, A. (2003). Technological value of spelt and common wheat hybrid. *Electronic Journal of Polish Agricultural Universities, 6*(1), art. no. 02.
8. Chrpová, J., Grausgruber, H., Weyermann, V., Buerstmayr, M., Palicová, J., Kozová, J., Trávníčková, M., Nguyen, Q.T., Amores, J.E.M., Buerstmayr, H., Janovská, D. (2021). Resistance of winter spelt wheat [*Triticum aestivum* subsp. *spelta* (L.) Thell.] to *Fusarium* head blight. *Frontiers in Plant Science, 12*, art. no. 661484. https://doi.org/10.3389/fpls.2021.661484
9. Dąbkowska, E. (2009). Wpływ odmiany ziarna orkiszu uzyskanego w warunkach produkcji ekologicznej na jakość mąki. Rozprawa doktorska. [The effect of spelt grain variety obtained under organic production conditions on flour quality. Doctoral thesis]. UWM w Olsztynie, Wydział Nauk o Żywności. Olsztyn. (doctoral thesis, in Polish). https://www.wbc.poznan.pl/Content/153050/PDF/Dabkowska_Ewa-rozprawa_doktorska.pdf (accessed: 29 May 2023).
10. Dinkel (2023). https://www.gzpk.ch/kulturen/dinkel/ (accessed: 29 May 2023)
11. Dinu, M., Whittaker, A., Pagliai, G., Benedettelli, S., Sofi, F. (2018). Ancient wheat species and human health: Biochemical and clinical implications. *The Journal of Nutritional Biochemistry, 52*, 1-9. https://doi.org/10.1016/j.jnutbio.2017.09.001
12. Diordiieva, I., Riabovol, L., Riabovol, I., Serzhyk, O., Novak, A., Kotsiuba, S. (2018). The characteristics of wheat collection samples created by *Triticum aestivum* L./*Triticum spelta* L. hybridisation. *Agronomy Research, 16*, 2005-2015.
13. Dubat, A., Bock, J. (2018). The Mixolab Profiler Good practices in the milling and baking industries and mistakes to avoid. A white paper. Chopin Technologies 2018, p. 35.
14. Dvorak, J., Deal, K.R., Luo, M.C., You, F.M., von Borstel, K., Dehghani, H. (2012). The origin of spelt and free-threshing hexaploid wheat. *Journal of Heredity, 103*(3), 426–441. https://doi.org/10.1093/jhered/esr152
15. Dziki, D., Cacak-Pietrzak, G., Gawlik-Dziki, U., Świeca, M., Miś, A., Różyło, R., Jończyk, K. (2017). Physicochemical properties and milling characteristics of spring wheat from different farming systems. *Journal of Agricultural Science and Technology, 19*, 1253-1266.
16. Fan, M.-S., Zhao, F.-J., Fairweather-Tait, S.J., Poulton, P.R., Dunham, S.J., McGrath, S.P. (2008). Evidence of decreasing mineral density in wheat grain over the last 160 years. *Journal of Trace Elements in Medicine and Biology, 22*(4), 315-324. https://doi.org/10.1016/j.jtemb.2008.07.002
17. Frakolaki, G., Giannou, V., Topakas, E., Tzia, C. (2018). Chemical characterization and breadmaking potential of spelt *versus* wheat flour. *Journal of Cereal Science, 79*, 50-56. https://doi.org/10.1016/j.jcs.2017.08.023
18. Gacek, E. (2013). Polish National List of Agricultural Varieties; Research Center for Cultivar Testing: Słupia Wielka, Poland.
19. Geisslitz, S., Longin, C.F.H., Scherf, K.A., Koehler, P. (2019). Comparative study on gluten protein composition of ancient (einkorn, emmer and spelt) and modern wheat species (durum and common wheat). *Foods, 8*(9), art. no. 409. https://doi.org/10.3390/foods8090409
20. Gulyás, G., Rakszegi, M., Bognár, Z., Láng, L., Bedõ, Z. (2012). Evaluation of genetic diversity of spelt breeding materials based on AFLP and quality analyses. *Cereal Research Communications, 40*(2), 185–193. https://doi.org/10.1556/CRC.40.2012.2.2
21. Haros, M., Ferrer, A., Rosell, C. (2006). Rheological behavior of whole wheat flour. 2006. *UFoST 13th World Congress of Food Sciences Technology, Nantes, France*, 1139-1148. https://doi.org/10.1051/IUFoST:20060681
22. ISO 17715:2013. Flour from wheat (*Triticum aestivum* L.) — Amperometric method for starch damage measurement.
23. ISO 20483:2013. Cereals and pulses — Determination of the nitrogen content and calculation of the crude protein content — Kjeldahl method.
24. ISO 21415-2:2015. Wheat and wheat flour — Gluten content — Part 2: Determination of wet gluten and gluten index by mechanical means.
25. ISO 2171:2007. Cereals, pulses and by-products — Determination of ash yield by incineration.
26. ISO 3093:2009. Wheat, rye and their flours, durum wheat and durum wheat semolina — Determination of the falling number according to Hagberg-Perten.
27. ISO 520:2010. Cereals and pulses — Determination of the mass of 1,000 grains.
28. ISO 5529:2007. Wheat — Determination of the sedimentation index — Zeleny test.
29. ISO 712:2009. Cereals and cereal products — Determination of moisture content — Reference method.
30. ISO 7971-3:2019. Cereals — Determination of bulk density, called mass per hectolitre — Part 3: Routine method.

31. Jukić, M., Koceva Komlenić, D., Mastanjević, K., Mastanjević, K., Lučan, M., Popovici, C., Nakov, G., Lukinac, J. (2019). Influence of damage starch on the quality parameters of wheat dough and bread. *Ukrainian Food Journal, 8*(3), 512-521. https://doi.org/10.24263/2304-974X-2019-8-3-8
32. Kahraman, K., Sakryan, O., Ozturk, S., Koksel, H., Summu, G., Dubat, A. (2008). Utilization of Mixolab® to predict the suitability of flours in terms of cake quality. *European Food Research and Technology, 227*, 565-570. https://doi.org/10.1007/s00217-007-0757-y
33. Kaushik, R., Kumar, N., Kumar, Sihag, M., Ray, A. (2015). Isolation, characterization of wheat gluten and its regeneration properties. *Journal of Food Science and Technology, 52*, 5930-5937. https://doi.org/10.1007/s13197-014-1690-2
34. Krawczyk, P., Ceglińska, A., Kardialik, J. (2008). Porównanie wartości technologicznej ziarna orkiszu z pszenicą zwyczajną. [Comparing the technological value of spelt grains to common wheat grains]. Żywność. *Nauka. Technologia. Jakość, 5*(60), 43-51 (in Polish; English abstract and tables).
35. León, A.E., Barrera, G.N., Pérez, G.T., Ribotta, P.D., Rosell, C.M. (2006). Effect of damaged starch levels on flour-thermal behaviour and bread staling. *European Food Research and Technology, 224*, 187-192. https://doi.org/10.1007/s00217-006-0297-x
36. Litvyak, V. (2018). Size and morphological features of native starch granules of different botanical origin. *Ukrainian Food Journal, 7*(4), 563–576. https://doi.org/10.24263/2304-974X-2018-7-4-3
37. Liu, X., Li, E., Jiang, Y., Tian, Y. (2018). Milling process of starch. In: Z. Sui, X. Kong (Eds.), *Physical Modification of Starch.* Springer Nature Singapore Pte Ltd, pp. 155-174. https://doi.org/10.1007/978-981-13-0725-6_9
38. Mixolab Applications Handbook. Rheological and enzyme analyses. Analysis methods. Studies and applications. (2012). Chopin Technologies, France. http://concereal.net/wp-content/uploads/2017/03/2012-CHOPIN-Mixolab-Applications-Handbook-EN-SPAIN-3.pdf (accessed: 29 May, 2023)
39. Packa, D., Wiwart, M., Suchowilska, E., Bieńkowska, T. (2015). Morpho-anatomical traits of two lowest internodes related to lodging resistance in selected genotypes of Triticum. *International Agrophysics, 29*, 475-483. https://doi.org/10.1515/intag-2015-0053
40. Packa, D., Załuski, D., Graban, Ł., Lajszner, W. (2019). An evaluation of spelt crosses for breeding new varieties of spring spelt. *Agronomy, 9*(4), art. no. 167. https://doi.org/10.3390/agronomy9040167
41. PN-A-74105:1992. Pieczywo pszenne zwykłe i wyborowe (Wheat baked goods) (in Polish).
42. Rachoń, L., Bobryk-Mamczarz, A., Kiełtyka-Dadasiewicz, A., (2020). Hulled wheat productivity and quality in modern agriculture against conventional wheat species. *Agriculture, 10*(7), art. no. 275. https://doi.org/10.3390/agriculture10070275
43. Rapp, M., Beck, H., Gütler, H., Heilig, W., Starck, N., Römer, P., Cuendet, C., Uhlig, F., Kurz, H., Würschum, T., Longin, C.F.H. (2017). Spelt: Agronomy, quality, and flavor of its breads from 30 varieties tested across multiple environments. *Crop Science, 57*(2), 739-747. https://doi.org/10.2135/cropsci2016.05.0331
44. Rodríguez-Quijano, M., Vargas-Kostiuk, M.-E., Ribeiro, M., Callejo, M.J. (2019). *Triticum aestivum* ssp. *vulgare* and ssp. *spelta* cultivars. 1. Functional evaluation. *European Food Research and Technology, 245*, 1561-1570. https://doi.org/10.1007/s00217-019-03263-7
45. Różyło, R., Dziki, D., Gawlik-Dziki, U., Cacak-Pietrzak, G., Miś, A., Rudy, S. (2015). Physical properties of gluten-free bread caused by water addition. *International Agrophysics, 29*, 353-364. https://doi.org/10.1515/intag-2015-0042
46. Sapirstein, H., Wu, Y., Koksel, F., Graf, R. (2018). A study of factors influencing the water absorption capacity of Canadian hard red winter wheat flour. *Journal of Cereal Science, 81*, 52-59. https://doi.org/10.1016/j.jcs.2018.01.012
47. Sen, M., Li, L., Wang, X., Zheng, X., Bian, K., Bao, Q. (2016). Effect of mechanically damaged starch from wheat flour on the quality of frozen dough and steamed bread. *Food Chemistry, 202*, 120-124. https://doi.org/10.1016/j.foodchem.2016.01.075
48. Shewry, P.R. (2018). Do ancient types of wheat have health benefits compared with modern bread wheat? *Journal of Cereal Science, 79*, 469-476. https://doi.org/10.1016/j.jcs.2017.11.010
49. Shewry, P.R., Hassall, K.L., Grausgruber, H., Andersson, A.A.M, Lampi, A.-M., Piironen, V., Rakszegi, M., Ward, J.L., Lovegrove, A. (2020). Do modern types of wheat have lower quality for human health? *Nutrition Bulletin, 45*(4), 362-373. https://doi.org/10.1111/nbu.12461
50. Shewry, P.R., Hey, S. (2015). Do "ancient" wheat species differ from modern bread wheat in their contents of bioactive components? *Journal of Cereal Science, 65*, 236-243. https://doi.org/10.1016/j.jcs.2015.07.014
51. Sobczyk, A., Pycia, K., Stankowski, S., Jaworska, G., Kuźniar, P. (2017). Evaluation of the rheological properties of dough and quality of bread made with the flour obtained from old cultivars and modern breeding lines of spelt *(Triticum aestivum* ssp. *spelta*). *Journal of Cereal Science, 77*, 35-41. https://doi.org/10.1016/j.jcs.2017.07.013
52. Suchowilska, E., Szafrańska, A., Słowik, E., Wiwart, M. (2019). Flour from *Triticum polonicum* L. as a potential ingredient in bread production. *Cereal Chemistry, 96*(3), 554-563. https://doi.org/10.1002/cche.10155
53. Suchowilska, E., Wiwart, M., Kandler, W., Krska, R. (2012). A comparison of macro- and microelement concentrations in the whole grain of four *Triticum* species. *Plant, Soil and Environment, 58*, 141-147. https://doi.org/10.17221/688/2011-PSE
54. Sugár, E., Fodor, N., Sándor, R., Bónis, P., Vida, G., Árendás, T. (2019). Spelt wheat: an alternative for sustainable plant production at low n-levels. *Sustainability*, *11*(23), art. no. 6726. https://doi.org/10.3390/su11236726
55. Szafrańska, A., Rachoń, L., Szumiło, G. (2015). Estimation of protein-starch complex of selected wheat species depending on production technology intensity. *Zeszyty Problemowe Postępów Nauk Rolniczych, 582*, 81-90. https://docplayer.pl/53486226-Estimation-of-protein-starch-complex-of-selected-wheat-species-depending-on-production-technology-intensity.html (accessed: 13 Mar, 2023).
56. Takač, V., Tóth, V., Rakszegi, M., Mikić, S., Mirosavljević, M., Kondić-Špika, A. (2021). Differences in processing quality traits, protein content and composition between spelt and bread wheat genotypes grown under conventional and organic production. *Foods, 10*(1), art. no. 156. https://doi.org/10.3390/foods10010156
57. TIBCO Software Inc. (2017). Statistica (data analysis software system), version 13.
58. Tóth, V., Láng, L., Vida, G., Mikó, P., Rakszegi, M. (2022). Characterization of the protein and carbohydrate related quality traits of a large set of spelt wheat genotypes. *Foods, 11*(14), art. no. 2061. https://doi.org/10.3390/foods11142061
59. Tran, K.D., Konvalina, P., Capouchova, I., Janovska, D., Lacko-Bartosova, M., Kopecky, M., Tran, P.X.T. (2020). Comparative study on protein quality and rheological behavior of different wheat species. *Agronomy, 10*(11), art. no. 1763. https://doi.org/10.3390/agronomy10111763
60. Valli, V., Taccari, A., Di Nunzio, M., Danesi, F., Bordoni, A. (2018). Health benefits of ancient grains. Comparison among bread made with ancient, heritage and modern grain flours in human cultured cells. *Food Research International, 107*, 206-215. https://doi.org/10.1016/j.foodres.2018.02.032
61. Wang, J., Chatzidimitriou, E., Wood, L., Hasanalieva, G., Markellou, E., Iverseng, P.O., Seala, C., Baranski, M., Vigar, V., Ernst, L., Willson, A., Thapa, M., Barkla, B.J., Leifert, C., Rempelos, L. (2020). Effect of wheat species (*Triticum aestivum* vs *T. spelta*), farming system (organic vs conventional) and flour type (wholegrain vs white) on composition of wheat flour – Results of a retail survey in the UK and Germany – 2. Antioxidant activity, and phenolic and mineral content. *Food Chemistry: X, 6,* art. no. 100091. https://doi.org/10.1016/j.fochx.2020.100091
62. Wilson, J.D., Bechtel, D.B., Wilson, G.W.T., Seib, P.A. (2008). Bread quality of spelt wheat and its starch. *Cereal Chemistry, 85*(5), 629-638. https://doi.org/10.1094/CCHEM-85-5-0629
63. Winterspelz, Winterdinkel: Sorte Divimar. (2023). https://www.proplanta.de/Pflanzenbauberater/Sorten/Divimar-Winterspelz-Winterdinkel_sks_2610SPW1.html (accessed: 29 May, 2023).
64. Witzenberger, A.H., Hack, H., van den Boom, T. (1989). Erläuterungen zum BBCH-Dezimal-Code für die Entwicklungsstadien des Getreides—mit Abbildungen. *Gesunde Pflanzen, 41*, 384–388 (in German).
65. Wiwart, M., Szafrańska, A., Wachowska, U., Suchowilska, E. (2017). Quality parameters and rheological dough properties of 15 spelt (*Triticum spelta* L.) varieties cultivated today. *Cereal Chemistry, 94*(6), 1037-1044. https://doi.org/10.1094/CCHEM-05-17-0097-R
66. Zhygunov, D., Barkovska, Y., Yehorshyn, Y., Zhyhunova, H., Barikian, K. (2020). Type 600 wheat-spelt flour with improved bakery properties. *Food Science and Technology, 14*(1), 53-62. https://doi.org/10.15673/fst.v14i1.1646

ORIGINAL ARTICLE
http://journal.pan.olsztyn.pl

Polish Journal of Food and Nutrition Sciences
2023, Vol. 73, No. 3, 278–288
DOI: 10.31883/pjfns/170815
ISSN 1230-0322, e-ISSN 2083-6007

Effect of Extrusion on the Functional Properties and Bioactive Compounds of Tamarind (*Tamarindus indica* L.) Shell

Dalia S. Aguilar-Ávila[1,2], Héctor E. Martínez-Flores[3]*, Eduardo Morales-Sánchez[4], Rosalía Reynoso-Camacho[5], Ma. Guadalupe Garnica-Romo[6]

[1]Programa Institucional de Maestría en Ciencias Biológicas, Universidad Michoacana de San Nicolás de Hidalgo, Avenida Francisco J. Múgica S/N, Ciudad Universitaria, C.P. 58030, Morelia, Mich., México
[2]Laboratorio de Investigación y Desarrollo Farmacéutico (LIDF) and Laboratorio de Ingeniería y Biotecnología de los Alimentos (LIBA), Centro Universitario de Ciencias Exactas e Ingenierías (CUCEI), Universidad de Guadalajara, Blvd. Gral. Marcelino García Barragán 1421, Olímpica, C.P. 44430 Guadalajara, Jal., México
[3]Facultad de Químico Farmacobiología, Universidad Michoacana de San Nicolás de Hidalgo, Tzintzuntzan 173. Col. Matamoros, C.P. 58240, Morelia, Mich., México
[4]Instituto Politécnico Nacional, Centro de Investigación en Ciencia Aplicada y Tecnología Avanzada, Cerro Blanco 141, Colinas del Cimatario, CP 76090, Santiago de Querétaro, Qro., México
[5]Facultad de Química, Universidad Autónoma de Querétaro, C.U. Cerro de las Campanas, C.P. 76010, Santiago de Querétaro, Qro, México
[6]Facultad de Ingeniería Civil, Universidad Michoacana de San Nicolás de Hidalgo, Santiago Tapia 403, Col. Centro, CP 58000, Morelia, Mich., México

The food-use of the tamarind (*Tamarindus indica* L.) fruit produces shell and seeds as by-products. In this work, the effects of the tamarind shell moisture content and the temperature of their extrusion on the dietary fiber content and physiochemical properties, such as water absorption capacity (WAC), oil absorption capacity (OAC), and glucose dialysis retardation index (GDRI) of the extrudates, were estimated. Moreover, the effects of the extrusion variables on the total phenolic and total flavonoid contents and on the antioxidant capacity of the tamarind shell were evaluated. The dry powdered tamarind shell was conditioned to have 32 or 39 g of water *per* 100 g of shell, prior to being subjected to extrusion. Subsequently, the conditioned samples were processed at 90°C, 100°C and 110°C in a single screw extruder. A non-extruded tamarind shell was taken as a control. The extrusion resulted in a 138.3% increase in the soluble dietary fiber content, along with 40.3% and 18.4% reductions of total phenolic and total flavonoid contents, respectively. The antioxidant capacity of the tamarind shell with moisture content of 32 g/100 g extruded at 100°C and 110°C was similar to that of non-extruded material. Moreover, the extruded products had the higher OAC compared to that of the control and they displayed an excellent response with regard to controlling the GDRI. The extrusion advantageously modified properties of the tamarind shell particularly when material with a moisture content of 32 g/100 g at 100°C was processed.

Key words: thermomechanical treatment, tamarind shell, dietary fiber, phenolic compounds, antioxidant capacity

ABBREVIATIONS

ABTS$^{\bullet+}$, radical cation of 2,2'-azino-bis(3-ethylbenzothiazoline-6-sulfonic acid); ANOVA, analysis of variance; DPPH$^{\bullet}$, 2,2-diphenyl-1-picrylhydrazyl radical; FTIR, Fourier transform infrared spectroscopy; GAE, gallic acid equivalents; GDRI, glucose dialysis retard index; IDF, insoluble dietary fiber; OAC, oil absorption capacity; SEM, scanning electron microscopy; RE, rutin equivalents; SDF, soluble dietary fiber; TDF, total dietary fiber; WAC, water absorption capacity.

***Corresponding Author:**
e-mail: hector.martinez.flores@umich.mx (H. Martinez-Flores)

Submitted: 2 April 2023
Accepted: 4 August 2023
Published on-line: 31 August 2023

INTRODUCTION

The agro-industrial by-products generated during the processing of fruits and vegetables are potential sources of bioactive compounds, such as carotenoids, phytosterols, phenolics, and dietary fiber [Lemes *et al.,* 2022; Reguengo *et al.,* 2022]. In this context, some authors have focused their attention on the study of by-products obtained from fruits and vegetables as sources of dietary fiber (DF) [Garcia-Amezquita *et al.,* 2018]. According to Gan *et al*. [2021], the ultimate purpose is to apply the DF in the functional food industry. Specifically, DF is associated with the reduced risks of coronary heart disease, type-2 diabetes, inflammatory bowel disease, constipation, and colon cancer [Gustafson & Rose, 2022; Martínez-Flores *et al.,* 2009; Yusuf *et al.,* 2022]; these beneficial physiological effects of DF are directly related to its physicochemical and technological properties, such as water retention capacity, swelling capacity, viscosity, and the ability to bind bile salts and organic molecules such as glucose and lipids [Elleuch *et al.,* 2011; Larrea *et al.,* 2010]. Phenolics, other phytochemicals present in fruits and vegetables, are antioxidants that delay or inhibit the oxidation of molecules in the human body and, therefore, reduce the risk of oxidative stress and diseases such as cancer, diabetes, and cardiovascular disease [Kumar & Goel, 2019].

Relevant to this study, the tamarind plant (*Tamarindus indica* L.) is a multipurpose tree whose roots, wood, leaves, fruits, seeds, and pod shells are used to make food items, drugs, herbal medicine, fuel, timber, fodder, and textile industry products [Chimsah *et al.,* 2020; De Caluwé *et al.,* 2010]. Upon the separation of the tamarind fruit, the residues – constituted by the seed and the shell – that remain are considered as its by-products. The tamarind shell is used as a biosorbent to remove chemical substances, such as malachite green [Saha *et al.,* 2010], and to produce briquettes [Ujjinappa *et al.,* 2018] and tannins, the latter being used as potential green rust converter [Abdulmajid *et al.,* 2019]. Another potential use of the tamarind shell entails the modification of its properties, particularly by modification of its DF, to obtain new functional characteristics [Gan *et al*., 2019]. Some investigations have focused on the functional and physicochemical changes of the DF generated by the extrusion process [Benítez *et al*., 2023; Huang *et al*., 2019; Zhang *et al*., 2011; Zhong *et al*., 2019]. The tamarind shell is characterized by the presence of mostly insoluble dietary fiber (IDF) and very little soluble dietary fiber (SDF). Thus, a thermomechanical modification by extrusion, that converts IDF to SDF, could be a viable alternative for obtaining a product designed for application purposes in the food industry [Menis-Henrique *et al.,* 2020]. Barak & Mudgil [2014], mentioned that soluble fiber, such as locust gum bean, was used as a thickener, stabilizer and gelling agent in various food products, such as baked foods, beverages, dairy products, and processed fruit products. Increasing the amount of soluble fiber in a sample, could be useful in products that require greater water absorption capacity, for example, in preventing syneresis in products such as yogurt [Mudgil, 2018].

Unfortunately, there is a lack of research addressing the application of the extrusion technology to the tamarind shell. Therefore, the objective of this study was to apply the extrusion process to modify some physicochemical properties of the tamarind shell without affecting bioactive compounds such as phenolics, as well as their antioxidant capacity.

MATERIALS AND METHODS

Raw material

Ten kilograms of tamarind shells meant for extrusion were obtained from the company La Estrella® located in the city of Morelia, Michoacán, Mexico. Tamarind shells were oven-dried at 40°C (FE-292 oven, Felisa®, Zapopan, Jalisco Mexico) for 48 h and crushed in a Pulvex model 200 mill (Molinos Pulvex, S.A. de C.V., México city, Mexico) using a mesh of 800 µm. The tamarind shell samples were blended with water for 10 min using a mixer (Kitchen Aid model K45SS, St. Joseph, MI, USA) until reaching a moisture content of 32 g/100 g and 39 g/100 g. Samples were placed at 4°C, in Ziploc® hermetic bags (SC Johnson and Son Inc., Racine, WI, USA) for 12 h until they were processed by extrusion.

Extrusion of tamarind shells

The crushed tamarind shells with moisture content of 32 g/100 g or 39 g/100 g were extruded using and extruder designed and built in the Mechatronics Laboratory of the Center for Research in Applied Science and Advanced Technology, National Polytechnic Institute (CICATA-IPN), Querétaro, Mexico. It consisted of a single screw with a ratio of length to diameter of 21, a channel length of 18 mm, and a channel depth of 3 mm. The output die was a metal plate with a 6 mm diameter hole. The extruder had two heating zones: zone one was maintained at a constant temperature of 60°C and zone two was set at temperatures of 90°C, 100°C and 110°C, respectively, according to previously established conditions. Additionally, the extruder allowed speed control by means of a Baldor VS1 inverter at 15 RPM. A complete factorial design was used, with two factors: temperature and moisture content, the first with three levels (90°C, 100°C and 110°C) and the second with two levels (32 g/100 g and 39 g/100 g), with a total of six treatments. An amount of 250 g of sample was used in each treatment, with two repetitions *per* treatment. The extrudates were stored at 4°C in sealed bags until analysis. The non-extruded tamarind was taken as a control.

Proximate and dietary fiber composition analyses

Chemical analyses were performed on the non-extruded sample and the extrudates, *i.e.*, tamarind shells with different moisture contents extruded under different temperatures. The proximate composition of the non-extruded samples was determined by the American Association of Cereal Chemists (AACC) methods [AACC, 2000], for contents of moisture (AACC method 44-19), ash (AACC method 08-01), crude protein (AACC method 46-13), and fat (AACC method 30-25). The soluble, insoluble, and total dietary fiber contents in tamarind shell and extrudates were determined by the method of Prosky *et al.* [1988]. The pectin level in tamarind shells was quantified using the method recommended by Carré & Haynes [1922]. Briefly, 5 g of sample was added to

100 mL of distilled water, the blend was boiled three times, filtered, and in each filtrate the volume was recovered by adding 100 mL of water, having a final volume of 400 mL. An amount of 100 mL of 0.1 M sodium hydroxide were added to the filtrate, which was left to stand for 12 h. Subsequently, 50 mL of 1 M acetic acid were added, and the mixture was allowed to settle for 5 min to finally add 50 mL of 1 M calcium chloride and allowing the mixture to settle again for 1 h; after which it was boiled for 5 min and filtered. After the residue was washed with 500 mL of hot distilled water to remove chlorine, the obtained precipitate was redissolved in 100 mL of distilled water at 25°C and boiled for 5 min. Finally, it was filtered on open-pore filter paper previously set to constant weight, the paper with the residue was washed and dried until constant weight. The pectin content was expressed in g *per* 100 g of dry matter (DM) of tamarind shell.

Extractable-free samples were obtained to determine lignin, cellulose and hemicellulose contents. Briefly, 5 g of the non-extruded and extruded dried tamarind shells were placed in cellulose cartridges in the Soxhlet equipment, 150 mL of cyclohexane were added to a balloon flask and refluxed for 6 h of extraction. After, the equipment was allowed to cool, it was disassembled and the cartridges were left to air overnight. The same procedure was carried out with acetone, methanol, and water. Finally, the sample was spread on a filter paper to dry at room temperature overnight.

The lignin content was estimated according to the Runkel & Wilke [1951 method. Briefly, 2 g of extractable-free samples from non-extruded tamarind shells or extrudates were weighed and placed in a 200 mL Erlenmeyer flask; then, 50 mL of 72% sulfuric acid, 5 mL of 49% hydrobromic acid were added and left to settle for 2 h in an extraction hood. After this time, 200 mL of cold distilled water were added to stop the reaction, and the mixture was boiled for 5 min, filtered and rinsed with hot water until a neutral pH. The sediment with lignin was left to dry on a glass Petri dish in an oven at 105°C for 6 h, tempered and weighed. The lignin content (g/100 g DM) was calculated on the basis of the mass balance.

Before cellulose determination, extractable-free samples from non-extrude material and extrudates were delignified by the method of Wise *et al*. [1946]. Five g of extractable-free samples were placed in a 200 mL Erlenmeyer flask, to which 1.5 g of sodium chlorite, 160 mL of distilled water and 10 drops of acetic acid were added. The flask was covered with aluminum foil and placed in a water bath at 75°C for 1 h. After this time 1.5 g of sodium chlorite and 10 drops of acetic acid were added again. This procedure was repeated two more times until 4 h of digestion was completed. Upon completion, the reaction was stopped by placing the flask in an ice bath and when it cooled, it was filtered and washed with cold water and acetone, dried in an oven at 40°C for three days, and weighed. The cellulose content was determined according to the American National Standards Institute (ANSI) standard method D1103-60 [ANSI/ASTM, 1977]. To this end, 2 g of holocellulose extracted from non-extruded and extrudates samples were added with 10 mL of 17.5% sodium hydroxide at room temperature. The mixture was left to stand for 5 min and another 5 mL of NaOH were added, and the mixture was again left to stand for 5 min. The procedure was repeated once more to finally let it rest for 30 min. Then, 33 mL of distilled water were added at room temperature, and the sample was left to rest for 1 h. After filtration in a Gooch crucible, sediment with cellulose was washed with 35 mL of 8.3% NaOH solution distilled water and 10% acetic acid, allowed to stand for 3 min, dried in an oven overnight at 105°C, and weighed. The results were expressed as g of cellulose *per* 100 g of DM of tamarind shell or extrudate.

The hemicellulose content was obtained by difference, by subtracting the holocellulose content minus the cellulose content, and was expressed as a g of hemicellulose per 100 g of DM of tamarind shell or extrudate.

Glucose dialysis retardation index determination

The glucose dialysis retardation index (GDRI) was determined according to the method described by Adiotomre *et al*. [1990] with some modifications. Ten milliliters of a 50 mM (900 mg/dL) glucose solution containing 0.2 g of each sample were taken, these were placed in dialysis cellulose bags 11 cm long. Each sample was previously hydrated in the glucose solution for 45 min. Each bag was closed and suspended in 100 mL of distilled water and then placed in a constantly shaking bath at 37°C for 4 h. A 2 mL aliquot was taken to measure its glucose concentration by means of the glucose oxidase method with a Randox (Crumlin, County Antrim, UK) brand kit at a time of 0, 10, 20, 30, 60, 120, 150, 180, 210 and 240 min. GDRI of non-extruded tamarind shell and its extrudates was calculated according to Liu *et al*. [2018] using the formula (1):

$$\text{GDRI (\%)} = \left(1 - \frac{\text{Tamarind shells GC}}{\text{Control GC}}\right) \times 100 \quad (1)$$

where: GC, glucose content.

Determination of water and oil absorption capacities

The water absorption capacity (WAC) and oil absorption capacity (OAC) were determined according to the methodology proposed by Anderson *et al.* [1969]. To WAC determination, 1 g of non-extruded tamarind shell and extrudates samples were weighed in a Falcon tube, and 10 mL of distilled water was added. They were left to rest for 30 min, shaking every 30 s. Subsequently, suspensions were centrifuged at 670×*g* for 10 min (Z 400 K centrifuge, Hermle AG, Gosheim, Germany). The supernatant was discarded, and the solid residue was weighed. The amount of water absorbed was calculated by measurement of difference in the weights of the samples before and after centrifugation. The results were expressed in terms of DM of tamarind shell and extrudates. The same procedure was used with the replacement of distilled water with soybean oil to determine OAC.

Extraction of bioactive compounds

An aliquot of 10 mL of methanol was added to 1 g of each non-extruded an extrudates samples, and then the samples, protected from light, were stirred for 24 h. Subsequently, they

were centrifuged using a Hermle Z 400 K centrifuge at 2,680×*g* for 10 min. Thereafter, the extracts were kept at 4°C until they were used to determine the total phenolic content, total flavonoid content, and antioxidant capacity.

Total phenolic content determination

Total phenolic content of non-extruded tamarind shell and extrudates was determined using the Folin-Ciocalteu's reagent by the method of Singleton & Rossi [1965]. The absorbance was measured at 765 nm on a UV/Vis Smartec Plus spectrophotometer (Bio-Rad, Philadelphia, PA, USA). The results were expressed as mg of gallic acid equivalents *per* g of DM of non-extruded and extruded samples (mg GAE/g DM).

Total flavonoid content determination

Total flavonoid content of non-extruded tamarind shell and extrudates was determined using the method described by Oomah *et al.* [2005]. A total of 200 µL of the extract from the tamarind shell or extrudates were reacted with 80 µL of 2-aminoethyl diphenylborate and 720 µL of distilled water. The mixture was incubated for 30 min in the dark, and absorbance was read at 404 nm. Rutin was used as standard. The results were expressed as mg of rutin equivalents *per* g of DM of sample (mg RE/g DM).

Determination of DPPH$^{\bullet}$ scavenging capacity

The ability of tamarind shell and extrudates to scavenge the 2,2-diphenyl-1-picrylhydrazyl radical (DPPH$^{\bullet}$) was determined using the method described by Brand-Williams *et al.* [1995]. The DPPH$^{\bullet}$ was dissolved in methanol until an absorbance of 0.75–0.78 at 517 nm was obtained (using UV/Vis Smartec Plus spectrophotometer, Bio-Rad). Then, 50 µL of each extract was added to 2.95 mL of DPPH$^{\bullet}$ solution, mixtures were shaken and kept in a dark space at room temperature for 30 min. Thereafter, absorbance (A_e) was read at 517 nm. A blank sample containing methanol instead of extract was prepared, and its absorbance (A_b) was measured. The percentage of DPPH$^{\bullet}$ inhibition was calculated using the formula (2):

$$\text{DPPH}^{\bullet}\ \text{inhibition}\ (\%) = \frac{A_b - A_e}{A_b} \times 100 \qquad (2)$$

Determination of ABTS$^{\bullet+}$ scavenging capacity

The scavenging of the radical cation of 2,2′-azino-bis(3-ethylbenzothiazoline 6-sulfonic acid) (ABTS$^{\bullet+}$) by extracts was evaluated using the Re *et al.* [1999] method. This cation radical was formed after incubation of the ABTS (7 mM) with potassium persulfate (2.45 mM) at room temperature, under dark conditions, for 12 h. Once formed, it was diluted with ethanol until an absorbance value of 0.700±0.100 at 754 nm was obtained. The absorbance of ABTS$^{\bullet+}$ solution, reaction mixtures (A_e) and blank samples (A_b) was measured using UV/Vis Smartec Plus spectrophotometer (Bio-Rad). Reaction mixtures were obtained after reaction of 50 µL of extracts with 2.95 mL of ABTS$^{\bullet+}$ solution. A blank sample contained ethanol instead of extract. The percentage of ABTS$^{\bullet+}$ inhibition was calculated using the formula (3):

$$\text{ABTS}^{\bullet+}\ \text{inhibition}\ (\%) = \frac{A_b - A_e}{A_b} \times 100 \qquad (3)$$

Fourier transform infrared spectroscopy analysis

The non-extruded and extrudate samples were dried for 24 h at 60°C and Fourier transform infrared spectroscopy (FTIR) analysis was carried out using a Spectrum 400 FTIR spectrometer (Perkin-Elmer, Waltham, Massachusetts, USA). The analysis conditions were marked by 40 scan cycles and by 2 cm^{-1} resolution being measured in the range of wavenumbers of 500–4,000 cm^{-1}, using the transmittance mode.

Scanning electron microscopy analysis

The scanning electron microscope (SEM) images were only taken for the non-extruded tamarind shell and in extrudates that presented the best results of the chemical and physicochemical characterization, which corresponded to the treatment of tamarind shell with 32 g moisture/100 g at 100°C. Both samples were sieved with 60 mesh to obtain a uniform particle size of 250 µm, and were submitted to dehydration for 24 h at 60°C. Then, the samples were coated with copper and analyzed at 500× magnification using JMS-6400 scanning electron microscope with Bruker X FLASH 4010 SEM microanalysis detector (JEOL, Peabody, MA, USA).

Statistical analysis

All the chemical analyses were performed in triplicate and were later statistically processed with the JMP®6.0 software (Cary, NC, USA), using an analysis of variance (ANOVA) and a Tukey's test in order to compare the treatments and observe whether differences were statistically significant at $p<0.05$. Finally, the correlations between the response variables were evaluated with the Pearson correlation coefficient (r).

RESULTS AND DISCUSSION

Chemical composition of tamarind shell

The chemical composition of the raw tamarind shell is shown in Table 1. Evidently, the total dietary fiber (TDF) was the major component of the shell and it consisted of IDF (56.80 g/100 g DM) and SDF (1.20 g/100 g DM). In turn, the IDF portion was formed mainly by lignin (31.57 g/100 g DM) and cellulose (16.21 g/100 g DM) while the SDF was formed by pectin (0.93 g/100 g DM). The TDF content quantified in the tamarind shell was higher to that reported in commercial products such as Metamucil®, Fibra Kania®, Fibra Tarasca®, Nopalinaza Plus®, and Fibra Xotzil®, which reportedly contribute 52.72 g/100 g, 50.57 g/100 g, 33.60 g/100 g, 33.32 g/100 g, and 21.90 g/100 g of TDF, respectively [Martínez-Flores *et al.,* 2009]. Thereafter, the next-largest component in the tamarind shell was the nitrogen-free extract (35.24 g/100 g DM), followed by ash (3.60 g/100 g DM) and protein (2.43 g/100 g DM).

Effect of the extrusion on the dietary fiber composition of tamarind shell

The contents of the TDF, IDF and SDF of both the extruded and non-extruded tamarind shells are shown in Table 2.

TABLE 1. Chemical composition of the tamarind shell.

Component	Content (g/100 g DM)
Total dietary fiber (TDF)	58.00±0.69
Insoluble dietary fiber (IDF):	56.80±0.53
Lignin	31.57±0.38
Cellulose	16.21±0.03
Hemicellulose	9.00±0.34
Others	0.02
Soluble dietary fiber (SDF):	1.20±0.35
Pectin	0.93±0.1
Others	0.27
Ash	3.60±0.02
Protein	2.43±0.19
Fat	0.73±0.12
Free nitrogen extract [1]	35.24

[1]Obtained by the following formula: Free nitrogen extract=100–(TDF+ash+protein+fat). Values are presented as mean ± standard deviation. DM, dry matter.

The extruded samples exhibited increases, on average, by 9.3%, 6.9%, and 138.3% of the TDF, IDF, and SDF, respectively, in comparison with their respective levels in the non-extruded material. In a study done by Stojceska *et al.* [2010] using extrusion to obtain gluten-free products with fruit as a source of dietary fiber, extrusion significantly increased the total dietary fiber content in gluten-free products. This increase could be a result of the interaction between DF and phenolics (hydroxycinnamic acids, resveratrol, tannins, and flavonoids), which possibly formed insoluble complexes that were quantified as DF. According to Bader *et al.* [2019], extrusion modifies dietary fiber by applying high temperature, pressure, and shear force on food to break down glycosidic bond of insoluble polysaccharides and converts them into lower molecular weight soluble compounds. Arribas *et al.* [2017; 2019] mentioned that extrusion caused a considerable redistribution of insoluble dietary fiber to the soluble form and documented that increase in SDF could be attributable to the formation of other compounds, such as, polysaccharide--protein complex, which are measured as soluble fiber. Chen *et al.* [2018] indicated that the insoluble fiber of extruded powder may be converted into soluble oligosaccharide by extrusion. In our study, with moisture level of 32 g/100 g and temperatures of 90°C and 100°C, the greatest changes were recorded in the three DF portions of the tamarind shell (Table 2).

In general, lignin and cellulose contents in the extruded samples were higher, on average, by 12.5% and 29.9%, respectively, while hemicellulose content was lower, on average, by 58.0% than in the tamarind shell (Table 3). In particular, lignin content

TABLE 2. Content of total dietary fiber (TDF), insoluble dietary fiber (IDF), soluble dietary fiber (SDF), as well as water absorption capacity (WAC) and oil absorption capacity (OAC) of non-extruded tamarind shell (control) and its extrudates.

Treatment	TDF (g/100 g DM)	IDF (g/100 g DM)	SDF (g/100 g DM)	WAC (g water/g DM)	OAC (g oil/g DM)
Control	58.00±0.69^{c}	56.80±0.53^{cd}	1.20±0.35^{c}	1.85±0.02^{a}	2.42±0.20^{a}
32 g/100 g (M), 90°C (T)	64.02±1.07^{b}	60.10±0.85^{bc}	3.93±0.29^{a}	1.77±0.14^{a}	2.71±0.18^{a}
32 g/100 g (M), 100°C (T)	74.30±0.40^{a}	70.40±0.40^{a}	3.91±0.01^{a}	1.78±0.05^{a}	2.82±0.16^{a}
32 g/100 g (M), 110°C (T)	59.59±0.51^{c}	55.94±0.35^{d}	3.65±0.15^{a}	1.69±0.10^{a}	2.88±0.22^{a}
39 g/100 g (M), 90°C (T)	58.41±2.74^{c}	56.99±2.79^{cd}	1.42±0.34^{c}	1.76±0.04^{a}	2.93±0.03^{a}
39 g/100 g (M), 100°C (T)	60.32±1.41^{bc}	58.90±0.40^{bcd}	2.12±0.31^{b}	1.75±0.08^{a}	2.92±0.09^{a}
39 g/100 g (M), 110°C (T)	63.76±1.71^{b}	62.00±2.00^{b}	2.16±0.11^{b}	1.75±0.14^{a}	2.55±0.64^{a}

Values are presented as mean ± standard deviation. Different letters in the same column indicate that the treatments are significantly different ($p<0.05$). M, moisture content in tamarind shell subjected to extrusion; T, extrusion temperature; DM, dry matter.

TABLE 3. Content of lignin, cellulose, and hemicellulose in non-extruded tamarind shell (control) and its extrudates (g/100 g DM).

Treatment	Lignin	Cellulose	Hemicellulose
Control	31.57±0.38^{cd}	16.21±0.03^{d}	9.00±0.34^{a}
32 g/100 g (M), 90°C (T)	33.29±1.00^{c}	21.96±0.99^{b}	4.83±0.02^{b}
32 g/100 g (M), 100°C (T)	43.23±0.83^{a}	22.64±0.65^{ab}	3.53±0.39^{cd}
32 g/100 g (M), 110°C (T)	30.12±0.93^{d}	21.82±0.81^{b}	3.70±0.02^{bcd}
39 g/100 g (M), 90°C (T)	30.68±0.79^{d}	23.93±1.35^{a}	3.26±0.35^{cd}
39 g/100 g (M), 100°C (T)	37.01±0.86^{b}	16.51±0.36^{d}	2.95±0.63^{d}
39 g/100 g (M), 110°C (T)	38.75±0.01^{b}	19.49±0.37^{c}	4.42±1.02^{bc}

Values are presented as mean ± standard deviation. Different letters in the same column indicate that the treatments are significantly different ($p<0.05$). M, moisture content in tamarind shell subjected to extrusion; T, extrusion temperature; DM, dry matter.

increased compared to the non-extruded material in the treatments at 100°C where the initial tamarind shell moisture content was 32 g/100 g and at 100°C and 110°C with tamarind shell having the moisture content of 39 g/100 g of sample. Likewise, the cellulose content increased compared to the non-extruded material when a sample with moisture content of 32 g/100 g was used at each of the temperatures tested, as well as in the treatment of tamarind shell containing 39 g water/100 g treated at 90°C and 100°C. The hemicellulose content, regardless of the extrusion conditions, was lower in the extrudates compared to the non-extruded material.

Effect of the extrusion on water and oil absorption capacities and glucose dialysis retardation index of tamarind shell

The results of OAC and WAC measurements of tamarind shell and its extrudates are shown in Table 2. The OAC of the control sample was 2.42 g oil/g DM and a tendency to increase OAC as a result of extrusion was observed (an average 16%), although the differences between values for non-extruded and extruded samples were not significant ($p \geq 0.05$). OAC has been attributed to the physical entrapment of oil [Abah *et al*., 2020], and such oil entrapment in dietary fibers is mainly related to the surface properties of the particles, the overall charge density, and the hydrophilic nature of the fiber [Elleuch *et al.,* 2011]. A high OAC of food product is important because, according to the information documented by Kesselly *et al*. [2022], fats act as flavor retainers and improve mouthfeel of foods. Moreover, ingredients with high OAC can be used as emulsifiers in food items that are rich in fat. In addition, the ability of reduction of cholesterol levels in blood is linked with a high OAC of dietary fiber of extrudates, as documented by Khan *et al.* [2018]. The OAC depends mainly on the porosity of the material, since the oil is lodged in the said sites, as well as on the surface area and the hydrophobicity character found in chemical structure of IDF. The WAC of non-extruded tamarind shell was 1.85 g water/g DM, and for extrudates, an average decrease in WAC of 5.4% was noted; however, these changes were statistically insignificant ($p \geq 0.05$) (Table 2).

The glucose dialysis retardation index (GDRI) is a useful *in vitro* indicator of the effect of dietary fiber on gastrointestinal glucose absorption delay [Li *et al*., 2022]. In Figure 1, it was observed that the greatest retardation capacity in the diffusion of glucose in the extruded tamarind shells and the control was in the first 30 min. It should be noted that the highest GDRI was obtained both in tamarind shell with 32 g/100 g of moisture treated at 90°C, 100°C and 110°C (the values oscillated between 52.3–59.7%) and in control (54.2%). On average, tamarind shells processed with 32 g/100 g of moisture had a GDRI of 57.2% compared to a GDRI of 18.8% for tamarind shells containing 39 g/100 g. At 60 and 120 min, a strong effect of tamarind shells extruded with 32 g/100 g of moisture, regardless of the temperature used on the GDRI was still observed. The GDRI was gradually lower at the end of 240 min in all the treatments and the control.

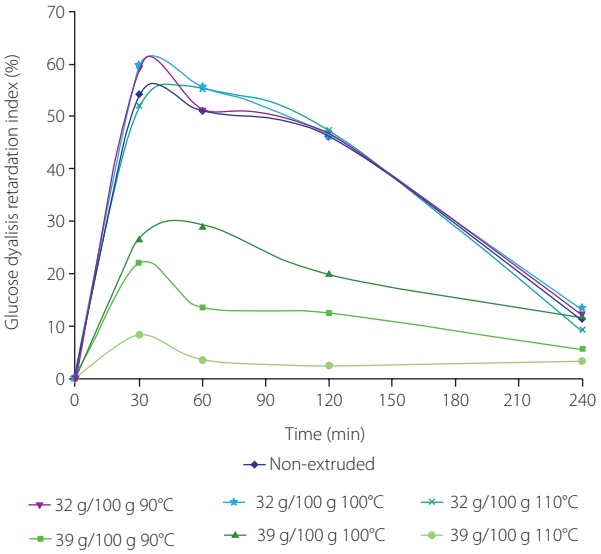

FIGURE 1. Glucose dialysis retardation index over time of the non-extruded tamarind shell and its extrudates obtained from raw material with moisture contents of 32 g/100 g and 39 g/100 g at extrusion temperature of 90–110°C.

One of the salient physicochemical properties of a dietary fiber is its ability to retain organic molecules, such as glucose and lipids, in its structural matrix and form of a viscous gel [Martínez-Flores *et al.,* 2009]. These viscous fibers can delay the gastric emptying of ingested food into the small intestine, providing a feeling of satiety, reducing postprandial blood glucose concentrations, and ensuring a beneficial effect on insulin sensitivity and weight control. As *per* available research, the extrusion process of a given raw material helps to increase the amount of its SDF, as persuasively documented by Bader *et al.* [2019]. Larrea *et al.* [2010], studying the effect of the fiber from the orange bagasse on the GDRI before and after the extrusion process, claimed that extruded samples presented a higher retardation rate compared to that of the non-extruded sample.

Effect of the extrusion on total phenolic content, total flavonoid content, and antioxidant capacity of tamarind shell

The total phenolic content of the tamarind shell was 19.86 mg GAE/g DM. In general, the extrudates exhibited significantly ($p<0.05$) lower total phenolic content (an average 40.3%) compared to the raw tamarind shell (Figure 2A). The lowest total phenolic content was 5.9 mg GAE/g DM, occurring in the tamarind shell with moisture content of 39 g/100 g extruded at 100°C. In turn, the total flavonoid content of the unprocessed tamarind shell was 13.54 mg RE/g DM. After the extrusion, a reduction in total flavonoid content of 7.16% was observed in the tamarind shell with a moisture content of 32 g/100 g treated at 100°C (Figure 2B). This sample had the highest total flavonoid content between extrudates. An average reduction in total flavonoid content in the extrudates compared to the non-extruded sample was 18.4%. The phenolic content was reduced in the extruded tamarind shell, probably due to its instability of phenolics in the conditions of process. The change

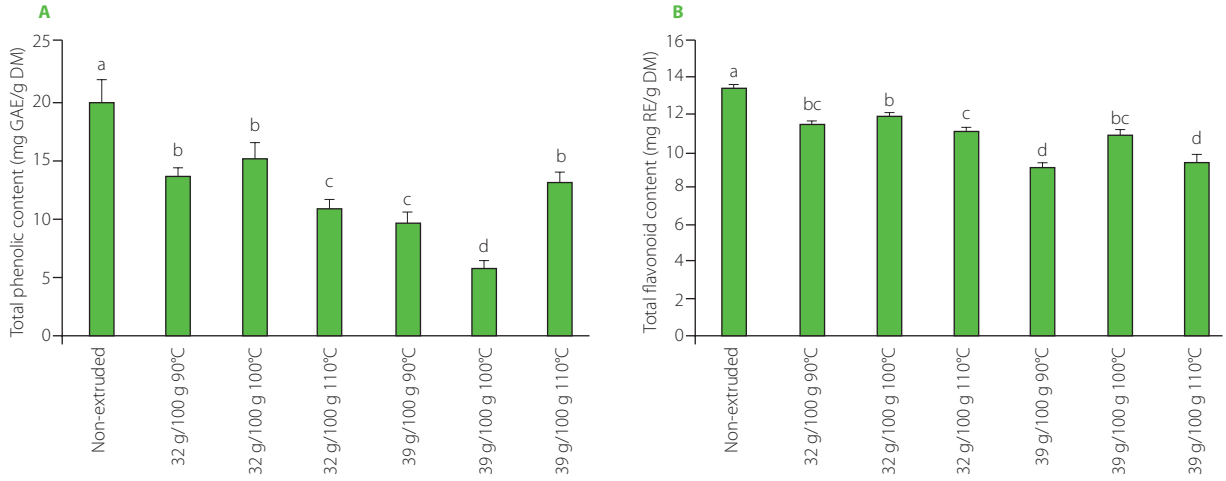

FIGURE 2. Total phenolic content (**A**) and total flavonoid content (**B**) of the non-extruded tamarind shell and its extrudates obtained from raw material with moisture contents of 32 g/100 g and 39 g/100 g at extrusion temperature of 90–110°C. Different letters above bars indicate that the treatments are significantly different (p<0.05). GAE, gallic acid equivalents; RE, rutin equivalents; DM, dry matter.

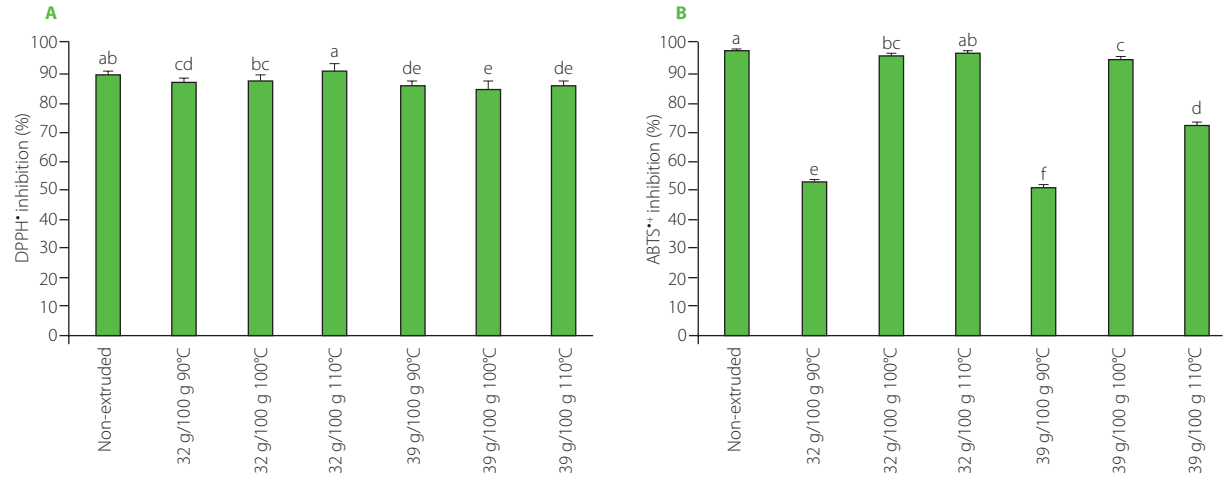

FIGURE 3. DPPH• (**A**) and ABTS•+(**B**) scavenging capacity of the non-extruded tamarind shell and its extrudates obtained from raw material with moisture contents of 32 g/100 g and 39 g/100 g at extrusion temperature of 90–110°C. Different letters above bars indicate that the treatments are significantly different (p<0.05).

of the chemical structure of phenolic compounds was attributed to the combined effect of moisture and extrusion temperature. In this regard, Sharma *et al.* [2012] mentioned that the use of high moisture was more destructive for these compounds. The synergistic effect of moisture and temperature above 80°C mainly generates the decarboxylation [Brennan *et al.*, 2011], malonic conjugation, and de-esterification of phenolics [Mahungu *et al.*, 1999].

Figure 3A and 3B depict the results of measurements of the antioxidant capacity of non-extruded tamarind shell and its extrudates in ABTS and DPPH assays. There was an average decrease in the scavenging capacity of extrudates against both radicals compared to raw tamarind shell (by 2.8% in DPPH and 19.6% in ABTS assay), but, for both radicals, the scavenging capacity of tamarind shell with a moisture level of 32 g/100 g treated at 100°C and 110°C was similar to that for the non-extruded sample, indicating the maintenance of their antioxidant capacity.

Correlation analysis

The TDF content showed a significant (p<0.001), positive, correlation with the IDF and with lignin contents (r=0.978 and r=0.825, respectively) (Table 4). Likewise, lignin correlated significantly (p<0.001) with IDF (r=0.881). The hemicellulose content also exhibited affinity for total phenolic content (r=0.732, p<0.001) and total flavonoid content (r=0.586, p<0.01). Total flavonoid content had a significant (p<0.01) affinity towards the ABTS•+ scavenging capacity (r=0.646) and DPPH• scavenging capacity (r=0.561), while total phenolic content was significantly (p<0.01) correlated with the DPPH• scavenging capacity (r=0.552).

FTIR spectra and SEM micrographs of tamarind shell and its extrudates

The FTIR spectra obtained from the extruded samples were similar among themselves as well as with respect to the non-extruded sample (Figure 4). The signals that corresponded to different functional groups are present in the spectra. A broad band at

TABLE 4. Coefficients of Pearson correlations of response variables for the non-extruded tamarind shell and its extrudates.

	TDF	IDF	SDF	Total phenolic content	Total flavonoid content	DPPH assay	ABTS assay	Lignin	Cellulose
IDF	0.978***								
SDF	0.639**	0.476							
Total phenolic content	0.223	0.222	0.013						
Total flavonoid content	0.120	0.085	0.162	0.490					
DPPH assay	0.011	–0.100	0.285	0.552**	0.561**				
ABTS assay	0.139	0.151	0.070	0.148	0.646**	0.452			
Lignin	0.825***	0.881***	0.313	0.079	0.053	–0.308	0.264		
Cellulose	0.323	0.224	0.469	–0.090	–0.493	0.027	–0.526	–0.050	
Hemicellulose	–0.256	–0.226	–0.366	0.732***	0.586**	0.501*	0.191	–0.277	–0.498

*Significance at $p<0.05$; **significance at $p<0.01$; ***significance at $p<0.001$. TDF, total dietary fiber; IDF, insoluble dietary fiber; SDF, soluble dietary fiber; DPPH assay, assay with 2,2-diphenyl--1-picrylhydrazyl radical; ABTS assay, assay with 2,2'-azino-bis-(3-ethylbenzothiazoline-6-sulfonic acid radical cation.

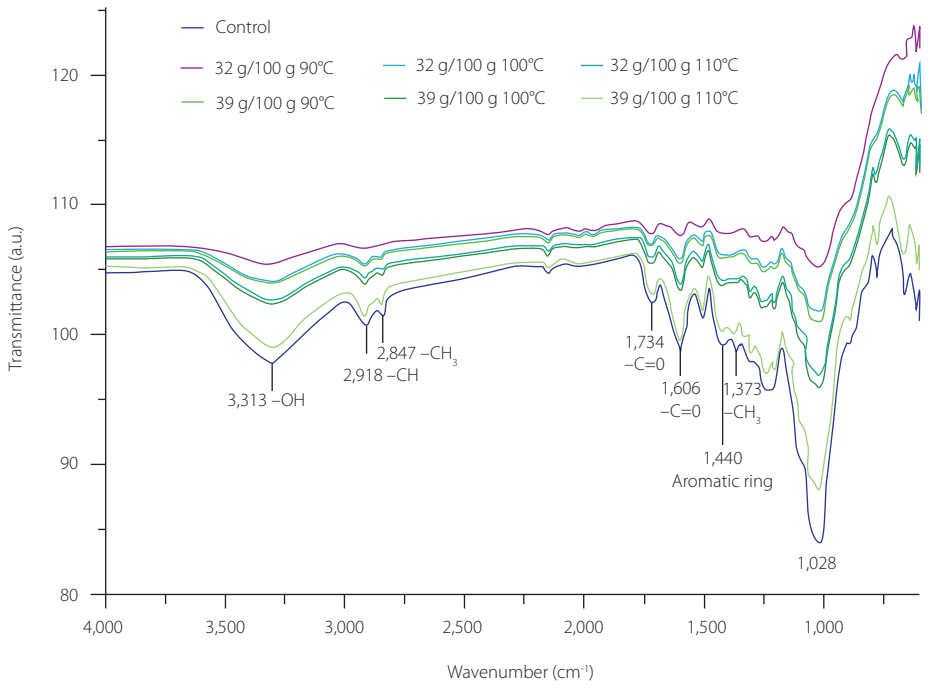

FIGURE 4. Fourier transform infrared spectra of the non-extruded tamarind shell (control) and its extrudates obtained from raw material with moisture contents of 32 g/100 g and 39 g/100 g at extrusion temperature of 90–110°C.

a wavenumber of 3,313 cm^{-1} (Figure 4) would indicate the stretching of the hydroxyl groups (–OH) of cellulose, lignin, and polyphenols [Anirudhan *et al.,* 2008], in addition to the stretching vibration generated by the –OH of the carboxyl groups (–COOH) of pectin and hemicellulose molecules [Arroyo *et al.,* 2008; Sivam *et al.,* 2011]. Pectin is a linear polysaccharide comprising several D-galacturonic acid molecules connected by α-1,4 glycosidic bonds [Liu et al., 2021]. The stretching vibration of the hydroxyl groups in pectin is generally attributed to the presence of D-galacturonic acids [Arroyo *et al.,* 2008]. On the other hand, hemicelluloses, having a heterogeneous chemical structure, exhibit the said stretching vibrations in their different functional groups, corresponding to those of the monosaccharides such as arabinose, xylose, glucose, mannose, galactose, and uronic acids [Arroyo *et al.,* 2008]. In this study, the characteristic signal of hydroxyl groups was also observed at a wavenumber of 1,232 cm^{-1}, corresponding with lignin, and at wavenumbers of 2,916 cm^{-1}, 2,847 cm^{-1}, and 1,373 cm^{-1}, associated with the elongation vibrations of the carbon-hydrogen

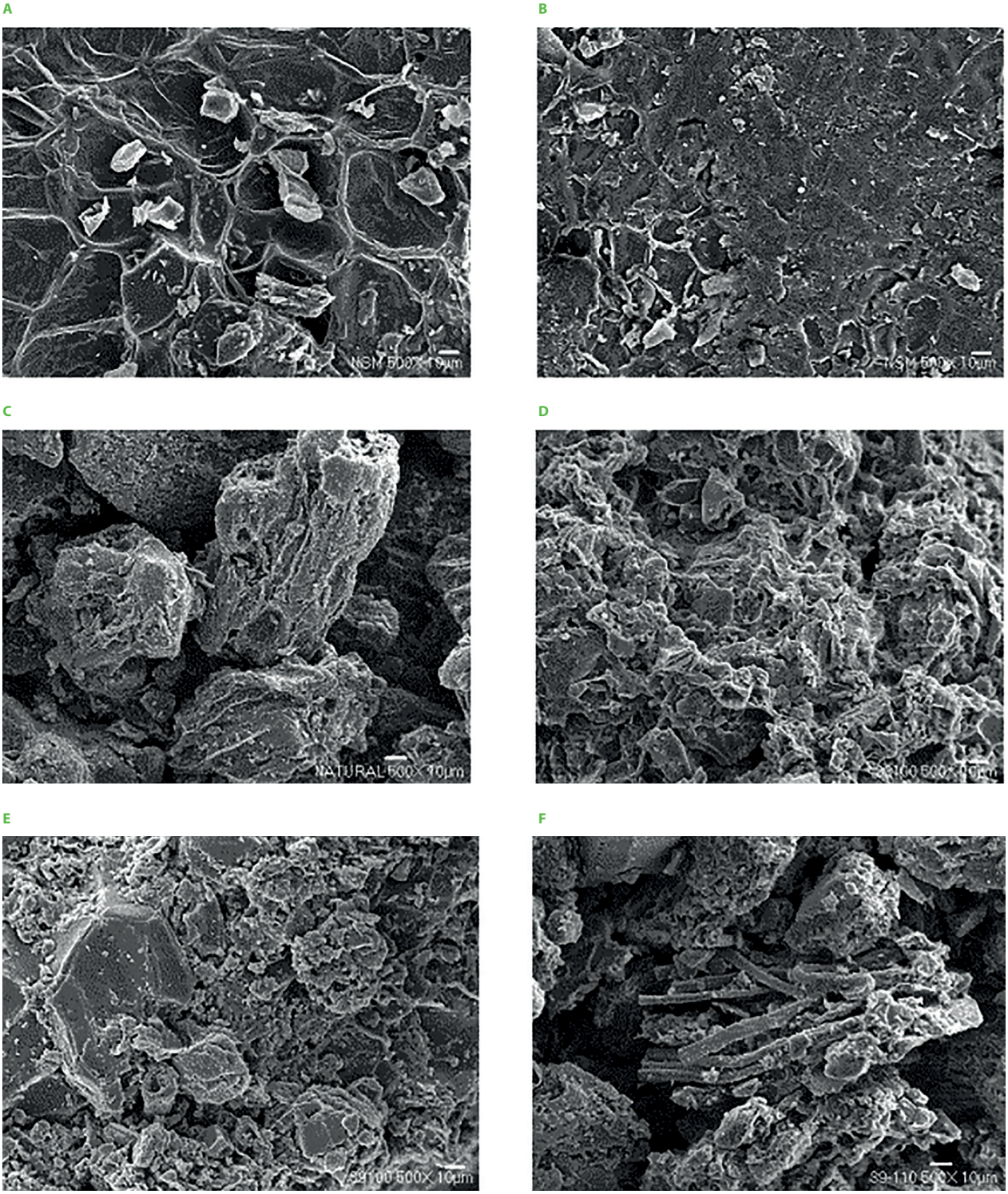

FIGURE 5. Scanning electron micrographs of internal (**A**) and external (**B**) part of the non-extruded and non-ground tamarind shells, non-extruded ground tamarind shell (**C**), extruded tamarind shells at 100°C and initial moisture contents of 32 g/100 g (**D**) and 39 g/100 g (**E**), and cellulose microfibrils in the extrudate obtained at 110°C and initial moisture content of 39 g/100 g (**F**). Magnification 500×.

of the alkane group (–CH) of cellulose, hemicellulose, and lignin, respectively [Arroyo *et al.,* 2008]. The bands at 1,734 cm^{-1} and 1,605 cm^{-1} of the carbonyl group (–C=O) were associated with the aldehydes and ketones of simple and complex carbohydrates and the esterified carboxylic acids from pectin, hemicellulose, and lignin [Arroyo *et al*., 2008]. Sivam *et al.* [2011] related the 1,734 cm^{-1} wavenumber with the presence of methylated pectin. The C–O asymmetric stretching of the hydroxyl groups of phenolics was observed at 1,028 cm^{-1} wavenumber. The band at 2,916 cm^{-1} wavenumber is characteristic of catechin, in addition to 2,847 cm^{-1} being associated with gallic acid and, 3313 cm^{-1} being related to tannic acid.

The micrographs obtained for the tamarind shell under different conditions are shown in Figure 5. The morphology

of the inner part of the tamarind shell without grinding (Figure 5A) showed a heterogeneous surface with smooth and rough parts, while the external part (Figure 5B) displayed a much rougher surface resembling that of a honeycomb. Similar morphology of tamarind shell was also reported by Sivasankar *et al.* [2012]. Figure 5C presents the micrograph of ground non-extruded tamarind shell. Small, isolated fragments with a porous structure were visible along with striations due to the presence of cellulose microfibrils. This characteristic porosity would give DF the ability to trap oil molecules, as was documented by Zhuang *et al.* [2019]. Further, the micrographs presented in Figures 5D–E show the morphology of the ground and extruded shell, implying a more interconnected (homogenized) structure where the isolated shell fragments were not observed. In addition, the extruded material had small pores on its surface. After the extrusion process, the cellulose present in the extruded tamarind shell (Figure 5F) presented a well-defined cylindrical cell structure, which also coincided with the report documented by Maheswari *et al.* [2008].

CONCLUSION

The temperature of the extrusion and moisture content of the tamarind shell subjected to extrusion affected changes in the chemical composition of the extrudates, mainly in terms of their soluble dietary fiber content and improved some of the raw material's physiochemical properties, such as OAC and GDRI, suggesting the potential benefits of using the extruded tamarind shell. The treatment of shell with a moisture content of 32 g/100 g at 100°C was particularly beneficial for improving these parameters. Although the general aim of extrusion of tamarind shell was to reduce the content of phenolic compounds, extrusion of shells with a moisture content of 32 g/100 g at 100°C and 110°C allowed to maintain antioxidant capacity, and the extrudates had $DPPH^{\bullet}$ and $ABTS^{\bullet+}$ scavenging activity at the level of the starting material. In light of the above findings, this item, hitherto considered by the food industry as waste material, could be used in the future as a raw material in the production of functional foods.

ACKNOWLEDGEMENTS

The student Dalia Samanta Aguilar Ávila thanks CONACyT for the scholarship granted during her master's studies.

RESEARCH FUNDING

The study received no external funding.

CONFLICT OF INTERESTS

The authors declare that they have no competing interests.

ORCID IDs

D.S. Aguilar-Ávila https://orcid.org/0000-0003-3820-3180
M.G. Garnica-Romo https://orcid.org/0000-0002-2260-2489
H.E. Martínez-Flores https://orcid.org/0000-0002-0044-9399
E. Morales-Sánchez https://orcid.org/0000-0002-0855-5460
R. Reynoso-Camacho https://orcid.org/0000-0002-7223-0062

REFERENCES

1. AACC. 2000. American Association of Cereal Chemists. Approved Methods. 10th edition. Edited by the AACC. Minneapolis, MN, USA.
2. Abah, C.R., Ishiwu, C.N., Obiegbuna, J.E., Oladejo, A.A. (2020). Nutritional composition, functional properties and food applications of millet grains. *Asian Food Science Journal*, *14*(2), 9–19. https://doi.org/10.9734/AFSJ/2020/v14i230124
3. Abdulmajid, A., Hamidon, T.S., Rahim, A.A., Hussin, M.H. (2019). Tamarind shell tannin extracts as green corrosion inhibitors of mild steel in hydrochloric acid medium. *Materials Research Express*, *6*(10), art. no. 106579. https://doi.org/10.1088/2053-1591/ab3b87
4. Adiotomre, J., Eastwood, M.A., Edwards, C., Brydon, W.G. (1990). Dietary fiber: *in vitro* methods that anticipate nutrition and metabolic activity in humans. *The American Journal of Clinical Nutrition*, *52*(1), 128-134. https://doi.org/10.1093/ajcn/52.1.128
5. Anderson, R.A., Conway, H.F., Pfeifer, V.F., Griffin, E.L. (1969). Roll and extrusion-cooking of grain sorghum grits. *Cereal Science Today*, *14*(11), 371-381.
6. Anirudhan, T.S., Radhakrishnan, P.G., Suchithra, P.S. (2008). Adsorptive removal of mercury (II) ions from water and wastewater by polymerized tamarind fruit shell. *Separation Science and Technology*, *43*(13), 3522–3544. https://doi.org/10.1080/01496390802222459
7. ANSI/ASTM. (1977). Standard test methods for alpha-cellulose in wood D 1103-60. American National Standard Institute, Washington DC.
8. Arribas, C., Cabellos, B., Cuadrado, C., Guillamón, E., Pedrosa, M.M. (2019). Extrusion effect on proximate composition, starch and dietary fibre of ready-to-eat products based on rice fortified with carob fruit and bean. *LWT – Food Science and Technology*, *111*, 387–393. https://doi.org/10.1016/j.lwt.2019.05.064
9. Arribas, C., Cabellos, B., Sánchez, C., Cuadrado, C., Guillamón, E., Pedrosa, M.M. (2017). The impact of extrusion on the nutritional composition, dietary fiber and *in vitro* digestibility of gluten-free snacks based on rice, pea and carob flour blends. *Food & Function*, *8*(10), 3654–3663. https://doi.org/10.1039/C7FO00910K
10. Arroyo, S.Y., Carrasco, C.M., Bueno, L.A., Cardeña, C., Luízar, O.C. (2008). Obtención y caracterización fisicoquímica y funcional de las fibras dietéticas del níspero común (*Mesillas germánica*). *Revista de la Sociedad Química del Perú*, *74*(4), 269–281 (in Spanish; English abstract).
11. Bader Ul Ain, H., Saeed, F., Ahmed, A., Asif Khan, M., Niaz, B., Tufail, T. (2019). Improving the physicochemical properties of partially enhanced soluble dietary fiber through innovative techniques: A coherent review. *Journal of Food Processing and Preservation*, *43*(4), art. no. e13917. https://doi.org/10.1111/jfpp.13917
12. Barak, S., Mudgil, D. (2014). Locust bean gum: Processing, properties and food applications – A review. *International Journal of Biological Macromolecules*, *66*, 74–80. https://doi.org/10.1016/j.ijbiomac.2014.02.017
13. Benítez, V., Rebollo-Hernanz, M., Braojos, C., Cañas, S., Gil-Ramírez, A., Aguilera, Y., Martín-Cabrejas, M.A. (2023). Changes in the cocoa shell dietary fiber and phenolic compounds after extrusion determine its functional and physiological properties. *Current Research in Food Science*, *6*, art. no. 100516. https://doi.org/10.1016/j.crfs.2023.100516
14. Brand-Williams, W., Cuvelier, M.E., Berset, C. (1995). Use of a free radical method to evaluate antioxidant activity. *LWT – Food Science and Technology*, *28*(1), 25–30. https://doi.org/10.1016/S0023-6438(95)80008-5
15. Brennan, C., Brennan, M., Derbyshire, E., Tiwari, B.K. (2011). Effects of extrusion on the polyphenols, vitamins and antioxidant activity of foods. *Trends in Food Science and Technology*, *22*(10), 570–575. https://doi.org/10.1016/j.tifs.2011.05.007
16. Carré, M.H., Haynes, D. (1922). The estimation of pectin as calcium pectate and the application of this method to the determination of the soluble pectin in apples. *Biochemistry Journal*, *16*(1), 60–69. https://doi.org/10.1042/bj0160060
17. Chen, H., Zhao, C., Li, J., Hussain, S., Yan, S., Wang, Q. (2018). Effects of extrusion on structural and physicochemical properties of soluble dietary fiber from nodes of lotus root. *LWT – Food and Science Technology*, *93*, 204–211. https://doi.org/10.1016/j.lwt.2018.03.004
18. Chimsah, G.F.A., Nyarko, G., Abubakari, A.-H. (2020). A review of explored uses and study of nutritional potential of tamarind (*Tamarindus indica* L.) in Northern. *African Journal of Food Science*, *14*(9), 285–294. https://doi.org/10.5897/AJFS2018.1744
19. De Caluwé, E., Halamová, K., Van Damme, P. (2010). *Tamarindus indica* L. – A review of traditional uses, phytochemistry and pharmacology. *Afrika Focus*, *23*(1), 53–83. https://doi.org/10.21825/af.v23i1.5039
20. Elleuch, M., Bedigian, D., Roiseux, O., Besbes, S., Blecker, C., Attia, H. (2011). Dietary fibre and fibre-rich by products of food processing: Characterisation,

technological functionality and commercial applications: a review. *Food Chemistry, 124*(2), 411–421. https://doi.org/10.1016/j.foodchem.2010.06.077
21. Gan, J., Xie, L., Peng, G., Xie, J., Chen, Y., Yu, Q. (2021). Systematic review on modification methods of dietary fiber. *Food Hydrocolloids*, 19, art. no. 106872. https://doi.org/10.1016/j.foodhyd.2021.106872
22. Garcia-Amezquita, L.E., Tejada-Ortigoza, V., Serna-Saldivar, S.O., Welti-Chanes, J. (2018). Dietary fiber concentrates from fruit and vegetable by-products: processing, modification, and application as functional ingredients. *Food and Bioprocess Technology*, *11*(2), 1439–1463. https://doi.org/10.1007/s11947-018-2117-2
23. Gustafson, C.R., Rose, D.J. (2022). US consumer identification of the health benefits of dietary fiber and consideration of fiber when making food choices. *Nutrients*, *14*(11), art. no. 2341. https://doi.org/10.3390/nu14112341
24. Huang, Y.L., Ma, Y.S., Tsai, Y.H., Chang, S.K. (2019). *In vitro* hypoglycemic, cholesterol-lowering and fermentation capacities of fiber-rich orange pomace as affected by extrusion. *International Journal of Biological Macromolecules*, *124*, 796–801. https://doi.org/10.1016/j.ijbiomac.2018.11.249
25. Kesselly, S.R., Mugabi, R., Byaruhanga, Y. (2022). Effect of extrusion on the functional and pasting properties of high-quality cassava flour (HQCF). *Journal of Food Research*, *11*(4), 1–12. https://doi.org/10.5539/jfr.v11n4p1
26. Khan, G.M., Khan, N.M., Khan, Z.U., Ali, F., Jan, A.K., Muhammad, N., Elahi, R. (2018). Effect of extraction methods on structural, physiochemical and functional properties of dietary fiber from defatted walnut flour. *Food Science and Biotechnology*, *27*, 1015–1022. https://doi.org/10.1007/s10068-018-0338-9
27. Kumar, N, Goel, N. (2019). Phenolic acids: Natural versatile molecules with promising therapeutic applications. *Biotechnology Reports*, *24*, art. no. e00370. https://doi.org/10.1016/j.btre.2019.e00370
28. Larrea Céspedes, M.A., Martínez-Bustos, F., Chang, Y.K. (2010). The effect of extruded orange pulp on enzymatic hydrolysis of starch and glucose retardation index. *Food and Bioprocess Technology*, *3*, 684–692. https://doi.org/10.1007/s11947-008-0166-7
29. Lemes, A.C., Buranelo, E.M., Gonçalves de O.F.J., Gautério, G.V., Bernardo Días, R.B., Zarur, C.M.A. (2022). Biological approaches for extraction of bioactive compounds from agro-industrial by-products: A review. *Frontiers in Bioengineering and Biotechnology*, *9*, art. no. 802543. https://doi.org/10.3389/fbioe.2021.802543
30. Li, L., Liu, J., Zhang, Y., Wang, Q., Wang, J. (2022). Qualitative and quantitative correlation of microstructural properties and in vitro glucose adsorption and diffusion behaviors of pea insoluble dietary fiber induced by ultrafine grinding. *Foods*, *11*(18), art. no. 2814. https://doi.org/10.3390/foods11182814
31. Liu, J., Wang, T., Huang, B., Zhuang, Y., Hu, Y., Fei, P. (2021). Pectin modified with phenolic acids: Evaluation of their emulsification properties, antioxidation activities, and antibacterial activities. *International Journal of Biological Macromolecules*, *174*, 485–493. https://doi.org/10.1016/j.ijbiomac.2021.01.190
32. Liu, L., Kerr, W.L., Kong, F., Dee, D.R., Lin, M. (2018). Influence of nano-fibrillated cellulose (NFC) on starch digestion and glucose absorption. *Carbohydrate Polymers, 196*, 146–153. https://doi.org/10.1016/j.carbpol.2018.04.116
33. Maheswari, C.U., Guduri, B.R., Rajulu, A.V. (2008). Properties of lignocellulose tamarind fruit fibers. *Journal of Applied Polymer Science*, *110*(4), 1986–1989. https://doi.org/10.1002/app.27915
34. Mahungu, S.M., Diaz-Mercado, S., Li, J., Schwenk, M., Singletary, K., Faller, J. (1999). Stability of isoflavones during extraction processing of corn/soy mixture. *Journal of Agricultural and Food Chemistry*, *47*(1), 279–284. https://doi.org/10.1021/jf980441q
35. Martínez-Flores, H.E., Maya-Cortés, D.C., Figueroa-Cárdenas, J.D., Garnica Romo, M.G., Ponce-Saavedra, J. (2009). Chemical composition and physicochemical properties of shiitake mushroom and high fiber products. *CyTA-Journal of Food*, *7*(1), 7–14. https://doi.org/10.1080/11358120902850537
36. Menis-Henrique, M.E.C., Scarton, M., Piran, M.V.F., Clerici, M.T.P.S. (2020). Cereal fiber: Extrusion modifications for food industry. *Current Opinion in Food Science*, *33*, 141–148. https://doi.org/10.1016/j.cofs.2020.05.001
37. Mudgil, D. (2018). Influence of partially hydrolyzed guar gum as soluble fiber on physicochemical, textural and sensory characteristics of yoghurt. *The Journal of Microbiology, Biotechnology and Food Sciences*, *8*(2), 794-797. https://doi.org/10.15414/jmbfs.2018.8.2.794-797
38. Oomah, B.D., Cardador-Martínez, A., Loarca-Piña, G. (2005). Phenolics and antioxidative activities in common beans (*Phaseolus vulgaris* L). *Journal of the Science of Food and Agriculture*, *85*(6), 935–942. https://doi.org/10.1002/jsfa.2019
39. Ou, S., Kwok, K., Li, Y., Fu, L. (2001). *In vitro* study of possible role of dietary fiber in lowering postprandial serum glucose. *Journal of Agriculture and Food Chemistry*, *49*(2), 1026–1029. https://doi.org/10.1021/jf000574n
40. Prosky, L., Asp, N.G., Scheweizer, T.F., Furda, I. (1988). Determination of insoluble, soluble, and total dietary fiber in food and products: Interlaboratory study. *Journal- Association of Official Analytical Chemists*, *71*(5), 1017–1023. https://doi.org/10.1093/jaoac/71.5.1017
41. Re, R., Pellegrini, N., Proteggente, A., Pannala, A., Yang, M., Rice-Evans, C. (1999). Antioxidant activity applying an improved ABTS radical cation decolorization assay. *Free Radical Biology and Medicine*, *26*(9-10), 1231–1237. https://doi.org/10.1016/s0891-5849(98)00315-3
42. Reguengo, L.M., Kawata, S.M., Sivieri, K., Maróstica, J.M.R. (2022). Agro-industrial by-products: Valuable sources of bioactive compounds. *Food Research International*, *152*, art. no. 110871. https://doi.org/10.1016/j.foodres.2021.110871
43. Runkel, R.O.H., Wilke, K.D. (1951). Zur Kenntnis des thermoplastischen Verhaltens von Holz. *Holz Roh Werkstoff*, *9*, 260–270 (in German). https://doi.org/10.1007/BF02617370
44. Saha, P., Chowdhury, S., Gupta, S., Kumar, I., Kumar, R. (2010). Assessment on the removal of malachite green using tamarind fruit shell as biosorbent. *CLEAN – Soil, Air, Water, 38*(5–6), 437-455. https://doi.org/10.1002/clen.200900234
45. Sharma, P., Gujral, H.S., Singh, B. (2012). Antioxidant activity of barley as affected by extrusion. *Food Chemistry*, *131*(4), 1406–1413. https://doi.org/10.1016/j.foodchem.2011.10.009
46. Singleton, V.L., Rossi, J.A. (1965). Colorimetry of total phenolics with phosphomolybdic-phosphotungstic acid reagents. *American Journal of Enology and Viticulture*, *16*, 144–158. https://doi.org/10.5344/ajev.1965.16.3.144
47. Sivam, A.S., Sun-Waterhouse, D., Perera, C.O., Waterhouse, G.I.N. (2011). Application of FT-IR and Raman spectroscopy for the study of biopolymers in breads fortified with fibre and polyphenols. *Food Research International*, *50*(2), 574–585. https://doi.org/10.1016/j.foodres.2011.03.039
48. Sivasankar, V., Rajkumar, S., Murugesh, S., Darchen, A. (2012). Tamarind (*Tamarindus indica*) fruit shell carbon: a calcium-rich promising adsorbent for fluoride removal from groundwater. *Journal of Hazardous Materials*, *225–226*, 164–172. https://doi.org/10.1016/j.jhazmat.2012.05.015
49. Stojceska, V., Ainsworth, P., Plunkett, A., Ibanoglu, S. (2010). The advantage of using extrusion processing for increasing dietary fibre level in gluten-free products. *Food Chemistry*, *121*(1), 156–164. https://doi.org/10.1016/j.foodchem.2009.12.024
50. Ujjinappa, S., Sreepathi, L.K. (2018). Production and quality testing of fuel briquettes made from pongamia and tamarind shell. *Sādhanā*, *43*, art. no. 58. https://doi.org/10.1007/s12046-018-0836-8
51. Wise, L.E., Maxine M, D'Addieco, A.A. (1946). Chlorite holocellulose, its fractionation and bearing on summative wood analysis and on studies on the hemicelluloses. *Paper Trade Journal, 122*, 35–43
52. Yusuf, K., Saha, S., Umar, S. (2022). Health benefits of dietary fiber for the management of inflammatory bowel disease. *Biomedicines*, *10*(6), art. no. 1242. https://doi.org/10.3390/biomedicines10061242
53. Zhang, M., Bai, X., Zhang, Z. (2011). Extrusion process improves the functionality of soluble dietary fiber in oat bran. *Journal of Cereal Science*, *54*(1), 98-103. https://doi.org/10.1016/j.jcs.2011.04.001
54. Zhong, L., Fang, Z., Wahlqvist, M. L., Hodgson, J.M., Johnson, S.K. (2019). Extrusion cooking increases soluble dietary fibre of lupin seed coat. *LWT – Food Science and Technology*, *99*, 547–554. https://doi.org/10.1016/j.lwt.2018.10.018
55. Zhuang, Z., Chen, M., Niu, J., Qu, N., Ji, B., Duan, X., Liu, Z., Liu, X., Wang, Y., Zhao, B. (2019). The manufacturing process of kiwifruit fruit powder with high dietary fiber and its laxative effect. *Molecules*, *24*(21), art. no. 3813. https://doi.org/10.3390/molecules24213813

ORIGINAL ARTICLE
http://journal.pan.olsztyn.pl

Polish Journal of Food and Nutrition Sciences
2023, Vol. 73, No. 3, 289–296
DOI: 10.31883/pjfns/170938
ISSN 1230-0322, e-ISSN 2083-6007

Physicochemical Properties, Antioxidant Capacity, and Consumer Acceptability of Ice Cream Incorporated with Avocado (*Persea Americana* Mill.) Pulp

Jutamas Moolwong[1], Worasaung Klinthong[2], Thanida Chuacharoen[1,*]

[1]Faculty of Science and Technology, Suan Sunandha Rajabhat University, 1 U Thong Nok Road, Dusit, Bangkok 10300, Thailand
[2]Greenday Global Co., Ltd., 829 Moo 2 Bangpoo Industrial Estate (North), Mueang Samutprakarn, Samutprakarn 10280, Thailand

Avocado pulp is low in sugar contents but quite high in dietary fiber, nutrients, and phytochemicals with potential health benefits. In this study, the avocado pulp was incorporated into ice cream. The effects of replacing milk fat with avocado on the physical and chemical properties of ice cream and consumer acceptability were evaluated. Milk fat-based ingredients of the ice cream were partially replaced with avocado pulp at ratios of 10, 20, and 30% (*w/w*). All ice creams were subjected to physical and chemical analyses and were evaluated in sensory acceptability tests. Replacing milk fat with avocado pulp significantly reduced moisture content, protein, and fat content, while it increased the carbohydrate (3.70 to 7.91 g/100 g) and crude fiber content (0.39 to 1.38 g/100 g). A higher content of avocado pulp caused a reduction in overrun and retarded the melting rate due to the effect of high fiber content. Increased viscosity and hardness were observed. The ice cream with the highest avocado pulp content had approximately 3-fold higher total phenolic content determined by the Folin-Ciocalteau method and 2-fold higher antioxidant capacity evaluated as DPPH$^{\bullet}$ and ABTS$^{\bullet+}$ scavenging activity, and ferric reducing antioxidant power compared to that of the control. Sensory evaluation showed the 20% (*w/w*) avocado pulp was the suitable ratio for incorporating in the ice cream, which showed a good level of overall acceptability. Thus, our results suggest the potential use of avocado pulp to replace milk fat in frozen dairy products.

Key words: avocado pulp, fiber-rich ice cream, antioxidant capacity, textural property

INTRODUCTION

Consuming desserts incorporated with high amounts of fiber and phytochemical agents obtained from fruits and vegetables plays an essential role in maintenance of healthy eating. Avocado (*Persea Americana* Mill.) is a subtropical fruit native to Mexico, and it has recently become a popular fruit to grow in northern Thailand. The avocado is a nutrient- and phytochemical-dense food consisting of 17.34 g of crude fat, 6.94 g of carbohydrates, 5.55 g of dietary fiber, and 2.08 g of proteins per 100 g of fresh pulp, and it is a useful source of energy [Dreher & Davenport, 2013; Marlett & Cheung, 1997; Yahia & Woolf, 2011]. According to Dreher & Davenport [2013], avocado oil fatty acids consist of 71% monounsaturated fatty acids, 13% polyunsaturated fatty acids, and 16% saturated fatty acids, and are thus considered high in monounsaturated fatty acids. Potassium, sodium, magnesium, ascorbic acid, vitamin K, folate, vitamin B_6, niacin, pantothenic acid, riboflavin, choline, carotenoids, tocopherols, and phytosterols contained in avocado pulp appear to support a wide range of potential health effects [Dreher & Davenport, 2013; Krumreich *et al.*, 2018; Ramos-Aguilar *et al.*, 2021]. Due to its healthy fat

***Corresponding Author:**
e-mail: thanida.ch@ssru.ac.th (Thanida Chuacharoen)

Submitted: 16 April 2023
Accepted: 11 August 2023
Published on-line: 6 September 2023

content, consuming avocado helps to reduce total cholesterol, low-density lipoprotein cholesterol, and triglycerides, resulting in increased HDL cholesterol levels, which helps to promote a healthy blood lipid profile [Mahmassani *et al.*, 2018]. In addition, avocado is a source of phenolic compounds including phenolic acids, flavonoids, lignans, and stilbenes, the content of which correlates with its antioxidant potential [Lyu *et al*., 2023]. The avocado phenolics have also anti-inflammatory, as well as anticancer and antimicrobial activities, which are beneficial for health [Ford *et al*., 2023]. Avocado components such as fatty acids, carbohydrates (including dietary fiber) also confer potential cardiovascular health benefits. It is claimed by the United States Department of Agriculture (USDA) [2011] that the composition profile of avocado has qualified its heart health-improving potential similar to that of almonds, pistachios, and walnuts with less than half the calories.

In many countries, avocados are consumed as a vegetable in savory dishes, such as guacamole, and they are often used as a fresh cream in sweet dishes, such as shakes, smoothies, and ice creams [Cortés Rodríguez *et al.*, 2019]. Thus, because the avocado has potential functional components, such as healthy fatty acid, dietary fiber, and bioactive phytochemicals, its pulp is hypothesized to be able to substitute fat ingredients and enrich dietary fiber in various functional foods, including beverages along with dairy and bakery products for commercial use.

Milk-based ice cream is a frozen dairy dessert [Yeon *et al.*, 2017], which has gained in popularity with all age groups in Thailand. Its main ingredients are milk, whipped cream, and sugar, which can cause adverse health effects, such as diabetes, obesity, and high blood pressure. Thus, partially replacing milk-fat ingredients in ice cream with avocado pulp should reduce the risk of chronic diseases as well as enhance the nutritional values and health benefits of ice cream.

Given the aforementioned potential health benefits of using the avocado pulp as an alternative to dairy fats in desserts, we aimed to identify the ratio of avocado pulp substitution of dairy ingredients (*i.e.*, milk, whipped cream, and skimmed milk) in ice cream that affects the ice cream's physical properties and sensory acceptability to create a healthy functional ice cream with the benefits of high dietary fiber and antioxidant capacity.

MATERIALS AND METHODS

Preparation of the avocado ice cream

Avocado (*Persea Americana* Mill.) fruits were supplied by Greenday Global Co., Ltd., Samutprakarn, Thailand. Ingredients of ice cream production were purchased from a local market in Bangkok, Thailand. Avocado pulp was prepared according to Ospina *et al.* [2019] and Chuacharoen *et al.* [2021] by washing the avocados thoroughly with clean water, followed by vertically cutting avocados into four pieces, removing their seeds, and peeling them. Avocado pieces were blended into a paste using a kitchen blender, and 0.2% (*w/w*) of citric acid was added to reduce enzymatic activity. Four formulations of ice cream incorporated with the avocado pulp were prepared by the formulation of milk-based ice cream. Briefly, the liquid ingredients were pre-heated at 65°C and then the dried ones were mixed. Avocado pulp replaced 10% (A10), 20% (A20), and 30% (A30) (*w/w*) of the fat ingredients of the standard formulation, *i.e.*, fresh milk, whipped cream, and skimmed milk (Table 1). A sample without avocado (A0) was prepared as a control. The mixture was homogenized using a homogenizer (T25 Ultra-Turrax, IKA, Staufen im Breisgau, Germany) at 5,000 rpm for 2 min, pasteurized at 80°C for 25 s, and then immediately cooled down to 4°C before it was hardened at this temperature for 24 h. After hardening, the ice cream mix was produced and then frozen in an ice cream maker for 15 min. The avocado ice cream samples were stored at −18°C for further analyses.

Physicochemical analyses

To assess the quality of the ice cream, the physicochemical parameters including proximate composition, color, viscosity, melting rate, and overrun were determined.

Proximate analysis was performed based on the methodologies proposed by the Association of Official Analytical Chemists [Latimer, 2019]. Moisture content was determined by gravimetric method. In brief, the sample was dried in a convection oven at 110°C for 2 h (method 968.11). Ash content was quantified by burning the sample at 550°C in a muffle furnace (ELF11/14B, Carbolite, Derbyshire, UK) (method 945.38). Crude protein content was estimated in a digester (KI 11/26, Gerhardt, Koenigswinter, Germany) by the Kjeldahl method (method 971.09). Crude fiber content was determined by sequential acid and base

Table 1. Percentage (*w/w*) of ingredients in formulations of ice cream (A0) and ice cream with avocado pulp as a substitute of 10% (A10), 20% (A20), and 30% (A30) (*w/w*) of the fat ingredients.

Ingredient	A0 (control)	A10	A20	A30
Fresh milk	58.80	52.25	45.70	39.16
Whipped cream	23.00	20.44	17.88	15.32
Sugar	10.00	10.00	10.00	10.00
Skimmed milk	8.00	7.11	6.22	5.33
Guar gum	0.20	0.20	0.20	0.20
Avocado pulp	0.00	10.00	20.00	30.00

digestion (method 962.09). The total lipid content was extracted by the Soxhlet method for 80 min using *n*-hexane as the extraction solvent at 120°C (method 920.39) and carbohydrate content was established by difference and expressed as a nitrogen-free extract.

Color was measured using a MiniScan XE Plus colorimeter (Hunterlab, Reston, VA, USA). The *L**, *a**, and *b** values were determined. *L** characterized the lightness of the ice cream samples ranging from 0 (darkest) to 100 (lightest); *a** characterized the scale of green to red with negative values defined as hues of green and positive ones for hues of red; and *b** characterized the scale of blue to yellow with negative values for hues of blue and positive ones for hues of yellow.

Viscosity was measured using a Brookfield viscometer (DV-II, Brookfield, Middleboro, MA, USA) with spindle no. 2 at 100 rpm. A sample of 600 mL was analyzed at 14±1°C and was kept in cold water at 14±1°C to prevent temperature fluctuations during analysis. The results were expressed as cP.

Hardness was measured using a texture analyzer (XT-plus, Lloyd Ltd., Carlisle, UK) equipped with a 1 cm-diameter stainless steel cylindrical probe by the modified method of Bolliger *et al.* [2000]. The ice cream samples were stored at −22±1°C for 24 h before analysis. The conditions used for analysis were a penetration distance of 5 cm, a load cell of 1 kN, and a probe speed during penetration of 2.0 mm/s. The hardness (N) was measured as the peak compression force during the penetration of the sample.

Melting rates were measured by the modified method of Sofjan & Hartel [2004] in a controlled temperature chamber at 25°C. The frozen ice creams were tempered in a freezer at −18°C. A sample of 30 g was then placed on a 2 mm stainless steel screen with a funnel and graduated cylinder beneath it to collect the melt. The dripped weight was recorded once every 5 min for up to 60 min and the plot of the percentage of the melted ice cream was developed *versus* time. The slope of the plot indicated the melting rate expressed as g/min.

The percentage of overrun was measured by comparing the weight of melted ice cream in a fixed volume container with the weight of frozen ice cream [Aljewicz *et al.*, 2020]. The percentage of overrun was calculated according to the following formula (1):

$$\% \text{ Overrun} = \frac{W_{\text{melted IC}} - W_{\text{frozen IC}}}{W_{\text{frozen IC}}} \times 100 \quad (1)$$

where: $W_{\text{melted IC}}$ is weight of melted ice cream and $W_{\text{frozen IC}}$ is weight of frozen ice cream.

Antioxidant capacity determination

Extract preparation

Approximately 5 g of ice cream was extracted with 50 mL of methanol followed by vortexing and mechanical shaking for 4 h. The mixture was sonicated for 20 min and then filtered through Whatman No. 1 filter paper and centrifuged at 1,277×*g* for 30 min. The supernatant was separated and kept at −20°C for further analyses.

Total phenolic content determination

Total phenolic content (TPC) was determined with the Folin-Ciocalteau reagent, according to the method described by Singleton *et al.* [1999] and Chuacharoen *et al.* [2021] with a slight modification. Briefly, 20 µL of the extract, gallic acid standard, or blank sample taken in separate test tubes were mixed with 1.58 mL of distilled water, followed by the addition of 100 µL of Folin–Ciocalteau reagent, and the mixture was mixed thoroughly. Next, 300 µL of 7% aqueous sodium carbonate solution was added to the test tubes containing the mixtures within 8 min, and these were then immediately vortexed and allowed to stand in darkness for 30 min at room temperature. The absorbance was then recorded at 765 nm using a UV-Vis spectrophotometer (Spectronic™ GENESYS™2, Thermo Fisher Scientific, Waltham, MA, USA). TPC was calculated from a standard curve of gallic acid, and the results were expressed in mg gallic acid equivalent (GAE)/g of ice cream.

Antioxidant capacity determination

The antioxidant capacity of ice cream was measured by 1,1-diphenyl-2-picrylhydrazyl (DPPH) assay, 2,2′-azino-bis(3-ethylbenzothiazoline-6-sulfonic acid) (ABTS) assay, and ferric reducing antioxidant power (FRAP) assay.

DPPH assay was performed according to the procedure described by Ghafar *et al.* [2010] with a slight modification. Briefly, 200 µL of the extract was reacted with 2.8 mL of 100 µM $DPPH^{\bullet}$ dissolved in methanol for 30 min in darkness. A control containing only $DPPH^{\bullet}$ solution and 80% (*v/v*) methanol solution was used as the blank. The absorbance was then measured at 515 nm using a UV-Vis spectrophotometer (Spectronic™ GENESYS™2, Thermo Fisher Scientific). A standard curve was obtained by using a Trolox standard solution at various concentrations in 80% methanol solution. The results were expressed as mg of Trolox equivalents (TE)/g of ice cream

ABTS assay was carried out as described by Chuacharoen & Sabliov [2016] with a slight modification. Briefly, $ABTS^{\bullet+}$ solution was prepared by dissolving 7 mM of ABTS with 2.45 mM potassium persulfate and keeping the mixture in darkness for 15 h at room temperature. The $ABTS^{\bullet+}$ solution was then diluted with 5 mM sodium phosphate buffer at a pH of 7.4 to reach an absorbance of 0.70±0.02 using a UV-Vis spectrophotometer (Spectronic™ GENESYS™2, Thermo Fisher Scientific) read at 734 nm. Fifty µL of each extract was mixed thoroughly with 150 µL of the $ABTS^{\bullet+}$ solution, and incubated for 10 min at 25°C. The $ABTS^{\bullet+}$ scavenging activity was calculated from the calibration curve of Trolox. Results were expressed as mg of Trolox equivalent (TE)/g of ice cream.

FRAP assay was carried out according to the method described by Bakar *et al.* [2022] with a slight modification. Briefly, 100 µL of the extract was dissolved with 300 µL of distilled water, and the 100 µL of the diluted sample was pipetted into the test tube. The stock solutions including 300 mM acetate buffer (3.1 g sodium acetate trihydrate and 16 mL acetic acid) adjusted to pH 3.6, 20 mM $FeCl_3$ hexahydrate solution, and 10 mM 2,4,6-tri(2-pyridyl)-1,3,5-triazine (TPTZ) in 40 mM HCl solution were freshly prepared. Then, 3 mL of FRAP reagent (10:1:1 (*v/v/v*) of sodium acetate buffer, TPTZ, and $FeCl_3$ solutions) heated up to 37°C

was added to the sample test tube. The mixture was allowed to react for 30 min in darkness. Reading of the colored product (ferrous-tripyridyltriazine complex) was performed at 593 nm using a UV-Vis spectrophotometer (Spectronic™ GENESYS™2, Thermo Fisher Scientific). The FRAP was calculated from the calibration curve of Trolox. Results were expressed as mg of Trolox equivalent (TE)/g of ice cream.

Consumer acceptability test

Acceptability of avocado ice cream was evaluated by a semi-trained panel of 30 judges selected among graduate students, researchers, and academic staff of the Faculty of Science and Technology, Suan Sunandha Rajabhat University, Bangkok, Thailand. The semi-training consisted of presenting the aim of the study and introducing the sample properties to the panelists for 1 h. Subsequently, panel members were trained to identify the desired ice cream in terms of appearance, color, odor, taste, texture, resistance to melting, and overall acceptability. Ice cream samples stored at −20°C were removed from the freezer and tempered for 5 min at 20°C before sensory analysis. The samples of approximately 45 g were served in random code to panelists one by one to avoid melting of samples. During testing samples, the panelists were served drinking water to clean their palates. The sensorial properties were evaluated based on a 9-point hedonic scale for appearance, color, odor, taste, texture, resistance to melting, and overall acceptability using 1 – dislike and 9 – like, respectively [Di Criscio *et al.*, 2010; Karaman *et al.*, 2014; Kushwaha *et al.*, 2023; Tobin *et al.*, 2013].

Statistical analysis

The experiments were performed in triplicate, and the results were reported as mean ± standard deviation and analyzed using Statistical Package of the Social Science (SPSS) version 26 (IBM, Armonk, NY, USA) using one-way analysis of variance (ANOVA). Duncan's multiple range test was performed to determine the differences between mean values, and the differences were considered to be statistically significant at $p<0.05$.

RESULTS AND DISCUSSION

Proximate composition of avocado ice cream

The proximate compositions of the ice cream are shown in Table 2. Formulations having avocado pulp were significantly ($p<0.05$) higher in carbohydrates and crude fiber but significantly lower ($p<0.05$) in moisture, crude protein, total lipid, and ash contents compared with the control. Protein content was obviously reduced because the protein content of the controls was mainly obtained from fresh milk, whipped cream, and skimmed milk, which were partially replaced by avocado pulp.

Total lipid content of ice cream was reduced from 12.67 to 11.08 g/100 g (12%) and 9.1 g/100 g (28%) by partially replacing milk fat with 10% and 30% avocado pulp, respectively. Fat-reduced ice cream with avocado pulp should be a healthy choice. In addition, avocado contains oils that are rich in dietary beneficial monounsaturated fatty acids [Bes-Rastrollo *et al.*, 2008]. In a similar study, Harith *et al.* [2016] successfully used avocado puree as a fat replacer in muffins. They aimed to propose muffins with the benefit to promote healthy blood lipid profiles and regulate blood glucose levels. Additionally, the lipid fraction of avocado contains fat-soluble vitamins, including tocopherols [Green & Wang, 2020]. For this reason, this is a valuable phenomenon for substituting milk-fat ingredients of ice creams with avocado pulp.

Carbohydrate content in avocados includes about 80% dietary fiber, consisting of 70% insoluble and 30% soluble fiber [Marlett & Cheung, 1997]. Avocados contain 4.6 g of dietary fiber *per* 69 g approximately one-half of avocado fruit. Thus, consuming one-half an avocado can help to achieve about one-third of the adequate intake of 14 g dietary fiber *per* 1,000 kcal [USDA, 2011]. At this high level of carbohydrates, especially dietary fiber contained in an avocado, adding avocado pulp resulted in significantly ($p<0.05$) increased carbohydrate and fiber contents in the ice cream products, which was 2–3 times higher than that of the control (Table 2). It was hypothesized that adding cellulose fibers obtained from plants to ice cream could slow the melting rate. For example, citrus fiber was used to improve the melting quality of ice cream, but it failed to improve viscosity, overrun, and texture [Dervisoglu & Yazici, 2006]. Rice flour was a satisfactory fat replacer, but it caused a powdery mouthfeel in the ice cream [Cody *et al.*, 2007]. Soukoulis *et al.* [2009] studied the effects of four dietary fiber sources, which were oat, wheat, apple, and inulin, on the physicochemical properties of ice cream. They concluded that the enrichment of ice cream with dietary fibers was an effective way to enhance the nutritional and physiological

Table 2. Proximate composition (g/100 g) of ice cream (A0) and ice cream with avocado pulp as a substitute of 10% (A10), 20% (A20), and 30% (A30) (*w/w*) of the fat ingredients.

Component	A0 (control)	A10	A20	A30
Moisture	66.89±0.21^{a}	62.77±1.54^{b}	60.03±1.82^{bc}	59.59±1.12^{c}
Crude protein	15.50±0.21^{a}	12.49±1.09^{b}	10.15±0.96^{c}	9.29±0.38^{c}
Total lipids	12.67±0.11^{a}	11.08±0.98^{b}	10.14±0.83^{bc}	9.10±0.43^{c}
Carbohydrate	3.70±0.39^{c}	5.21±1.83^{b}	7.80±0.50^{a}	7.91±0.50^{a}
Ash	0.85±0.02^{a}	0.79±0.02^{b}	0.77±0.03^{b}	0.65±0.02^{c}
Crude fiber	0.39±0.07^{d}	0.84±0.22^{c}	1.11±0.55^{b}	1.38±0.60^{a}

Data are presented as mean ± standard deviation ($n=3$). $^{a-d}$ superscripts represent a significant difference within the same row ($p<0.05$) according to Duncan's multiple range test.

properties of the ice cream. Incorporating dietary fibers from plants not only affects the physical aspects of the food but also enhances the bioavailability of nutrients and phytochemicals [Unlu *et al.*, 2005]. Thus, ice cream incorporated with avocado may be healthier than the standard milk ice cream formulation because it has a lower fat content and higher fiber content.

The moisture content of ice cream was significantly (p<0.05) different between the samples having milk fat substituted with avocado pulp and control (Table 2). The control sample (A0) had the highest moisture content and moisture content decreased as the ratio of avocado pulp in the formulation was increased. This was due to decreasing the ratio of fresh liquid milk in the formulation. In general, a standard ice cream formulation should have a water content of about 55 to 65 g/100 g, and a mixture with high water content relates to a lower total solid content, and this proportion affects the physical properties of ice cream, particularly the texture and hardness [Choi & Shin, 2014].

Physical properties and color values of avocado ice cream

The physical parameters, including viscosity, melting rate, overrun, hardness, and color parameters, of control ice cream and ice cream with avocado pulp are shown in Table 3. The viscosity of ice cream differed significantly (p<0.05) among the formulations, and A30 had the highest value, followed by A20, A10, and A0, respectively. Overall viscosity increased as the ratio of avocado pulp added to the ice cream was increased. The viscosity of ice creams is particularly affected by adding stabilizer, sugar, or fiber [Syed, 2018]. In this study, guar gum was added at the same amount for all formulations, so crude fiber and sugar in avocado pulp incorporated into the ice cream played a significant role in its viscosity profile. The higher content of avocado pulp directly contributed to the increased sugar levels because of the natural sugars in avocados. Thus, higher contents of avocado pulp caused thicker and more viscous ice cream mixtures. Our results are consistent with the physical properties analysis of ice-cream frozen yogurts by Güven & Karaca [2002], who reported the amount of sugar and fruit increased viscosity values. Although avocado contains 1.2 g/100 g total sugar, it also contains 28 g/100 g dietary fiber [Dreher & Davenport, 2013]. Dietary fiber has the ability to bind with water, resulting in increased thickening of the ice cream mixture, as described by Soukoulis *et al.* [2009]. They explained that the increased viscosity of the fiber-enriched ice cream is caused by both the soluble and insoluble fibers. The contribution of the soluble fibers promotes soluble matter to the composition of the aqueous phase. Similarly, the contribution of insoluble fibers increases total solids affecting the three-dimensional conformation of the hydrated fibers. It is well known for its gel-forming ability and hydrogel structure reinforcement.

The melting rate of ice cream with avocado pulp differed significantly (p<0.05) between the formulations (Table 3). The control (A0) had the highest melting rate, followed by A10, A20, and A30. The melting rate decreased as the ratio of avocado pulp was increased, which may have been the dietary fiber in the avocado pulp that decreased the melting rate due to binding ability with water as mentioned earlier. A similar study on frozen dairy dessert by Soukoulis *et al.* [2009] reported that adding dietary fiber to a frozen dairy dessert could improve the melting quality of the ice cream, and insoluble fiber was able to increase the shear-thinning properties of the ice cream mixture as well.

Generally, a higher overrun level significantly contributes to a higher melting rate in the ice cream [Sofjan & Hartel, 2004]. In the present study, the overrun of ice cream was significantly (p<0.05) different among the formulations, which had the same trend as the melting rate. Increasing the ratio of avocado pulp to replace the milk fat in the ice cream mixture significantly reduced the overrun of the ice cream. The controls had a high overrun value resulting in a high melting rate due to the instability of air bubbles incorporated in the ice cream mixture. These air bubbles may have caused the temperature to increase while the ice cream was melting.

Overrun also affected the hardness profile of ice cream (Table 3). The hardness refers to the resistance of the ice cream to deform affected by an external force and it has an inverse relationship with the overrun [Muse & Hartel, 2004]. The highest hardness value was determined in the samples with the highest avocado pulp added, followed by A20 and A10, which were significantly (p<0.05) higher than those found in the controls. It can

Table 3. Physical properties of ice cream (A0) and ice cream with avocado pulp as a substitute of 10% (A10), 20% (A20), and 30% (A30) (*w/w*) of the fat ingredients.

Parameter		A0 (control)	A10	A20	A30
Viscosity (cP)		175.50±1.25^{d}	212.49±1.09^{c}	250.15±0.96^{b}	296.29±0.38^{a}
Melting rate (g/min)		7.85±0.63^{a}	3.54±0.29^{b}	1.23±0.20^{c}	0.42±0.18^{d}
Overrun (%)		21.05±0.21^{a}	19.90±1.18^{b}	17.46±0.14^{c}	10.89±1.17^{d}
Hardness (N)		9.74±0.54^{d}	13.16±0.88^{c}	16.87±0.25^{b}	18.48±0.13^{a}
Color	L^*	86.08±0.23^{a}	69.29±1.50^{b}	67.19±0.45^{c}	61.48±0.61^{d}
	a^*	−0.43±0.39^{a}	−1.71±0.28^{b}	−2.80±0.21^{c}	−3.34±0.49^{c}
	b^*	13.28±0.25^{d}	30.10±0.80^{c}	33.36±0.25^{b}	36.77±0.21^{a}

Data are presented as mean ± standard deviation (n=3). $^{a-d}$ superscripts represent a significant difference within the same row (p<0.05) according to Duncan's multiple range test. L^*, lightness; a^*, greenness to redness; b^*, blueness to yellowness.

be attributed to the gelling properties of avocado fibers which favor the ability to bind water molecules and form a particle gel network improving the firmness of the ice cream [Akalın *et al.*, 2018]. This was consistent with the findings of Crizel *et al.* [2014], who used orange fiber as a fat replacer in ice cream; the result showed that the greater amount of the orange fiber significantly increased ice cream's hardness compared to the control. For the texture perception, it can be concluded that ice cream enrichment with fiber may contribute to the improvement of melting rate and the formation of tiny ice crystals favoring the stability of ice crystals during frozen storage.

The color of ice cream brings visual attractiveness, which is relevant to the acceptability of a product for consumers. The images and color parameters of ice cream incorporated with avocado pulp are presented in Figure 1 and Table 3, respectively. Adding avocado pulp created a green-colored ice cream, and adding higher ratios of it caused less brightness along with changes in yellow and green hues, which were visually perceptible to the naked eyes. The L^* values of ice cream color decreased as the ratio of avocado was increased, and the hue of yellow (b^*) increased significantly ($p<0.05$). The green hue of the ice cream was less dark when the ratio of avocado pulp was increased (A20 and A30) and compared with the control (A0).

Total phenolic content and antioxidant capacity of avocado ice cream

The antioxidant capacity of avocado ice cream was evaluated as DPPH$^{\bullet}$ and ABTS$^{\bullet+}$ scavenging activities and as ferric reducing antioxidant power (FRAP). The DPPH assay is based on an electron transfer mechanism to stabilize radicals with a high affinity to lipophilic antioxidants, whereas more polar antioxidant compounds are easily determined by FRAP and/or ABTS assays [Martysiak-Żurowska & Wenta, 2012]. A significant relationship between antioxidant potential and phenolic compounds which are the major contributors to antioxidant activity is seen in Table 4. The TPC and antioxidant capacity of the ice cream incorporated with avocado pulp were significantly ($p<0.05$) higher than those without avocado pulp. It is not surprising as the strong antioxidant potential of avocado pulp was reported in previous studies [Chuacharoen *et al.*, 2021; Lyu *et al.*, 2023; Nguyen *et al.*, 2022]. The TPC of the ice cream with incorporated avocado ranged from 5.25 to 12.19 GAE mg/g ice cream, and the highest value was determined in the sample with the highest amount of avocado pulp (A30). The DPPH$^{\bullet}$ scavenging activity ranged from 32.3 to 45.7 µmol TE/g of avocado ice cream with increasing values as avocado pulp ratio was increased. This was attributed to the fact that fresh avocado pulp contains the bioactive compounds, which possessed the stronger antioxidant capacities when incorporated in higher amount proportionally [Chimuti *et al.*, 2021]. ABTS$^{\bullet+}$ scavenging activity and FRAP of avocado ice cream ranged from 73.0 to 104.9 µmol TE/g and 240 to 325 µmol TE/g, respectively. The results of ABTS and FRAP assays, demonstrate again higher antioxidant capacity of ice cream with higher amounts of avocado pulp mixed into the ice cream. Martysiak-Żurowska & Wenta [2012] reported that the ABTS test was more precise and sensitive to characterize the total antioxidant capacity in milk-based products compared to the DPPH test. In our study, all assays were useful to show the antioxidant capacity of avocado ice cream. In general, the addition of avocado pulp as a fat replacement ingredient can enhance the content of health-promoting phenolic compounds and antioxidant characteristics of ice cream.

Assessment of consumer acceptability of avocado ice cream

Consumer ratings of the avocado ice cream samples are shown in Table 5. Adding avocado pulp affected the sensory properties of the ice cream and decreased the overall acceptability of the product due to the grassy smell of the avocado pulp. The higher content of avocado pulp added into ice cream samples resulted in significantly ($p<0.05$) lower scores for odor and taste. The taste property is one of the most important sensory criteria for food products, especially for ice cream.

A significant ($p\geq0.05$) difference was not detected regarding the appearance and color of the samples except for A20, which received the highest score on both attributes. Texture score became lower as the ratio of avocado pulp was increased. The lower texture score was related to the ice cream's resistance to melting.

Figure 1. The appearance of ice cream (**A**) and ice cream incorporated with avocado pulp at different levels: 10%, *w/w* (**B**), 20%, *w/w* (**C**), and 30%, *w/w* (**D**).

Table 4. Total phenolic content (TPC) and antioxidant capacity of ice cream (A0) and ice cream with avocado pulp as a substitute of 10% (A10), 20% (A20), and 30% (A30) (*w/w*) of the fat ingredients.

Parameter	A0 (control)	A10	A20	A30
TPC (mg GAE/g)	3.57±0.08^{d}	5.25±0.02^{c}	8.56±0.10^{b}	12.19±0.07^{a}
DPPH$^{\bullet}$ scavenging activity (μmol TE/g)	24.2±3.5^{c}	32.3±8.6^{b}	39.3±6.7^{ab}	45.6±11.8^{a}
ABTS$^{\bullet+}$ scavenging activity (μmol TE/g)	62.1±0.7^{d}	73.0±1.2^{c}	83.5±5.2^{b}	104.9±3.1^{a}
FRAP (μmol TE/g sample)	169±18^{d}	240±21^{c}	290±11^{b}	325±20^{a}

Data are presented as mean ± standard deviation (n=3). $^{a-d}$ superscripts represent a significant difference within the same row (p<0.05) according to Duncan's multiple range test. DPPH$^{\bullet}$, 1,1-diphenyl-2-picrylhydrazyl radical; ABTS$^{\bullet+}$, 2,2'-azino-bis(3-ethylbenzothiazoline-6-sulfonic acid) radical cation; FRAP, ferric reducing antioxidant power; GAE, gallic acid equivalent; TE, Trolox equivalent.

Table 5. Consumer ratings of ice cream (A0) and ice cream with avocado pulp as a substitute of 10% (A10), 20% (A20), and 30% (A30) (*w/w*) of the fat ingredients.

Attribute	A0 (control)	A10	A20	A30
Appearance	7.17±1.05^{b}	7.23±1.19^{b}	7.57±0.86^{a}	7.10±1.06^{b}
Color	7.15±1.18^{b}	7.23±1.10^{b}	7.43±0.86^{a}	7.37±0.93^{b}
Odor	7.07±1.06^{a}	7.17±1.23^{a}	7.13±1.17^{a}	6.57±1.17^{b}
Taste	7.36±1.17^{a}	7.47±1.19^{a}	7.47±1.59^{a}	6.00±1.66^{b}
Texture	7.66±1.05^{a}	7.33±0.99^{b}	7.27±1.11^{b}	6.70±1.18^{c}
Resistance to melting	6.06±1.66^{c}	6.22±1.05^{c}	6.69±1.09^{b}	7.35±1.66^{a}
Overall acceptability	7.43±0.94^{a}	7.47±0.99^{a}	7.39±1.07^{a}	6.47±1.38^{b}

Data are presented as mean ± standard deviation (n=30). $^{a-c}$ superscripts represent a significant difference within the same row (p<0.05) according to Duncan's multiple range test.

The incremental increase in avocado pulp ratio provided resistance to melting, confirmed by the consumer ratings. The higher the amount of avocado pulp added to ice creams, the greater the amount of dietary fiber was retarding the melting rate of the ice cream. It was also confirmed by physical measurements of the melting rate and hardness. The highest amount of avocado pulp (A30) incorporated caused the ice cream to melt slowest and be difficult to consume. Thus, the consumers preferred the ice cream with a good combination of a medium green, a moderate rate of melting, and a texture with a slightly high overrun level, which were found from the characteristics of the ice cream samples incorporated avocado pulp at 10–20%.

CONCLUSIONS

Fresh avocado pulp could be used as a fat-replacing ingredient in dairy products (*e.g.*, ice cream), which would alter their physical and chemical aspects as a function of avocado content in the ice cream. Regarding the proximate composition, avocado ice cream showed a healthier content of crude fiber and was low in total lipid content, compared with a standard milk ice cream formulation. The substitution of milk fat with avocado pulp affected the texture perception in the ice cream mixture. In addition, the effect of avocado pulp compositions on air content in the ice cream mixture also contributed to the physical properties of the ice cream such as melting properties, overrun, hardness, and other sensorial characteristics. Health-promoting phenolic compounds and antioxidant capacity of the avocado ice cream increased as the ratio of avocado content was increased. To produce antioxidant-rich avocado ice cream, the incorporation of avocado pulp at contents higher than 20% increased the potential functional properties of the ice cream, but reduced some desirable physical properties, which significantly decreased the overall acceptability of the ice cream.

ACKNOWLEDGEMENTS

The authors would like to thank the Departments of Food Science and Technology and Home Economics, Faculty of Science and Technology, Suan Sunandha Rajabhat University for providing facilities, and Greenday Global Co., Ltd. for supplying avocado fruits during the research period.

RESEARCH FUNDING

The study received no external funding.

CONFLICT OF INTERESTS

Authors declare no conflict of interests.

ORCID IDs

T. Chuacharoen https://orcid.org/0000-0002-2668-942X

REFERENCES

1. Akalın, A.S., Kesenkas, H., Dinkci, N., Unal, G., Ozer, E., Kınık, O. (2018). Enrichment of probiotic ice cream with different dietary fibers: Structural characteristics and culture viability. *Journal of Dairy Science, 101*(1), 37-46. https://doi.org/10.3168/jds.2017-13468
2. Aljewicz, M., Florczuk, A., Dąbrowska, A. (2020). Influence of β-glucan structures and contents on the functional properties of low-fat ice cream during storage. *Polish Journal of Food and Nutrition Sciences, 70*(3), 233-240. https://doi.org/10.31883/pjfns/120915

3. Bakar, M.F.A., Ranneh, Y., Kamil, N.F.M. (2022). Development of high fiber rich antioxidant biscuits from purple and orange sweet potato peels. *Food Research*, *6*(1), 12-19. https://doi.org/10.26656/fr.2017.6(1).036
4. Bes-Rastrollo, M., van Dam, R.M., Martinez-Gonzalez, M.A., Li, T., Sampson, L.L., Hu, F.B. (2008). Prospective study of dietary energy density and weight gain in women. *The American Journal of Clinical Nutrition, 88*(3), 769-777. https://doi.org/10.1093/ajcn/88.3.769
5. Bolliger, S., Kornbrust, B., Goff, H.D., Tharp, B.W., Windhab, E.J. (2000). Influence of emulsifiers on ice cream produced by conventional freezing and low--temperature extrusion processing. *International Dairy Journal, 10*(7), 497-504. https://doi.org/10.1016/S0958-6946(00)00071-6
6. Chimuti, N., Takalani, T.K., Anyasi, T. (2021). Organoleptic and physicochemical properties of 'Hass' avocado (*Persea americana* Mill.) oil extract obtained using cold press technology. *Food Research, 5*(4), 360-365. https://doi.org/10.26656/fr.2017.5(4).032
7. Choi, M.J., Shin, K.S. (2014). Studies on physical and sensory properties of premium vanilla ice cream distributed in Korean market. *Korean Journal for Food Science of Animal Resources, 34*(6), 757-762. https://doi.org/10.5851/kosfa.2014.34.6.757
8. Chuacharoen, T., Sabliov, C.M. (2016). The potential of zein nanoparticles to protect entrapped β-carotene in the presence of milk under simulated gastrointestinal (GI) conditions. *LWT - Food Science and Technology, 72*, 302-309. https://doi.org/10.1016/j.lwt.2016.05.006
9. Chuacharoen, T., Moolwong, J., Chysirichote, T. (2021). Effects of maltodextrin on physicochemical properties of freeze-dried avocado powder. *Food Research, 5*(6), 178-186. https://doi.org/10.26656/fr.2017.5(6).739
10. Cody, T.L., Olabi, A., Pettingell, A.G., Tong, P.S., Walker, J.H. (2007). Evaluation of rice flour for use in vanilla ice cream. *Journal of Dairy Science, 90*(10), 4575-4585. https://doi.org/10.3168/jds.2006-531
11. Cortés Rodríguez, M., Orrego Vargas, F.S., Rodriguez-Sandoval, E. (2019). Optimization of guacamole formulation made with avocado powder and fresh avocado. *DYNA, 86*(209), 126-134. https://doi.org/10.15446/dyna.v86n209.72930
12. Crizel, T., Araujo, R., Rios, A., Rech, R., Flôres, S. (2014). Orange fiber as a novel fat replacer in lemon ice cream. *Food Science and Technology (Campinas), 34*(2), 332-340. https://doi.org/10.1590/fst.2014.0057
13. Dervisoglu, M., Yazici, F. (2006). Note. The effect of citrus fibre on the physical, chemical and sensory properties of ice cream. *Food Science and Technology International, 12*(2), 159-164. https://doi.org/10.1177/1082013206064005
14. Di Criscio, T., Fratianni, A., Mignogna, R., Cinquanta, L., Coppola, R., Sorrentino, E., Panfili, G. (2010). Production of functional probiotic, prebiotic, and synbiotic ice creams. *Journal of Dairy Science, 93*(10), 4555-4564. https://doi.org/10.3168/jds.2010-3355
15. Dreher, M.L., Davenport, A.J. (2013). Hass avocado composition and potential health effects. *Critical Reviews in Food Science and Nutrition, 53*(7), 738-750. https://doi.org/10.1080/10408398.2011.556759
16. Ford, N.A., Spagnuolo, P., Kraft, J., Bauer, E. (2023). Nutritional composition of hass avocado pulp. *Foods, 12*(13), art. no. 2516. https://doi.org/10.3390/foods12132516
17. Ghafar, M., Prasad, K.N., Weng, K.K., Ismail, A. (2010). Flavonoid, hesperidine, total phenolic contents and antioxidant activities from Citrus species. *African Journal of Biotechnology, 9*(3), 326-330.
18. Green, H.S., Wang, S.C. (2020). First report on quality and purity evaluations of avocado oil sold in the US. *Food Control, 116*, art. no. 107328. https://doi.org/10.1016/j.foodcont.2020.107328
19. Güven, M., Karaca, O.B. (2002). The effect of varying sugar content and fruit concentration on the physical properties of vanilla and fruit ice-cream-type frozen yogurts. *International Journal of Dairy Technology, 55*(1), 27-31. https://doi.org/10.1046/j.1471-0307.2002.00034.x
20. Harith, S., Manaf, A.M., Othman, N.A. (2016). The effect of avocado puree as fat replacer on the physical quality of muffin. *Malaysian Applied Biology, 45*(2), 11-16.
21. Karaman, S., Toker, Ö.S., Yüksel, F., Çam, M., Kayacier, A., Dogan, M. (2014). Physicochemical, bioactive and sensory properties of persimmon-based ice cream: Technique for order preference by similarity to ideal solution to determine optimum concentration. *Journal of Dairy Science, 97*(1), 97-110. https://doi.org/10.3168/jds.2013-7111
22. Krumreich, F.D., Borges, C.D., Mendonça, C.R.B., Jansen-Alves, C., Zambiazi, R.C. (2018). Bioactive compounds and quality parameters of avocado oil obtained by different processes. *Food Chemistry, 257*, 376-381. https://doi.org/10.1016/j.foodchem.2018.03.048
23. Kushwaha, R., Gupta, A., Singh, V., Kaur, S., Puranik, V., Kaur, D. (2023). Jackfruit seed flour-based waffle ice cream cone: Optimization of ingredient levels using response surface methodology. *Heliyon, 9*(2), art. no. e13140. https://doi.org/10.1016/j.heliyon.2023.e13140
24. Latimer, G.W. (2019). *Official Methods of Analysis of AOAC International*. Rockville, Md: AOAC International. https://doi.org/10.1093/9780197610145.001.0001
25. Lyu, X., Agar, O.T., Barrow, C.J., Dunshea, F.R., Suleria, H.A.R. (2023). Phenolic compounds profiling and their antioxidant capacity in the peel, pulp, and seed of Australian grown avocado. *Antioxidants, 12*(1), art. no. 185. https://doi.org/10.3390/antiox12010185
26. Mahmassani, H.A., Avendano, E.E., Raman, G., Johnson, E.J. (2018). Avocado consumption and risk factors for heart disease: a systematic review and meta--analysis. *The American Journal of Clinical Nutrition, 107*(4), 523-536. https://doi.org/10.1093/ajcn/nqx078
27. Marlett, J.A., Cheung, T.F. (1997). Database and quick methods of assessing typical dietary fiber intakes using data for 228 commonly consumed foods. *Journal of the American Dietetic Association, 97*(10), 1139-1151. https://doi.org/10.1016/S0002-8223(97)00275-7
28. Martysiak-Żurowska, D., Wenta, W. (2012). A comparison of ABTS and DPPH methods for assessing the total antioxidant capacity of human milk. *Acta Scientiarum Polonorum, Technologia Alimentaria, 11*(1), 83-89.
29. Muse, M.R., Hartel, R.W. (2004). Ice cream structural elements that affect melting rate and hardness. *Journal of Dairy Science, 87*(1), 1-10. https://doi.org/10.3168/jds.S0022-0302(04)73135-5
30. Nguyen, T.V.L., Nguyen, Q.D., Nguyen, P.B.D. (2022). Drying kinetics and changes of total phenolic content, antioxidant activity and color parameters of mango and avocado pulp in refractance window drying. *Polish Journal of Food and Nutrition Sciences, 72*(1), 27-38. https://doi.org/10.31883/pjfns/144835
31. Ospina, S., Ortiz, D.L., Orrego, C.E. (2019). Enzymatic browning and color evolution in frozen storage of two kinds of minimally processed avocado puree. *International Journal of Food Engineering, 15*(11-12). https://doi.org/10.1515/ijfe-2018-0431
32. Ramos-Aguilar, A.L., Ornelas-Paz, J., Tapia-Vargas, L.M., Gardea-Bejar, A.A., Yahia, E.M., Ornelas-Paz, J.d.J., Perez-Martinez, J.D., Rios-Velasco, C., Escalante-Minakata, P. (2021). Metabolomic analysis and physical attributes of ripe fruits from Mexican Creole (*Persea americana* var. *Drymifolia*) and 'Hass' avocados. *Food Chemistry, 354*, 129571. https://doi.org/10.1016/j.foodchem.2021.129571
33. Singleton, V.L., Orthofer, R., Lamuela-Raventós, R.M. (1999). Analysis of total phenols and other oxidation substrates and antioxidants by means of Folin-Ciocalteu reagent. *Methods in Enzymology, 299*, 152-178. https://doi.org/10.1016/S0076-6879(99)99017-1
34. Sofjan, R.P., Hartel, R.W. (2004). Effects of overrun on structural and physical characteristics of ice cream. *International Dairy Journal, 14*(3), 255-262. https://doi.org/10.1016/j.idairyj.2003.08.005
35. Soukoulis, C., Lebesi, D., Tzia, C. (2009). Enrichment of ice cream with dietary fibre: Effects on rheological properties, ice crystallisation and glass transition phenomena. *Food Chemistry, 115*(2), 665-671. https://doi.org/10.1016/j.foodchem.2008.12.070
36. Syed, Q.A. (2018). Effects of different ingredients on texture of ice cream. *Journal of Nutritional Health and Food Engineering, 8*(6), 422-435. https://doi.org/10.15406/jnhfe.2018.08.00305
37. Tobin, R., Moane, S., Larkin, T. (2013). Sensory evaluation of organic and conventional fruits and vegetables available to Irish consumers. *International Journal of Food Science and Technology, 48*(1), 157-162. https://doi.org/10.1111/j.1365-2621.2012.03172.x
38. Unlu, N.Z., Bohn, T., Clinton, S.K., Schwartz, S.J. (2005). Carotenoid absorption from salad and salsa by humans is enhanced by the addition of avocado or avocado oil. *Journal of Nutrition, 135*(3), 431-436. https://doi.org/10.1093/jn/135.3.431
39. USDA. (2011). Avocado, almond, pistachio and walnut Composition. *Nutrient Data Laboratory. USDA National Nutrient Database for Standard Reference, Release 24*.
40. Yahia, E.M., Woolf, A.B. (2011). Avocado (*Persea americana* Mill.). In E.M. Yahia (Ed.). *Postharvest Biology and Technology of Tropical and Subtropical Fruits*. Woodhead Publishing, Cambridge, UK, pp. 125-186. https://doi.org/10.1533/9780857092762.125
41. Yeon, S.J., Kim, J.H., Hong, G.E., Park, W., Kim, S.K., Seo, H.G., Lee, C.H. (2017). Physical and sensory properties of ice cream containing fermented pepper powder. *Korean Journal for Food Science of Animal Resources, 37*(1), 38-43. https://doi.org/10.5851/kosfa.2017.37.1.38

REVIEW ARTICLE
http://journal.pan.olsztyn.pl

INSTRUCTIONS FOR AUTHORS

SUBMISSION. Original contributions relevant to food and nutrition sciences are accepted on the understanding that the material has not been, nor is being, considered for publication elsewhere. All papers should be submitted and will be processed electronically via Editorial Manager system (available from PJFNS web site: http://journal.pan.olsztyn.pl). On submission, a corresponding author will be asked to provide: Cover letter; Files with Manuscripts, Tables, Figures/Photos; and Names of two potential reviewers (one from the author's homeland – but outside author's Institution, and the other from abroad). All papers which have been qualified as relevant with the scope of our Journal are reviewed. All contributions, except the invited reviews are charged. Proofs will be sent to the corresponding author and should be returned within one week since receipt. No new material may be inserted in the text at proof stage. It is the author's duty to proofread proofs for errors.

Authors should very carefully consider the preparation of papers to ensure that they communicate efficiently, because it permits the reader to gain the greatest return for the time invested in reading. Thus, we are more likely to accept those that are carefully designed and conform the instruction. Otherwise, papers will be rejected and removed from the online submission system.

SCOPE. The Polish Journal of Food and Nutrition Sciences publishes original, basic and applied papers, and reviews on fundamental and applied food research, preferably these based on a research hypothesis, in the following Sections:

Food Technology:
- Innovative technology of food development including biotechnological and microbiological aspects
- Effects of processing on food composition and nutritional value

Food Chemistry:
- Bioactive constituents of foods
- Chemistry relating to major and minor components of food
- Analytical methods

Food Quality and Functionality:
- Sensory methodologies
- Functional properties of food
- Food physics
- Quality, storage and safety of food

Nutritional Research:
- Nutritional studies relating to major and minor components of food (excluding works related to questionnaire surveys)

"News" section:
- Announcements of congresses
- Miscellanea

OUT OF THE SCOPE OF THE JOURNAL ARE:
- Works which do not have a substantial impact on food and nutrition sciences
- Works which are of only local significance i.e. concern indigenous foods, without wider applicability or exceptional nutritional or health related properties
- Works which comprise merely data collections, based on the use of routine analytical or bacteriological methods (i.e. standard methods, determination of mineral content or proximate analysis)
- Works concerning biological activities of foods but not providing the chemical characteristics of compounds responsible for these properties
- Nutritional questionnaire surveys
- Works related to the characteristics of foods purchased at local markets
- Works related to food law
- Works emphasizing effects of farming / agricultural conditions / weather conditions on the quality of food constituents
- Works which address plants for non-food uses (i.e. plants exhibiting therapeutic and/or medicinal effects)

TYPES OF CONTRIBUTIONS. *Reviews*: (at least: 30 pages and 70 references) these are critical and conclusive accounts on trends in food and nutrition sciences; *Original papers*: (maximally: 30 pages and 40 references) these are reports of substantial research; *Reports on post and forthcoming scientific events, and letters to the Editor* (all up to three pages) are also invited (free of charge).

REVIEW PROCESS. All scientific contributions will be peer-reviewed on the criteria of originality and quality. Submitted manuscripts will be preevaluated by Editor-in-Chief and Statistical Editor (except for review articles), and when meeting PJFNS' scope and formal requirements, they will be sent to a Section Editor who upon positive preevaluation will assign at least two reviewers from Advisory Board Members, reviewers suggested by the author or other experts in the field. Based on the reviews achieved, Section Editor and Editor-in--Chief will make a decision on whether a manuscript will be accepted for publication, sent back to the corresponding author for revision, or rejected. Once a manuscript is sent back to the corresponding author for revision, all points of the reviews should be answered or rebuttal should be provided in the Explanation letter. The revised manuscripts will be checked by Section Editor and by the original reviewers (if necessary), and a final decision will be made on acceptance or rejection by both Section Editor and Editor-in-Chief.

Polish Journal of Food and Nutrition Sciences uses CrossCheck's iThenticate software to detect instances of similarity in submitted manuscripts. In publishing only original research, PJFNS is committed to deterring plagiarism, including self-plagiarism.

COPYRIGHT LICENSE AGREEMENT referring to Authorship Responsibility and Acknowledgement, Conflict of Interest and Financial Disclosure, Copyright Transfer, are required for all authors, i.e. *Authorship Responsibility and Acknowledgement*: Everyone who has made substantial intellectual contributions to the study on which the article is based (for example, to the research question, design, analysis, interpretation, and written description) should be an author. It is dishonest to omit mention of someone who has participated in writing the manuscript ("ghost authorship") and unfair to omit investigator who have had important engagement with other aspects of the work. All contributors who do not meet the criteria for authorship should be listed in an Acknowledgments section. Examples of those who might be acknowledged include a person who provided purely technical help, writing assistance, or a department chairperson who provided only general support. Any financial and material support should also be acknowledged. *Conflict of Interest and Financial Disclosure*: Authors are responsible for disclosing financial support from the industry or other conflicts of interest that might bias the interpretation of results. *Copyright License Agreement*: Authors agree to follow the Creative Commons Attribution-Non--Commercial-NoDerivs 4.0 License.

A manuscript will not be published once the signed form has not been submitted to the Editor with the manuscript revised after positive reviews.

CHANGES TO AUTHORHIP. Authors are expected to consider carefully the list and order of authors before submitting their manuscript and provide the definitive list of authors at the time of the original submission. Any addition, deletion or rearrangement of author names in the authorship list should be made only before the manuscript has been accepted and only if approved by the journal Editor. To request such a change, the Editor must receive the following from the corresponding author: (a) the reason for the change in author list and (b) written confirmation (e-mail, letter) from all authors that they agree with the addition, removal or rearrangement. In the case of addition or removal of authors, this includes confirmation from the author being added or removed.

ETHICAL APPROVAL OF STUDIES AND INFORMED CONSENT. For all manuscripts reporting data from studies involving human participants or animals, formal approval by an appropriate institutional review board or ethics committee is required and should be described in the Methods section. For those investigators who do not have formal approval from ethics review committees, the principles outlined in the Declaration of Helsinki should be followed. For investigations of humans, state in the Methods section the manner in which informed consent was obtained from the study participants (i.e., oral or written). Editors may request that authors provide documentation of the formal review and recommendation from the institutional review board or ethics committee responsible for oversight of the study.

UNAUTHORIZED USE. Unauthorized use of the PJFNS name, logo, or any content for commercial purposes or to promote commercial goods and services (in any format, including print, video, audio, and digital) is not permitted by IAR&FR PAS.

MANUSCRIPTS. A manuscript in English must be singlesided, preferably in Times New Roman (12) with 1.5-point spacing, without numbers of lines. The Editor reserves the right to make literary corrections and to make suggestions to improve brevity. English is the official language. The English version of the paper will be checked by Language Editor. Unclear and unintelligible version will be returned for correction.

Every paper should be divided under the following headings in this order: a **Title** (possibly below 150 spaces); the **Name(s)** of the author(s) in full. In paper with more than one author, the asterisk indicates the name of the author to whom correspondence and inquiries should be addressed, otherwise the first author is considered for the corre-spondence. Current full postal address of the indicated corresponding author or the first author must be given in a footnote on the title page; the **Place(s)** where the work was done including the institution name, city, country if not Poland. In papers originated from several institu-tions the names of the authors should be marked with respective superscripts; the **Key words** (up to 6 words or phrases) for the main topics of the paper; an **Abstract** (up to 250 words for regular papers and reviews) summarizing briefly main results of the paper, no literature references; an **Introduction** giving essential background by saying why the research is important, how it relates to previous works and stating clearly the objectives at the end; **Materials and Methods** with sufficient experimental details permitting to repeat or extend the experiments. Literature references to the methods, sources of material, company names and location (city, country) for specific instruments must be given. Describe how the data were evaluated, including selection criteria used; **Results and Discussion** presented together (in one chapter). Results should be presented concisely and organized to supplement, but not repeat, data in tables and figures. Do not display the data in both tabular and graphic form. Use narrative form to present the data for which tables or figures are unnecessary. Discussion should cover the implications and consequences, not merely recapitulating the results, and it must be accomplished with concise **Conclusions**; **Acknowledgements** should be made to persons who do not fill the authorship criteria (see: Authorship forms); **Research funding** should include financial and material support; **Conflict of Interests**: Authors should reveal any conflicts of interest that might bias the interpretation of results; and **References** as shown below.

REFERENCES each must be listed alphabetically at the end of the paper (each should have an Arabic number in the list) in the form as follows: **Periodicals** – names and initials of all the authors, year of publication, title of the paper, journal title as in Chemical Abstracts, year of publication, volume, issue, inclusive page numbers, or article id.; **Books** – names and initials of all the authors, names of editors, chapter title, year of publication, publishing company, place of publication, inclusive page numbers; **Patents** – the name of the application, the title, the country, patent number or application number, the year of publication.

For papers published in language other than English, manuscript title should be provided in English, whereas a note on the original language and English abstract should be given in parentheses at the end.

The reference list should only include peer-reviewed full-text works that have been published or accepted for publication. Citations of MSc/PhD theses and works unavailable to international Editors, Reviewers, and Readers should be limited as much as possible.

References in the text must be cited by name and year in square parentheses (e.g.: one author – [Tokarz, 1994]; two authors – [Słonimski & Campbell, 1987]; more than two authors – [Amarowicz *et al*., 1994]). If more than one paper is published in the same year by the same author or group of authors use [Tokarz, 1994a, b]. Unpublished work must only be cited where necessary and only in the text by giving the person's name.

Examples:

Article in a journal:

Słonimski, B.A., Campbell, L.D., Batista, E., Howard B. (2008). Gas chromatographic determination of indole glucosinolates. Journal of Science and Food Agriculture, 40(5), 131–143.

Asher, A., Tintle, N.L., Myers, M., Lockshon, L., Bacareza, H., Harris, W.S. (2021). Blood omega-3 fatty acids and death from COVID-19: A pilot study. *Prostaglandins, Leukotrienes and Essential Fatty Acids, 166*, art. no. 102250.

Book:

Weber, W., Ashton, L., Milton, C. (2012). Antioxidants – Friends or Foes? 2nd edition. PBD Publishing, Birmingham, UK. pp. 218–223.

Chapter in a book:

Uden, C., Gambino, A., Lamar, K. (2016). Gas chromatography. In M. Queresi, W. Bolton (Eds.), CRC Handbook of Chromatography, CRC Press Inc., Boca Raton, Florida, USA, pp. 44–46.

ABBREVIATIONS AND UNITS. Abbreviations should only be used when long or unwieldy names occur frequently, and never in the title; they should be given at the first mention of the name. Metric SI units should be used. The capital letter L should be used for liters. Avoid the use of percentages (% g/g,% w/w; Mol%; vol%), ppm, ppb. Instead, the expression such as g/kg, g/L, mg/kg, mg/mL should be used. A space must be left between a number and a symbol (e.g. 50 mL not 50mL). A small x must be used as multiplication sign between numeric values (e.g. 5 × 102 g/mL). Statistics and measurements should be given in figures, except when the number begins a sentence. Chemical formulae and solutions must specify the form used. Chemical abbreviations, unless they are internationally known, Greek symbols and unusual symbols for the first time should be defined by name. Common species names should be followed by the Latin at the first mention, with contracting it to a single letter or word for subsequent use.

FIGURES should be submitted in separate files. Each must have an Arabic number and a caption. Captions of all Figures should be provided on a separate page "Figure Captions". Figures should be comprehensible without reference to the text. Self-explanatory legend to all figures should be provided under the heading "Legends to figures"; all abbreviations appearing on figures should be explained in figure footnotes. Three-dimensional graphs should only be used to illustrate real 3D relationships. Start the scale of axes and bars or columns at zero, do not interrupt them or omit missing data on them. Figures must be cited in Arabic numbers in the text.

TABLES should be submitted in separate files. They should be as few in number and as simple as possible (like figures, they are expensive and space consuming), and include only essential data with appropriate statistical values. Each must have an Arabic number and a caption. Captions of all Tables should be provided on a separate page "Table Captions". Tables should be self-explanatory; all abbreviations appearing in tables should be explained in table footnotes. Tables must be cited in Arabic numbers in the text.

PAGE CHARGES. A standard publication fee has been established at the rate of 450 EUR + tax (if applicable, e.g. for private persons) irrespective of the number of pages and tables/figures. For Polish Authors an equivalent fee was set at 1950 PLN + VAT. Payment instructions will be sent to Authors via e-mail with acceptance letter.

Information on publishing and subscription is available from:

Ms. Joanna Molga
Editorial Office of Pol. J. Food Nutr. Sci.
Institute of Animal Reproduction and Food Research Tuwima 10 Str., 10–748 Olsztyn 5, Poland
phone (48 89) 523–46–70, fax (48 89) 523–46–70;
e-mail: pjfns@pan.olsztyn.pl; http://journal.pan.olsztyn.pl